Pahute Mesa Well Development and Testing Analyses for Wells ER-20-7, ER-20-8 #2, and ER-EC-11

Navarro-Intera

Revision No.: 1

December 2011

Available for sale to the public from:

Printed on
recycled paper

PAHUTE MESA WELL DEVELOPMENT AND TESTING ANALYSES FOR WELLS ER-20-7, ER-20-8 #2, AND ER-EC-11

Revision No.: 1
December 2011

Navarro-Intera, LLC
c/o U.S. DOE
P.O. Box 98952
Las Vegas, NV 89193-8952

Reviewed and determined to be UNCLASSIFIED.
Derivative Classifier: _____ Joseph P. Johnston/N-I CO _____
(Name/personal identifier and position title)
Signature: /s/ Joseph P. Johnston
Date: 12/14/2011

Prepared for U.S. Department of Energy under Contract No. DE-AC52-09NA28091.

PAHUTE MESA WELL DEVELOPMENT
AND TESTING ANALYSES
FOR WELLS ER-20-7, ER-20-8#2, AND ER-EC-11

Approved by: **/s/ Sam Marutzky**   Date: 12-14-11

Sam Marutzky, UGTA Project Manager
Navarro-Intera, LLC

TABLE OF CONTENTS

TABLE OF CONTENTS *(CONTINUED)*

Appendix A - Groundwater Chemistry Results

Appendix B - LLNL Isotopic Analyses: 2009 ER-20-7 Drilling Fluids

Appendix C - LLNL Isotopic Analyses: 2009 ER-20-8#2 Drilling Fluids

Appendix D - LLNL Isotopic Analyses: 2009 ER-EC-11 Drilling Fluids

LIST OF FIGURES

LIST OF FIGURES (CONTINUED)

LIST OF TABLES

LIST OF ACRONYMS AND ABBREVIATIONS

Am	Americium
amsl	Above mean sea level
bgs	Below ground surface
BP	Barometric pressure
Br	Bromide
C	Carbon
°C	Degrees Celsius
Ca	Calcium
$CaCO_3$	Calcium carbonate
CAIP	Corrective action investigation plan
CAU	Corrective action unit
CD-ROM	Compact disc-read only memory
Cl	Chloride
Cm	Curium
CO_3	Carbonate
CS	Carbon steel
Cs	Cesium
D	Deuterium
DO	Dissolved oxygen
DOE	U.S. Department of Energy
DRI	Desert Research Institute
EC	Electrical conductivity
EMRL	Environmental Monitoring Radioanalytical Laboratory
EPA	U.S. Environmental Protection Agency
ER	Environmental restoration
e-tape	Electric tape
Eu	Europium
F	Fluoride
°F	Degrees Fahrenheit
FFACO	*Federal Facility Agreement and Consent Order*
ft	Foot
ft^2/d	Square feet per day
FY	Fiscal year
gal	Gallon

LIST OF ACRONYMS AND ABBREVIATIONS *(CONTINUED)*

gpm	Gallons per minute
GMWL	Global meteoric water line
H	Hydrogen
HCO_3	Bicarbonate
HFM	Hydrostratigraphic framework model
HSU	Hydrostratigraphic unit
I	Iodine
in.	Inch
IT	IT Corporation
K	Potassium
LANL	Los Alamos National Laboratory
LiBr	Lithium bromide
LLNL	Lawrence Livermore National Laboratory
LMWL	Local meteoric water line
m	Meter
mbar	Millibar
MCL	Maximum contaminant level
Mg	Magnesium
mg/L	Milligrams per liter
min/ft^2	Minutes per square foot
mmhos/cm	Millimhos per centimeter
N/A	Not applicable
Na	Sodium
NAD 27	North American Datum 1927
NAD 83	North American Datum 1983
ND	Not detected
NDEP	Nevada Division of Environmental Protection
N-I	Navarro-Intera, LLC
NNES	Navarro Nevada Environmental Services, LLC
NNSA/NSO	U.S. Department of Energy, National Nuclear Security Administration Nevada Site Office
NNSS	Nevada National Security Site
NTS	Nevada Test Site
NTTR	Nevada Test and Training Range
NTU	Nephelometric turbidity unit

LIST OF ACRONYMS AND ABBREVIATIONS *(CONTINUED)*

O	Oxygen
pCi/L	Picocuries per liter
PM	Pahute Mesa
pmc	Percent modern carbon
Pu	Plutonium
PXD	Pressure transducer
RPM	Reservoir performance monitor
S	Sulfur
SDWA	*Safe Drinking Water Act*
SEC	Specific electrical conductivity
SO_4	Sulfate
Sr	Strontium
SS	Stainless steel
SU	Standard unit
Tc	Technetium
TFM	Thermal flowmeter
U	Uranium
UGTA	Underground Test Area
USGS	U.S. Geological Survey
UTM	Universal Transverse Mercator
WDT	Well development and testing
%meq/L	Percent milliequivalents per liter
µg/L	Micrograms per liter
µS/cm	Microsiemens per centimeter

LIST OF STRATIGRAPHIC, GEOLOGIC, HYDROSTRATIGRAPHIC, AND HYDROGEOLOGIC UNIT ABBREVIATIONS AND SYMBOLS

BA	Benham aquifer
BFCU	Bullfrog confining unit
BRA	Belted Range aquifer
CFCM	Crater Flat composite unit
CHCU	Calico Hills confining unit
CHZCM	Calico Hills zeolitic composite unit
CPA	Comb Peak aquifer
DWT	Densely welded ash-flow tuff
FCCU	Fluorspar Canyon confining unit
IA	Inlet aquifer
LPCU	Lower Paintbrush confining unit
MPCU	Middle Paintbrush confining unit
MWT	Moderately welded ash-flow tuff
NTMMSZ	Northern Timber Mountain moat structural zone
NWT	Nonwelded ash-flow tuff
PBRCM	Pre-Belted Range composite unit
PVTA	Paintbrush vitric-tuff aquifer
PWT	Partially welded ash-flow tuff
SCCC	Silent Canyon caldera complex
SPA	Scrugham Peak aquifer
TCA	Tiva Canyon aquifer
TCU	Tuff confining unit
TCVA	Thirsty Canyon volcanic aquifer
Tf	Volcanics of Fortymile Canyon
Tfb	Beatty Wash Formation
THCM	Tannenbaum Hill composite unit
THLFA	Tannenbaum Hill lava-flow aquifer
Thp	Mafic-poor Calico Hills formation
Tm	Timber Mountain Group
TMA	Timber Mountain aquifer
Tmab	Bedded Ammonia Tanks tuff
Tmap	Mafic-poor Ammonia Tanks tuff

LIST OF STRATIGRAPHIC, GEOLOGIC, HYDROSTRATIGRAPHIC, AND HYDROGEOLOGIC UNIT ABBREVIATIONS AND SYMBOLS (CONTINUED)

Tmar	Mafic-rich Ammonia Tanks tuff
Tmat	Rhyolite of Tannenbaum Hill
Tmrf	Rhyolite of Fluorspar Canyon
Tmrp	Mafic-poor Rainier Mesa tuff
Tmrr	Mafic-rich Rainier Mesa tuff
Tp	Paintbrush Group
Tpb	Rhyolite of Benham
Tpc	Tiva Canyon tuff
Tpcm	Pahute Mesa lobe of Tiva Canyon tuff
Tpcyp	Crystal-poor tuff of Pinyon Pass
Tpk	Rhyolite of Comb Peak
Tps	Rhyolite of Scrugham Peak
Tpt	Topopah Spring tuff
Tptm	Pahute Mesa lobe of Topopah Spring tuff
TSA	Topopah Spring aquifer
Ttp	Pahute Mesa tuff
Ttr	Rocket Wash tuff
Ttt	Trail Ridge tuff
UPCU	Upper Paintbrush confining unit
VTA	Vitric-tuff aquifer

1.0 INTRODUCTION

In 2009, the *Phase II Corrective Action Investigation Plan* (CAIP) *for Corrective Action Units 101 and 102: Central and Western Pahute Mesa, Nevada Test Site, Nye County, Nevada* (NNSA/NSO, 2009) was published. This plan describes activities governed by the *Federal Facility Agreement and Consent Order* (FFACO) Underground Test Area (UGTA) strategy (FFACO, 1996; as amended 2010) and forms an essential part of corrective action unit (CAU) compliance overseen by the Nevada Division of Environmental Protection (NDEP). Characterization activities described in this plan were initiated for the U.S. Department of Energy (DOE), National Nuclear Security Administration Nevada Site Office's (NNSA/NSO) UGTA Sub-Project. Wells were drilled at three locations during fiscal year (FY) 2009 and FY 2010: ER-20-7, ER-20-8, and ER-EC-11 (NNSA/NSO, 2010a, 2011a, and 2010b). The closest underground nuclear tests to the area of investigation are TYBO (U-20y), BELMONT (U-20as), MOLBO (U-20ag), and BENHAM (U-20c) (Figure 1-1). The TYBO, MOLBO, and BENHAM tests had working points located below the regional water table. The BELMONT test working point was located just above the water table, and the cavity for this test is calculated to extend below the water table (Pawloski et al., 2002). The broad purpose of these wells is to determine the extent of radionuclide-contaminated groundwater (radiochemistry), the geologic formations, groundwater geochemistry as an indicator of age and origin, and the water-bearing properties and hydraulic conditions that influence radionuclide migration. The area location, wells, underground nuclear tests, and other features are shown in Figure 1-1.

Hydrostratigraphic cross sections A-A', B-B', and C-C' are shown in Figures 1-2, 1-3, and 1-4, respectively.

A striking feature of the area is its structural complexity. Some faulting is due to Basin-and-Range tectonic activity, and some is due to multiple stages of caldera collapse associated with the coalesced Silent Canyon caldera complex (SCCC) (Warren et al., 2000; BN, 2002). The Northern Timber Mountain moat structural zone (NTMMSZ) has between 1,000 and 2,200 feet (ft) of displacement (Figure 1-2), with other major faults having displacement of hundreds of feet
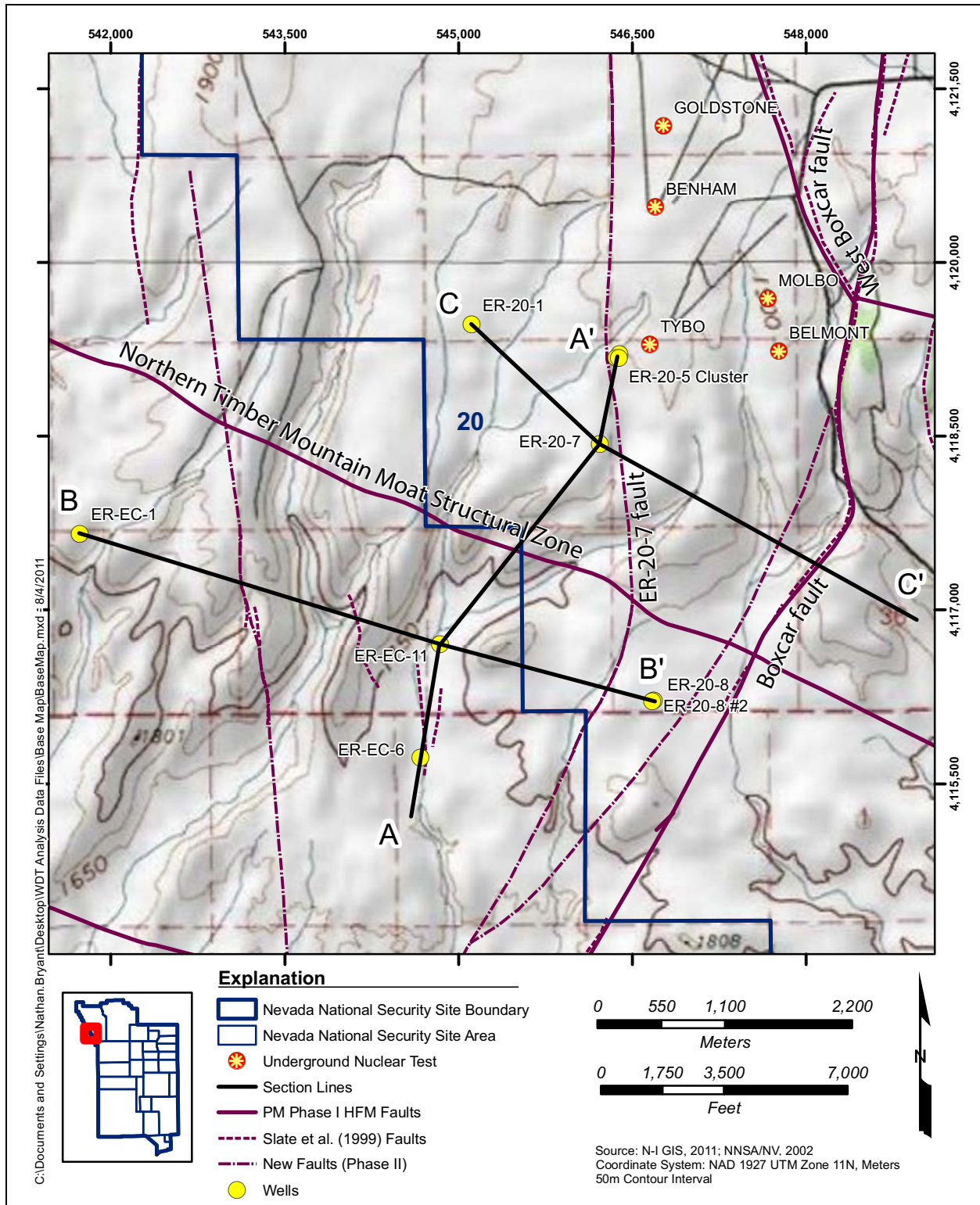
Figure 1-1
Study Area Base Map
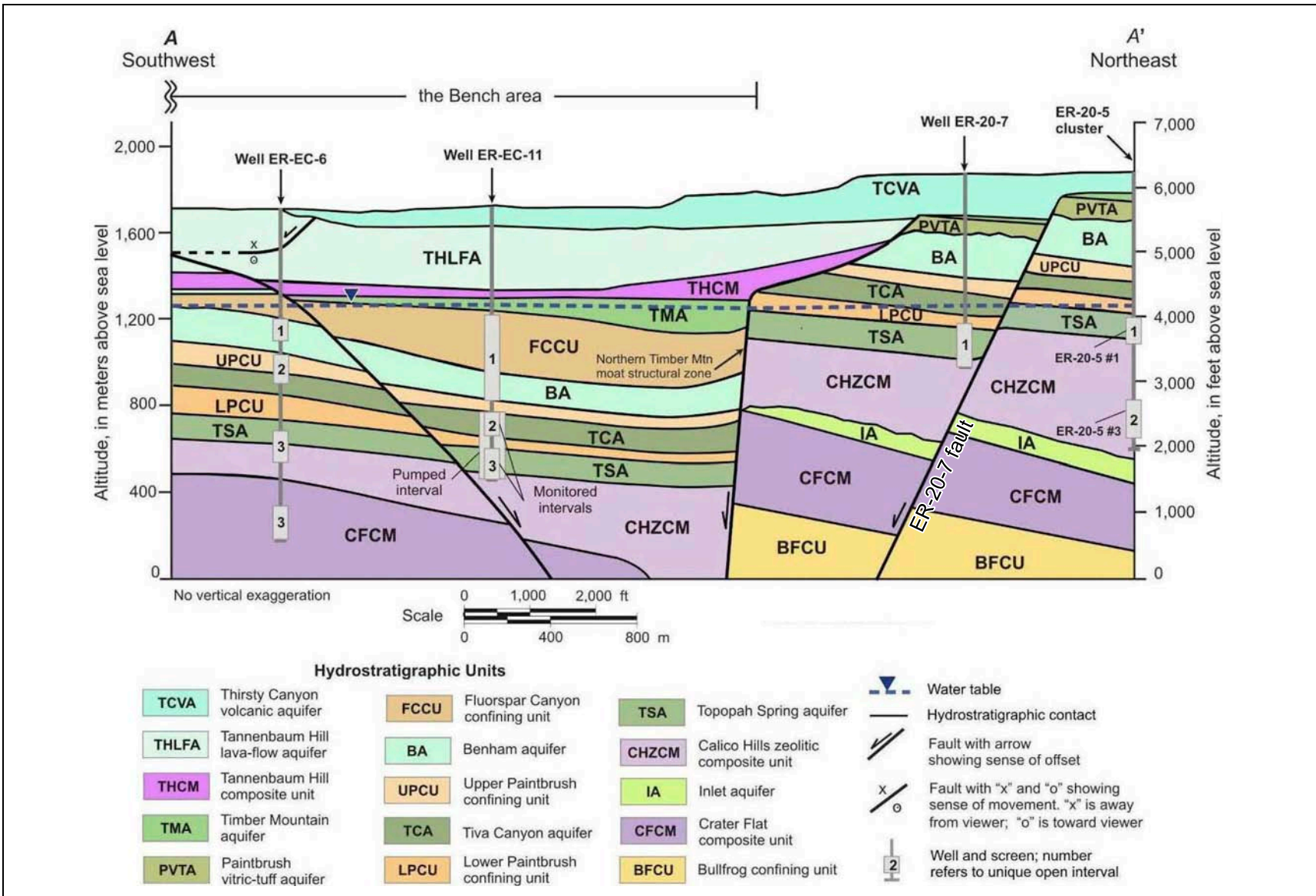
Figure 1-2
Hydrostratigraphic Section A-A', Pahute Mesa
Source: Modified from Halford et al., 2010
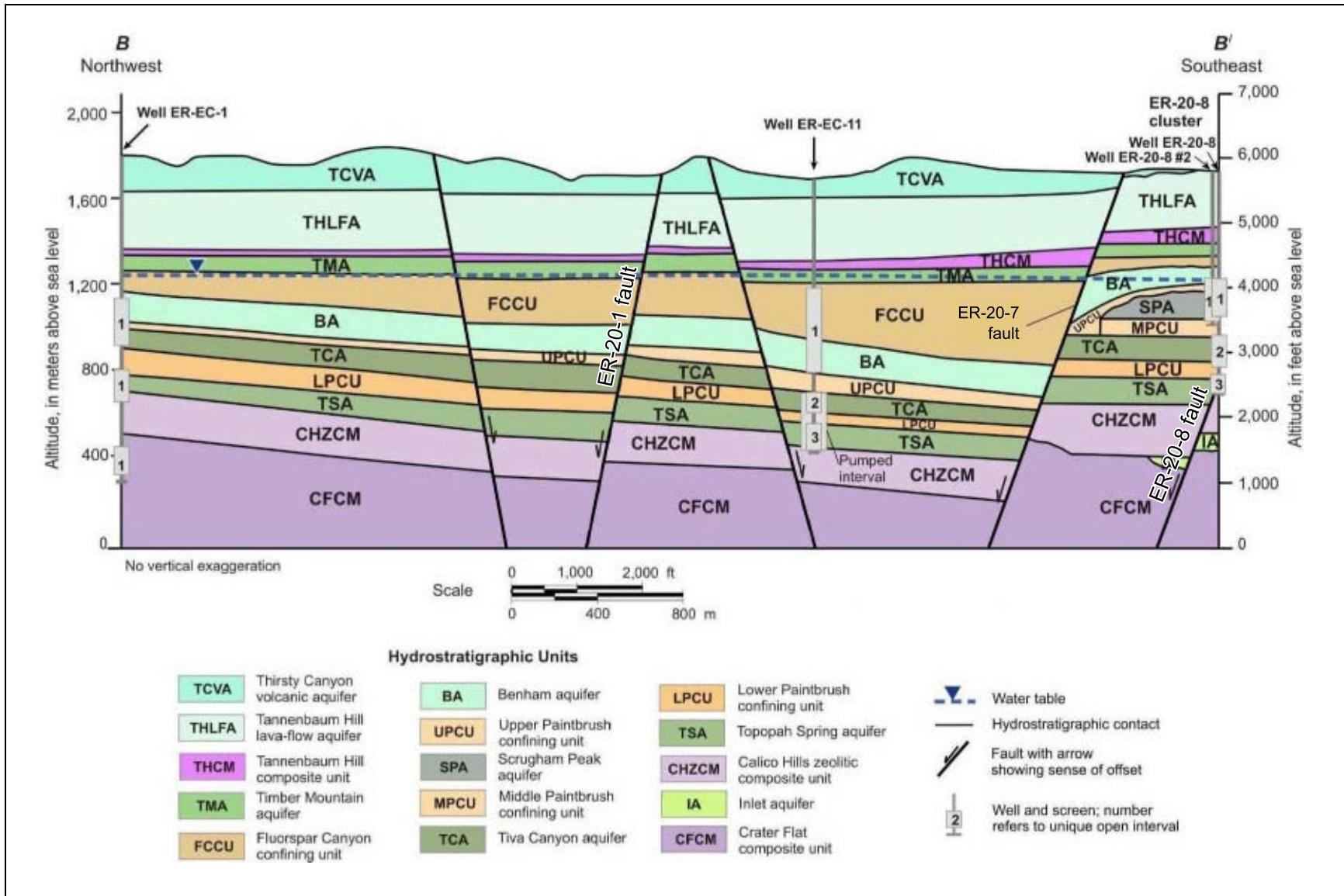
Figure 1-3
Hydrostratigraphic Section B-B', Pahute Mesa
Source: Modified from Halford et al., 2010
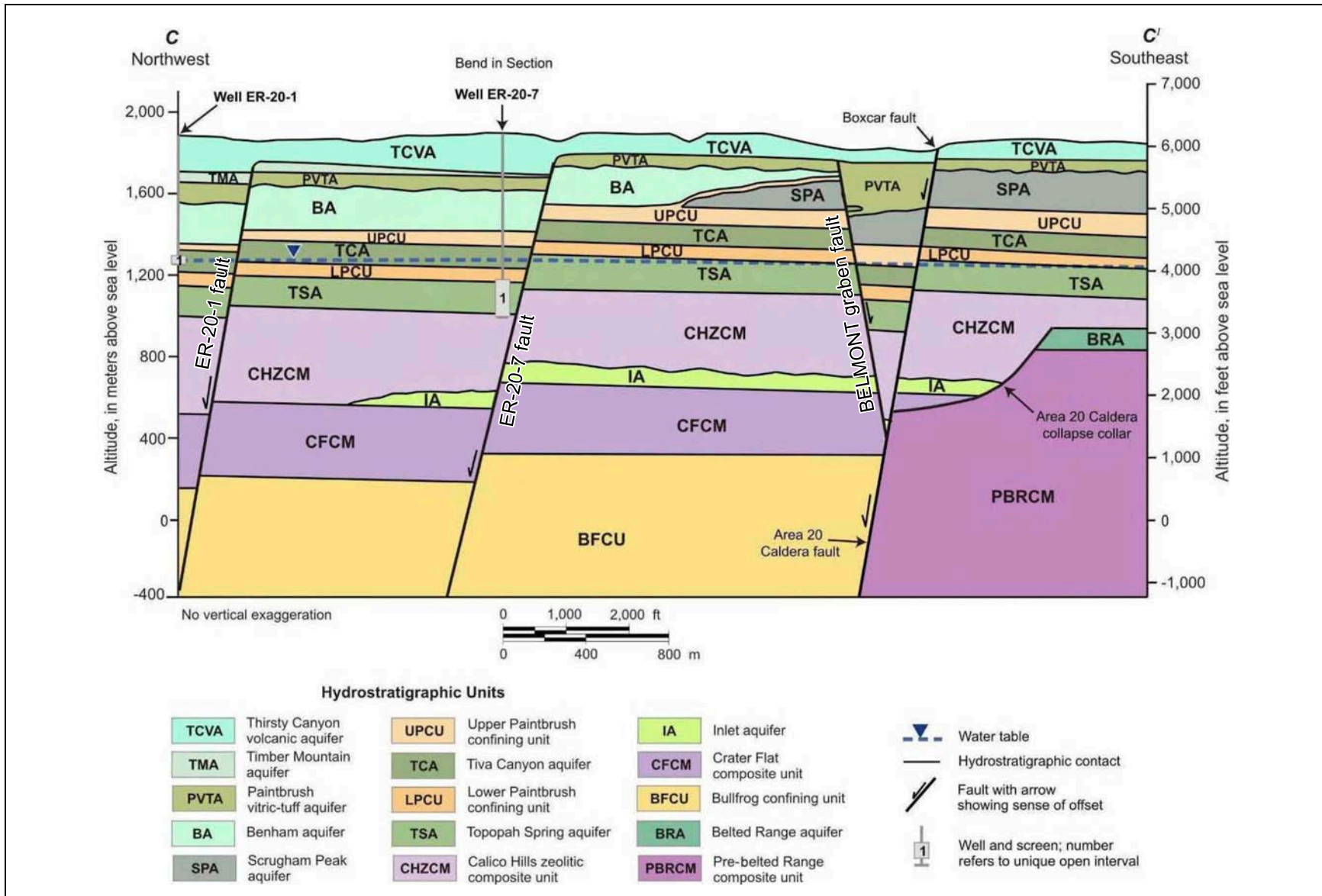
Figure 1-4
Hydrostratigraphic Section C-C', Pahute Mesa
Source: Modified from Halford et al., 2010

(Figures 1-2 through 1-4). Fracture density may increase with proximity to faults; however, the hydrologic properties, if any, of faults themselves in the area are not well known. Limited data suggest that the full spectrum of hydraulic properties, from barrier to conduit, may be possible (Blankennagel and Weir, 1973; Faunt, 1997). In the area of interest, it may be that the major influence of faults is to juxtapose formations creating complex flow paths, as generally suggested by Faunt (1997). The area known as the Bench, on the downthrown side of the NTMMSZ, is of interest because radionuclide-contaminated groundwater has been observed to be migrating through the structure and off the Nevada National Security Site (NNSS), formerly the Nevada Test Site (NTS) (NNSA/NSO, 2010b and 2011a).

Well ER-20-7 (NNSA/NSO, 2010a), located on southern Pahute Mesa in southwest operational Area 20, was drilled and constructed between June 6 and July 7, 2009. Its primary objective was to characterize groundwater contamination downgradient of the TYBO and BENHAM tests—it was found to be contaminated and was completed only in the TSA (Figure 1-5). Well development and testing (WDT) operations occurred between August 30 and October 12, 2010, and are described in the Navarro Nevada Environmental Services, LLC (NNES), report (NNES, 2010b).

The Well ER-20-8 pad is located just south of the southern topographical margin of Pahute Mesa in NNSS operational Area 20. Well ER-20-8 #2 (NNSA/NSO, 2010b and 2011a) is located on the Well ER-20-8 pad in the southwestern portion of Area 20. Well ER-20-8 #2 was the second well constructed at the Well ER-20-8 site but the first tested. Drilling and construction of Well ER-20-8 #2 occurred between August 22 and September 2, 2009, and was completed in the Scrugham Peak aquifer (SPA) and the lower portion of the overlying Benham aquifer (BA) (Figure 1-6). Well development and testing operations occurred at ER-20-8 #2 between November 16 and December 18, 2009, and are described in NNES (2010c).

Well ER-EC-11 is located just south of the southern topographical margin of Pahute Mesa on the Nevada Test and Training Range (NTTR), approximately 716 meters (m) (2,350 ft) south of the southwestern NNSS boundary. Well ER-EC-11 was drilled and constructed between September 13 and October 22, 2009 (Figure 1-7). Well development and testing operations occurred between April 29 and May 19, 2010, and are described in NNES (2010d).
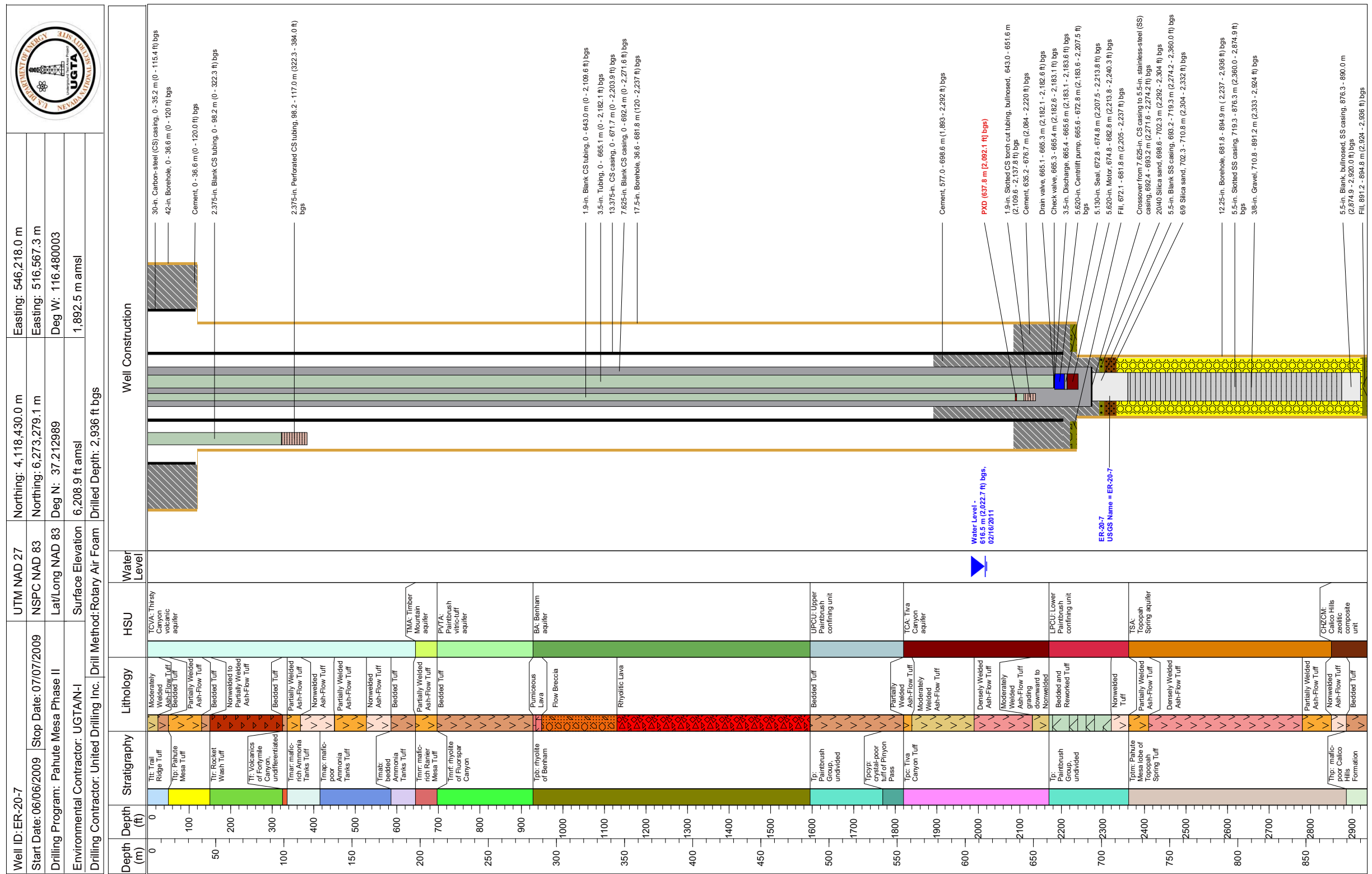
Figure 1-5
ER-20-7 Well Configuration and Geology
Source: Modified from N-I, 2010a; NNSA/NSO, 2010a
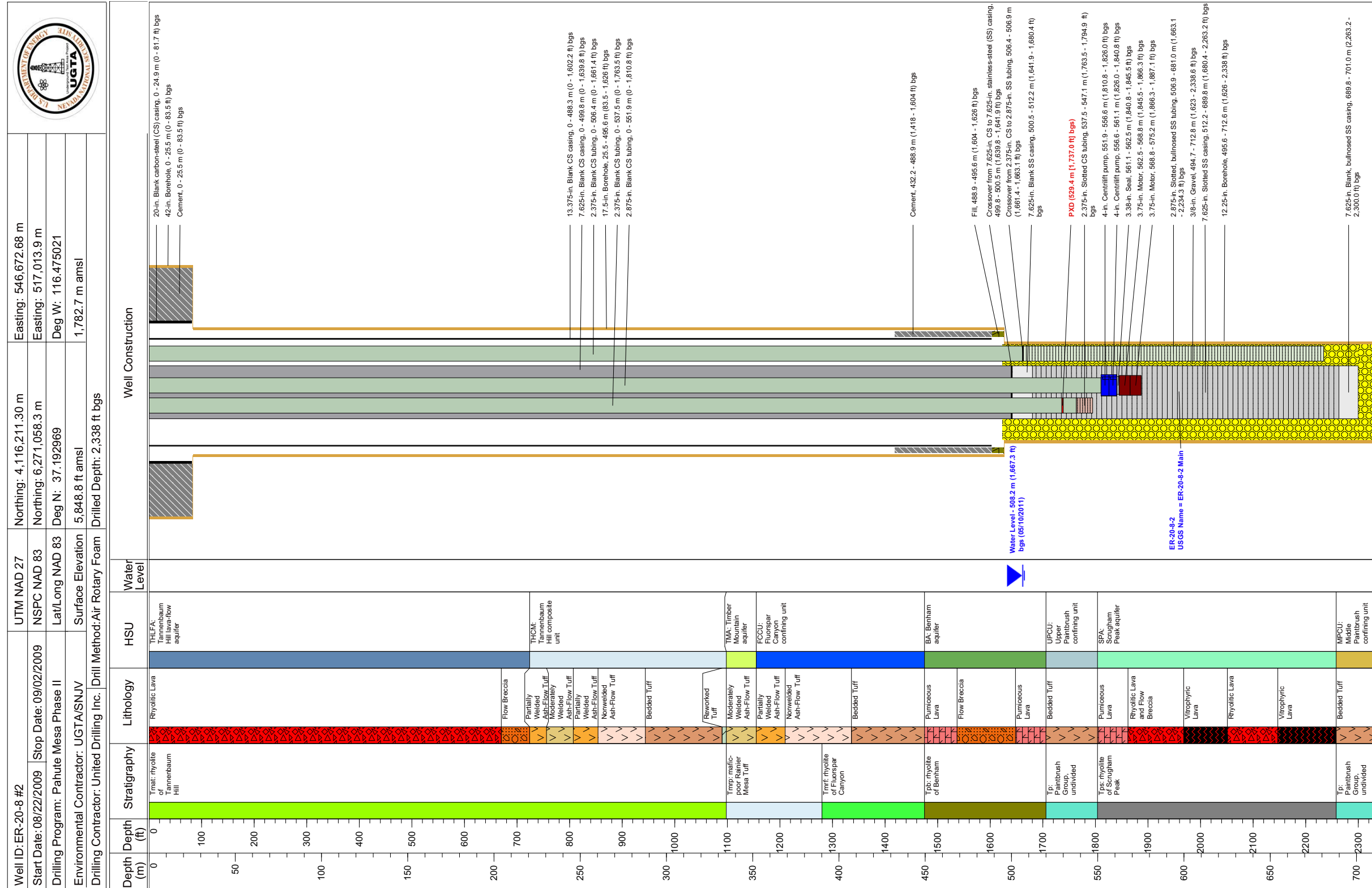
Figure 1-6
ER-20-8 #2 Well Configuration and Geology
Source: Modified from N-I, 2010b; NNSA/NSO, 2011a
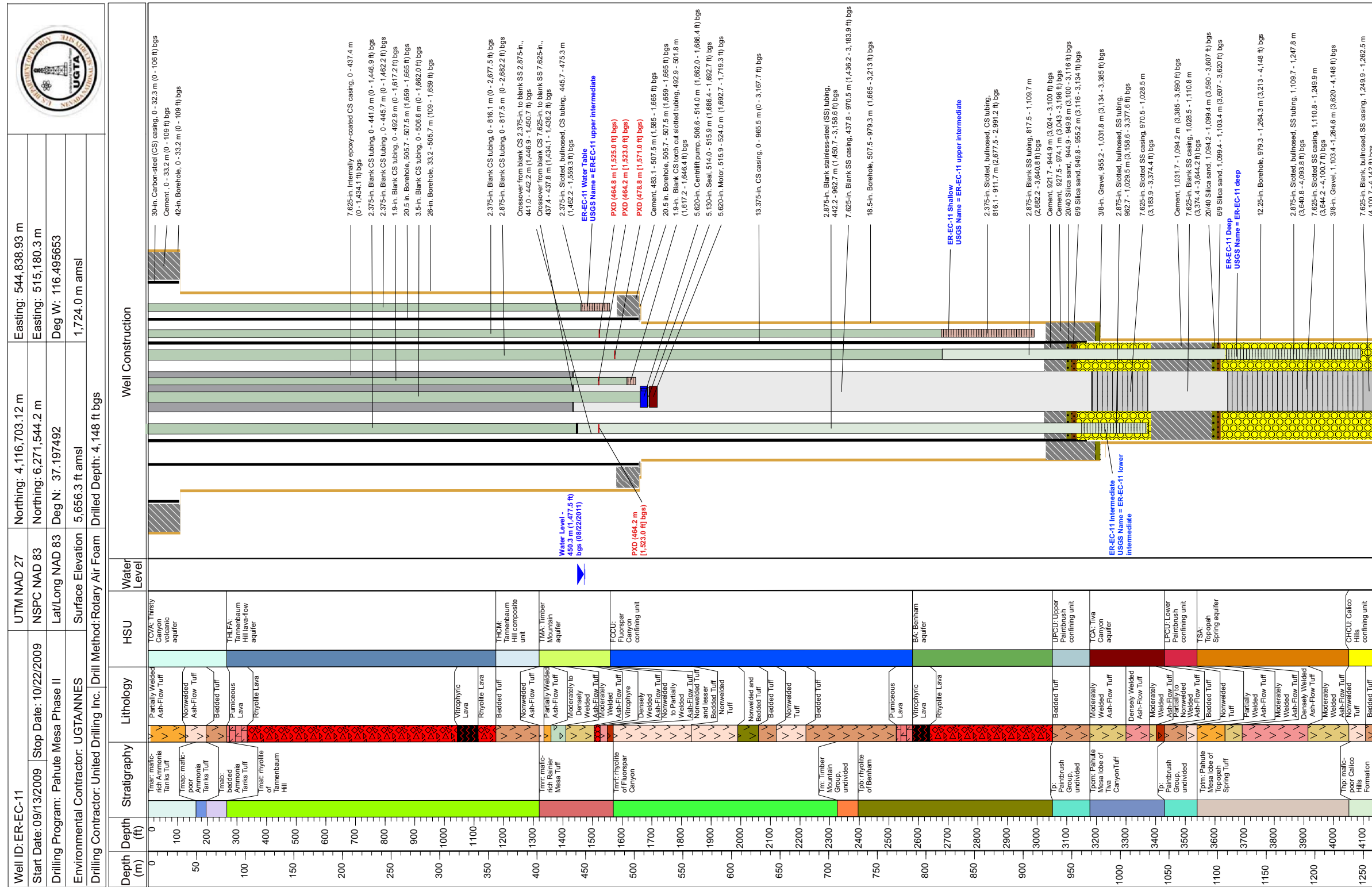
Figure 1-7
ER-EC-11 Well Configuration and Geology
Source: Modified from N-I, 2010c; NNSA/NSO, 2010b

This report analyzes the following data collected from ER-20-7, ER-20-8 #2, and ER-EC-11 during WDT operations:

- Chemical indicators of well development (Section 2.0)
- Static hydraulic head (Section 3.0)
- Radiochemistry and geochemistry (Section 4.0)
- Drawdown observed at locations distal to the pumping well (Section 5.0)
- Drilling water production, flow logs, and temperature logs (Section 6.0)

The new data are further considered with respect to existing data as to how they enhance or change interpretations of groundwater flow and transport, and an interim small-scale conceptual model is also developed and compared to Phase I concepts.

2.0   WELL DEVELOPMENT

The purpose of well development is to remove drilling fluids and drilling-associated fines from the formation adjacent to a well so samples reflecting ambient groundwater water quality can be collected, and to restore hydraulic properties near the well bore. Drilling fluids can contaminate environmental samples from the well, resulting in nonrepresentative measurements. Both drilling fluids and preexisting fines in the formation adjacent to the well can impede the flow of water from the formation to the well, creating artifacts in hydraulic response data measured in the well.

Well development can be monitored by measuring several water-quality indicators during pumping. Dissolved oxygen (DO), pH, turbidity (nephelometric turbidity unit [NTU]), and specific conductivity (SEC) stabilize as fluid introduced during drilling is removed (EPA, 2001). This stabilization is an indication that water produced from the well is representative of the formation.

Wells drilled for UGTA are drilled with an air-foam/polymer drilling fluid. Drilling fluids in UGTA wells are tagged with lithium bromide (LiBr) in order to estimate groundwater production during drilling, and to aid in determining well development (N-I, 2010a, b, and c). Bromide (Br) is typically found in low concentrations in NNSS groundwater, so the tagging allows removal of drilling fluid to be monitored. Bromide levels in non-environmental restoration (ER) wells in Table A.1-4 of Appendix A are variable but generally indicate concentrations ≤ 0.1 milligrams per liter (mg/L) in Area 20 wells. Bromide concentration in the drilling fluid varies with the amount of groundwater inflow but is generally 30 to 100 mg/L for the injected fluid. Detailed logs of the concentrations in the injected fluid and the discharge during drilling can be found in the drilling data report for each well (e.g., NNES, 2010b, c, and d).

Bromide concentrations are also monitored during WDT to gauge the removal of drilling fluid. Grab samples are collected every two hours (or as needed) from the discharge line while personnel are on site. The Br concentration is measured with a HORIBA F-53 meter equipped with an 8005-10C Br$^-$ electrode. The measurement range of the 8005-10C electrode is 0.8 to 80,000 mg/L

(HORIBA, 2003). During WDT, the instrument is calibrated daily at 0.5, 1, and 5 mg/L. Readings below the measurement range for the Br$^-$ electrode do not follow Nernst's equation (HORIBA, 2003), so it is difficult to make solid conclusions based on such measurements. However, the nature of the measurements below the measurement range is such that lower readings are indicative of lower concentrations when the instrument is calibrated in the same manner.

The cement slurry used to fix casing in the well and isolate completion intervals is alkaline and, in most groundwater, this slurry raises the pH of fluid it mixes with before it cures. As the well is cleaned out during development, residual cement-tainted fluids will be removed, and pH from produced water should stabilize to a representative level for the water in the formation.

Turbidity is an indication of fines suspended in the water, and the trend and absolute values of turbidity indicate whether fines are still being removed from the well. As drilling fluid and sediment are removed from the well, clarity improves and turbidity drops. Wells tend to show spikes in turbidity when the pump is turned on initially. The U.S. Environmental Protection Agency (EPA) standard operating procedure for well development recommends that wells be developed until the water has a turbidity of less than 50 NTU (EPA, 2001).

The SEC is a measure of the capacity of water produced from the well to conduct an electrical current. Electrical conductance of water is a function of the types and quantities of dissolved substances in water, but there is no universal linear relation between total dissolved substances and conductivity (USGS, 2011).

To frame the discussion of well development in the new wells, it is useful to look at water-quality samples from a previously developed well. Well ER-EC-6 was drilled and developed as part of Phase I Pahute Mesa activities. For WDT, 1.7 million gallons (gal) of water were produced from the well between January 14 and February 11, 2000 (IT, 2000b). Observations from thermal flow logging in 2000 indicate 0.58 gal per minute (gpm) downward flow within the upper flow completion under static conditions. This flow could allow as much as 2.7 million gal to flow through the well over the nine years the well was open, although this estimate should be treated as an upper bound because the gradient between the sections of the well—and, therefore, the flow—will decrease with time.

Well ER-EC-6 was pumped from April 7 to April 12, 2009, so georadiochemistry samples could be obtained (SNJV, 2009). Water-quality parameter monitoring data from the 2009 sampling are provided in Table 2-1 and Figure 2-1 to allow comparison of the new wells to a previously developed well.

Table 2-1
Well ER-EC-6 Grab Sample Summary Statistics (April 8 to April 12, 2009)

	pH	EC (mmhos/cm)	DO (mg/L)	Turbidity (NTU)	Br (mg/L)
Average	8.04	0.54	3.48	2.62	0.91
Standard Deviation	0.32	0.08	0.36	4.51	0.44

EC = Electrical conductivity
mmhos/cm = Millimhos per centimeter

2.1 Well ER-20-7

Well development and testing operations for ER-20-7 produced a total of 2.4 million gal of water from September 14 to September 24, 2010. Of this total, 1.1 million gal were produced during the formal development operations (September 14 to September 17, 2010). Figure 2-2 shows production rates and water-quality measurements for the WDT period. The time of geochemical and radiochemical sampling (further described in Section 4.0) is also shown.

There are no Br measurements available for ER-20-7 from the first day of production. Measurements of Br concentration in grab samples on September 15, 2010, average 2.45 mg/L with a standard deviation of 3.42 mg/L. After September 15, 2010, measurements average 0.27 mg/L with a standard deviation of 0.09 mg/L. Bromide concentration clearly drops at the start of development and remains well below the measurement range thereafter. The final Br concentration is lower than the concentrations in the other wells discussed in this report.

Overall, there is little change in the pH measurements of grab samples from ER-20-7 over the course of pumping. There is a statistically significant difference in the mean populations of pH measurements during the first two days of development (September 14 and September 15, 2010) and the remainder of development (September 16 to September 24, 2010). The mean pH during the first two days is 8.23 with a standard deviation of 0.16. The mean pH for the rest of testing is 7.44 with a
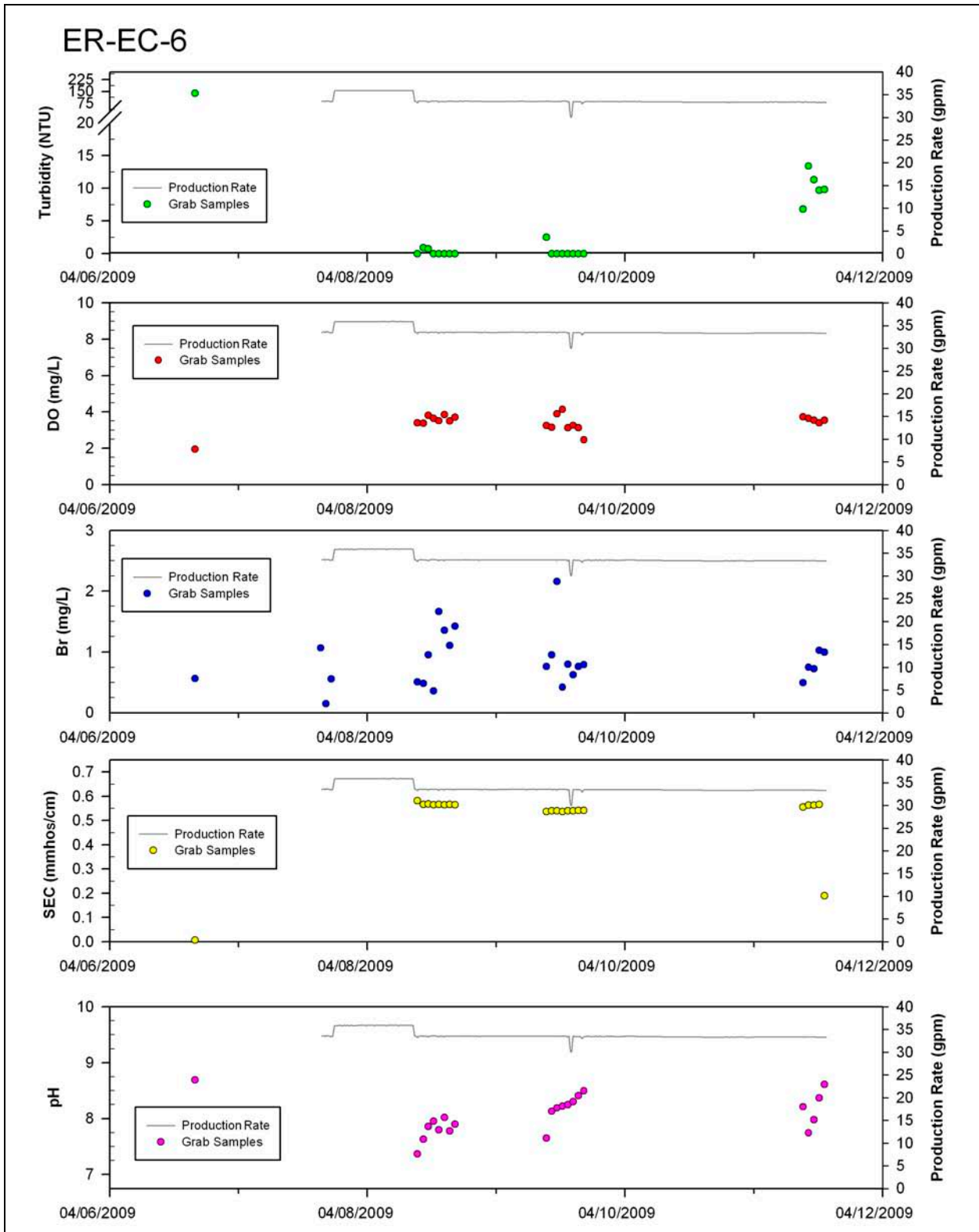
Figure 2-1
Well ER-EC-6 Water-Quality Monitoring Values
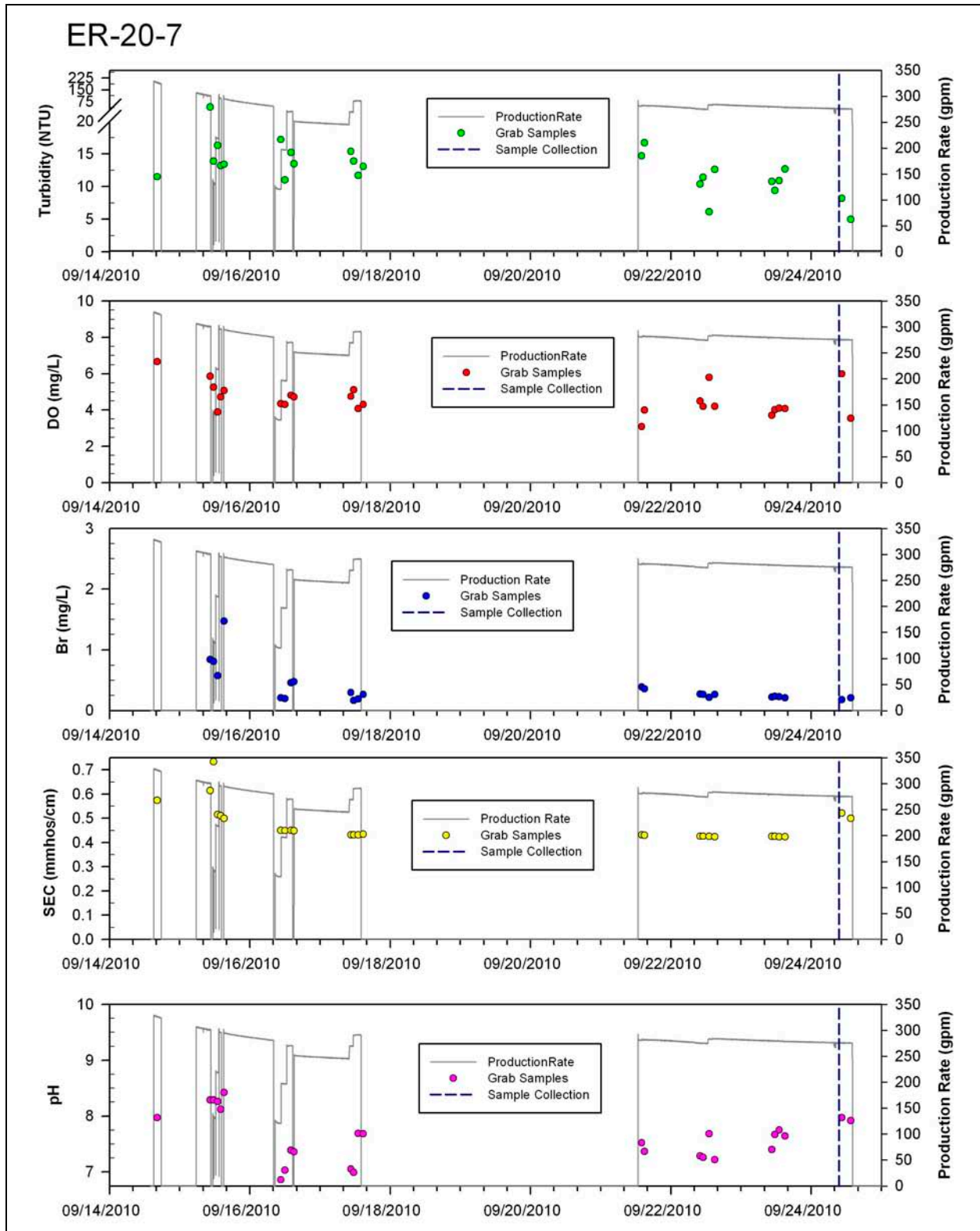
Figure 2-2
Well ER-20-7 Water-Quality Monitoring Values

standard deviation of 0.31. This difference is likely caused by the removal of drilling fluids including residuals from cement slurry.

There is a lot of variability in the turbidity measurements from the grab samples. On September 15, 2010, there is a single measurement of 40 NTU. After this measurement, the average turbidity measurement is 12.4 NTU with a standard deviation of 3.1 NTU. There is a slightly downward slope to a linear trend fit through the measurements data; however, the scatter makes this trend uncertain. While the turbidity in this well is higher than the others discussed in this report, it is still well below the EPA recommended values.

During the first two days of production, the SEC of samples from the well was slightly elevated and much more variable than the remainder of operations. The average SEC measurement of samples collected on September 14 and September 15, 2010, is 0.57 mmhos/cm, and the standard deviation is 0.09 mmhos/cm. The average measurement of samples collected after this period is 0.44 mmhos/cm with standard deviation of 0.03 mmhos/cm. Some variability in specific conductivity is expected in Pahute Mesa groundwater, and the variability in measurements compares favorably to ER-EC-6.

2.2   Well ER-20-8 #2

Well development and testing operations for ER-20-8 #2 produced a total of 1.9 million gal of water from November 28 to December 18, 2009. Of this total, 0.8 million gal were produced during the formal development operations (November 28 to December 3, 2009). Figure 2-3 shows production rates and water-quality measurements for the WDT period. The time of geochemical and radiochemical sampling (further described in Section 4.0) is also shown.

There is a single high Br measurement of 76.4 mg/L on the first day of well development but no discernible trend after this. The average Br concentration measured after the first day of development is 0.77 mg/L with a standard deviation of 0.47 mg/L. These measurements hover around the lower range of measurement for the Br⁻ electrode, so there is evidence of some residual Br in the well. As with ER-EC-11, the final Br concentration is much lower than the concentrations found in drilling fluids.
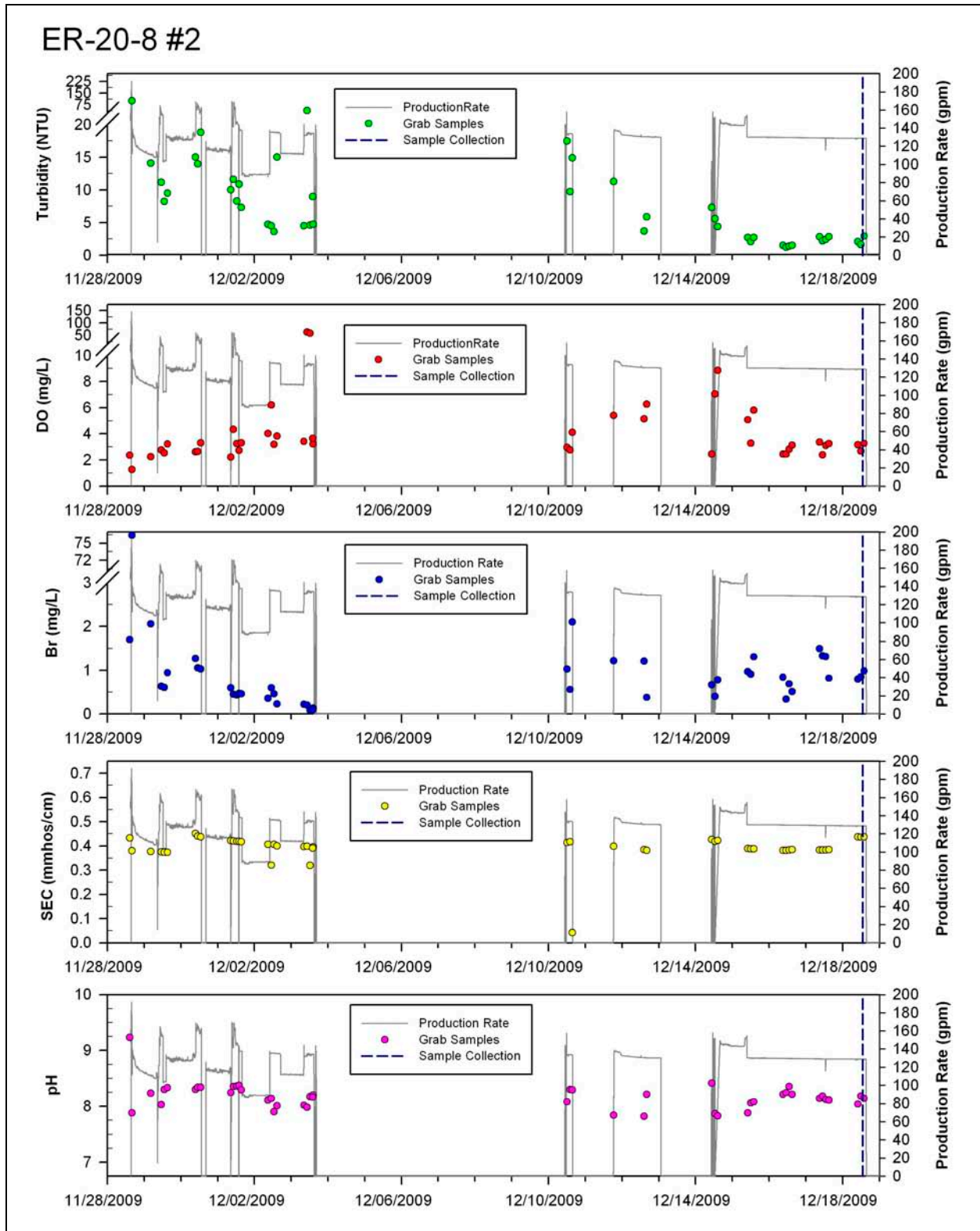
Figure 2-3
Well ER-20-8 #2 Water-Quality Monitoring Values

The pH measurement of a single grab sample during the first day of production (November 28, 2010) is 9.23. After this first measurement, the pH averages 8.15 with a standard deviation of 0.16. There is no significant trend in the pH measurements after the first day. The average pH is higher than ER-EC-6, but some variation is expected between wells. The standard deviation of the ER-20-8 #2 measurements is less than the ER-EC-6 measurements.

There is a lot of variability in the turbidity measurements from the well. There is a single turbidity measurement of 101 NTU during the first day of production. Excluding the first day, the average turbidity measurement is 7.68 NTU with a standard deviation of 6.83 NTU. No definitive trend can be assigned, given the scatter in the measurement. The range of measured turbidity near the end of the constant rate test agrees favorably with measurements from ER-EC-6 and is well below the recommended criteria specified by the EPA (2001).

Specific conductivity stays steady for most of the development period. The average SEC measurement of the all the grab samples is 0.40 mmhos/cm, and the standard deviation of the population is 0.028 mmhos/cm. Some variability in specific conductivity is expected in Pahute Mesa groundwater, and the variability in measurements compares favorably to ER-EC-6.

2.3   Well ER-EC-11

Well development and testing operations for ER-EC-11 produced a total of 5.6 million gal of water from April 29 to May 20, 2010. Of this total, 1.8 million gal were produced during the formal development of operations (April 29 to May 4, 2010). Figure 2-4 shows production rates and water-quality measurements for the WDT period. The time of geochemical and radiochemical sampling (further described in Section 4.0) is also shown.

There is a clear drop in the Br levels comparing first and second days of development, but no discernible trend after this. Bromide levels drop from 4 to 18 mg/L on the first day of development to an average of 0.79 mg/L, with a standard deviation of 0.58 mg/L for the rest of development and testing. Although many of these measurements are below the measurement range of the Br⁻ electrode used to measure them, there are occasional measurements within the range, indicating the Br level is close to the detection limit. However, the final concentration of Br is less than 3 percent of the initial concentration, indicating that the majority of the Br has been removed. The average Br concentration
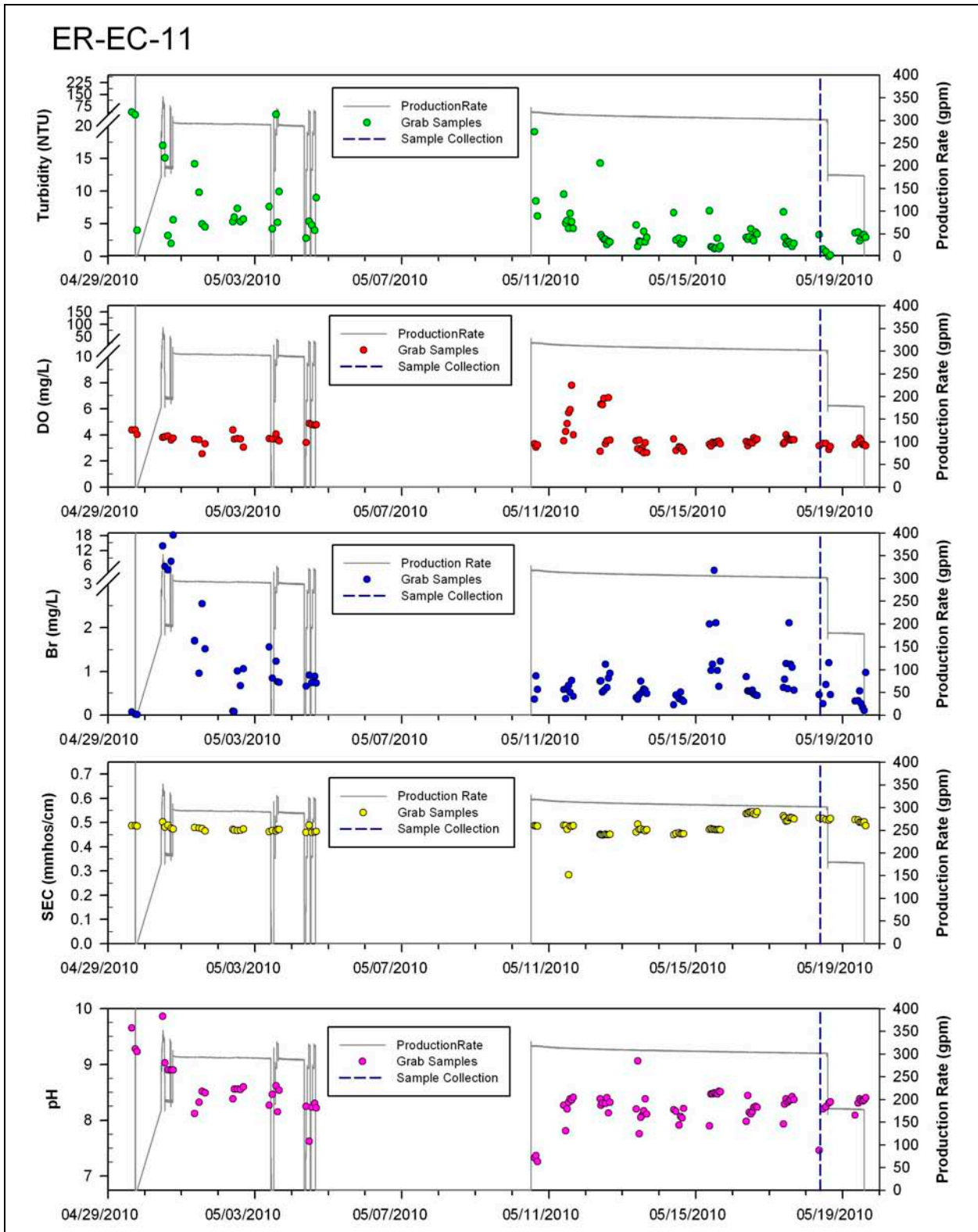
Figure 2-4
Well ER-EC-11 Water-Quality Monitoring Values

after the first day in ER-EC-11 is also below the average concentration for Phase II sampling in ER-EC-6.

The pH measurements of grab samples during the first two days of production range from 8.90 to 9.86. After the first day, the pH averages 8.24 with a standard deviation of 0.29. There is no significant trend in the pH measurements after the first day. The average pH is higher than ER-EC-6, but some variation is expected between wells. The standard deviation of the ER-EC-11 measurements is less than the ER-EC-6 measurements.

There is a lot of variability in the turbidity measurements from the well. Samples measured on or before April 30, 2010, vary from 2.0 to 37.8 NTU. A linear trend fitted to the measurements during the constant rate test shows a decrease with time, but there is a lot of scatter. The range of measured turbidity near the end of the constant rate test agrees favorably with measurements from ER-EC-6 and is well below the recommended criteria specified by the EPA (2001).

Specific conductivity stays steady for most of the development period. There is a small jump between May 15 and May 16, 2010, but it is difficult to determine what caused this difference. The average SEC measurement of all the grab samples is 0.48 mmhos/cm, and the standard deviation of the population is 0.033 mmhos/cm. Some variability in specific conductivity is expected in Pahute Mesa groundwater, and the variability in measurements compares favorably to ER-EC-6.

2.4   Conclusion

Wells ER-20-7, ER-20-8 #2, and ER-EC-11 have all been successfully developed. In general, the variations in the water-quality parameters monitored in the three wells compare favorably with those measured in ER-EC-6 during supplementary Phase II sampling. All three wells had elevated Br concentrations during the first few days of pumping that leveled off to a steady-state tail. The steady-state tail is higher than the expected natural concentration; however, Br is a spiked constituent of the drilling fluid, and the residual concentrations are much lower than the initial concentrations in the drilling fluid. The specific conductivity and pH show some measurement variation, but there were no definitive trends after the first several days of pumping, which indicates the residual fluids from drilling no longer have a large effect on the chemistry of water produced from the well. Radiochemistry and geochemistry samples collected near the end of pumping are representative of *in situ* conditions in the formation.

3.0 STATIC HEAD

Static head data from wells provide information about potentiometric gradients and groundwater flow. Fenelon et al. (2010) conducted a broad study of wells across the NNSS that covers the area surrounding ER-20-7, ER-20-8 #2, and ER-EC-11. The contours developed and locations of data used in Fenelon et al. (2010) are shown in Figure 3-1. These contours provide a good overview of the general direction of flow that is consistent with the interpretations of radionuclide transport data in the vicinity of southwest Area 20.

To better understand smaller-scale variations and the degree that the data support interpretations of local flow direction and the potentiometric gradient, the data and interpretation from Fenelon et al. (2010) have been combined with new water levels acquired during Pahute Mesa Phase II characterization operations (ER-20-7, ER-20-8 #2, and ER-EC-11) and the detailed geologic model. Table 3-1 shows the wells, water levels, and hydrostratigraphic units (HSUs) discussed in this section. The complexity of the geology makes it difficult to develop a clear picture of smaller-scale phenomena; however, a discussion of the data with respect to flow directions and the geologic framework is still instructive, particularly in understanding the effects of the many faults and structures in the area.

Figure 3-2 shows water levels that have been separated out by aquifer HSU as defined by Bechtel Nevada (BN) (2002) in the Phase I hydrostratigraphic framework model (HFM) along with contours from Fenelon et al. (2010). Well ER-EC-1 was not considered because all the completions are open, and assigning the water level to a particular HSU is ambiguous. As Figure 3-2 shows, water levels can vary between aquifer units at the same well. The clearest instance of this is in U-20y. The average of water levels in the TCA in U-20y is 1,340.8 m above mean sea level (amsl), while those in the deeper TSA in the same well are 1,277.1 m amsl. The TCA and TSA are separated by a 60-m section of the LPCU composed of zeolitized tuffs. In this case, it is likely that the well samples an isolated portion of the TCA and the higher water level is caused by local recharge, held above a larger flow system by the limited permeability of the LPCU. Fenelon et al. (2010) calls these water levels perched or semiperched.
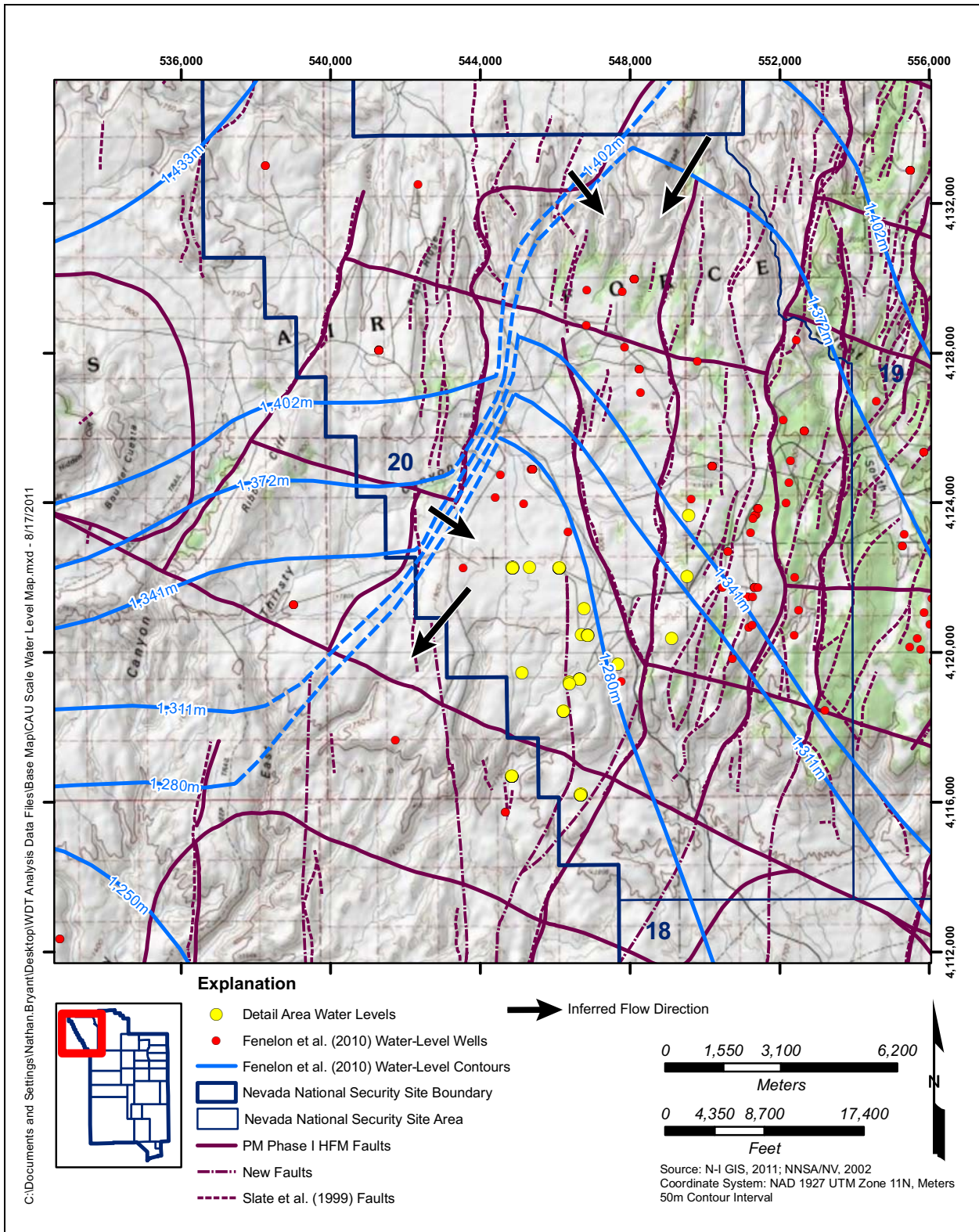
Figure 3-1
Southwest Area 20 and Vicinity Water-Level Contours

Table 3-1
Water Levels with Intersected Aquifer HSUs

Well Name	Water Level (m amsl)	HSU	Source
ER-20-1	1,277.7	TCA	Fenelon et al., 2010
ER-20-5-1	1,276.5	TSA	Fenelon et al., 2010
U-20ag	1,285.6	BA	Fenelon et al., 2010
U-20ak	1,278.3	BA	Fenelon et al., 2010
U-20ao	1,317.7	BA	Fenelon et al., 2010 [a]
U-20ax	1,329.8	CHZCM	Fenelon et al., 2010 [a]
U-20ay	1,360.9	CHZCM	Fenelon et al., 2010
U-20bb	<1,272.8	BA	Fenelon et al., 2010
U-20bb 1	1,279.6	BA	Fenelon et al., 2010
U-20bf	≥1,339.0	CHZCM	Fenelon et al., 2010
U-20c	1,273.5	CHZCM	Fenelon et al., 2010
U-20y	1,340.8	TCA	Fenelon et al., 2010 [a]
U-20y	1,277.1	TSA	Fenelon et al., 2010
UE-20c	≥1,266.7	TCA, TSA	Fenelon et al., 2010
UE-20d	1,273.8	TSA	Fenelon et al., 2010
UE-20d	1,272.5	TCA	Fenelon et al., 2010
UE-20d	≤1,295.4	CHZCM	Fenelon et al., 2010 [a]
ER-20-7	1,276.0	TSA	N-I, 2011b
ER-20-8 Deep	1,274.6	TSA	N-I, 2011b
ER-20-8 Intermediate	1,274.7	TCA	N-I, 2011b
ER-20-8-2	1,274.5	BA	N-I, 2011b
ER-EC-11 Deep (Tptm)	1,274.2	TSA	N-I, 2011b
ER-EC-11 Intermediate (Tpcm)	1,274.0	TCA	N-I, 2011b
ER-EC-11 Main	1,274.1	TCA, TSA	N-I, 2011b
ER-EC-11 Shallow (Tpb)	1,273.9	BA	N-I, 2011b
ER-20-5-3	1,275.4	CHZCM	N-I, 2011b

[a] Water level marked as "anomalously high" in Fenelon et al. (2010). Not used in contouring.
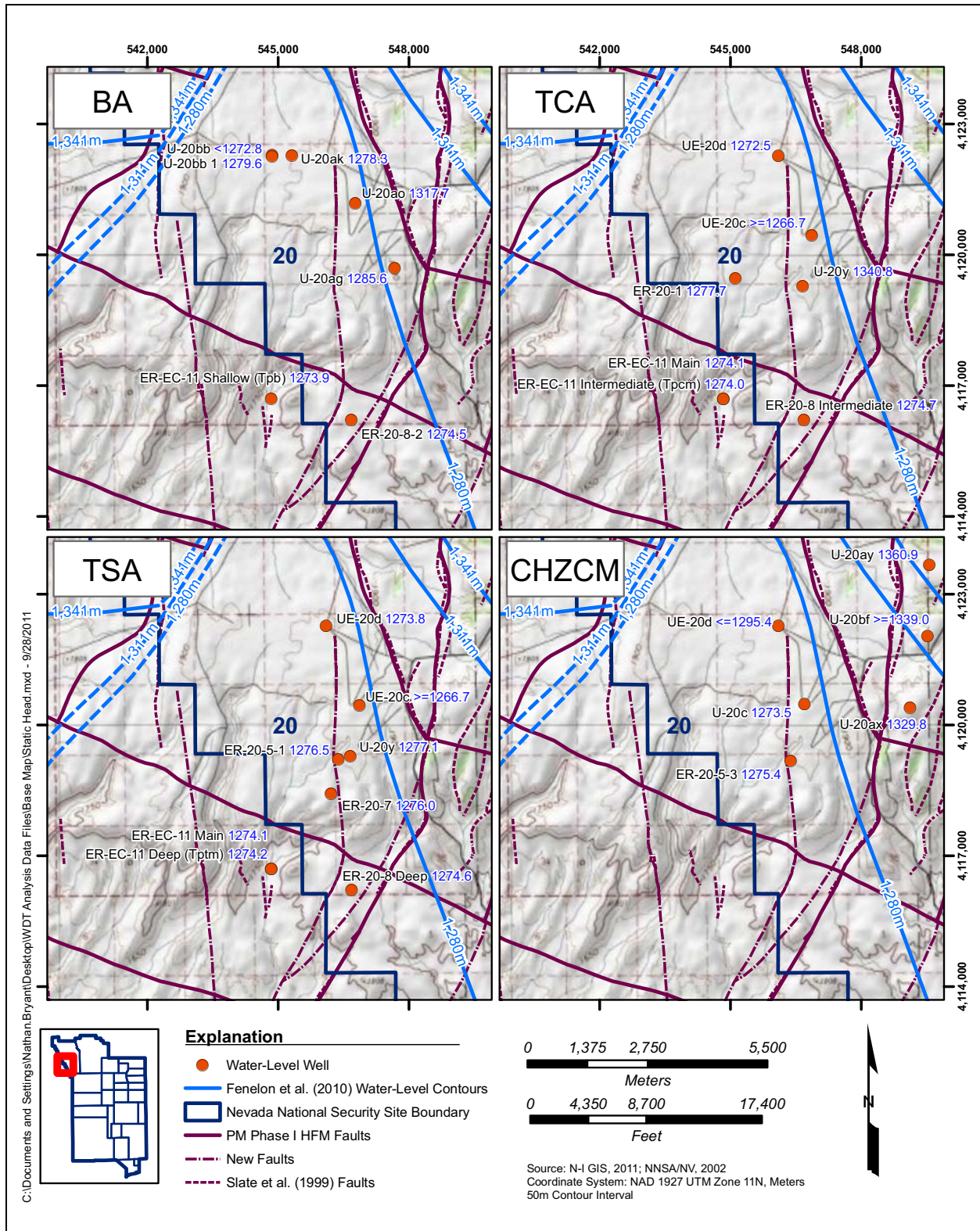
Figure 3-2
Water Levels by Aquifer

With the exceptions of U-20ao and U-20ag, there is only a modest amount of variation in the water levels of wells completed in the BA in southwestern Pahute Mesa. Both U-20ao and U-20ag are close to the West Boxcar fault. The elevated water levels in the two wells reflect the higher water levels found in the CHZCM wells across the fault. The range of water levels in the rest of the BA wells is 1,272.8 to 1,279.6 m. This entire range is expressed in two different wells (U-20bb and U-20bb 1, respectively) that are very close to each other, illustrating the amount of noise in the water-level data. Across the NTMMSZ, water levels in ER-EC-11 and ER-20-8 #2 differ by only 0.5 m.

There are several anomalous water levels in wells in the TCA. The water level in the TCA/TSA in UE-20c is only 1,266.8 m amsl. The water level is the last measurement in a recovery test that recovered about 15 m in 1 hour 40 minutes. The recovery rate over the last 40 minutes is 2 m per hour, so it appears the last water level is within a few meters of recovery. It is difficult to reconcile this water-level measurement with the surrounding wells. The measurement is a local minimum at a point where there is no known discharge sink. The water level in U-20y is anomalously high compared to the surrounding wells. There is only a 13-m column of water at the bottom of the TCA above a section of zeolitized tuff in the well. This water is likely local recharge retarded by the zeolitized tuff. There is only a modest difference (about 3 m) between ER-EC-11 and ER-20-8 #2 and the wells on the other side of the NTMMSZ. Across the NTMMSZ, water levels in ER-EC-11 and ER-20-8 #2 differ by only 0.6 m in the TCA.

There is little variation in the water levels in the TSA in southwestern Pahute Mesa. Excluding the anomalously low level in the TCA/TSA in UE-20c, the range is 1,273.8 to 1,277.1 m expressed in UE-20d and U-20y, respectively. Across the NTMMSZ, water levels in ER-EC-11 and ER-20-8 differ by only 0.4 m. These levels are noticeably lower than the three closest wells in the TSA north of the NTMMSZ. It is difficult to say if this is more than coincidence due to the amount of unexplained variance in the water-level measurements.

In the CHZCM east of the Boxcar fault, three wells (U-20ay, U-20bf, and U-20ax) have water levels of 1,360.9, 1,339.0, and 1,329.8 m, respectively. Well U-20ay is completed in the upper LFA portion of the HSU and should be representative of an extended portion of the aquifer. Wells U-20bf and U-20ax are both completed in zeolitized tuffs below the upper LFA and may be less representative. Across the Boxcar and West Boxcar faults, water levels in the CHZCM are significantly lower.

Over southwest Area 20, a large number of wells have water levels between 1,271.5 and 1,279.5 m. This supports the current (Fenelon et al., 2010) and past (DOE/NV, 1997; O'Hagan and Laczniak, 1996; Blankennagel and Weir, 1973) characterization of southwest Area 20 as a flatter valley in the potentiometric surface. New characterization data do not suggest that an abrupt change in this interpretation is necessary (at least for the BA/SPA, TCA, and TSA), even with the NTMMSZ present in a configuration most likely to make the effects of the fault detectable (Faunt, 1997). The presence of tritiated groundwater at ER-20-7, ER-20-8 #2, and ER-EC-11 is an unambiguous indication that groundwater is flowing from southwest Area 20.

3.1 Vertical Head Differences

The aquifer system in the area of the Bench has a distinct layered sequence of aquifers (fractured welded tuffs and lavas) and aquitards (zeolitized bedded tuff). A preliminary assessment of the propensity for vertical flow between formations can be made by examining differences in static head. In the southwest Area 20 region, three well pads are currently configured to monitor the BA/SPA, TCA, and TSA water levels separately: ER-EC-6 (packers were installed in 2009 to isolate the intervals), ER-20-8 (not discussed in this report), and ER-EC-11. Elliot and Fenelon (2010) report the initial interval water levels in ER-EC-6 after the packers were set; additional new data are presented here. Well ER-EC-1 has intervals open to multiple HSUs, but the formations are free to cross flow under natural conditions.

As part of transducer installation, depths to water are recorded with calibrated electric tapes (e-tapes). These data are summarized in Tables 3-2 and 3-3 for ER-EC-6 and ER-EC-11, respectively. Data sources are the 2010 long-term head monitoring report (N-I, 2011b), and field data forms (N-I, 2011a). Higher frequency data are available from pressure transducer records, but the smaller dataset is easier to understand for this reconnaissance.

Table 3-2
ER-EC-6 Static Head Measurements

Date	Time	Interval	HSU	BP (mbar)	Depth to Water (ft bgs)	Head (ft amsl)	Adjusted Head [a]		Source
							(ft amsl)	(m amsl)	
06/20/2009	09:54	Shallow Piezometer	BA	821	1,425.21	4,179.19	4,179.19	1273.82	NI, 2011b
06/20/2009	10:20	Deep Piezometer	TSA	821	1,426.14	4,178.26	4,178.26	1273.53	NI, 2011b
06/20/2009	16:35	Intermediate Piezometer	TCA	821	1,425.42	4,178.98	4,178.98	1273.75	NI, 2011b
04/05/2011	15:30	Intermediate Piezometer	TCA	819	1,425.43	4,178.97	4,178.92	1273.73	NI, 2011a
04/06/2011	12:55	Deep Piezometer	TSA	826	1,426.11	4,178.29	4,178.46	1273.60	NI, 2011a
04/06/2011	16:40	Shallow Piezometer	BA	826	1,425.42	4,178.98	4,179.15	1273.80	NI, 2011a

Source: N-I, 2011a and b

[a] Head adjusted to the barometric pressure change from 06/20/2009.

bgs = Below ground surface
BP = Barometric pressure
mbar = Millibar

Table 3-3
ER-EC-11 Static Head Measurements

Date	Time	Interval	HSU	BP (mbar)	Depth to Water (ft bgs)	Head (ft amsl)	Adjusted Head [a]		Source
							(ft amsl)	(m amsl)	
11/12/2009	08:50	Deep Piezometer	TSA	821	1,476.22	4,180.04	4,180.04	1274.08	NI,2011b
11/12/2009	09:15	Intermediate Piezometer	TCA	821	1,477.08	4,179.18	4,179.18	1273.81	NI,2011b
11/12/2009	08:20	Shallow Piezometer	BA	821	1,476.93	4,179.33	4,179.33	1273.86	NI,2011b
04/07/2010	14:30	Deep Piezometer	TSA	834	1,476.94	4,179.32	4,179.74	1273.99	NI,2011b
04/07/2010	17:30	Intermediate Piezometer	TCA	832	1,477.35	4,178.91	4,179.28	1273.84	NI,2011b
04/08/2010	14:00	Shallow Piezometer	BA	827	1,477.31	4,178.95	4,179.14	1273.80	NI,2011b
04/08/2011	12:55	Intermediate Piezometer	TCA	815	1,476.50	4,179.76	4,179.54	1273.92	NI, 2011a
04/15/2011	11:45	Shallow Piezometer	BA	833	1,477.61	4,178.65	4,179.04	1273.77	NI, 2011a

Source: N-I, 2011a and b

[a] Head adjusted to the barometric pressure change from 06/20/2009.

3.1.1 Well ER-EC-6

Packers were installed on May 13, 2009, along with tubing to allow monitoring of the upper three
(BA, TCA, and TSA) intervals. On June 20, 2009, and between April 4 and 6, 2010, depth to water
was measured for each open piezometer (the bottom completion was inaccessible because of the
bridge plug). Additionally, data for each interval were collected in 2000 with bridge plugs to isolate
each interval as described in IT Corporation (IT) (2002) and shown in Table 3-4.

Table 3-4
ER-EC-6 2000 Interval Static Head Measurements

Interval	HSU	Head (ft amsl)	Head (m amsl)
Shallow	BA	4,178.57	1,273.63
Upper intermediate	TCA	4,178.01	1,273.46
Lower intermediate	TSA	4,176.66	1,273.05
Lower	CFCM	4,173.00	1,271.93

Figure 3-3 shows the head profiles for the three available datasets; the center of the screen is used for
the elevation reference, although given the permeability variation in fractured rock, this is more
convenient than accurate. The barometric efficiency of this well is high (N-I [2011b] assumed a
barometric efficiency of 1), and barometric pressure changes were included. The newer data show
smaller differences (less than 0.5 m across all three intervals), although still directed downward, than
the 2000 data. This interpretation is consistent with that of Elliot and Fenelon (2010).

Density variations can have an important effect on interpreting groundwater systems (Hickey, 1989;
Post et al., 2007), and temperature corrections for groundwater analysis at NNSS have been described
by Winograd (1970). Three temperature logs were considered for use in temperature correction.
One was collected immediately after drilling, during development but before the constant rate test,
and the other about a month after WDT operations finished in 2000 (Figure 3-4). Computations were
performed with Desert Research Institute (DRI) pre-WDT data using the method of Winograd (1970)
as described by Fenelon et al. (2010). The resulting corrections were about 1 and 5 m for the upper
middle or intermediate (TCA), and lower middle or deep (TSA) piezometers. The downward sense is
maintained after the temperature correction but is larger with respect to the TSA. However, these
adjustments should be considered approximate and preliminary because insufficient time elapsed for
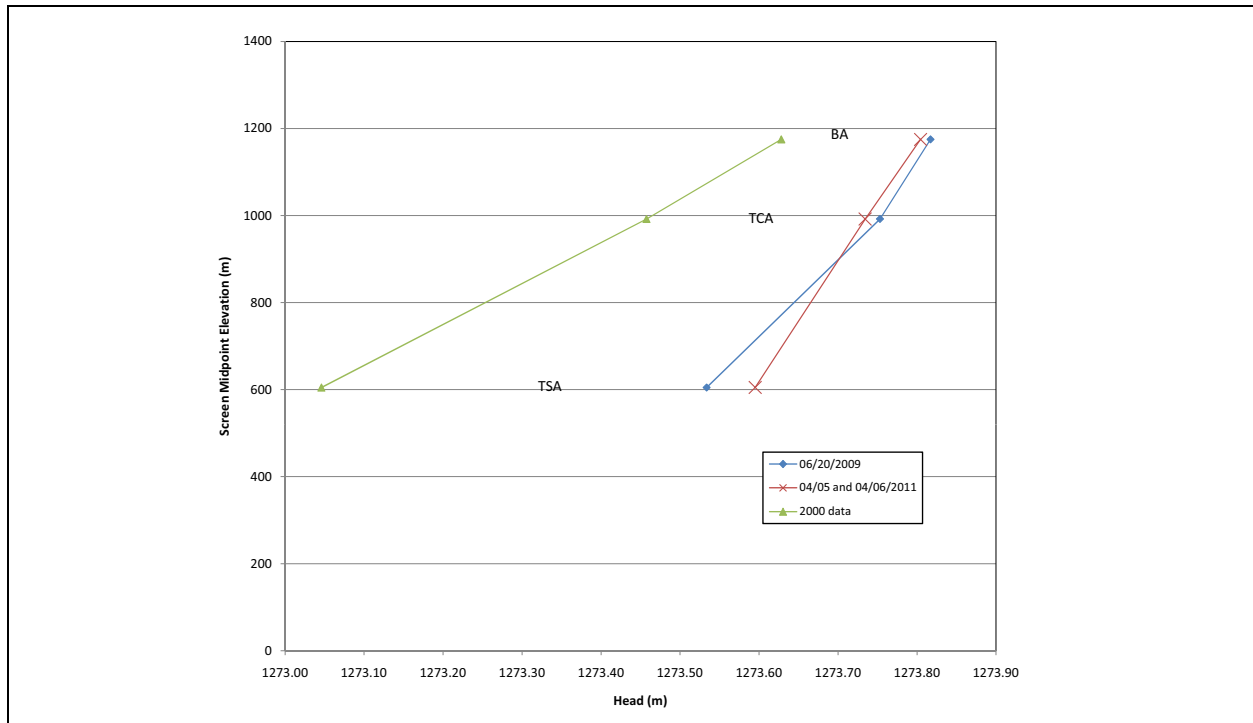
Figure 3-3
Vertical Hydraulic Head Profile at ER-EC-6
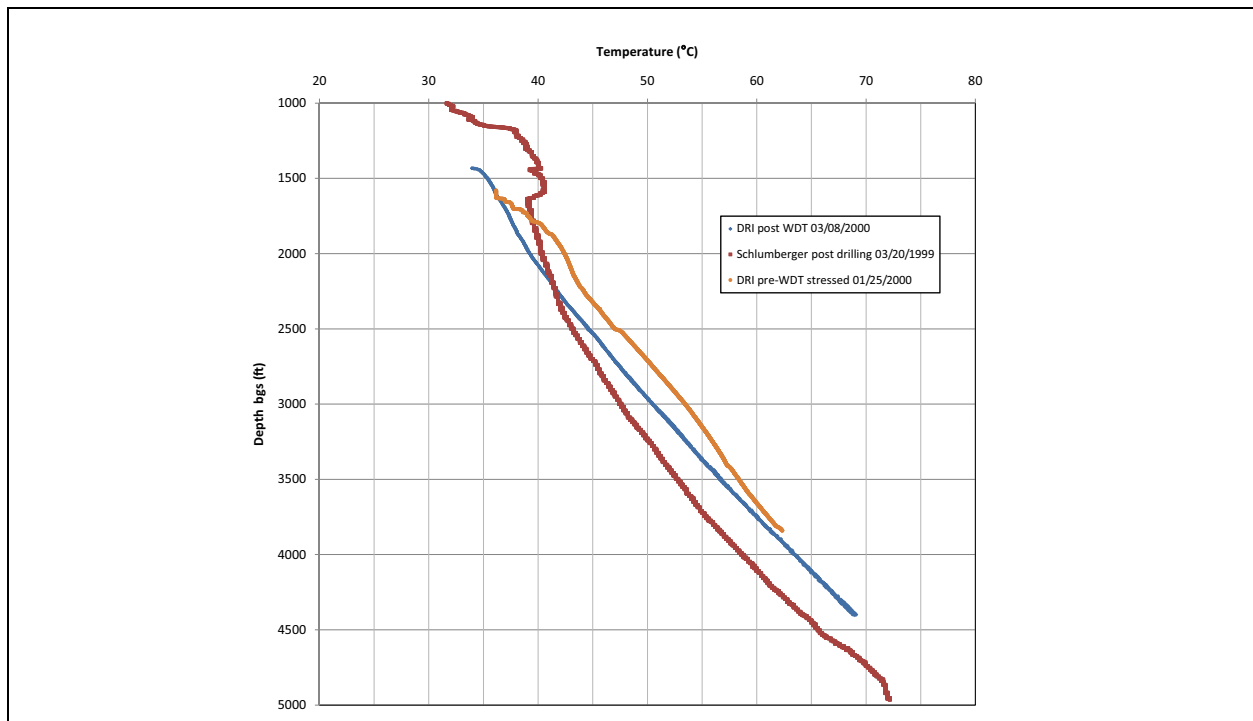
Figure 3-4
Well ER-EC-6 Temperature Profiles

the temperature profile to return to undisturbed conditions. Gillespie (2005) suggested a year was necessary for this to occur.

3.1.2   Well ER-EC-11

On November 12, 2009, transducers were installed in each of ER-EC-11's piezometers. Depth to water was measured again in April 2010 and April 2011 (Table 3-3). Head profiles for the three datasets are shown in Figure 3-5. Changes in barometric pressure were accounted for using a barometric efficiency of one. The apparent vertical hydraulic gradient is upward, and is less than 0.3 m. Two temperature logs are available (Figure 3-6): one immediately after drilling, and the other not quite six months later about five days before the start of WDT operations. Using the latter log to compute temperature corrections using the method of Winograd (1970) as described by Fenelon et al. (2010) gives head reductions of about 2, 3, and 4 m for the shallow (BA), intermediate (TCA), and deep (TSA) completions, respectively. As noted for ER-EC-6, these corrections should be considered preliminary, however, it is likely that the true vertical hydraulic gradient is downward, not upward, at ER-EC-11.
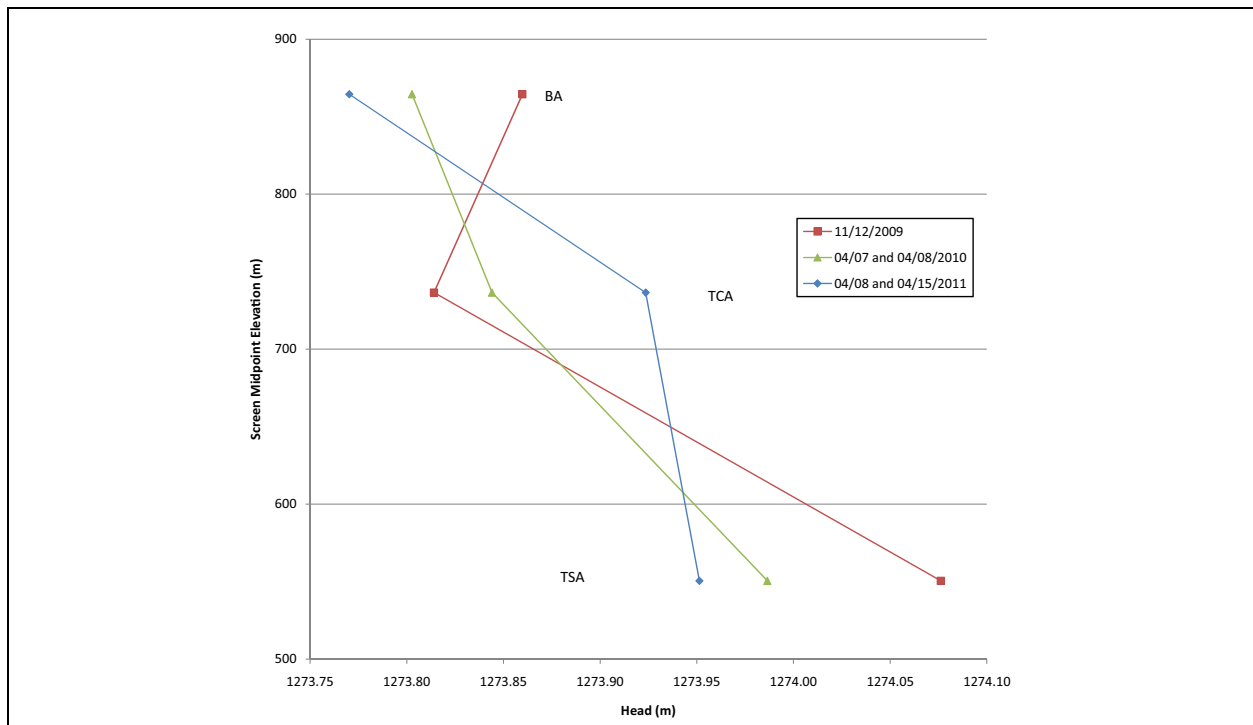
Figure 3-5
Well ER-EC-11 Vertical Head Profiles
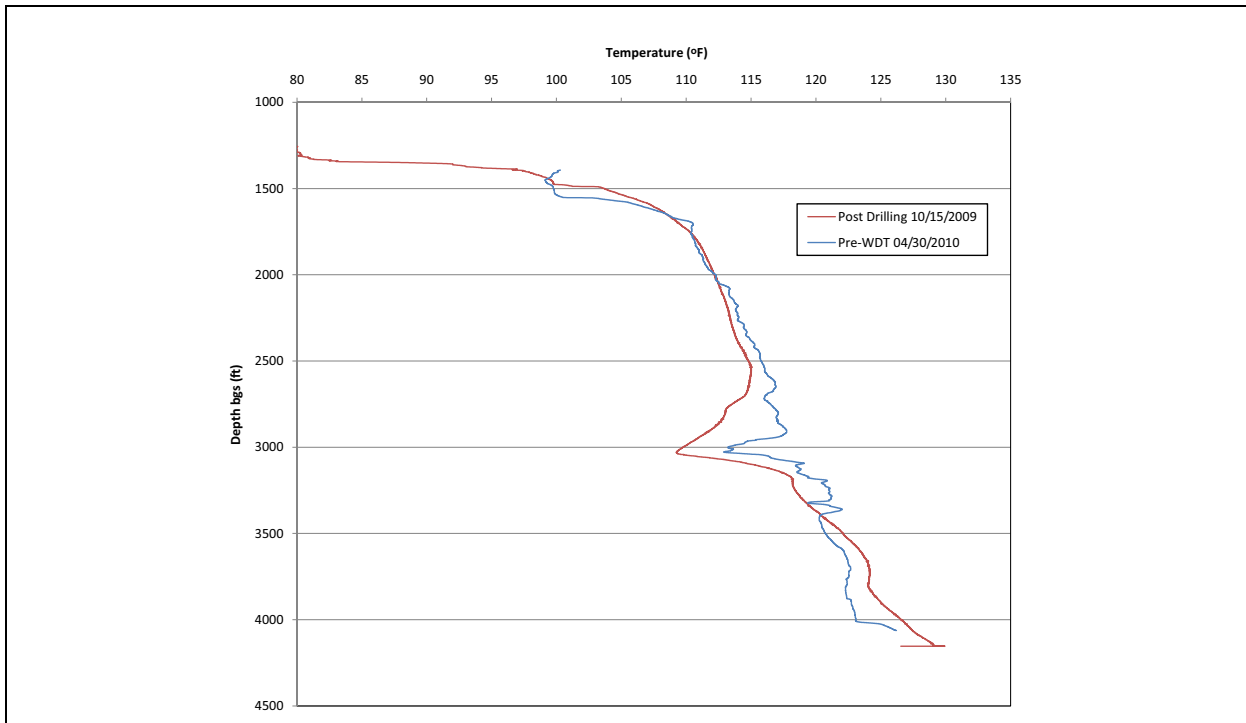
Figure 3-6
Well ER-EC-11 Temperature Profiles

3.2 Summary

Static head data collected at Phase II characterization boreholes provide information to refine the understanding of potentiometric gradients and groundwater flow in the bench area of southwest Area 20. Observed head conditions indicate that groundwater flow is consistent with previous estimates of flow to the south and west. Generally, heads are lower in deeper aquifer units, possibly indicating that recharge is limited to deeper units by the presence of thick tuff confining units. Analysis of static groundwater heads in the vicinity of faults did not show discontinuities in the groundwater gradients, indicating that faults in this area are unlikely to significantly impede groundwater flow.

4.0 GROUNDWATER CHEMISTRY

This section presents chemistry data for ER-20-7, ER-20-8 #2, and ER-EC-11; and provides a qualitative evaluation of trends in the groundwater chemistry of these wells and of others in their vicinity. The wells included in this evaluation, along with the primary HSU sampled within each well, are presented in Figure 4-1. In general, the primary HSU is the HSU that extends the largest length within the effective open interval. The chemistry data included in the evaluation are presented in Appendix A. Comprehensive groundwater chemistry evaluations for Pahute Mesa are presented in Thomas et al. (2002), Kwicklis et al. (2005), and Rose et al. (2006). This section integrates the new data with these earlier investigations in a qualitative manner.

Samples were collected from ER-20-7, ER-20-8 #2, and ER-EC-11 during drilling operations and also during WDT. The samples collected during drilling operations are more likely to be impacted by drilling fluids but provide depth-discrete groundwater chemistry data that can be evaluated with respect to samples collected during WDT, once large quantities of water are purged from the well.

4.1 Evaluation of Samples Collected during Drilling Operations

During drilling, fluid-discharge samples were collected from each well for onsite and/or laboratory analysis of tritium. Additional analyses were performed on the fluid-discharge samples on a case by case basis as described in Sections 4.1.1 through 4.1.3. Samples were also collected at the end of drilling using a depth-discrete wireline bailer and analyzed for a limited number of parameters by a commercial laboratory certified by the State of Nevada (i.e., ALS Laboratory Group and/or Eberline Services). Details of the sampling activities are presented in NNES (2010b, c, and d) for ER-20-7, ER-20-8 #2, and ER-EC-11, respectively.

4.1.1 Well ER-20-7

Elevated levels of tritium (approximately 53,000 picocuries per liter [pCi/L]) were encountered in the fluid-discharge samples when the borehole reached 2,063 ft bgs (TCA HSU), approximately 40 ft
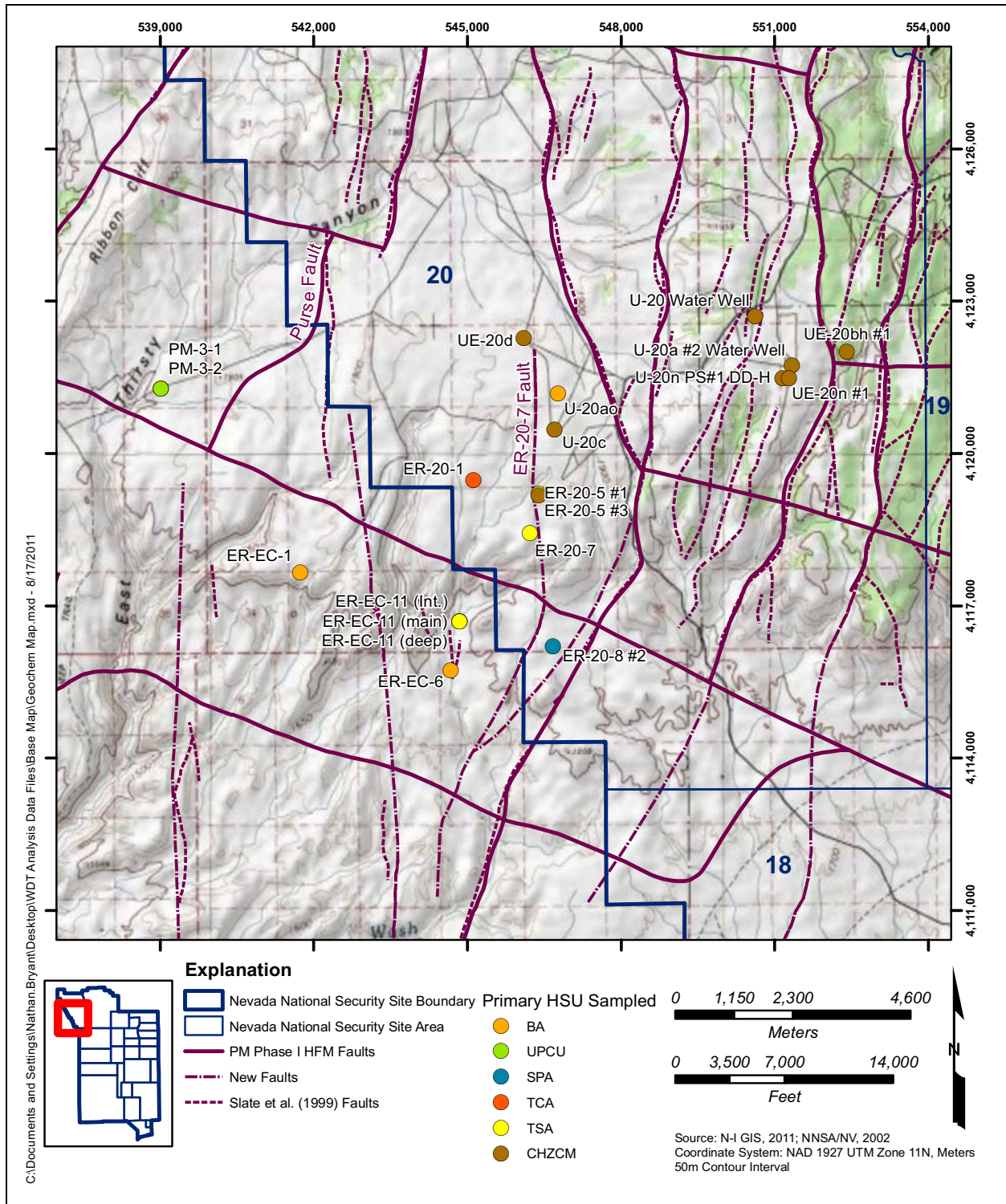
Figure 4-1
Wells Included in the Groundwater-Chemistry Evaluation

Note: The primary HSUs are as follows for wells that sample multiple completions: PM-3-1 (TCA),
PM-3-2 (UPCU), ER-20-5 #1 (TSA), ER-20-5 #3 (CHZCM), ER-EC-11 int (TCA), ER-EC-11 deep (TSA),
ER-EC-11 main (TSA).

below the static water level. Tritium activities averaged approximately 3.3 million pCi/L between 2,063 and 2,375 ft bgs within the TCA, LPCU, and TSA HSUs; and increased to an average of 20 million pCi/L, with a maximum of 61.7 million pCi/L at 2,645 ft bgs, within the TSA (NNES, 2010b).

Seven fluid-discharge samples, collected between 2,115 to 2,930 ft bgs, were analyzed by Lawrence Livermore National Laboratories (LLNL) for gamma-emitting radionuclides, tritium, and anions; and three samples were analyzed for isotopic plutonium ($^{239, 240}$Pu). These analyses are described in the LLNL letter report presented in Appendix B. The concentrations of Br ranged from 0.4 to 7.0 mg/L with the exception of the sample collected at 2,115 ft bgs with a Br concentration reported as 321 mg/L. The low Br suggests that fluid in the samples is predominantly formation water. Fluoride (F$^-$) concentrations ranged from 2.3 to 6.2 mg/L, chloride (Cl$^-$) from 27.9 to 32.6 mg/L, and sulfate (SO$_4^{2-}$) from 52.4 to 65.8 mg/L (see Appendix B). No detectable gamma-emitting radionuclides were reported except for the sample collected between 2,842 to 2,930 ft; cesium-137 (^{137}Cs) was reported as approximately 4 pCi/L (a value very near the detection limit) for this sample (see Appendix B). Tritium activities range from 1.82 million to 18.3 million pCi/L, and the $^{239, 240}$Pu activities range from approximately 0.005 to 0.12 pCi/L (Table 4-1). The $^{239, 240}$Pu activities are well below the 15 pCi/L EPA *Safe Drinking Water Act* (SDWA) maximum contaminant level (MCL) for alpha-emitting radionuclides (CFR, 2011). The Pu isotope measurements of LLNL suggest that the Pu contamination is attributable, in both the TCA and TSA, at least in part to the BENHAM test (see Appendix B).

Depth-discrete bailer samples were collected within the TSA at ER-20-7 at depths of 2,535 and 2,650 ft bgs on June 30 and July 1, 2009 (Figure 1-5), and analyzed by ALS Laboratory Group. The results of the analyses are presented in Table A.1-1 of Appendix A. Similar chemistry is observed between the depth-discrete samples. For instance, F$^-$ concentrations ranged from 5.5 to 5.6 mg/L, Cl$^-$ from 29 to 30 mg/L, SO$_4^{2-}$ from 49 to 50 mg/L, calcium (Ca^{2+}) from 4.1 to 4.4 mg/L, potassium (K$^+$) from 4.1 to 4.3 mg/L, and magnesium (Mg^{2+}) from 0.13 to 0.15 mg/L. These results are also consistent with LLNL's for the fluid-discharge samples (see Appendix B) with the exception of SO$_4^{2-}$, which was lower in the bailer samples.

Table 4-1
Results of LLNL Analysis of ER-20-7 Fluid-Discharge Samples

Sample Date	Depth (ft)	HSU	Br⁻ (mg/L)	Tritium (pCi/L)	^{239,240}Pu (pCi/L)
06/17/2009	2,115	TCA	321	1.98 (± 0.01) E+06	~0.005
06/17/2009	2,208	LPCU	3.5	2.35 (± 0.01) E+06	--
06/21/2009	2,211	LPCU	7.0	1.82 (± 0.01) E+06	--
06/21/2009	2,237	LPCU	4.0	6.08 (± 0.03) E+06	0.04
06/24/2009	2,193–2,526	LPCU/TSA	2.7	1.37 (± 0.007) E+07	--
06/25/2009	2,540–2,809	TSA	0.4	1.83 (± 0.009) E+07	--
06/27/2009	2,842–2,930	TSA/CHZCM	0.8	1.80 (± 0.009) E+07	0.12

Source: LLNL letter report (see Appendix B); NNSA/NSO, 2010a

-- = Not analyzed

Tritium activities in the depth-discrete bailer samples were reported as 17.9 million pCi/L at 2,535 ft bgs, and 18.1 million pCi/L and 18.2 million pCi/L (duplicate sample) at 2,650 ft bgs. In addition, the ^{239,240}Pu activity was reported as 0.068 pCi/L in the sample collected at 2,650 ft bgs (see Table A.1-1 of Appendix A). The ^{239,240}Pu activity in the other two samples, reported as 0.030 pCi/L (2,535 ft) and 0.046 pCi/L (2,650 ft), are less than the detection limit (0.020 pCi/L and 0.025 pCi/L, respectively) plus the analytical error (0.020 pCi/L and 0.027 pCi/L, respectively), and are considered highly uncertain.   The bailer samples were also analyzed for gamma-emitting radionuclides. Although no gamma emitters were detected in these samples, only those listed as potential contaminants of concern in NNSA/NSO (2011b) (i.e., identified in the inventory from Bowen et al., 2001) are presented in Table A.1-1. Gamma emitters include americium-241 (^{241}Am), cesium-137 (^{137}Cs), curium-244 (^{243,244}Cm), europium-152 (^{152}Eu), ^{154}Eu, and uranium-235 (^{235}U).

4.1.2   Well ER-20-8 #2

Although fluid-discharge samples were measured on site for tritium, inconsistencies were observed and the results were determined to be unreliable (NNES, 2010c). Thirteen composite samples, collected over 50-ft intervals from 1,700 ft bgs to the total depth of the borehole, were analyzed by LLNL for tritium and anions. The samples are believed to be primarily from the SPA; samples were collected during drilling within the SPA and top of the UPCU. These analyses are described in the LLNL letter report presented in Appendix C.

Tritium analyses were performed by the LLNL UGTA laboratory and the LLNL low-level tritium analysis laboratory (Environmental Monitoring Radioanalytical Laboratory [EMRL]) to test for consistency among laboratories and methods. Eichrom tritium columns were used by the LLNL UGTA laboratory to remove possible interference from organics (chemiluminescence) and other radionuclides. Tritium activities were low in shallow samples but started increasing with depth at 1,953 ft (Table 4-2). The highest activities were reported as 1,395 and 1,500 pCi/L using the two methods at LLNL. All measured values are below the 20,000 pCi/L MCL (CFR, 2011).

Table 4-2
Results of LLNL Analysis of Bromide and Tritium in ER-20-8 #2 Drilling Fluids

Sample Date	Depth (ft)	HSU	Br⁻ (mg/L)	Tritium (pCi/L)	
				LLNL UGTA Lab[a]	EMRL
08/29/2009	1,744	UPCU	8.4	ND [b]	67 ± 48
08/29/2009	1,808	SPA	6.2	ND [b]	39 ± 47
08/29/2009	1,843	SPA	5.1	ND [b]	183 ± 50
08/29/2009	1,936	SPA	3.3	ND [b]	68 ± 48
08/29/2009	1,953	SPA	2.0	179 ± 158	230 ± 51
08/29/2009	2,001	SPA	2.6	262 ± 159	244 ± 52
08/29/2009	2,050	SPA	3.1	201 ± 156	329 ± 54
08/29/2009	2,104	SPA	1.9	763 ± 159	873 ± 64
08/30/2009	2,157	SPA	1.1	836 ± 157	962 ± 65
08/30/2009	2,203	SPA	2.3	883 ± 158	940 ± 65
08/30/2009	2,250	SPA	1.2	1,043 ± 160	1,220 ± 70
08/30/2009	2,310	MPCU	0.7	1,337 ± 163	1,410 ± 72
08/30/2009	2,338	MPCU	0.8	1,395 ± 163	1,500 ± 74

Source: LLNL letter report (see Appendix C); NNSA/NSO, 2011a

[a] Analyzed using Eichrom column purification followed by liquid scintillation counting.
[b] Detection limit is approximately 100 pCi/L.

ND = Not detected

The concentrations of Br decreased from 8.4 mg/L at 1,744 ft bgs to 0.8 mg/L at 2,338 ft bgs (Table 4-2); the decrease in Br concentrations with depth suggests the portion of formation water in the drilling fluid returns increased with depth. The other anion concentrations tended to be more dilute in the samples collected between 1,744 to 1,843 ft bgs (F⁻ ranges from 2.5 to 3.4 mg/L, Cl⁻

from 19.0 to 21.1 mg/L, and SO_4^{2-} from 42.2 to 44.0 mg/L) when compared the concentrations in the deeper samples (F^- ranges from 3.9 to 4.5 mg/L, Cl^- from 24.1 to 26.1 mg/L, and SO_4^{2-} from 44.5 to 46.4 mg/L) (see Appendix C).

Depth-discrete bailer samples were collected from ER-20-8 #2 at depths of 1,710 ft bgs (BA HSU) and 2,200 ft bgs (SPA HSU) on August 31, 2009 (Figure 1-6) (NNES, 2010c). The results of these analyses are presented in Table A.1-2 of Appendix A. The ALS Laboratory Group reported tritium activities of 680 ± 230 pCi/L and 850 ± 250 pCi/L for the duplicate well samples collected at 1,710 ft bgs, and 900 ± 250 pCi/L for the sample collected at 2,200 ft bgs. Although a $^{239, 240}Pu$ activity of 0.016 pCi/L is reported for one of the samples collected at 1,710 ft bgs, the measured value is less than the detection limit (0.009 pCi/L) plus the error (± 0.015) and is thus highly uncertain. No other radionuclides were detected in these depth-discrete samples (see Table A.1-2).

The sample collected from 2,200 ft bgs tended to exhibit higher concentrations of most of the chemical constituents when compared to the samples collected at 1,710 ft bgs. These results are also consistent with LLNL's for the fluid-discharge samples (see Appendix C).

4.1.3 Well ER-EC-11

Elevated levels of tritium (10,730 pCi/L) were encountered in the fluid discharge when the borehole reached a depth of 2,719 ft bgs within the BA HSU, approximately 1,242 ft below the static water level (NNES, 2010d). Tritium activities measured on site averaged approximately 14,400 pCi/L within the BA HSU and the upper portion of the TCA HSU (between 2,719 and 3,212 ft bgs). A maximum tritium activity of 37,229 pCi/L was reported at 2,808 ft bgs within the BA HSU.

Fluid-discharge samples were also analyzed at two laboratories, LLNL and Eberline Services. The analyses performed at LLNL are described in the LLNL letter report presented in Appendix D. Tritium, measured by LLNL, ranged from 6,480 to 13,600 pCi/L in samples collected at 2,847 to 3,244 ft bgs within the BA HSU and top of the TCA HSU (Table 4-3). Tritium was below the detection limits (222 to 229 pCi/L) in samples collected above 2,290 ft and ranged from less than 150 pCi/L to 280 pCi/L below a depth of 3,244 ft. Tritium levels measured by Eberline Services ranged from 3,295 to 12,533 pCi/L within the BA HSU and top of the TCA HSU; other samples ranged from nondetect to 180 pCi/L.

Table 4-3
Results of LLNL Analysis of Tritium in ER-EC-11 Drilling Fluids

Sample Date	Depth (ft)	HSU	Tritium (pCi/L)	Sample Date	Depth (ft)	HSU	Tritium (pCi/L)
09/18/2009	1,542	TMA	<229	10/03/2009	2,949	BA	13,300 ± 300
09/18/2009	1,582	FCCU	<222	10/03/2009	3,004	BA	12,700 ± 300
09/18/2009	1,610	FCCU	<225	10/03/2009	3,043	BA	12,700 ± 300
09/29/2009	1,843	FCCU	<229	10/04/2009	3,103	UPCU	13,500 ± 300
09/29/2009	1,881	FCCU	<225	10/04/2009	3,148	UPCU	13,300 ± 300
09/30/2009	1,943	FCCU	<227	10/04/2009	3,206	TCA	12,800 ± 300
09/30/2009	1,988	FCCU	<223	10/12/2009	3,244	TCA	6,480 ± 150
09/30/2009	2,047	FCCU	<224	10/12/2009	3,300	TCA	<153
09/30/2009	2,090	FCCU	<226	10/12/2009	3,351	TCA	<152
09/30/2009	2,136	FCCU	<226	10/12/2009	3,403	TCA	<151
09/30/2009	2,185	FCCU	<224	10/12/2009	3,465	LPCU	<150
09/30/2009	2,236	FCCU	<226	10/12/2009	3,498	LPCU	200 ± 90
09/30/2009	2,290	FCCU	<226	10/12/2009	3,555	TSA	280 ± 100
10/03/2009	2,847	BA	13,600 ± 300	10/12/2009	3,601	TSA	<152
10/03/2009	2,900	BA	13,500 ± 300				

Source: LLNL letter report (see Appendix D); NNSA/NSO, 2010b

Depth-discrete bailer samples were collected from ER-EC-11 at depths of 2,450 (FCCU HSU), 2,750 (BA HSU), 3,150 (UPCU HSU), 3,285 (TCA HSU), and 3,755 (TSA HSU) ft bgs between October 9 and October 17, 2009 (Figure 1-7) (NNES, 2010d). The results of these analyses are presented in Table A.1-3 of Appendix A. Tritium activities in the samples associated with the FCCU, BA, and UPCU HSUs (i.e., 2,450, 2,750, and 3,150 ft bgs) ranged from 9,800 to 10,100 pCi/L, and were below the detection limits in the TCA and TSA HSUs (i.e., 3,285 and 3,755 ft bgs). These results are consistent with those measured by LLNL in the fluid-discharge samples (Table 4-3). No other radionuclides above detectable limits for these samples were reported (see Appendix A).

4.2   Evaluation of Samples Collected during WDT

Groundwater samples were collected during WDT and submitted to multiple laboratories for analysis for a wide range of chemical parameters including major ions, stable isotopes, trace metals, and radioisotopes (see Appendix A). Laboratories performing the analyses include the commercial

laboratory (ALS Laboratory Group), DRI, LLNL, Los Alamos National Laboratory (LANL), and the U.S. Geological Survey (USGS). The commercial laboratory is certified by the State of Nevada; the other laboratories provide state-of-the-art analyses not available from commercial laboratories in addition to analyses used to corroborate commercial laboratory results . Water-quality measurements were made on grab samples collected throughout the testing period to ensure sufficient well development to obtain samples representative of the formation water (Section 2.0).

4.2.1 Sample Collection

The following section summarizes sample collection and water-quality measurements performed during WDT operations. Details of these activities are presented in data reports (N-I, 2010a, b, and c) for ER-20-7, ER-20-8 #2, and ER-EC-11, respectively.

4.2.1.1 Well ER-20-7

Well samples were collected in duplicate on September 24, 2010, after pumping more than 2.2 million gal (N-I, 2010a). The water-quality measurements performed during development and testing for ER-20-7 are presented in Section 2.1. Figure 2-2 demonstrates stabilization of the water-quality parameters (temperature, pH, SEC, DO, and turbidity) before samples were collected for laboratory analysis. This stabilization along with the low Br concentrations (0.18 to 0.21 mg/L) suggest the samples likely represent formation waters. The water-quality measurements made during sample collection ranged from 34.0 to 34.1 degrees Celsius (°C) (temperature), 7.92 to 7.97 (pH), 0.500 to 0.522 mmhos/cm (SEC), 3.5 to 6.0 mg/L (DO), and 5.0 to 8.2 NTU (turbidity).

4.2.1.2 Well ER-20-8 #2

A depth-discrete sample was collected from ER-20-8 #2 on December 3, 2009, at a depth of 2,100 ft bgs (SPA HSU) while the well was pumped at approximately 132 to 136 gpm; the total production from the well increased from approximately 95,700 to 836,000 gal during sampling (N-I, 2010b). On December 18, 2009, samples were collected from the well after pumping nearly 1.9 million gal. The water-quality measurements performed during development and testing of ER-20-8 #2 are presented in Section 2.2 and those associated with the samples collected for laboratory analysis are presented in Table A.1-2 of Appendix A. Figure 2-3 demonstrates stabilization of these water-quality parameters (temperature, pH, SEC, DO, and turbidity) before

samples were collected for laboratory analysis. This stabilization along with the low Br concentrations suggest the samples likely represent formation waters. The water-quality measurements made during sample collection ranged from 41.4 to 41.9 °C (temperature), 8.04 to 8.18 (pH), 0.383 to 0.437 mmhos/cm (SEC), 2.4 to 3.3 mg/L (DO), and 1.6 to 2.9 NTU (turbidity).

4.2.1.3 Well ER-EC-11

Depth-discrete bailer samples were collected on May 2, 2010, at a depth of 3,750 ft bgs in the deep piezometer (TSA HSU), and from 3,300 ft bgs in the intermediate piezometer (TCA HSU) while the well was pumped at approximately 293 gpm (N-I, 2010c). Well-head samples were collected from the main completion (TSA HSU) on May 18, 2010, after pumping more than 5.2 million gal. The water-quality measurements performed during development and testing of ER-EC-11 are presented in Section 2.3. Figure 2-4 demonstrates stabilization of the water-quality parameters (temperature, pH, SEC, DO, and turbidity) before samples were collected for laboratory analysis. This stabilization along with the low Br concentrations (0.5 to 1.2 mg/L) suggest the samples likely represent formation waters. The water-quality measurements made during sample collection ranged from 38.7 to 43.5 °C (temperature), 7.46 to 8.24 (pH), 0.512 to 0.519 mmhos/cm (SEC), 3.2 to 3.4 mg/L (DO), and 0.7 to 3.3 NTU (turbidity).

4.2.2 Results

The following section presents an evaluation of the major-ion, stable-isotope, and radionuclide data for the samples collected from ER-20-7, ER-20-8 #2, and ER-EC-11 and from other wells in the vicinity. The data used for the evaluations are presented in Tables A.1-4 and A.1-5 of Appendix A. The evaluation focusses on the samples collected during WDT because these samples are considered most representative of the formation water. The mean concentrations are reported for the wells with multiple samples available.

4.2.2.1 Major Ions

As the dissolved constituents in groundwater provide a record of the minerals encountered as water moves through an aquifer, evaluation of the major-ion characteristics of groundwater can provide insights on the source areas and flow directions for groundwater movement. Major ions typically consist of calcium (Ca^{2+}), potassium (K^+), magnesium (Mg^{2+}), sodium (Na^+), chloride (Cl^-), sulfate

(SO_4^{2-}), bicarbonate (HCO_3^-), and carbonate (CO_3^{2-}). Other constituents (such as silica or boron) are occasionally at concentrations high enough to be considered major constituents of groundwater. These constituents, however, more commonly occur as minor or trace constituents at significantly lower concentration levels.

A Piper diagram—illustrating the relative major-ion chemistry of the groundwaters from ER-20-7, ER-20-8 #2, and ER-EC-11 and from other wells in the vicinity—is presented in Figure 4-2. The Piper diagram presents relative concentrations of major ions in percent milliequivalents per liter (%meq/L) and is used to classify various groundwater chemistry types, or facies, and illustrate the relationships that may exist between water samples. The relative concentrations of cations and anions are presented in the left and right triangles, respectively, and are projected onto the central diamond to present the combined major-ion chemistry (Figure 4-2).

The Piper diagram shows that Na + K are the dominant cations in all groundwaters in the study area. The relative concentrations of anions are substantially more variable (Figure 4-2); the dominant anion in several samples is HCO_3^-, but significant relative concentrations of Cl^- and SO_4^{2-} are also present in many of the samples. The groundwaters vary from a Na-HCO_3 type (greater than 50 percent HCO_3^- as the dominant anion) to a Na-HCO_3/SO_4/Cl type (relatively equal concentrations of the three anions are present). These groundwater types are characteristic of waters that have dissolved volcanic rhyolitic lava, ash-fall and ash-flow tuffs, and associated volcanic alluvium. The elevated levels of Cl^- and SO_4^{2-} observed in samples are thought to result from interaction with hydrothermally altered zones; drill core and cuttings from wells in the area show evidence of hydrothermal alteration (IT, 1998).

The groundwaters of ER-20-7, ER-20-8 #2, and ER-EC-11 plot quite similarly on the Piper diagram, and lie in the middle of a rough trend line connecting the Na-HCO_3 and Na-HCO_3/SO_4/Cl type waters. The end members of this trend line consist of samples collected from the cluster of wells in the northeastern portion of the study area including UE-20bh#1, U-20ao, and U-20c (Na-HCO_3 type) and the wells located west of the Purse fault including ER-EC-1 and PM-3 (Na-HCO_3/SO_4/Cl type). With the exception of the sample from the intermediate piezometer of ER-EC-11, the pumped well and depth-discrete samples plot quite close together; the Ca^{2+} to Na^+ ratio is greater in this intermediate
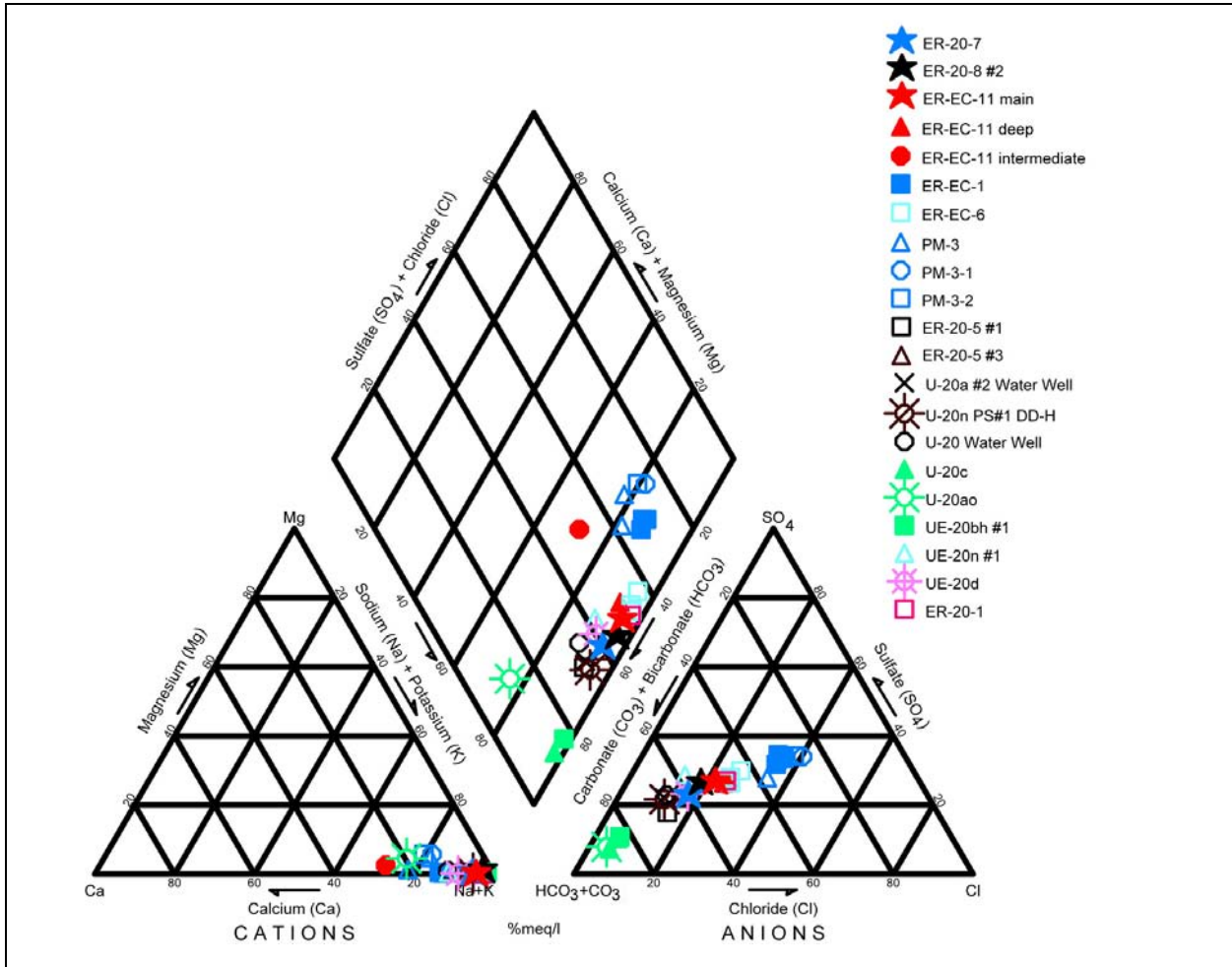
Figure 4-2
Piper Diagram Illustrating Groundwater Major-Ion Chemistry of
ER-20-7, ER-20-8 #2, and ER-EC-11 and Wells in Their Vicinity

piezometer sample. This may be due to the presence of cement and insufficient purging of this
piezometer. The Ca^{2+} to Na^+ ratio is also greater in the samples from U-20ao, ER-EC-1, and PM-3.

Chloride typically behaves conservatively in groundwater; it is highly soluble and does not
participate in any common geochemical reactions at concentrations typical of most groundwaters.
Therefore, preliminary flow paths can be evaluated based on Cl^- concentrations. The concentration of
Cl^- ranges from 29 to 31 mg/L in bailed and pumped samples from ER-20-7, all of which are from the
TSA (see Table A.1-1 of Appendix A). The ER-20-8 #2 samples analyzed by LLNL (31 mg/L) are
slightly higher than those analyzed by the commercial laboratory (22 to 27 mg/L) (see Table A.1-2).
The Cl^- concentrations for ER-EC-11 are greater (56 to 57 mg/L) in the depth-discrete samples

collected from depths of 2,450, 2,750, and 3,150 ft after drilling (FCCU, BA, and UPCU HSUs); Cl^- concentrations are reported as 38 to 49 mg/L for samples collected between 3,285 ft (TCA HSU) and 3,755 ft (TSA HSU) (see Table A.1-3).

Figure 4-3 presents a spatial representation of Cl^- concentrations along with the primary HSU sampled. For ER-EC-1 and ER-EC-6, the primary HSU is specified as the BA because flow logs show that production in these wells was derived from the upper completions (IT, 2000a and b). The reported Cl^- concentrations are associated with the samples collected during WDT because these samples are considered most representative of the formation water. The mean Cl^- concentrations are reported for the wells with multiple samples available. This is the case for ER-EC-1 and ER-EC-6, for which concentrations range from 88 to 100 mg/L and 44 to 54 mg/L, respectively, for samples collected in 2000, 2003, and 2009.

Some trends are apparent from Figure 4-3. First, the highest Cl^- concentrations, ranging from 84 to 112 mg/L, are observed in ER-EC-1 and PM-3 located in Thirsty Canyon (see Table A.1-4). Next, the lowest Cl^- concentrations, ranging from 3 to 13 mg/L, are observed in wells located in the northeastern portion of the study area (U-20 Water Well, UE-20bh #1, U-20n PS 1D, UE-20 n1, U-20a #2 Water Well, U-20ao, and U-20c). The samples from these wells are primarily associated with the CHZCM HSU. Groundwater samples from the remaining wells (including ER-20-7, ER-20-8 #2, and ER-EC-11) exhibit a range in Cl^- concentrations intermediate to these values and are potentially a mixture of groundwater from these two areas. These trends were described in the earlier investigations (Thomas et al., 2002; Kwicklis et al., 2005; and Rose et al., 2006). The inference from these results was that the relatively dilute groundwater from Pahute Mesa flows southwest toward Thirsty Canyon, where it mixes with more concentrated groundwater flowing from the north.

4.2.2.2 Stable Isotopes

The stable isotopes of hydrogen ($^2H/^1H$ or $D/^1H$) and oxygen ($^{18}O/^{16}O$) are intrinsic to the water molecule and therefore behave conservatively in most groundwater systems. In the water cycle, these isotopes are fractionated (partitioned) between the liquid and vapor phases during evaporation and condensation processes. Once the precipitation has infiltrated to the water table, the stable isotope values are unaffected by water-rock interaction at temperatures below approximately 100 °C (Criss, 1999). These isotopes are therefore used along with Cl^- as conservative tracers for evaluating
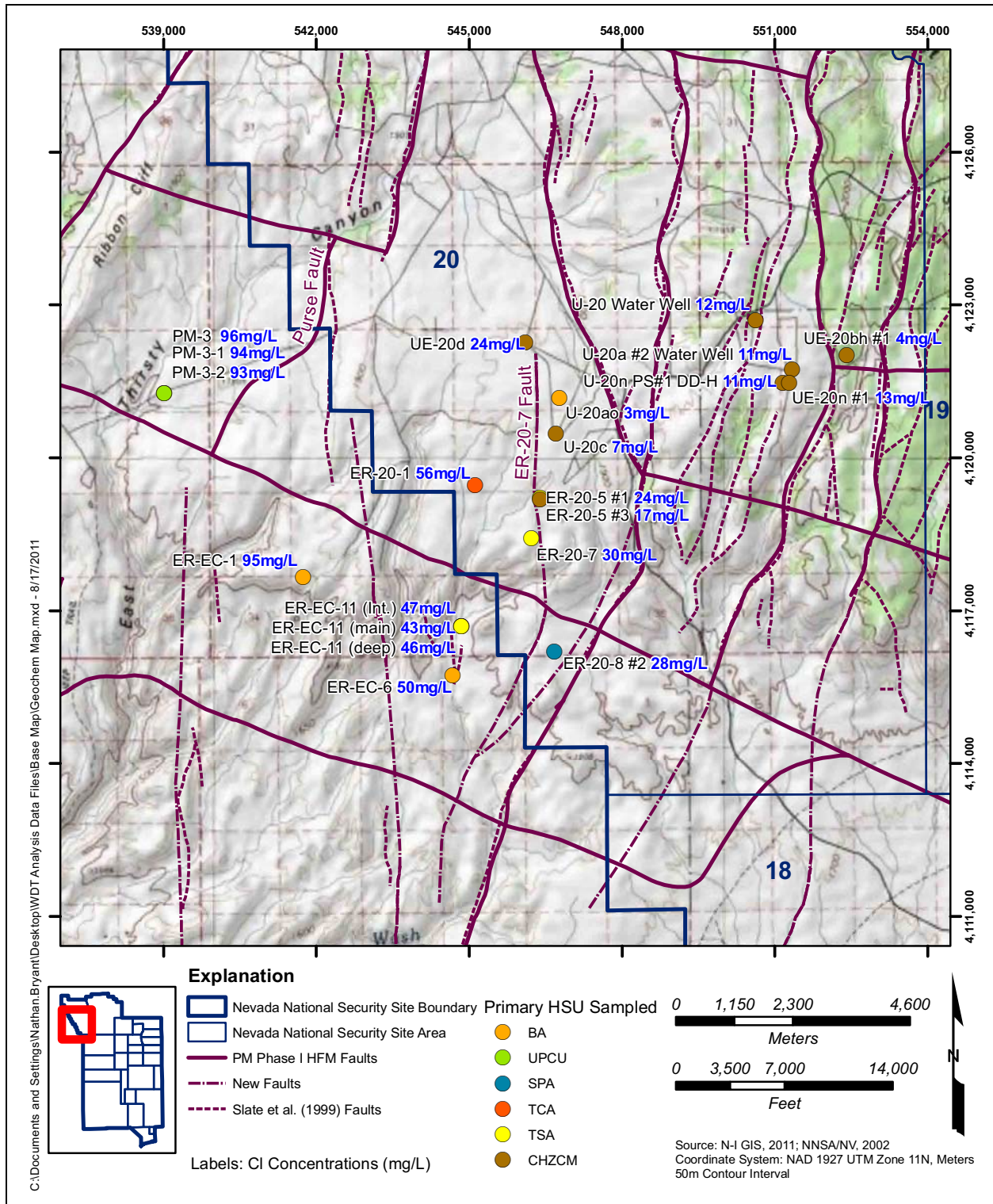
Figure 4-3
Spatial Distribution of Cl within the Study Area

Note: The primary HSUs are as follows for wells that sample multiple completions: PM-3-1 (TCA), PM-3-2 (UPCU), ER-20-5 #1 (TSA), ER-20-5 #3 (CHZCM), ER-EC-11 int (TCA), ER-EC-11 deep (TSA), ER-EC-11 main (TSA).

groundwater origin and flow paths. Hydrogen and oxygen isotopes are conventionally reported as delta (δ) values representing permil (‰) variations in the isotope ratio of the sample relative to a reference standard.

Samples collected from ER-20-7 were analyzed by LLNL for δD (-113 ‰) and δ^{18}O (-15.4 ‰); DRI does not participate in hot-well analyses. The δD and δ^{18}O in samples collected from ER-20-8 #2 were measured by DRI (-115 and -15.2 ‰, respectively) and LLNL (-117 and -15.4 ‰, respectively). The δD in samples collected from ER-EC-11 was measured by DRI (-115 ‰), and the δ^{18}O was measured by DRI (-15.2 ‰) and LLNL (-15.3 ‰); the δD measurement by LLNL is in progress. Although within the analytical uncertainties associated with δD (±2 ‰) and δ^{18}O (±0.2 ‰) measurements (NNSA/NSO, 2011b), the isotopic values tend to be lower when measured by LLNL.

Plots of δD versus δ^{18}O and δD versus Cl⁻ are presented in Figures 4-4 and 4-5, respectively. The three data points for ER-EC-1 and ER-EC-6 represent averages of the multiple samples collected for each of the three sampling events. Unfortunately, the number of wells with isotope data is less than those with major-ion data. For reference, the global meteoric water line (GMWL) defined by Craig (1961) and the local meteoric water line (LMWL) defined by Ingraham et al. (1990) are included (Figure 4-4). The meteoric water lines represent the observed correlations in δ^{18}O-δD values of precipitation samples from around the world and from the NNSS, respectively. The GMWL is defined by the equation δD = $8\delta^{18}$O + 10 (Craig, 1961), while the LMWL is defined by the equation δD = $6.87\delta^{18}$O - 6.5 (Ingraham et al., 1990). The symbol colors correspond to the primary HSU sampled: green (UPCU), yellow (TSA), blue (SPA), orange (BA), red (TCA), and black (CHZCM). All samples (except ER-20-7) plot well below the present-day global or local meteoric water lines, suggesting that the groundwater is mostly fossil groundwater unrelated to present precipitation (Merlivat and Jouzel, 1979).

Although, δ^{18}O is not consistent within HSUs, there is rough trend in δD and Cl⁻. The δD values range from -117 to -115 ‰ for the BA HSU, -115 to -113 ‰ for the TSA HSU, and -114 to -110 ‰ for the CHZCM HSU; and Cl⁻ concentrations range from 48 to 96 mg/L for the BA HSU, 24 to 26 mg/L for the TSA HSU, and 4 to 17 mg/L for the CHZCM HSU (Figures 4-4 through 4-6). The other HSUs are represented by single samples and cannot be assessed.
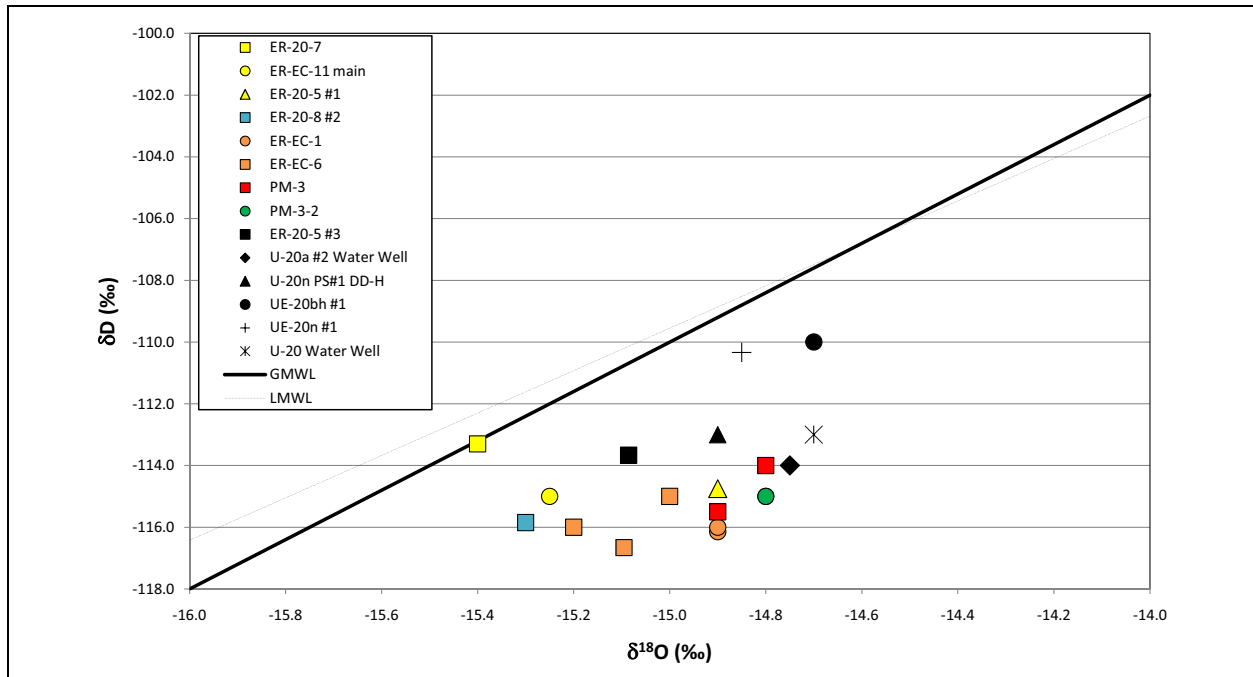
Figure 4-4
Plot of δD versus $\delta^{18}O$
Note: Symbol colors represent the primary HSU: yellow (TSA), blue (SPA),
green (UPCU), orange (BA), red (TCA), and black (CHZCM).
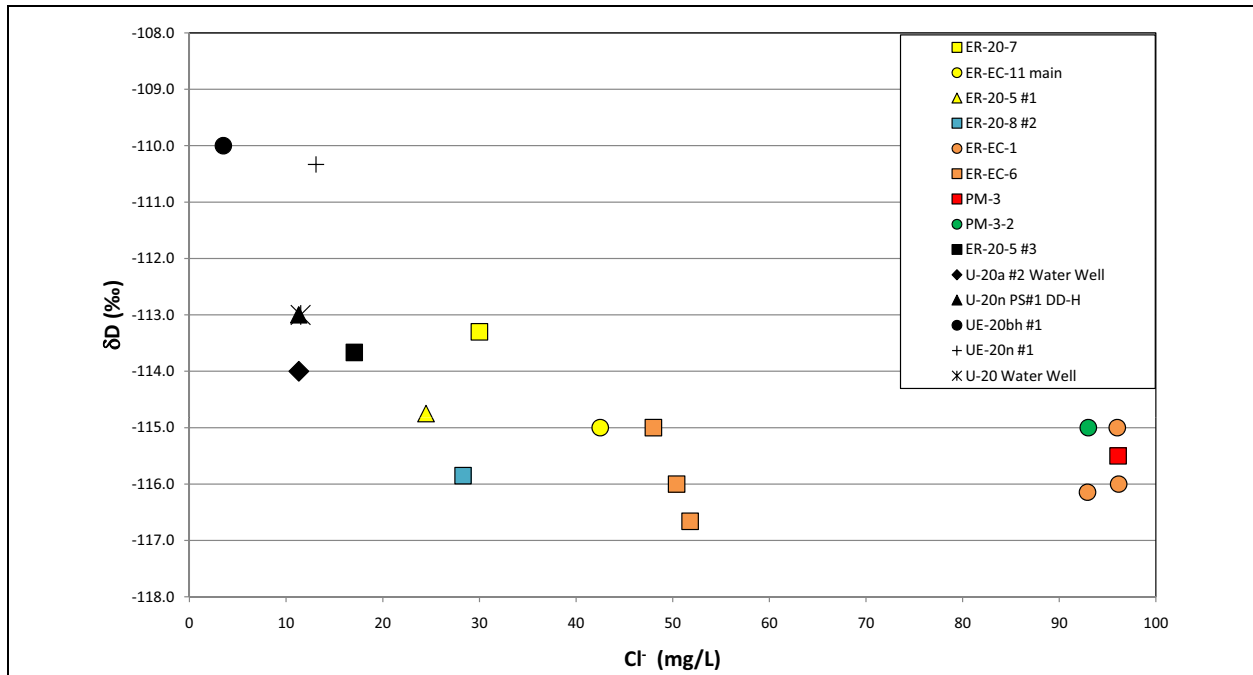
Figure 4-5
Plot of δD versus Cl
Note: Symbol colors represent the primary HSU: yellow (TSA), blue (SPA), orange (BA),
green (UPCU), red (TCA), and black (CHZCM).
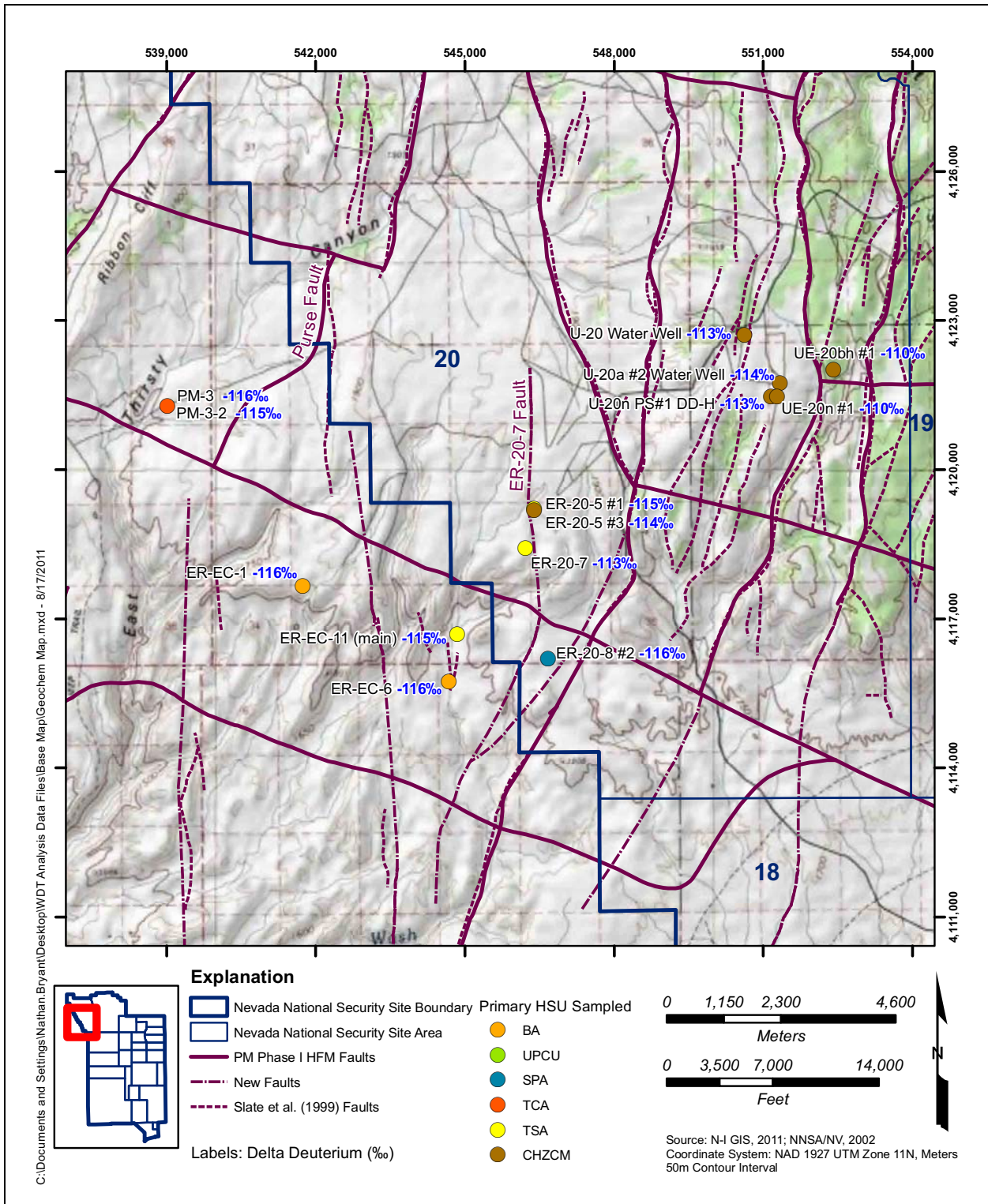
Figure 4-6
Spatial Distribution of δD within the Study Area

Note: The primary HSUs are as follows for wells that sample multiple completions: PM-3-1 (TCA),
PM-3-2 (UPCU), ER-20-5 #1 (TSA), ER-20-5 #3 (CHZCM), ER-EC-11 int (TCA), ER-EC-11 deep (TSA),
ER-EC-11 main (TSA).

Within the study area, $\delta^{18}O$ values range from -15.4 to -14.7 ‰, and δD values range from -117 to -110 ‰. The samples collected from the northeastern portion of the study area (U-20a #2 Water Well, UE-20bh #1, U-20n PS#1 DDH, and UE-20n #1) tend to have the most enriched δD and $\delta^{18}O$, with δD values ranging from -114 to -110 ‰ and $\delta^{18}O$ values ranging from -14.9 to -14.7‰. A rough inverse correlation is observed for δD and Cl^- (Figure 4-4). Relatively enriched δD and dilute Cl^- concentrations are observed for wells in the northeastern portion of the study area, and lighter δD and greater Cl^- concentrations are observed in the Thirsty Canyon wells located west of the Purse fault. The difference in the conservative tracer compositions of groundwater on either side of the Purse fault suggests two distinct water masses occur in this area. Immediately downgradient from this water-level discontinuity, intermediate δD and Cl values exist, implying the two water masses are mixing.

Kwicklis et al. (2005) applied the geochemical modeling code, PHREEQC, to groundwater chemistry data of Pahute Mesa to develop mixing models based on the conservative (Cl^-, SO_4^{2-}, δD, and $\delta^{18}O$) and reactive (cations, dissolved silica, pH, alkalinity, and carbon isotopes [$\delta^{13}C$ and ^{14}C]) components in groundwater. Based on the PHREEQC models, Kwicklis et al. (2005) determined that groundwater at ER-EC-6 is composed of roughly equal amounts of groundwater from ER-EC-1 and U-20 Water Well, with a possible minor contribution of groundwater from the vicinity of UE-19h (located northeast of U-20 Water Well).

4.2.2.3 Radionuclides

Samples collected during WDT are considered representative of the formation waters (Section 4.2.1). These samples were analyzed for a large suite of radionuclides by the commercial laboratory (ALS Laboratory Group) as well as LLNL and LANL (see Appendix A). The focus of these analyses is on those radionuclides listed as potential contaminants of concern in NNSA/NSO (2011b) (i.e., identified in the inventory from Bowen et al., 2001). Although these samples were analyzed for the full suite of gamma-emitting radionuclides, only ^{241}Am, ^{137}Cs, $^{243,244}Cm$, ^{152}Eu, ^{154}Eu, ^{235}U are presented in Appendix A.

Well ER-20-7

The ALS Laboratory Group reported tritium activities of 19.1 million and 18.9 million pCi/L for the duplicate well samples collected at the end of WDT (see Table A.1-1 of Appendix A). Isotopic plutonium ($^{239, 240}$Pu) activities were reported as 0.062 ± 0.032 pCi/L and 0.070 ± 0.040 pCi/L; the detection limits associated with these analyses are 0.010 and 0.041 pCi/L, respectively. Tritium and Pu activities of 17.7 million pCi/L and 0.10 pCi/L, respectively, were reported by LLNL for these samples. Technetium-99 (^{99}Tc) was reported by the ALS Laboratory Group as 13.4 ± 4.5 pCi/L and 16.4 ± 4.7 pCi/L for the duplicate well samples; detection limits were reported as 6.1 and 6.0 pCi/L, respectively. Strontium-90 (^{90}Sr) was reported by the ALS Laboratory Group as 1.47 ± 0.43 pCi/L and 1.52 ± 0.45 pCi/L for the duplicate well samples; detection limits were reported as 0.31 and 0.32 pCi/L, respectively. No other radionuclides were detected (see Appendix A). Tritium is the only radionuclide that exceeded the MCL (20,000 pCi/L); although detectable quantities of $^{239, 240}$Pu (MCL = 15 pCi/L), ^{99}Tc (MCL = 900 pCi/L), and ^{90}Sr (MCL = 8 pCi/L) were measured in the ER-20-7 samples, the levels were far below their associated MCL.

It is important to note that the ^{14}C values reported by Navarro-Intera, LLC (N-I), (2010a) as 23,500 and 38,700 pCi/L and by NNES (2010b) as 11,500 and 7,500 pCi/L were later determined to be in error. The analytical signal identified as ^{14}C was actually a result of an interference from the high concentration of tritium in the samples (see the LLNL letter report presented in Appendix B for discussion). Because of the tritium interference, the ALS Laboratory Group could not quantify ^{14}C in the samples. The ^{14}C analysis performed by LLNL uses instrumentation that is not impacted by the high level of tritium. Additional radionuclide analyses for ER-20-7 are in progress at LLNL and LANL (including ^{14}C analysis by LLNL).

Well ER-20-8 #2

The ALS Laboratory Group reported tritium activities of $1,040 \pm 270$ pCi/L and 880 ± 250 pCi/L for the duplicate well samples collected in the SPA HSU at the end of WDT. A tritium activity of $1,280 \pm 97$ pCi/L was reported by LLNL. No other radionuclides were detected by the ALS Laboratory Group (see Appendix A); the detection limits obtained by LLNL are generally much lower than for the commercial laboratories, including the ALS Laboratory Group. The activities of iodine-129 (^{129}I),

^{234}U, ^{235}U, ^{236}U, and ^{238}U are reported as 9.27E-05 pCi/L, 3.08 pCi/L, 0.0366 pCi/L, <2.3E-05 pCi/L, and 0.780 pCi/L, respectively (see Appendix A). Additional radionuclide analyses for ER-20-8 #2 are in progress at LLNL and LANL. No MCL exceedances were observed in the ER-20-8 #2 samples.

Well ER-EC-11

No radionuclides, including tritium, were detected by the commercial laboratory (ALS Laboratory Group) in the well samples collected during the pumping test or the samples collected at depths of 3,300 and 3,750 ft bgs, from the intermediate (TCA HSU) and deep piezometers (TSA HSU), respectively (see Appendix A). Uranium isotope data were reported by LLNL as 2.35 pCi/L, 0.0269 pCi/L, <1.7E-5 pCi/L, and 0.577 pCi/L for ^{234}U, ^{235}U, ^{236}U, and ^{238}U, respectively (see Appendix A). Additional radionuclide analyses for ER-EC-11 are in progress at LLNL and LANL.

No MCL exceedances were observed in the ER-20-8 #2 samples. Although tritium was detected in the drilling samples from the FCCU, BA, and UPCU HSUs, it did not exceed the 20,000 pCi/L MCL.

5.0   DRAWDOWN ANALYSIS

5.1   Geologic Conceptual Model

During WDT activities at ER-20-7, ER-20-8 #2, and ER-EC-11, hydraulic responses were observed in welded ash-flow tuffs and lavas (i.e., welded-tuff aquifers and lava-flow aquifers) throughout southwestern Pahute Mesa and the Bench (Figure 1-1). The lavas and ash-flow tuffs were laid down by sequential volcanic eruptions. The distribution of permeability in these aquifer units reflects a complex history of eruptive and cooling processes that have been overprinted by regional tectonic activity. The volcanic aquifers are separated by layers of tuff confining units that are typically low-permeability ash-fall tuffs that have become zeolitic in the saturated zone.

Lava-flow aquifers in the Bench area are composed of rhyolitic lavas. These are highly viscous, silicic lava flows that erupt from local vents or fissures and form relatively thick steep-sided flows that typically have thickness to lateral extent ratios considerably greater than more fluid volcanic deposits such as ash-flow tuffs and basalt. Phase II drill-hole data have refined the extent of lava flows in the area (NNSA/NSO, 2010a, 2011a, and 2010b) to differentiate three separate, overlapping rhyolitic lava flows that increase in age from west to east. Stratigraphically, from oldest to youngest, these rhyolitic lava flows are the rhyolite of Scrugham Peak (Tps), rhyolite of Benham (Tpb), and rhyolite of Comb Peak (Tpk). Interim interpretation of the extents of the lavas is shown in Figure 5-1. The three rhyolitic lava flows have been designated hydrostratigraphically as the Comb Peak aquifer (CPA), Benham aquifer (BA), and Scrugham Peak aquifer (SPA) and, as mentioned above, are separated from one another by relatively thin layers of tuff confining unit. The three lava-flow aquifers are thought to have similar hydrologic properties because they are related to the same eruptive cycle, are very similar mineralogically, and exhibit the same basic internal architecture
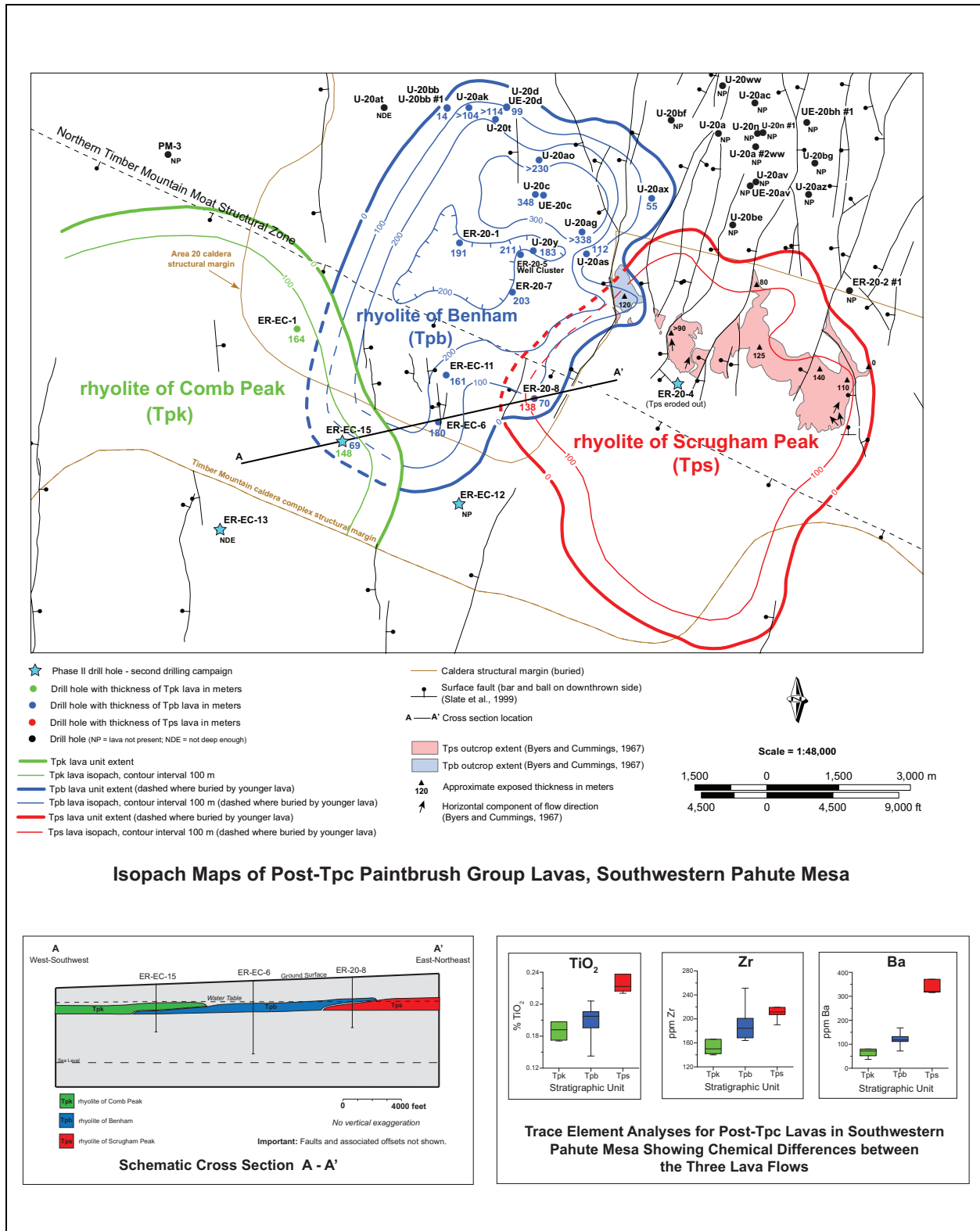
Figure 5-1
Extent of Lava-Flow Aquifers in Southwest Area 20
Source: Modified from Drellack, 2011a

consisting of five distinct lithofacies. (Figure 5-2 illustrates the general conceptual model of a rhyolitic, lava-flow aquifer.) From top to bottom, these lava lithofacies are as follows:

1. Pumiceous lava cap – porous and poorly fractured; included in the overlying tuff confining layer where zeolitic.

2. Upper vitrophyre – fractured with very low primary porosity.

3. Stony lava interior – fractured with double porosity.

Stratigraphic Unit	Hydrostratigraphic Unit [a]	Hydrogeologic Unit [b]	Lithologic Unit	Percent of lava flow thickness (N/A = Not applicable)	Fracture Intensity
rhyolite of Benham (Tpb)	FCCU	TCU	Bedded Tuff	N/A	Very low
	PVTA	VTA	Pumiceous Lava	10%	Low
	Benham aquifer (BA)	Lava-flow aquifer (LFA)	Upper Vitrophyre	10%	Moderate to high
			Stony Lava Interior	65%	Moderate to high
			Lower Vitrophyre	10%	Moderate to high
			Basal Flow Breccia	5%	Low
	UPCU	TCU	Bedded Tuff	N/A	Very low

Top of lava flow

Base of lava flow

[a] FCCU = Fluorspar Canyon confining unit
PVTA = Paintbrush vitric-tuff aquifer
UPCU = Upper Paintbrush confining unit

[b] TCU = Tuff confining unit
VTA = Vitric-tuff aquifer

Figure 5-2
Conceptual Hydrologic Model of a Rhyolitic, Lava-Flow Aquifer
Source: Modified from Drellack, 2010a

4. Lower vitrophyre – fractured with very low primary porosity.

5. Basal flow breccia – porous with lower fracture intensity than seen in the vitrophyre or stony interior. Depending on degree of alteration, may or may not be included within lava-flow aquifer.

In contrast to rhyolitic lavas, ash-flow tuffs are highly fluid pyroclastic deposits emplaced very quickly as the eruption column of a large volcanic eruption collapses. The resulting high-temperature density currents consisting of ash, pumice, mineral crystals, and rock fragments flow out at high rates away from the volcano. Many large-volume ash-flow tuffs are related to caldera formation when the land surface around the erupting volcano collapses rapidly as the underlying magma chamber is depleted. Caldera-forming ash-flow tuffs can accumulate to great thicknesses within the subsiding portions of calderas. Outside the caldera, the same large-volume, caldera-forming ash-flow tuff is typically much thinner with thickness to lateral extent ratios considerably less than more viscous volcanic deposits like rhyolitic lavas.

Ash-flow tuffs typically have an internal architecture defined by zones of varying degrees of welding with welding typically increasing inward toward the interior of the ash flow. This welding process occurs as the flow cools and compresses after emplacement. Thermal contraction during the cooling and welding processes results in the formation of cooling joints within the welded portions of the flow, particularly at the top and bottom. Figure 5-3 illustrates the general conceptual model of a non-lithophysal ash-flow tuff. This forms the initial fracture network from which the permeability of the rock is derived—the permeability of the matrix is orders of magnitude lower because of the welding. Lithophysae, small cavities caused by expanding gases before solidification, form if gas is entrapped in the center portion of the unit.

Two saturated welded ash-flow tuffs, the Tiva Canyon tuff (Tpc) and older Topopah Spring tuff (Tpt), are present in drill holes in southwestern Pahute Mesa and the Bench. Both represent outflow sheets from caldera sources located south of the Bench. These two welded ash-flow tuffs form welded-tuff aquifers and have been designated hydrostratigraphically as Tiva Canyon aquifer (TCA) and Topopah Spring aquifer (TSA). Although both are welded-tuff aquifers, they differ significantly in internal architecture, particularly with regards to the distribution of fractures and lithophysae. The TCA contains prominent and well-developed lithophysal zones within its interior, resulting in fractures concentrated at the top and bottom of the flow and few fractures in the lithophysal interior
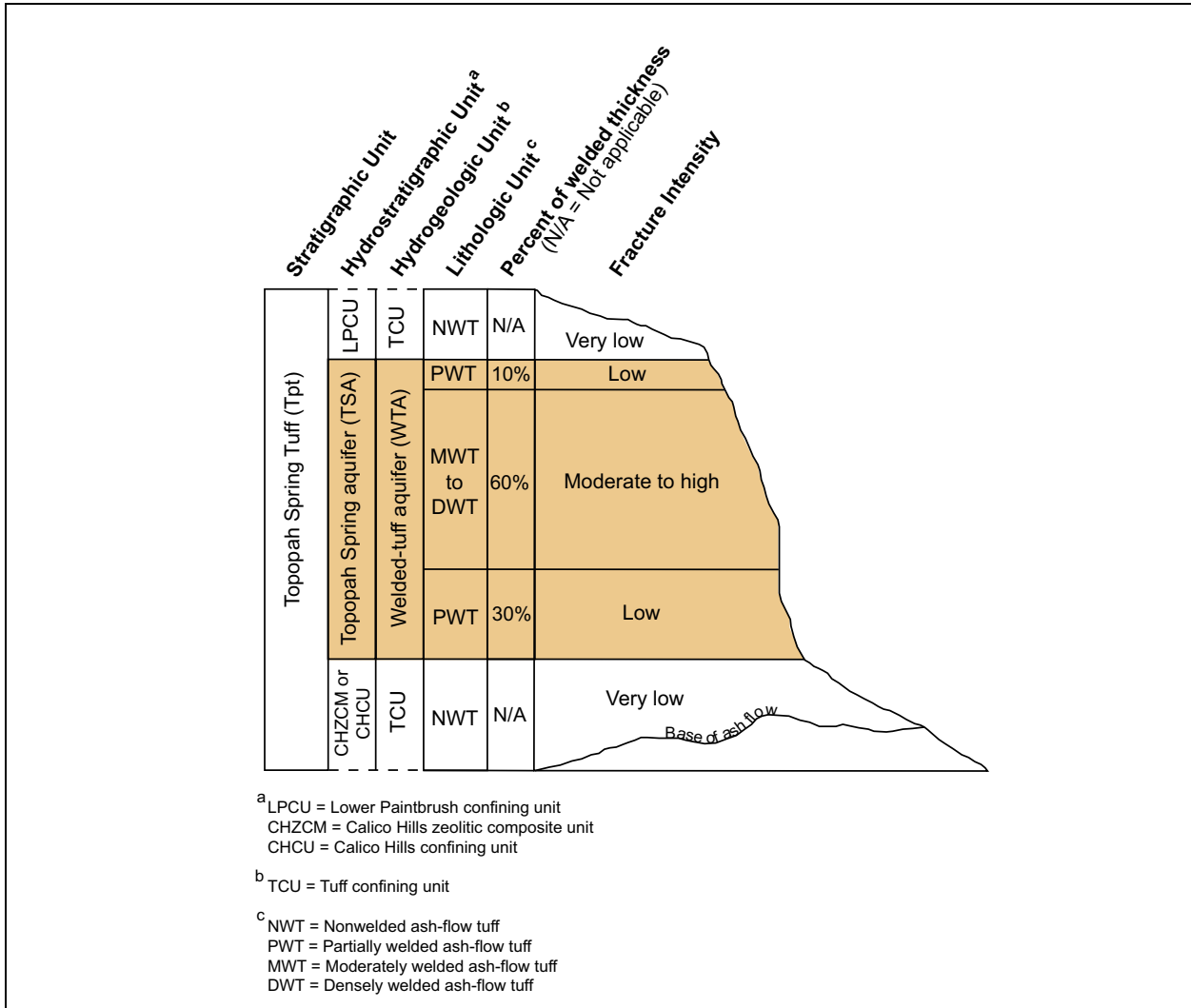
Figure 5-3
Preliminary Conceptual Model of the TSA in Southwestern Pahute Mesa Area
Source: Modified from Drellack, 2010b

(Prothro et al., 2009; Prothro, 2009 and 2010). The TSA lacks well-developed lithophysal zones, and borehole image logs indicate that fractures are distributed more evenly throughout the aquifer (Prothro et al., 2009; Prothro, 2009 and 2010).

For hydrologic purposes, rocks are categorized by their ability to transmit water (e.g., aquifer or aquitard) rather than stratigraphy as shown in Figures 5-2 and 5-3. As a result, the non-welded and pumiceous portions of ash-flow tuffs undergo zeolitic alteration in the presence of water and are included in adjacent tuff confining units. This results in the interleaved sequence of aquifers and aquitards seen in cross section.

The presence of aquitards between aquifers would conceptually restrict vertical communication resulting in vertical head changes through the geologic section, a feature noted by Blankennagel and Weir (1973) elsewhere on Pahute Mesa. However, one of the striking features of this area is the presence of faults and other large structures. Caine and Forster (1999) proposed a fault conceptual model that includes fault gouge and damage zones of altered permeability that result in a range, depending on the proportions of each component, of hydraulic behavior. Sweetkind and Drake (2007) noted that damage zones tend to scale with fault offset in volcanic rocks in Yucca Flat, and damage zones associated with large-offset faults (greater than 100 m) are many tens of meters wide, whereas damage zones associated with smaller offset faults are generally only a meter or two wide. They also noted that zeolitized tuff develops moderate-sized (on the scale of meters) damage zones. Prothro et al. (2009) also studied faults at the NNSS and observed the following: (1) faults often form discrete zones; (2) more recently active faults probably form permeable fault zones where they cut stronger rocks such as welded tuff and lava; (3) faults that intersect TCU form zones of enhanced permeability, relative to TCU protolith, although of less absolute permeability than those in welded tuff and lava; and (4) any enhanced fault-zone permeability will be generally controlled by fractures that will be subparallel to the strike of the fault resulting in anisotropic permeability. Blankennagel and Weir (1973) suggested that well yields could be enhanced in rocks otherwise unfavorable for pumping near large structures because of fault damage zone enhanced permeability. Geldon (2004) notes that, at Yucca Mountain, faults that cut tuffaceous rocks tend to locally enhance permeability. Due to the structural complexity, one of the goals of the Phase II characterization work is to better inform the geologic model of the area by incorporating feedback from hydrologic data. *That is, are the geology and hydrology consistent?* Figure 5-4 shows a preliminary fault distribution interpretation that will be considered in the analysis of well-test interference that follows.

In summary, an initial flow system conceptual model would have the following features:

- Multiple flow systems revealed by clear vertical head differences—because the mineralogy of the rocks is quite similar, geochemical differences may not be distinguishable.

- Areally extensive drawdown responses in the laterally extensive welded tuffs.

- Localized responses in the limited lava-flow aquifers, unless otherwise connected by permeable faults or offset to other permeable rocks.

- Fault structures through aquitards allowing vertical connections between otherwise laterally and vertically separated aquifers.
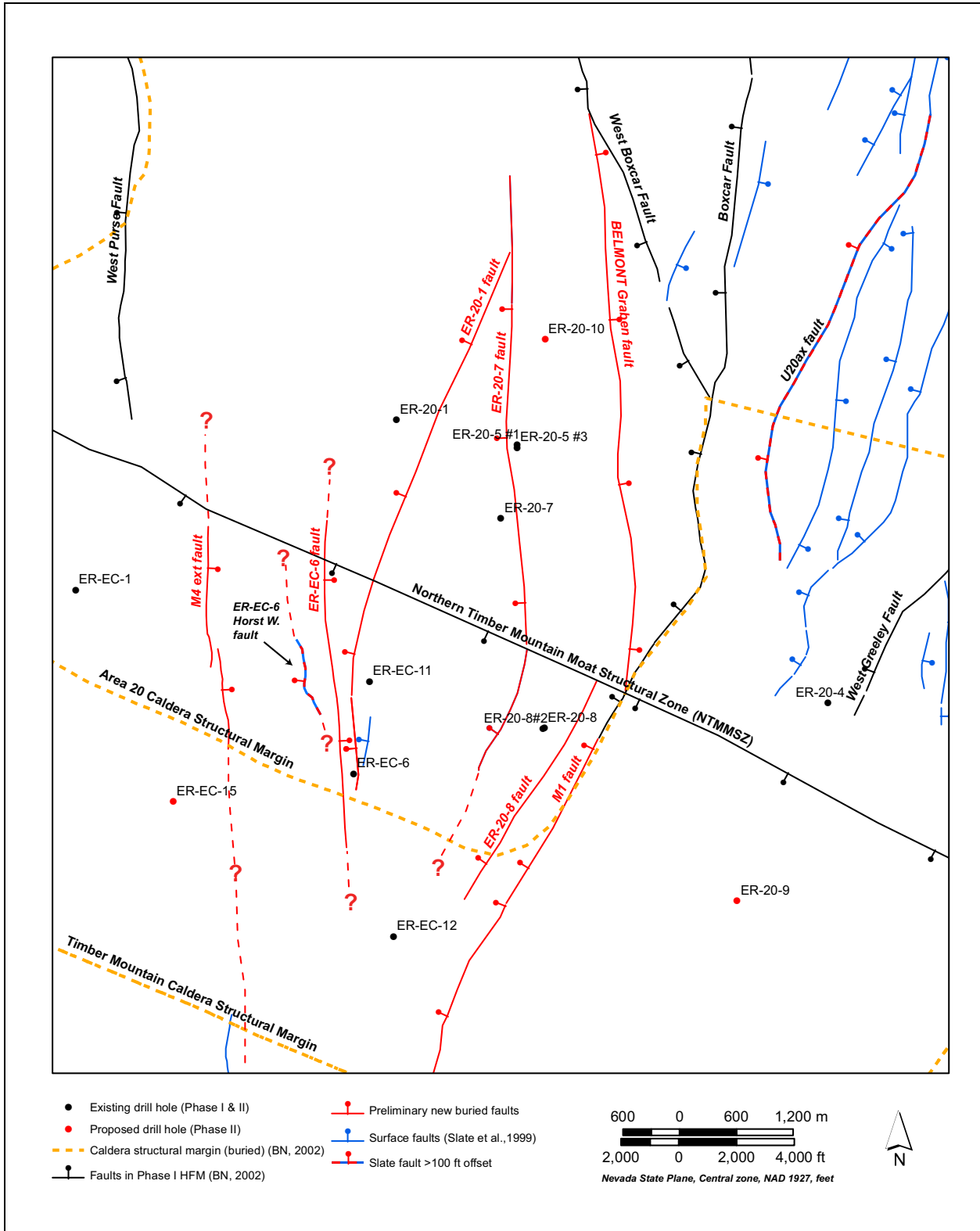
Figure 5-4
Preliminary Structure Map for Southwest Pahute Mesa
Source: Modified from Drellack, 2011b

5.2   Interference Data Analysis

The response of wells to pumping provides key information about formation properties and flow regime. The analysis of pressure/head transient data begins by reviewing the data with the log-log pressure and pressure derivative diagnostic plot in order to identify responses that are characteristic of certain types of flow regimes, and also to identify how changes over time further refine conceptual understanding (Horne, 1995). In the complexly faulted geology at Pahute Mesa, the assumptions inherent in prototypical conceptual models that are tractable with semianalytic methods are violated. Additionally, the assumption that the drawdown response seen by an observation well is due to the full discharge from the pumping well is violated in fractured rock. A small response at a distal well may result from a poor connection to the fracture system that is being pumped, rather than a high transmissivity. However, while it is true that properties may not be reliably estimated with simple solutions, they are still useful for comparing and contrasting the observed response to gain conceptual insight into what is actually occurring. Halford et al. (2010) bypassed this issue by constructing a numerical model of the ER-20-8 #2 and ER-EC-11 tests considered here. Streltsova (1988) defines the radius of investigation as $r = \sqrt{2\eta t}$, where η is hydraulic diffusivity (L^2/T) and t is transmissivity divided by storativity for a single aquifer or fracture—when data are normalized by t/r^2 different diffusivity, flow paths can be distinguished because if the diffusivity is the same, all the curves will plot on top of one another. Knudby and Carrera (2006) show that this approximate measure can be useful in mapping fracture connectivity. To examine the relationships among hydraulic responses and geologic structure, each set of test data was examined to determine trends in well behavior. This type of plot is termed a "composite" plot in well-test software such as AQTESOLV (Duffield, 2007).

Additional insight can be provided through distance-drawdown analysis. This approach examines the total drawdown (displacement) as a function of distance from the pumping well at a specific time. Deviations from the theoretical Theis solution provide guidance for determining whether specific hydraulic pathway connections are enhanced or attenuated compared to an anticipated response.

An analysis was completed using data processed by the USGS (Halford et al., 2010; Fenelon et al., 2011) (for consistency's sake and convenience) to examine hydraulic diffusivity, potential conceptual interpretations of the aquifer system, and the presence and absence of flow barriers or high-flow features such as faults. Because the test data presented here needed to be highly processed before these analyses, only wells with "high" to "moderate" relative certainty of drawdown (as classified by

Halford et al., 2010, and Fenelon et al., 2011) were examined. Beauheim (2007) illustrates such an analysis.

5.2.1 Hydraulic Responses from ER-20-7 Topopah Spring Aquifer Pumping

Table 5-1 shows the map distances between ER-20-7 and the observation wells (Fenelon et al., 2011).

Table 5-1
Distances between ER-20-7 and Observation Wells

Well Name	Distance from ER-20-7 (ft)
ER-20-5 #3	2,520
ER-20-5 #1	2,620
ER-20-8D	7,440
ER-20-8I	7,440
ER-20-8S	7,440
ER-EC-11-LI	7,250
ER-EC-11-UI	7,250
ER-EC-6D	10,230
ER-EC-6I	10,230
ER-EC-6S	10,230
ER-EC-1	14,920
ER-20-1	4,970

Source: Modified from Fenelon et al., 2011

When ER-20-7 (TSA) is pumped (composite plot shown in Figure 5-5; Theis solution also shown for comparison), the following observations can be made:

1. The responses at ER-20-5#1 (TSA) and ER-20-5#3 (CHZCM) are very similar in magnitude and timing. This is significant because ER-20-5#3 is separated from the TSA by about 150 m of zeolitized bedded tuffs while ER-20-5#1 is completed in the TSA. The ER-20-5 cluster lies on the opposite side of the ER-20-7 fault. The fault is possibly providing the vertical connection to both observation intervals.

2. ER-20-1 (TCA) responds less than the ER-20-5 cluster but is also open to only about 23 m of saturated TCA. The LPCU separates the TSA from the TCA. Explanations for the response include connection through the ER-20-1 fault and partial juxtaposition across the ER-20-1 fault.
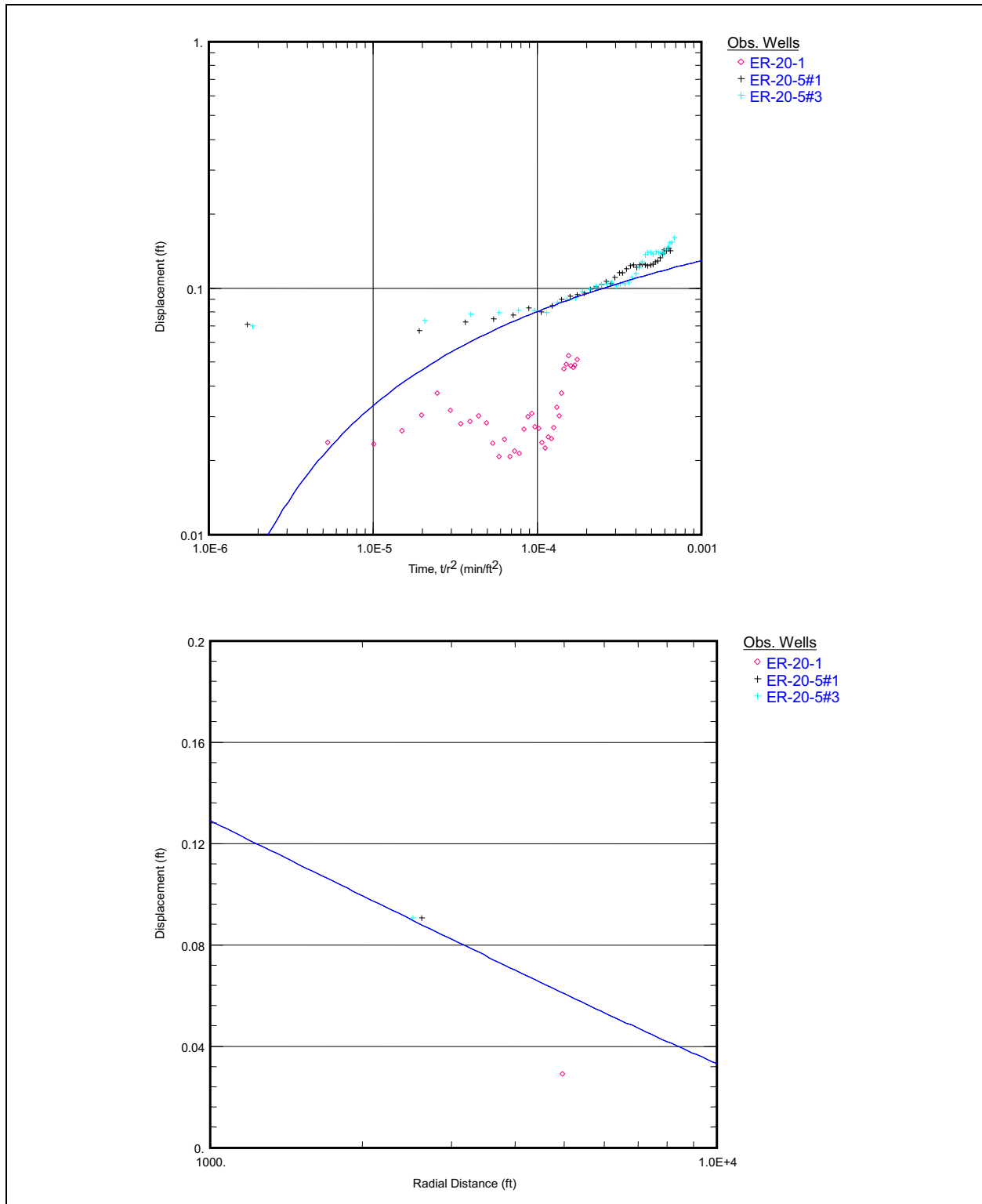
Figure 5-5
Composite Plot for ER-20-7 Pumping Observation Wells, and Distance-Drawdown Plot for ER-20-7 Pumping Observation Wells

3. Distance-drawdown analysis of these data indicates that ER-20-1 drawdown is much less than anticipated based on its distance from ER-20-7 (the pumping well). As mentioned above, this may be due to the relatively short screened interval and the fault disrupting the flow path.

4. Distance-drawdown analysis of ER-20-5 #1 and ER-20-5 #3 indicates that in both cases, drawdown is similar to that which would be anticipated if the system were uniform and fully connected. This is significant for ER-20-5 #3 because of the zeolitized bedded tuff between the TSA and the CHZCM rhyolitic lava.

Data from ER-20-7 were noisy when the pump was running. This was determined to be from electrical interference between the pump's power line and the transducer to data logger cable. However, when a similarly noisy signal (same transducer model) was compared with that from an integrated transducer/logger, the non-interfered data plotted approximately through the middle of the noisy data (Londergan, 2011). Processing the signal to identify the full response via the standard log-log diagnostic plot was not attempted. Rather, it was assumed that flow conditions were infinite acting and radial, and a Cooper-Jacob semi-log analysis was performed with the program AQTESOLV (Duffield, 2007). The results are shown in Figure 5-6. The transmissivity (16,000 square feet per day [ft^2/d]) is about five times higher than the total Paintbrush unit (UPCU, TCA, LPCU, and TSA) suggested by Halford et al. (2010); because this is the pumping well, the storativity estimate is not valid. Furthermore, because the analysis conceptual model was assumed, statistical measures of uncertainty are not valid. Depending on how the straight line is drawn through the data, the range of transmissivity is roughly between 5,000 and 40,000 ft^2/d.

5.2.2 Hydraulic Responses from ER-20-8 #2 Scrugham Peak Aquifer Pumping

Table 5-2 shows the map distances between ER-20-8 #2 and the observation wells (Halford et al., 2010).

When ER-20-8 #2 (SPA) is pumped (composite plot shown in Figure 5-7; Theis solution also shown for comparison), the following observations are made:

1. All the completions at ER-20-8 respond. The shallow SPA/BA completion shows the most response, which is consistent with a direct connection between the two horizons. However, the two deeper completions show responses not long thereafter, requiring some kind of vertical communication.
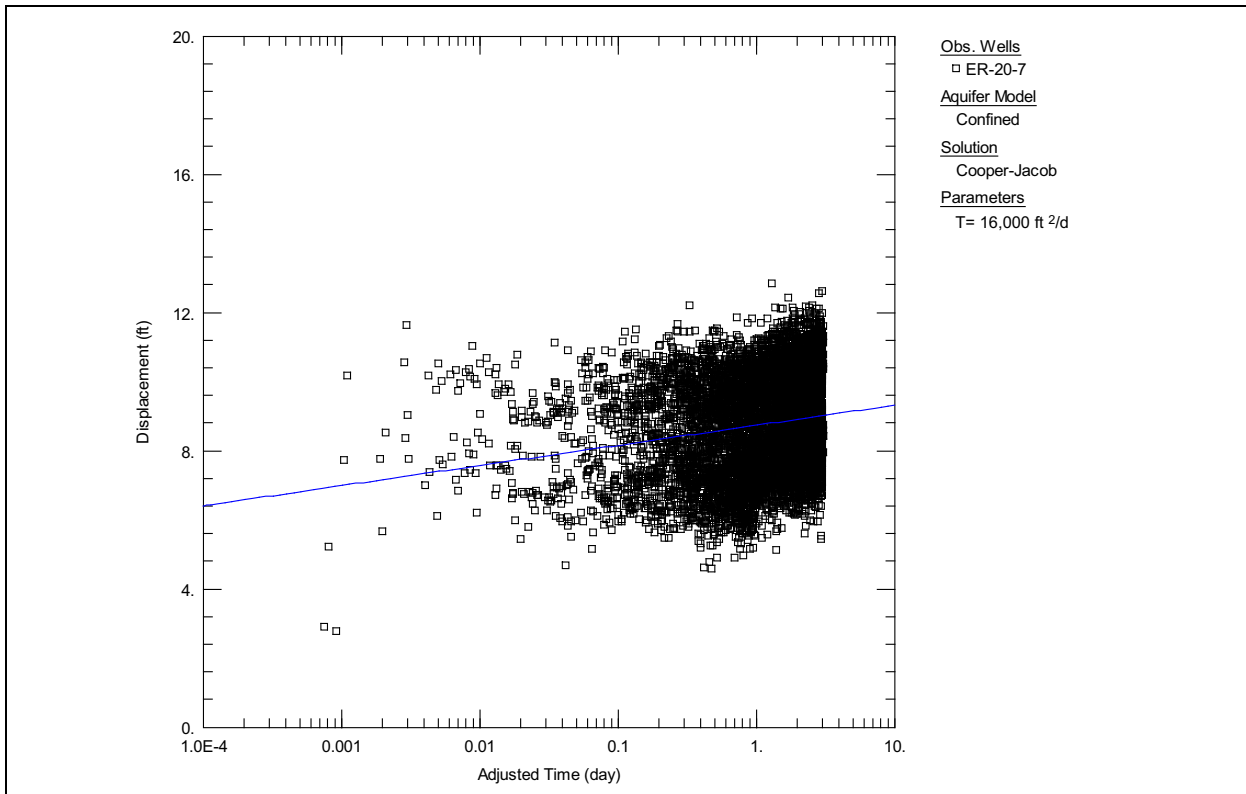
Figure 5-6
Cooper-Jacob Analysis of ER-20-7 Drawdown Data

Table 5-2
Distances between ER-20-8 #2 and Observation Wells

Well Name	Distance from ER-20-8 #2 (ft)
ER-20-7	7,450
ER-20-8D	50
ER-20-8I	50
ER-20-8S	50
ER-EC-11-LI	6,220
ER-EC-11-UI	6,220
ER-EC-6D	6,740
ER-EC-6I	6,740
ER-EC-6S	6,740
ER-EC-1	16,870
ER-20-1	11,770

Source: Modified from Halford et al., 2010
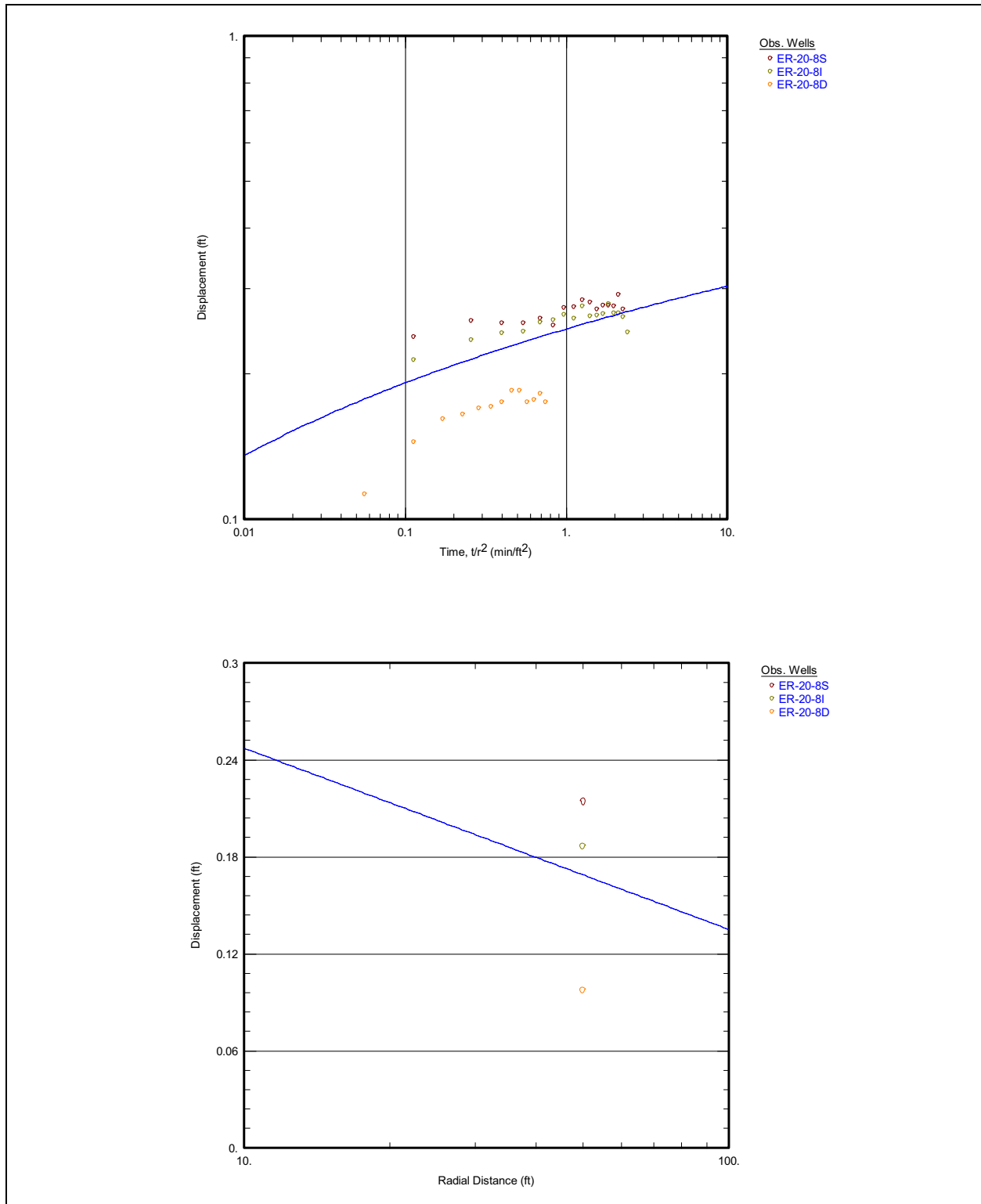
Figure 5-7
Composite Plot for ER-20-8 #2 Pumping Observation Wells

2. The intermediate completion shows more response than the deep, which suggests a shorter connection to the interval. The ER-20-8 fault (with about 300 ft of displacement [NNSA/NSO, 2011a]) could explain the observed behavior. Alternatively, Halford et al. (2010) suggests that leaky aquitards may exist between the SPA/BA, TCA, and TSA.

3. When ER-EC-11 main (TSA/TCA) was pumped, the response in the deeper TSA was earlier than the TCA. The difference may indicate that the TSA is the primary hydraulic pathway and indicate higher conductivity between ER-EC-11 and ER-20-8.

5.2.3 Hydraulic Responses from ER-EC-11 Main Topopah Spring and Tiva Canyon Aquifer Pumping

Table 5-3 shows the map distances between ER-EC-11 and the observation wells (Halford et al., 2010).

Table 5-3
Distances between ER-EC-11 and Observation Wells

Well Name	Distance from ER-EC-11 (ft)
ER-20-5 #1	9,670
ER-20-5 #3	9,650
ER-20-7	7,250
ER-20-8D	6,250
ER-20-8I	6,250
ER-20-8S	6,250
ER-EC-1	10,700
ER-EC-6D	3,250
ER-EC-6I	3,250
ER-EC-6S	3,250
ER-20-1	9,130

Source: Modified from Halford et al., 2010

The observation well data for the second, larger phase of drawdown (from about May 10 to May 19, 2010) was considered (Figure 5-8) and the following observations made:

1. Hydraulic responses are observed in TSA, TCA, BA, and SPA well completions. The ER-20-7 fault or the ER-20-1 fault could explain the observed behavior. Alternatively, Halford et al. (2010) suggests that leaky aquitards may exist between the SPA/BA, TCA, and TSA.
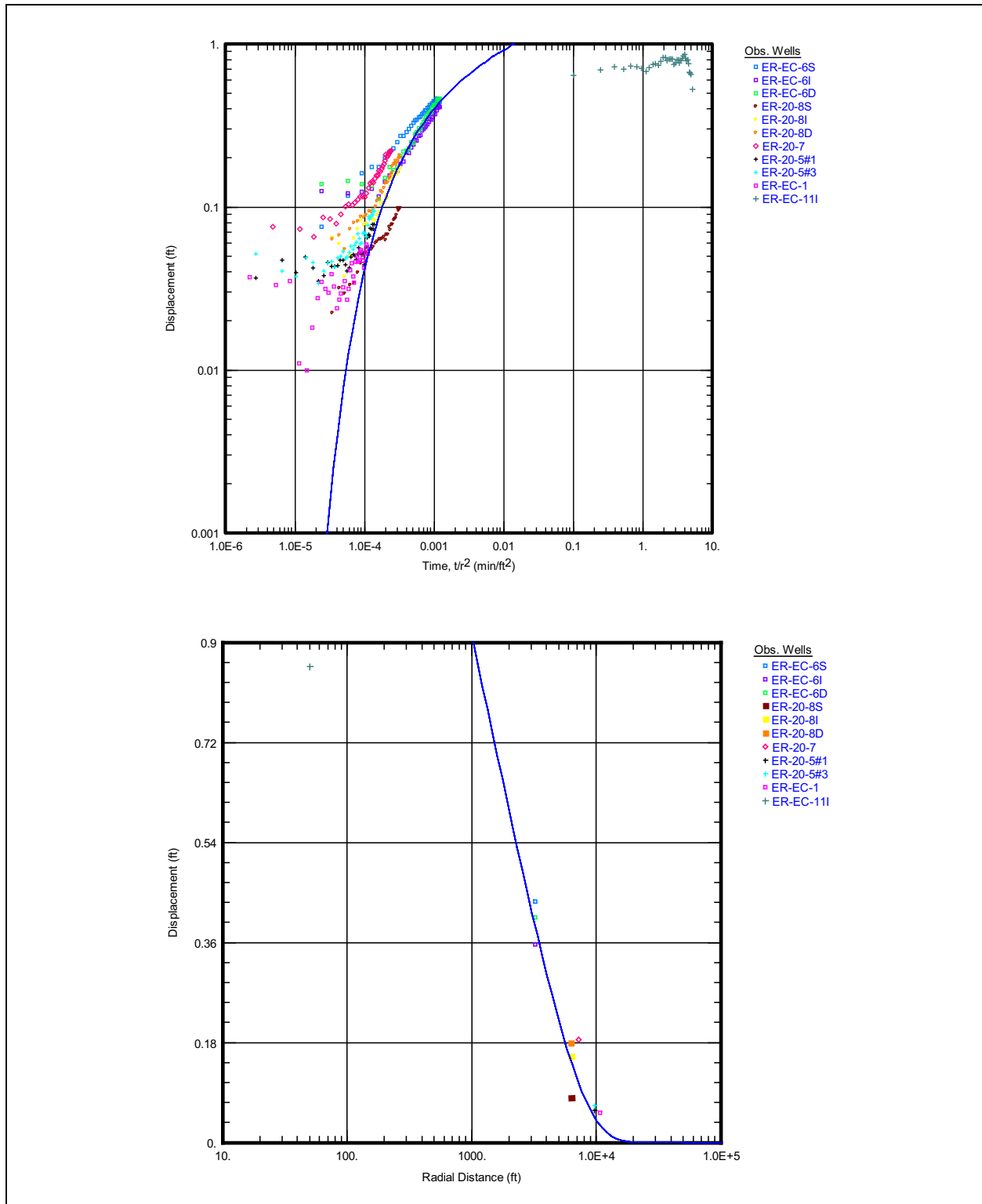
Figure 5-8
Composite Plot for ER-EC-11 Main Pumping Observation Wells,
and Distance-Drawdown Plot for ER-EC-11 Main Pumping Observations Wells

2. Hydraulic diffusivity is not equivalent among the responding well completions when the composite plot is examined (Figure 5-8). This result demonstrates that while the aquifers in this portion of Pahute Mesa are connected, the response is enhanced along some pathways (for instance, the BA and SPA might have been expected to show little response according to the initial conceptual model) and attenuated along others. The Theis solution is also shown for comparison.

3. Section B-B' (Figure 1-3) shows a tuff confining unit between the ER-20-7 fault and the SPA completion of ER-20-8 and ER-20-8 #2. The hydraulic response apparent at ER-20-8S indicates that the TCA and/or TSA of ER-EC-11 are connected to the shallow SPA at ER-20-8S, although not as well as the deeper intervals. This can be explained by drawdown transmission through a leaky aquitard (Halford et al., 2010), or through a fault such as the ER-20-7 fault. Depending on the transmissivity of the SPA, estimated to be quite high by Halford et al. (2010), this aquitard "wrapper" may not be permissible with the hydraulic data.

4. All the ER-EC-6 completions respond at similar time. One explanation is that the postulated ER-20-1 fault (Figure 5-4) cross connects all the formations, and that the fault-crossing zeolitic tuff confining units are permeable. Another explanation is that the aquitards are quite leaky (Halford et al., 2010). Because the shallow completion (BA) responds earlier than the TSA and TCA completions, this would require both leaky aquitards and a BA with higher diffusivity than the TCA and TSA, which is how the model of Halford et al. (2010) generates the fit to this data. In the absence of good single-well tests allowing diagnosis of the interpretive model, the conceptual uncertainty cannot be resolved.

5. Similar to the early response in the BA at ER-EC-6, the TSA response at ER-20-7 has a high diffusivity, responds nearly in concert with ER-EC-6S (BA), and is clearly better connected to the pumped interval of ER-EC-11 main than most of the other observation points. Of note is that the map distance to ER-20-7 is greater than the distance to several of the other responding wells, and the structure (Table 5-3, Figure 1-1) is thought to have up to 2,200 ft of vertical offset in the TSA across this distance. This response suggests alternative interpretations as follows: (1) the NTMMSZ itself provides a rapid connection (is a conduit) between these two well completions; and/or (2) the displacement across the NTMMSZ is not as large as previously thought, allowing juxtaposition or otherwise not causing as much head loss as might have been expected. The NTMMSZ does not appear to be a barrier.

6. The TCA and TSA completions of ER-20-8 behave similarly, in contrast to the SPA completion, which shows a lower peak response and a time lag in response relative to the distance between the wells. The ER-EC-11 pumped intervals, the TSA and TCA, show the clearest response in ER-20-8, based on proximity and the presence of all units of interest. The response in ER-20-8D (TSA) suggest a higher diffusivity than observed for ER-20-8I, reflecting the higher anticipated transmissivity of the TSA than the TCA.

7. The lower peak of the ER-20-8S (SPA piezometer) response implies different diffusivity along the path from ER-EC-11. It could be the degree of connection in the fault (less), path length of the connection (more), or in the transmissivity of the SPA (lower, assuming

the same storativity as TCA and TSA). The lower transmissivity of the SPA for this piezometer is reasonable given that the completion is a short interval (9.3 m) in the stony lava interior of the rhyolitic lava, which may have somewhat lower fracture intensity than the overlying and underlying vitrophyres (Prothro, 2010).

8. Responses were also observed in ER-20-5 #1, ER-20-5 #3, and ER-EC-1. These flow paths appear to have lower diffusivity values to the other observed pathways through the aquifer systems.

9. Distance-drawdown (Figure 5-8) shows that many of the wells respond within a reasonable range of a theoretical Theis response based on the total drawdown and the well locations. All wells located north of the NTMMSZ (ER-20-5 #1, ER-20-5 #3, and ER-20-7) respond with higher drawdown than anticipated based on their Euclidian distance. A particularly strong connection is observed at ER-20-7, further indicating that this pathway is significantly enhanced compared to the anticipate pressure wave propagation to this well location. Conversely, the distance-drawdown analysis shows that ER-20-8S (SPA) has significantly less drawdown than would be expected at this location.

5.3   Observations and Conclusions

1. The drawdown data do not show responses consistent with any prototypical aquifer response (e.g., infinite acting radial flow, linear flow).

2. Drawdown data suggest that enhanced pathways exist due to faulting, but that these enhancements are not uniform nor are they ubiquitous among all units in all directions.

3. The NTMMSZ appears to provide significant connections and enhancement in hydraulic responses across the structure.

4. Vertical connections between the three major water-bearing units (SPA/BA, TCA, and TSA) appear to exist along faults.

5. The hydraulic diffusivity observed in all aquifer tests indicates that the diffusivity value for the TSA is greater than the TCA.

6.0   OTHER SUPPORTING INFORMATION

During the drilling and testing of ER-20-7, ER-20-8 #2, and ER-EC-11, a large amount of information was collected, some of which can be used to support flow system interpretation. That information is summarized here.

6.1   Water Production during Drilling

The drilling method used for ER wells under saturated conditions is rotary tool with underbalanced air-foam and conventional circulation. This approach limits the amount of water and other drilling fluids that need to be introduced to the formations during drilling. As mentioned in Section 2.0, LiBr is added to drilling fluid to help estimate water production volumes during drilling and the efficacy of well development. During drilling operations, the bit advances down the hole, and the water inflow from the formation that reaches the bit is circulated up to the surface using pumps and hydraulic lines. This water quantity is shown in Figures 6-1 through 6-3 as estimated water production profiles for ER-20-7 (NNES, 2010b), ER-20-8 #2 (NNES, 2010c), and ER-EC-11 (NNES, 2010d). The relative change in flow can be considered a qualitative indicator of the formation hydraulic conductivity in the saturated zone. This information is qualitative and dependent on many unmeasured, downhole conditions including pump pressures, formation pressures, and other items.

Figure 6-1 (ER-20-7) shows that low water production began immediately below the water table in the Tiva Canyon moderately welded tuff (the TCA HSU) with low production through the bedded Paintbrush tuff. Production increased markedly in the Topopah Spring moderate to densely welded tuff (the TSA HSU), reaching a maximum about in the middle, with no clear pattern of diminution to the bottom of the unit, although reduced inflow is suggested in the bottom 100 ft of the hole. The hydrologic conceptual model of a welded-tuff aquifer is that flow will be concentrated in the fractures that will tend to be in the most densely welded middle of the ash flow (Figure 5-3). The onset location of flow is generally consistent with this conceptual model, and the reduction in flow toward
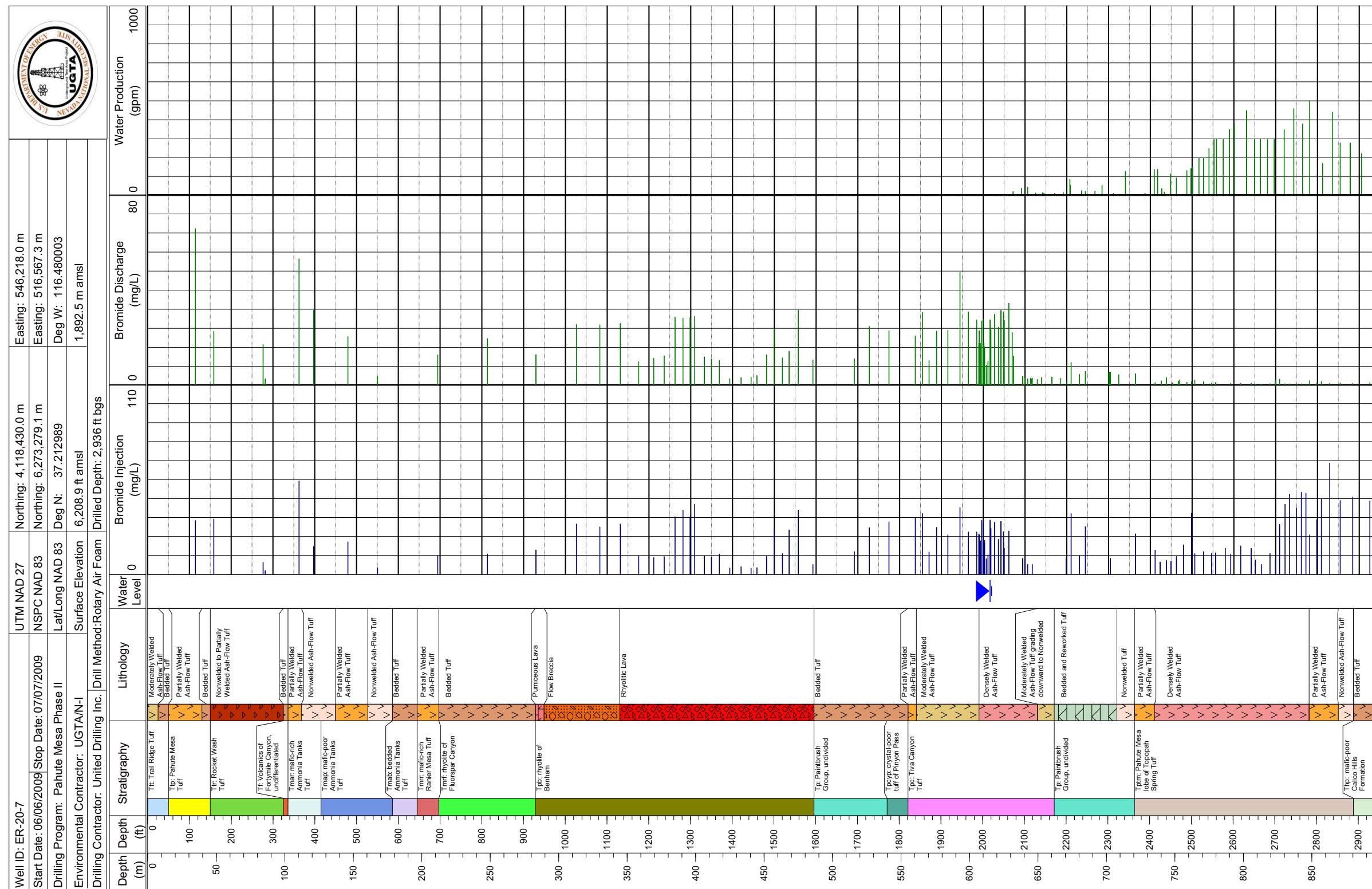
Figure 6-1
Well ER-20-7 Water Production during Drilling
Source: Modified from NNES, 2010b; NNSA/NSO, 2010a
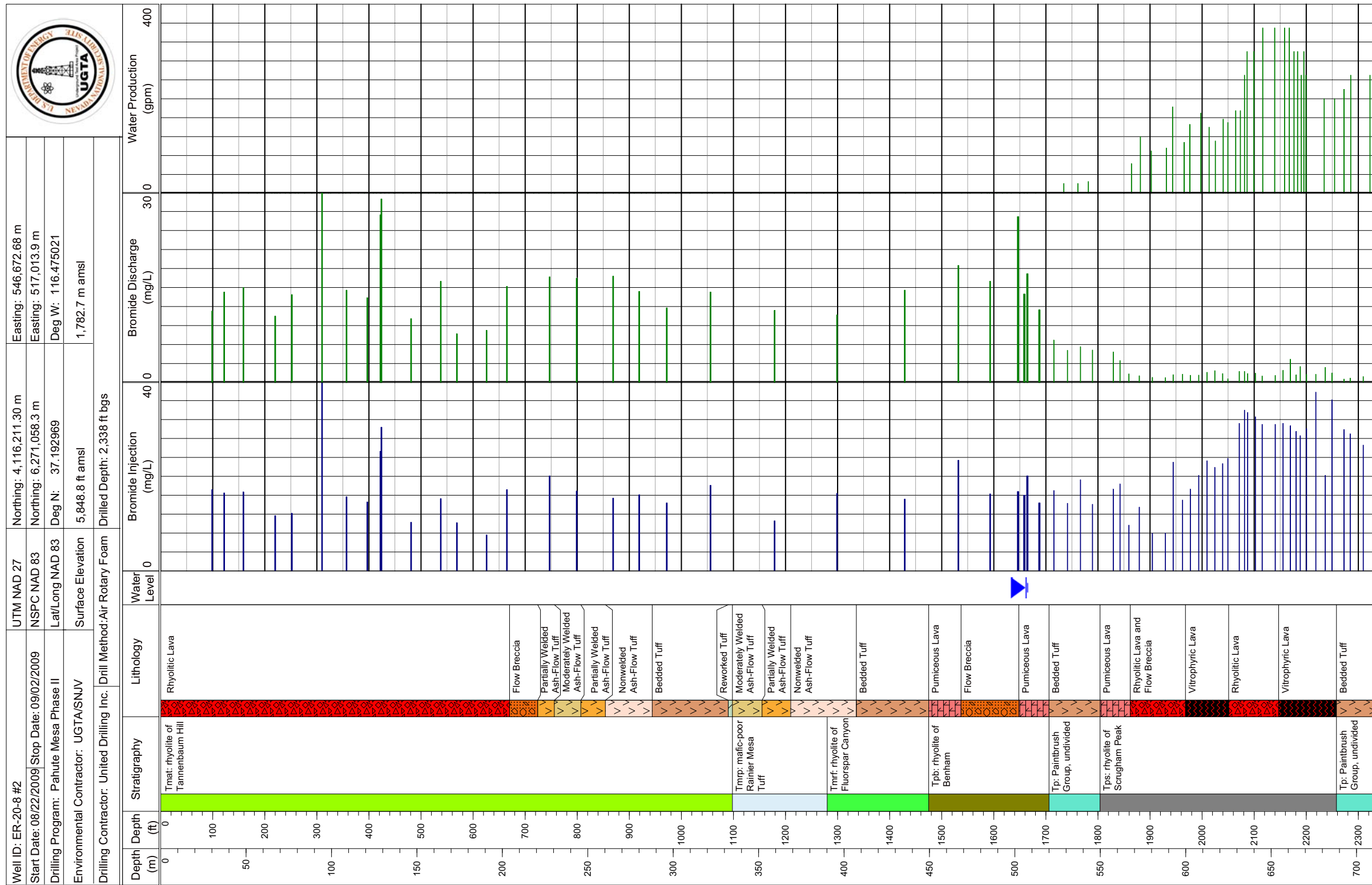
Figure 6-2
Well ER-20-8 #2 Water Production during Drilling
Source: Modified from NNES, 2010c; NNSA/NSO, 2011a
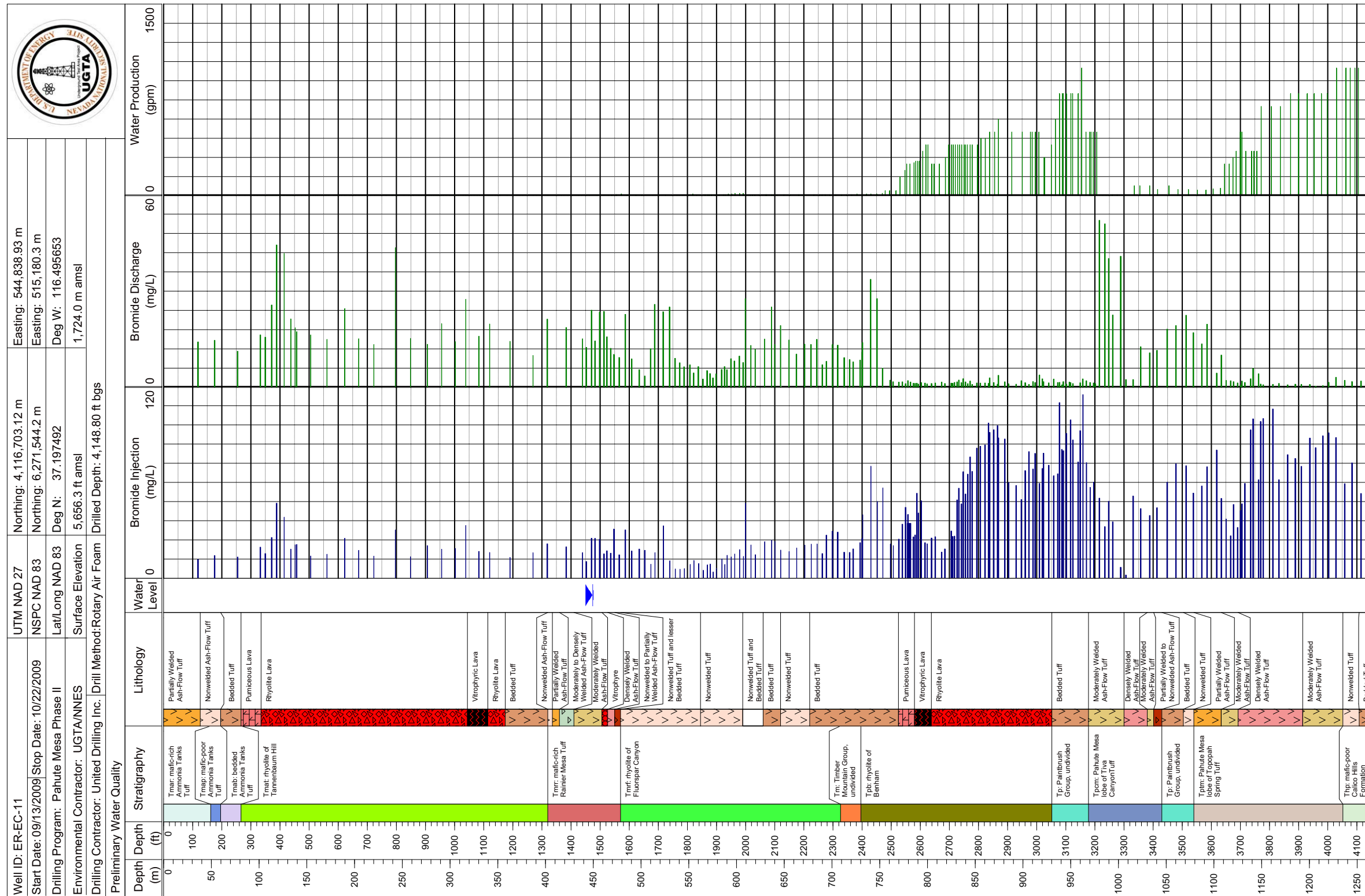
Figure 6-3
Well ER-EC-11 Water Production during Drilling
Source: Modified from NNES, 2010d; NNSA/NSO, 2010b

the bottom of the ash flow is consistent with the lower fracture intensity expected away from the center of the unit.

Sporadic low production began just below the water table when ER-20-8 #2 was drilled (Figure 6-2) in the bedded tuff at the bottom of the Benham formation. The hydrologic conceptual model for this interval is that it has very low fracture intensity and, if saturated, is zeolitized, implying flow should be minimal. Production increases slightly in the pumiceous lava at the top of the Scrugham Peak formation, consistent with the conceptual model, and continues to increase through the flow breccia and into the vitrophyric and rhyolitic lava where the fracturing is conceptualized to be most intense. There is some production decline at the bottom Scrugham Peak formation, which is broadly consistent with a reduction in fracture intensity at the base of rhyolitic lava flows. Observations of water production in the bedded ash-fall tuffs (TCU hydrogeologic unit [HGU]) may indicate that flow from overlying ash-flow tuffs or lava enters the hole after the bit advances, relieving local drilling-induced pressures, or may reflect the presence of flow in fractures that are noted in borehole image logs of Well ER-20-8.

When drilling ER-EC-11, there was almost no production through the bedded tuff from 1,560 to 2,520 ft bgs, which NNSA/NSO (2010b) states has undergone zeolitic alteration making the interval into the TCU HGU, which conceptually transmits water poorly. Production increased in the pumiceous top of the Benham formation lava and continued at about the same rate throughout the remainder of the Benham formation, even in the tuffaceous bottom interval. Once casing was set, production immediately decreased in the moderately to densely welded (but incorporating abundant) lithophysae Tiva Canyon tuff (the TCA HSU), and through the bedded Paintbrush tuffs. The production decline in the TCA compared to the rhyolitic lava is consistent with the conceptual model because of the extensive presence of lithophysae that can disrupt the formation of cooling fractures, which is the interpretation of the production data. Consistent with the conceptual model of an ash-flow tuff (Figure 5-3), increased production occurred at the top of the moderately to densely welded Topopah Spring tuff (the TSA HSU) and similarly to the bottom of the formation.

6.2   Flow Logging

Flow logging can be useful for determining the hydrologic significance of geologic features and, when run under static borehole conditions, for directly evaluating formation potential differences.

No usable flow logs were obtained for ER-20-7 (N-I, 2010a).

Flow logging during pumping at ER-20-8 #2 was performed by Baker Atlas (spinner, reservoir performance monitor [RPM] tools) and DRI (thermal flowmeter [TFM]) concurrent with the end of the well-development/step-drawdown pumping testing operations on December 1 and 2, 2009. The tools measured the vertical velocity of water in the cased portion of the well, and the resulting logs provide cumulative vertical flows in each interval shown as a blue bar (Figure 6-4). Most of the inflow occurs in the rhyolitic and vitrophyric lava, which is generally consistent with the conceptual model of a lava-flow aquifer.

Desert Research Institute performed non-stressed (static) TFM logging at ER-20-8 #2 on April 28 and 29, 2010, and on June 17, 2010; the results are shown in Figure 6-5. The static TFM logging provides information on natural-gradient driven flow in the well, which reflects head relationships (N-I, 2010b).

Flow logs (spinner, RPM, and thermal pulse) in ER-EC-11 were run by Baker Atlas in the intermediate and the deep piezometers (monitoring the TCA and TSA HSUs) while the well was being pumped. Figure 6-6 shows representative flow (RPM final station log results) and temperature logs for the stressed condition. The RPM flow logs are approximate indicators of flow in the main casing, but the results suggest that approximately 85 percent of the production during pumping came from the lower completion interval, and most of that from the upper 200 ft of the lower interval (3,800 to 3,600 ft bgs). Most of the production from the upper completion interval originated from a short interval near the center of the interval (approximately 3,350 to 3,000 ft bgs). The spinner and TFM logs reflect flow distribution in the piezometers, and generally indicate low flow rates, as expected. The static condition TFM logs run by DRI in the main completion yielded very little interpretable valid results. The logging of the intermediate and deep (TCA and TSA HSU) piezometers showed downward flow between the formations (the bridge plug between TCA and TSA was not yet replaced).
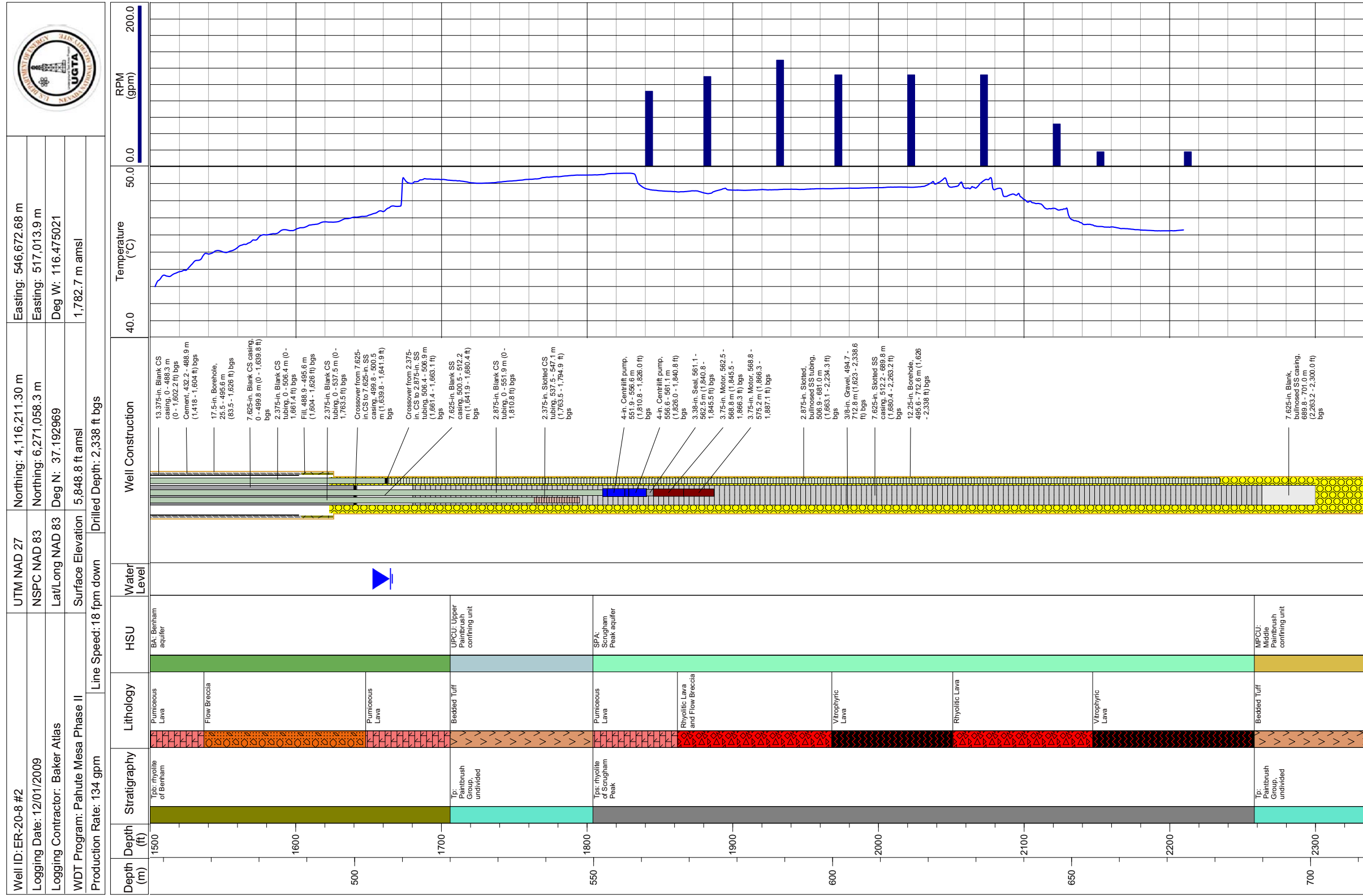
Figure 6-4
Spinner and RPM Logs for ER-20-8 #2 while Pumping
Source: Modified from N-I, 2010b; NNSA/NSO, 2011a
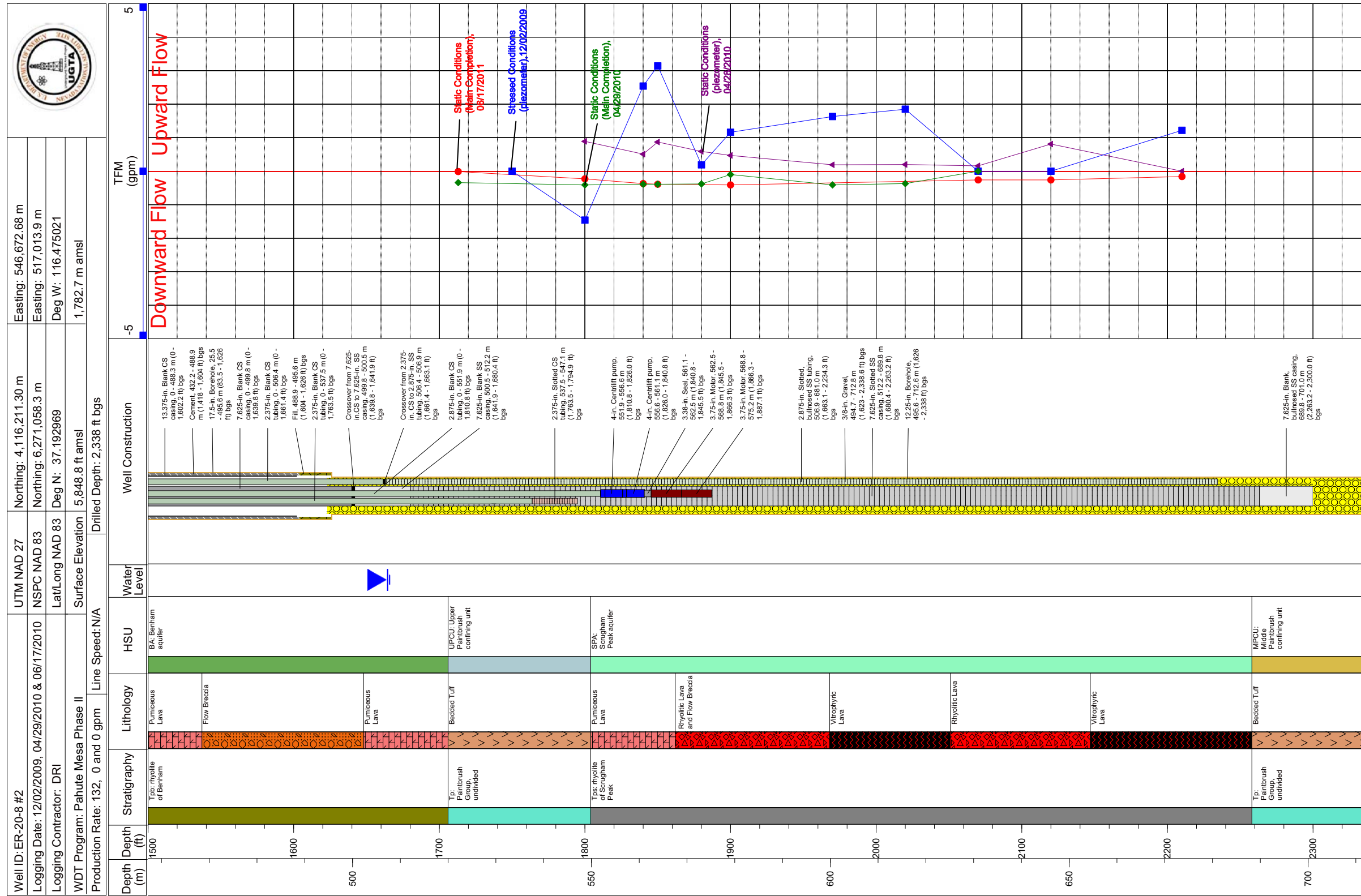
Figure 6-5
TFM Log under Static Conditions for ER-20-8 #2
Source: Modified from N-I, 2010b; NNSA/NSO, 2011a
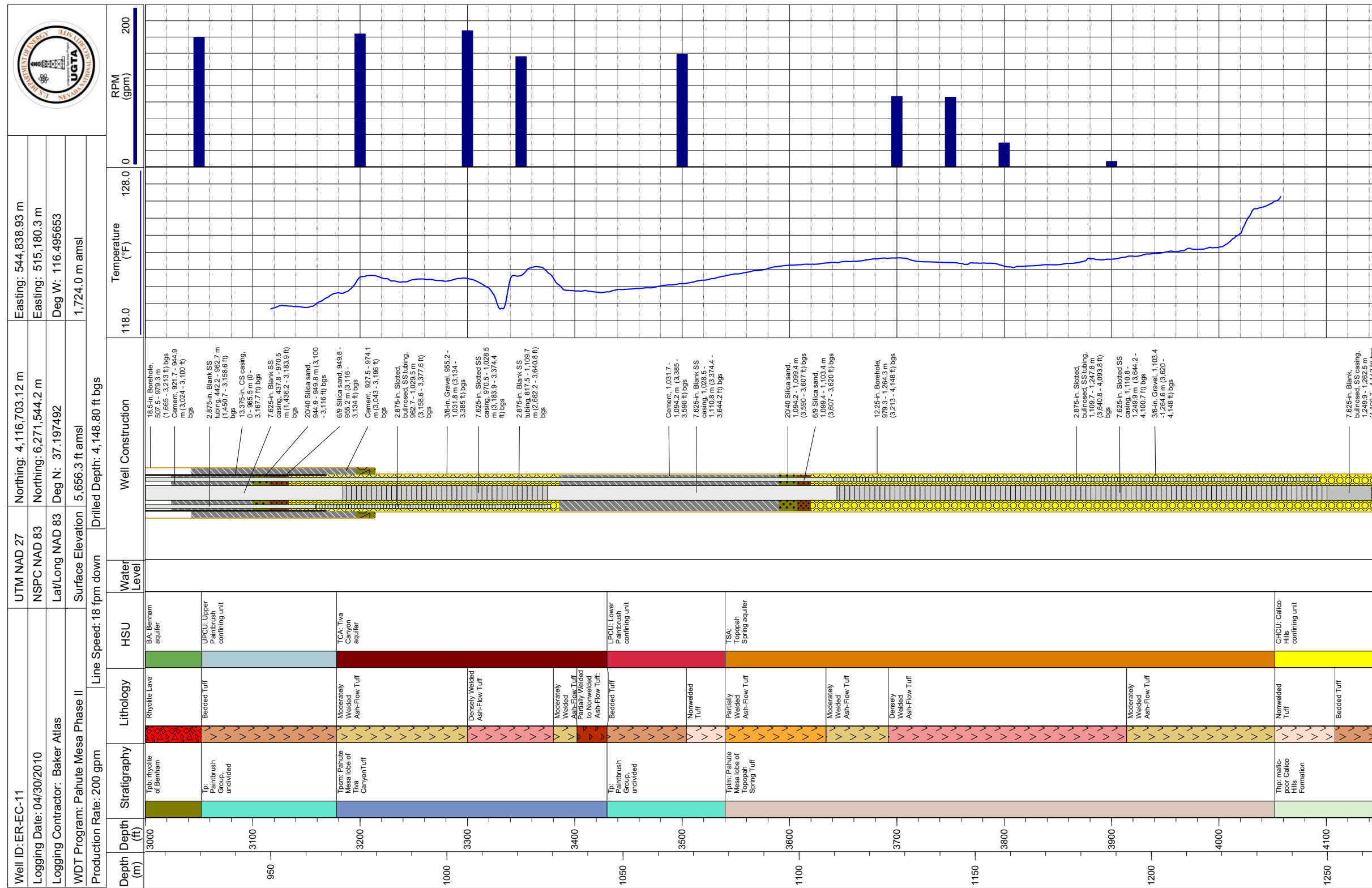
Figure 6-6
Temperature and RPM Logs from ER-EC-11 under Pumping Conditions
Source: Modified from N-I, 2010c; NNSA/NSO, 2010b

6.3   Temperature Logging

Variation in temperature can be used to infer hydraulic properties due to heat transport (Stallman, 1963; Anderson, 2005; Gillespie, 2005). Temperature logs collected at various stages of drilling and testing are qualitatively reviewed—no quantitative interpretation is attempted. The data are unlikely in thermal equilibrium due to the well drilling and development work, but can be evaluated to screen potential relationships associated with transitions between flowing and low/no flow intervals.

Gillespie (2005) provides an example of a temperature profile used during an earlier investigation of the relationship between flow distribution within formations and temperature distribution down a borehole (Figure 6-7). At Well PM-1, Gillespie (2005) identified four different regions: from the water table to 965 m bgs, 965 to 1,595 m bgs, 1,595 to 2,040 m bgs, and 2,040 m bgs. The interval below 1,595 m bgs is densely welded tuff, and Gillespie suggests that the low heat flow computed for the interval may be due to horizontal groundwater flow. More importantly, for the purpose of the qualitative analysis discussed here, there are minor variations in thermal gradient with lithology compared to what is seen in the wells considered by Gillespie, possibly reflecting that the boreholes have not achieved thermal equilibrium. However, the use of these data to further investigate and test conceptual distribution of flow in the subsurface allows for insight into the constraints and relationships among the aquifers and confining units.

On October 11, 2010, DRI logged temperature and pH under ambient conditions at ER-20-7 after the WDT activities shown in Figure 6-8 (N-I, 2010a). The stable groundwater temperatures from 2,420 ft bgs to approximately 2,750 ft bgs suggest advective dispersal of heat by groundwater flow—conceptually consistent with the presence of TSA in this interval and water production observed during drilling. The steadily increasing groundwater temperatures below 2,750 ft bgs indicate low flow in the less welded and bedded tuffs, although lower thermal conductivity of these rocks will result in a higher temperature gradient (Gillespie, 2005).

Well ER-20-8 #2 was logged for temperature at pumping and static conditions (N-I, 2010b) as shown in Figure 6-9. The static temperature log shows a cooler zone below about 2,080 ft bgs (in the vitrophyric lava), with a rise throughout the flow breccia, and pumiceous and bedded tuffs. The
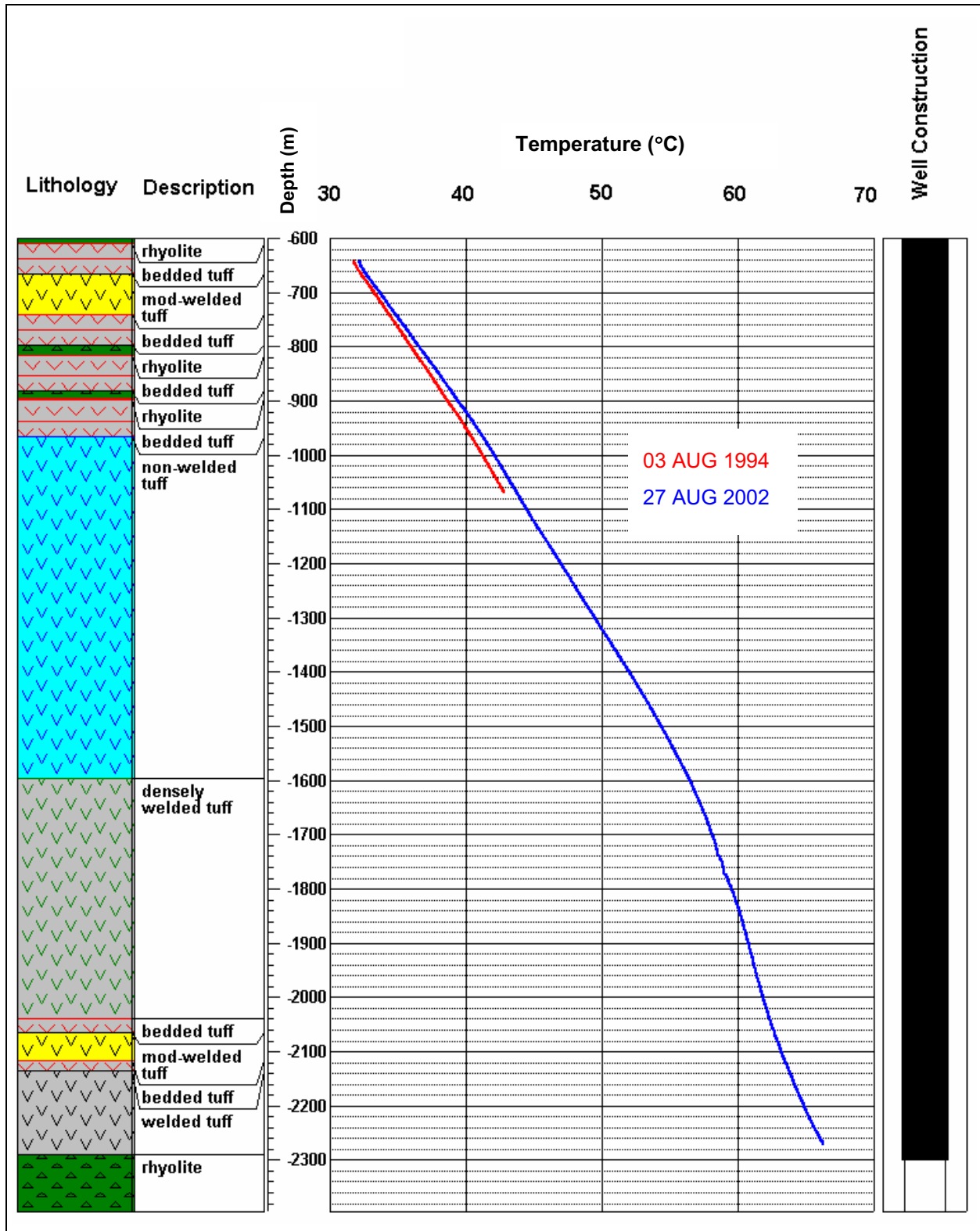
Figure 6-7
Temperature Profiles, Lithology, and Well Construction for Well PM-1
Source: Gillespie, 2005
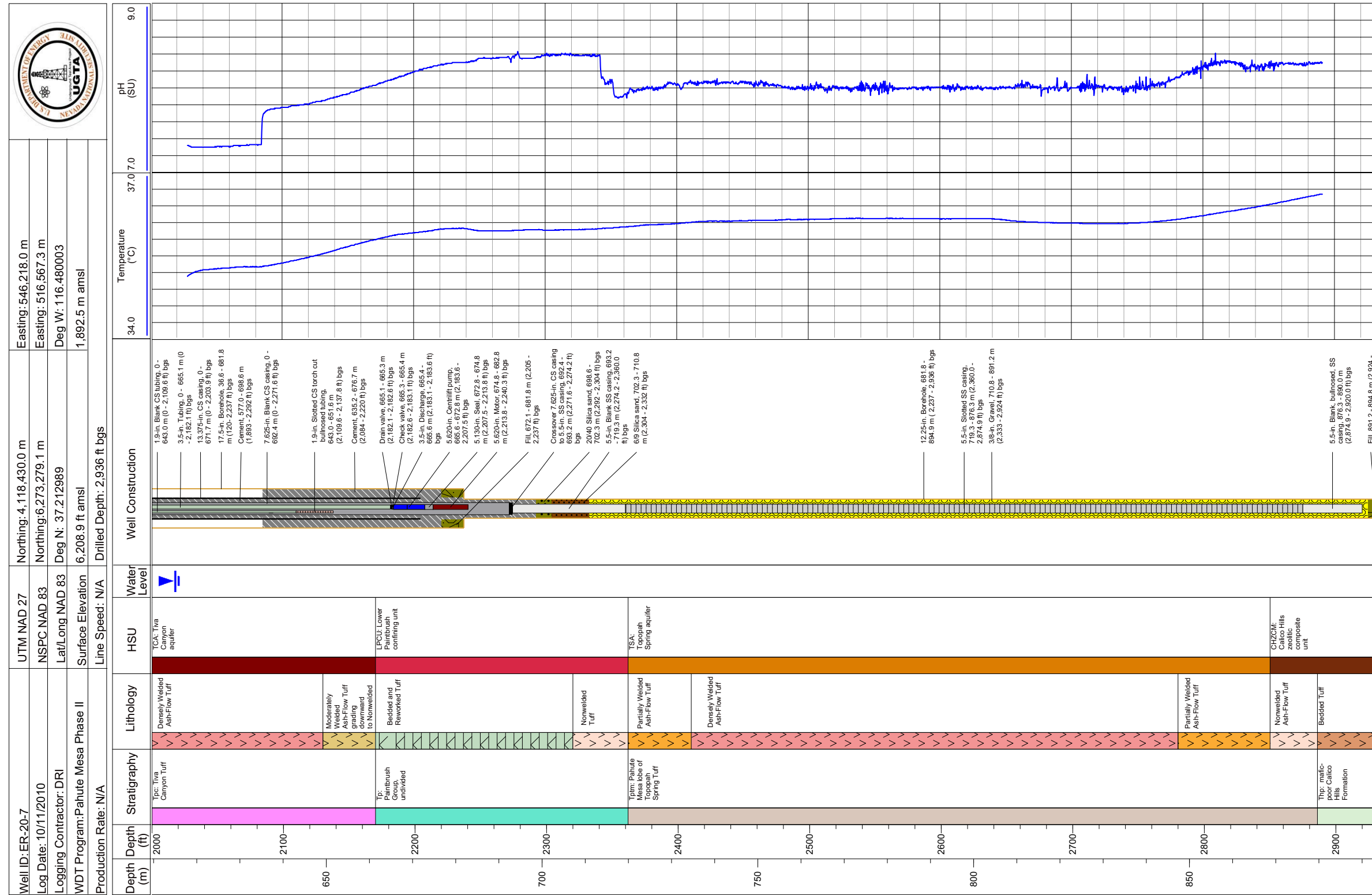
Figure 6-8
Temperature and pH Logs at ER-20-7 under Ambient Conditions
Source: Modified from N-I, 2010a; NNSA/NSO, 2010a
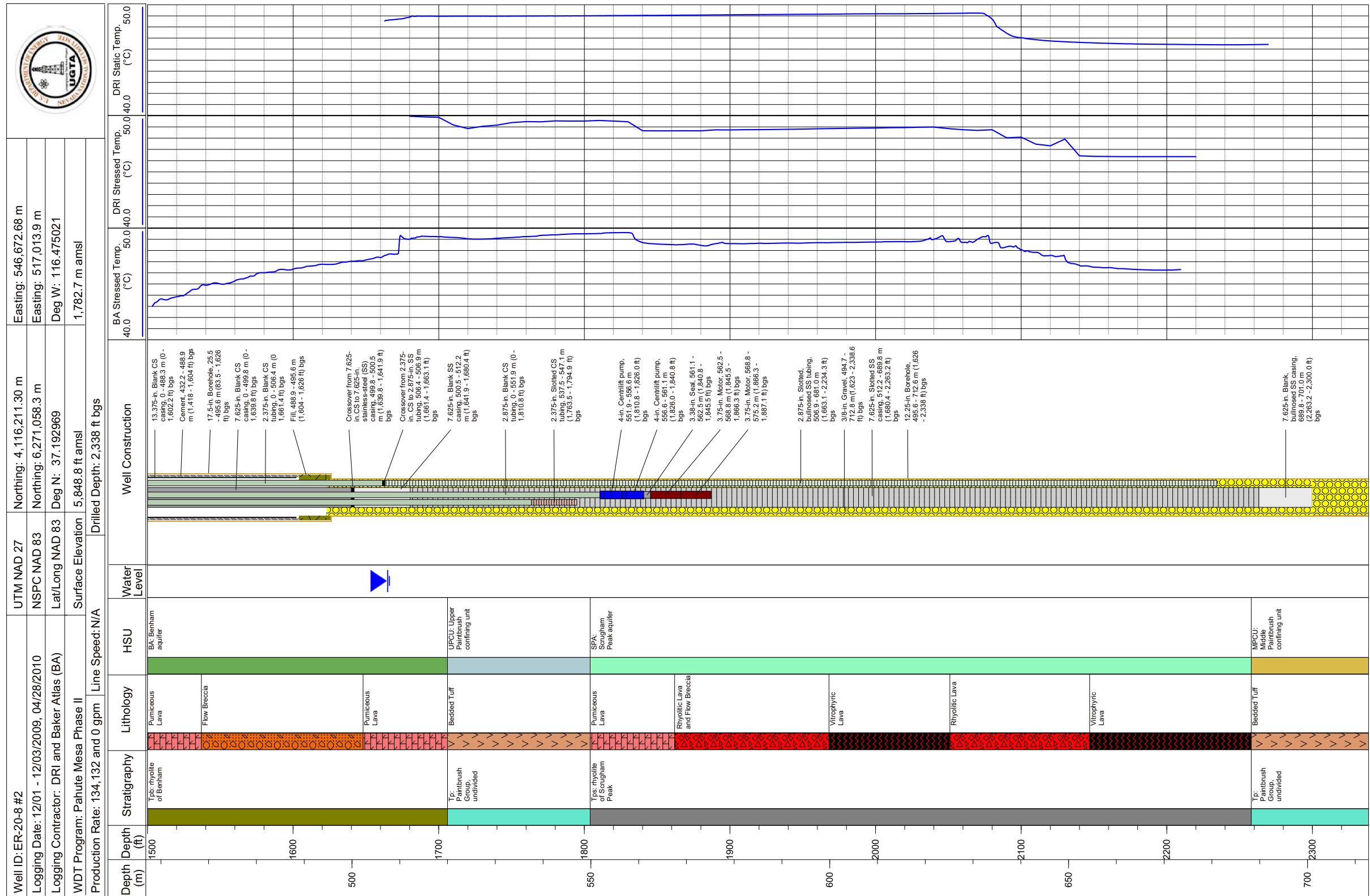
Figure 6-9
ER-20-8 #2 Temperature Logs under Stressed and Ambient Conditions
Source: Modified from N-I, 2010b; NNSA/NSO, 2011a

location of this temperature change is near the first major inflow detected in stressed flow logging (Figure 6-4); thus, this temperature perturbation is from lateral groundwater flow into the borehole and mixing the water vertically within the flowing interval.

The main completion and intermediate and deep piezometers of ER-EC-11 were logged on June 13 and 14, 2010 (bridge plug reinstalled June 29, 2010). The temperature, pH, and electrical conductivity results for the main completion are shown in Figure 6-10—the results for the piezometers are nearly identical. The low temperature gradients from 4,040 to 3,700 ft bgs, 3,380 to 3,200 ft bgs, and 3,020 to 2,740 ft bgs suggest lateral groundwater flow is disturbing the temperature profile. These zones are also generally coincident with drilling water production and flow logging inflow locations. Conversely, the presence of temperature gradients between 3,660 to 3,380 ft bgs, 3,200 to 3,040 ft bgs, and above 2,540 ft bgs suggests little lateral groundwater flow, consistent with these units comprising mostly bedded tuff.

The diverse volcanic rock lithologies encountered at ER-20-7, ER-20-8 #2, and ER-EC-11 include unaltered nonwelded and bedded tuffs, altered (zeolitic) tuffs, variably welded ash-flow tuffs, and pumiceous to vitrophyric rhyolitic lava. The dependency of any conclusions from the temperature on the variation in thermal conductivity should be considered. Gillespie (2005) has reviewed thermal properties for NNSS rocks and temperature profiles at selected NNSS wells. Laboratory thermal conductivity for volcanic rock types are shown in Figure 6-11. The range is relatively narrow.
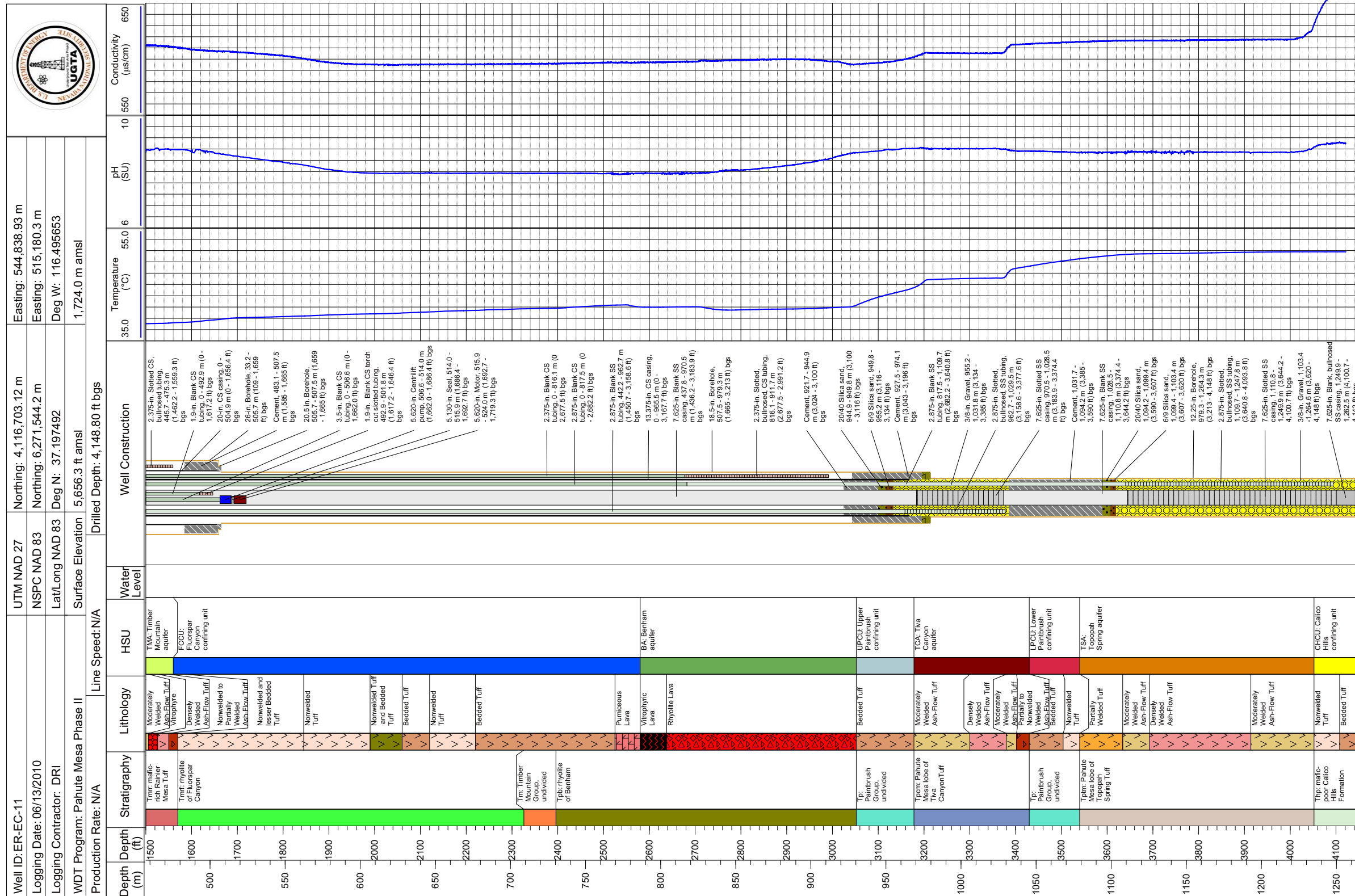
Figure 6-10
ER-EC-11 Main Completion Temperature, pH, and Electrical Conductivity Logs
Source: Modified from N-I, 2010c; NNSA/NSO, 2010b
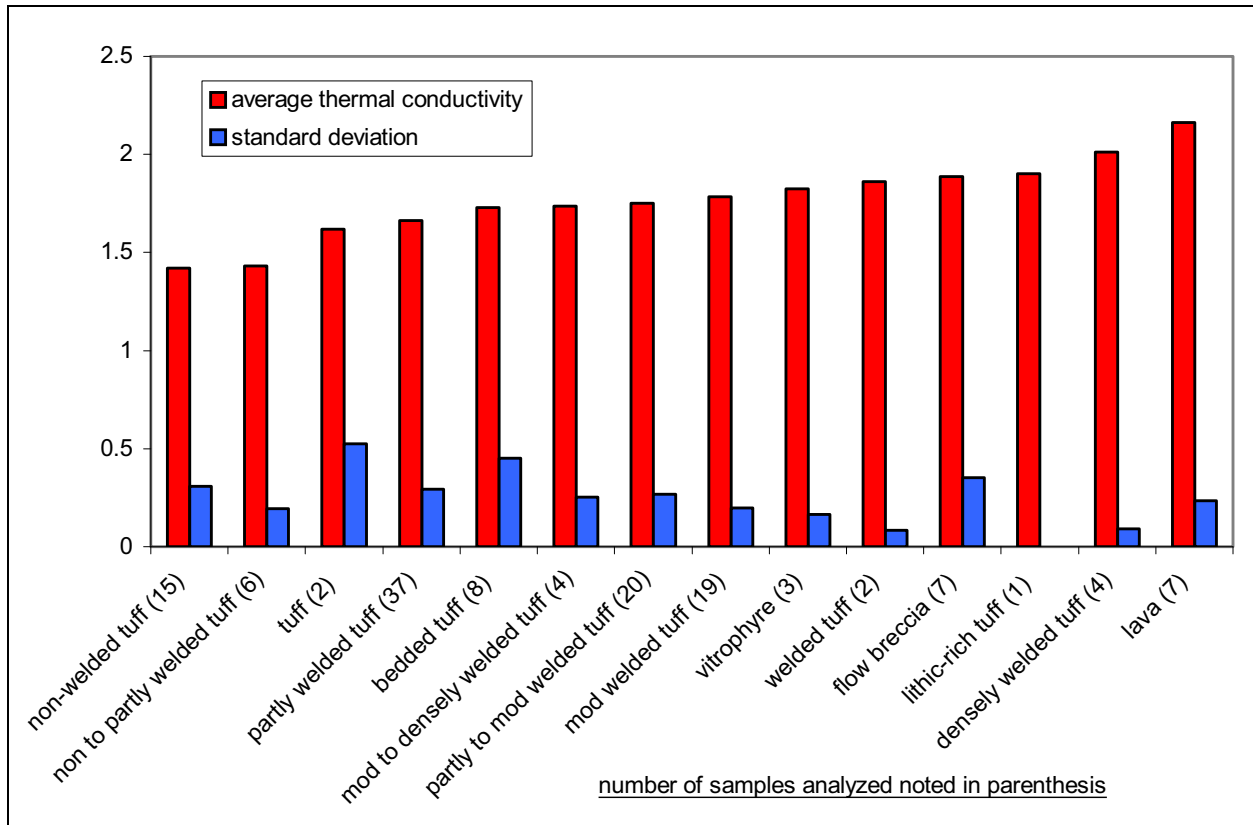
Figure 6-11
Laboratory Measured Thermal Conductivity Values (watt per m °C)
for Tertiary Lithologies
Source: Gillespie, 2005

7.0 *S*MALL-SCALE *C*ONCEPTUAL *M*ODEL OF *S*OUTHWEST *A*REA 20 AND THE *B*ENCH

The Phase II corrective action investigation for Pahute Mesa emphasizes the importance of understanding the flow path from southwest Area 20 to Oasis Valley. Of particular interest is the area between the SCCC and the Timber Mountain caldera structural margin where the rocks present in southwest Area 20 have been downdropped up to 2,200 ft along the NTMMSZ in an area known as the Bench (Section 1.0). Furthermore, the rocks in the area are reasonably permeable and contiguous, circumstances that are favorable for radioactive groundwater to migrate from underground tests. The flow paths through large structures, the properties of rocks on either side of the structure, and any flow and transport properties of the structures themselves are not directly measured, and are the focus of Phase II characterization activities. As part of the Phase II characterization effort, ER-20-7, ER-20-8#2, and ER-EC-11 were pumped for the purpose of development and sampling, HSU transmissivity estimation, and drawdown observations at distal wells in this critical area.

Characterization of the NTMMSZ was considered during WDT operations. Specifically, static head measurements—the new wells are closer to the NTMMSZ than any previous—were examined to see whether the NTMMSZ affects the potentiometric surface (Section 3.0). Although the structure is orthogonal to groundwater flow, similar to the Purse Fault in Figure 3-1, the new data indicate there is no detectable difference of the potentiometric due to the NTMMSZ. This result is in contrast to the obvious influence of the Purse Fault on the local flow directions. The new data are consistent with the *de facto* NTMMSZ conceptual model implemented in the Phase I model, which had the alteration of permeability in the structural zone mostly neutral, and relied upon juxtaposition and HSU properties to direct flow through the structure. The exact configuration of HSUs across the NTMMSZ is unknown, and it is possible that there is enough juxtaposed transmissivity across the structure to not significantly impede groundwater flow. This is the interpretation of Halford et al. (2010). It is also possible, based on the fault damage zone conceptual model (Caine and Forster, 1999), that the structure itself has a direct role in conducting groundwater flow through the

area—conceptually acting as a manifold. This could imply that there is little low-permeability core. In tension with this interpretation is Faunt's (1997) suggestion that, because of the regional stress field, faults that strike northwest-southeast should be in compression and closed. The NTMMSZ is thought to be related to the foundering of a block of the SCCC and the adjacent inter-caldera area into the Timber Mountain caldera (BN, 2002). Vertical profiles of hydraulic head generally showed a downward hydraulic gradient (Section 3.1), consistent with flow logging, with up to potentially several meters of head difference.

The drawdown response data at wells distal from the pumping wells provided additional insight into the role of structure and stratigraphy (Section 5.2). Overall, the most striking result from these data is how well connected the formations are vertically (through multiple aquitards) and laterally through faults and the NTMMSZ. Of particular interest is that ER-20-7, completed in the TSA on the upside of the NTMMSZ (closer to the underground nuclear tests), responded as fast to pumping at ER-EC-11 as ER-EC-6, which is closer to ER-EC-11 and the downdropped side of the NTMMSZ (Figures 5-5 and 5-4). These data confirm the concept that the NTMMSZ is more or less transparent to groundwater flow, but not how this transparency occurs. The vertical connection between formations is illustrated by the response to ER-EC-11 pumping at ER-EC-6, and the response at ER-20-8 from ER-20-8 #2 pumping (Figure 5-8). The postulated ER-20-1 fault (also roughly coincident with a fault segment identified at the surface by Slate et al. [1999] [Figure 5-4]), with either the fault-damage zone concepts in zeolitic rocks (Section 5.0) or juxtaposition (the fault offset is not known accurately), provides a straightforward explanation of why all three horizons respond nearly identically, when pumping at ER-EC-11 is only from the bottom two HSUs. In the case of ER-20-8 #2, pumping the uppermost HSU, the SPA, results in rapid drawdown in the *lowermost* HSUs, the TCA and the TSA (Figure 5-7). The NNSA/NSO (2011b) report states the following (references have been rewritten to reflect those in this document):

> *"The Topopah Spring Tuff in Well ER-20-8 is 88.4 to 110.6 m (290 to 363 ft) thinner than in other holes in the area such as Wells ER-EC-6 (DOE/NV, 2000), ER-20-7 (NNSA/NSO, 2010a), ER-EC-11 (NNSA/NSO, 2010b), and ER-20-5#3 (DOE/NV, 1997). The proximity of these wells to Well ER-20-8 suggests that the thinning is not related to depositional processes (i.e., stratigraphic thinning) but instead to faulting (i.e., structural thinning). This means that the Well ER-20-8 borehole intercepted a fault that effectively cuts out approximately 91.4 m (300 ft) of Topopah Spring Tuff in*

> *the well. Detailed analyses of data from the well…indicate that the fault is within the Topopah Spring Tuff and not at the top or base of the unit."*

That this fault, eliminating 300 ft of TSA, is acting as a conduit is the most direct explanation—juxtaposition is not a factor because both wells are in the same fault block.

Broadly, the flow paths from a two-dimensional potentiometric map (Figure 3-1) are the same as those estimated from geochemical data. Kwicklis et al. (2005) and Rose et al. (2006) analyzed flow paths from southwestern Pahute Mesa based upon several tracers, including Cl⁻ and δD. Samples from new and existing wells suggest that the general conclusions about the flow paths from geochemical data are still the same (Section 4.0). However, a more local inspection of the data shows that there is a transition zone from groundwater with a Cl⁻ concentration of about 10 mg/L to PM-3-type groundwater with a concentration of about 95 mg/L (Figure 4-3). Observations include the following:

- The Cl⁻ concentration in ER-EC-11 is virtually the same in all completions (although the intermediate TCA completion has a different calcium/magnesium concentration), and is about half of the PM-3 end member (Figure 4-3). Based on the analysis of Kwicklis et al. (2005) and Rose et al. (2006), a southeast flow direction from ER-EC-1 would be required to create the observed mixing.

- Well ER-20-1 has a Cl⁻ concentration about half of PM-3 (Figure 4-3). Hydraulically, it seems unlikely that water could flow due southeast across the Purse fault for 4.5 kilometers to mix with water from the east.

- The Cl⁻ concentration is only slightly greater in ER-20-1 than that in ER-EC-11 and ER-EC-6 suggesting possible flow from the north (along the ER-20-1 fault?) mixing with more dilute water from the northeast (e.g., U-20 Water Well [Figure 4-3]).

- The Cl⁻ concentration in ER-20-5 #1 and #3, and ER-20-8 #2 is about a quarter of PM-3, but about twice of the wells to the north (e.g., U-20 Water Well [Figure 4-3]). Hydraulically, it is not probable that water has crossed the southern part of the Purse fault to create this chemistry. The δD also shows a trend to heavier water in the Bench area that is difficult to explain with complete segregation of the flow system west of the Purse fault until the NTMMSZ is reached, inconsistent with the Phase I groundwater flow paths.

The entire Purse Fault was essentially a no-flow boundary in the Phase I flow model (SNJV, 2006). This did not allow for any water balance uncertainty in the northern inflow component, and forced the majority of the water flowing through the area roughly between the Purse and Boxcar faults to come

from the east, which did reasonably match the estimated mixing ratios in some cases. A somewhat different conceptual model of the Purse fault can be generated by noting that Fenelon et al. (2010) infer a small inflow component of what would be PM-3-type water across the Purse fault in north-central Area 20 (Figure 3-1). This flow would go due south and is a potential explanation for the Cl⁻ concentrations seen in the vicinity of southwest Area 20. However, the basic premise of the Purse fault, that it restricts flow into Area 20, does not change.

Groundwater samples for radionuclide analysis were collected during drilling, at discrete depths in piezometers with bailers, and from screened intervals during pumping (see Table A.1-5). Observations include the following:

- Although there is some imprecision in the sample depth, tritium concentrations increased during drilling ER-20-7 to a maximum in about the center of the TSA, roughly consistent with the conceptual model of a welded, non-lithophysal ash-flow tuff. The apparent tritium concentrations in the LPCU are probably an artifact of no groundwater inflow through the unit (Section 6.0), meaning the samples are really representative of the TCA.

- Tritium was reported during ER-20-8 #2 drilling, with the samples from the completion interval (SPA/BA) at the end of the WDT at roughly 1,000 pCi/L.

- Tritium was detected primarily in the BA at ER-EC-11 during drilling, with possible detection at the top of the TCA (which could be still circulating water from the BA). This suggests that the flow through the NTMMSZ does not result in complete mixing of water vertically among the aquifers of the Bench.

The Pahute Mesa Phase I (SNJV, 2009) and Frenchman Flat Phase II transport model (NNES, 2010a) results suggested that tritium, ^{14}C, ^{36}Cl, ^{99}Tc, and ^{129}I would be the radionuclide most likely encountered in groundwater away from underground nuclear tests. Results for ^{14}C and ^{36}Cl have yet to be obtained, but no ^{129}I was detected in any of the samples from these wells. Technetium-99 was detected in ER-20-7 groundwater at concentrations about 50 times lower than the regulatory limit of 900 pCi/L (CFR, 2011). These preliminary data suggest that either the mobility or inventory of ^{99}Tc and ^{129}I may have been overestimated in Phase I transport calculations.

In summary, a working conceptual model of the area has the following features and uncertainties:

1. Faulting has created vertical pathways for groundwater leakage. Geologic and drawdown data clearly support this concept. However, radionuclide concentration data do not indicate that the leakage is ubiquitous and/or homogenous.

    Uncertainty
    The fault damage zone is the mechanism that creates the pathway. How ubiquitous are these zones? Halford et al. (2010) did not simulate the effect of individual faults on the test interference data, but more broadly changed the TCU properties. Conceptually, this would allow diffuse leakage, rather than concentrated leakage, between aquifers. With respect to the radionuclide profile at ER-EC-11, if the relative flow rates are much different in the aquifers, the radionuclides may be diluted to low levels—there still may be migration in the other units. This effect would not become clear until (if) very high concentrations such as those at ER-20-7 cross the structure.

2. The distribution of secondary porosity (fracturing) influences groundwater flow pathways and the distribution of radionuclides within HSUs. The conceptual fracture distributions shown in Figures 7-1 and 7-2 for the TCA and TSA, respectively, indicate that the rock is not ubiquitously fractured through the entire HSU. Observations of tritium concentrations that are higher in the central portion of the TSA and the top of the TCA support this conclusion.

    Uncertainty
    The heterogeneity of the system is large, the permeability of the aquifer units is high, and the faulted TCU provides for leakage among the units. Vertical variations of radionuclide concentration within HSUs are only a reflection of local variations of vertical leakage, and these processes are effectively uniform at the scale of the Bench.

3. The hydraulic responses throughout the Bench, indicating that diffusivity of the TSA is higher than the TCA, support the more fractured nature of the TSA and the hypothesis that the presence of lithophysae in the TCA have disrupted the development of cooling fractures in the center of the unit as conceptualized in Figure 7-1. Sweetkind and Williams-Stroud (1996) observed that lower joint frequencies and connectivities occured in the lithophysal zones of the Tiva Canyon and Topopah Spring tuffs at Yucca Mountain.

    Uncertainty
    The large-scale diffusivity and apparent hydraulic responses in the ash-flow aquifers are a reflection of the juxtaposition of the aquifer units and may not be reflective of the extent of fracturing within the unit.
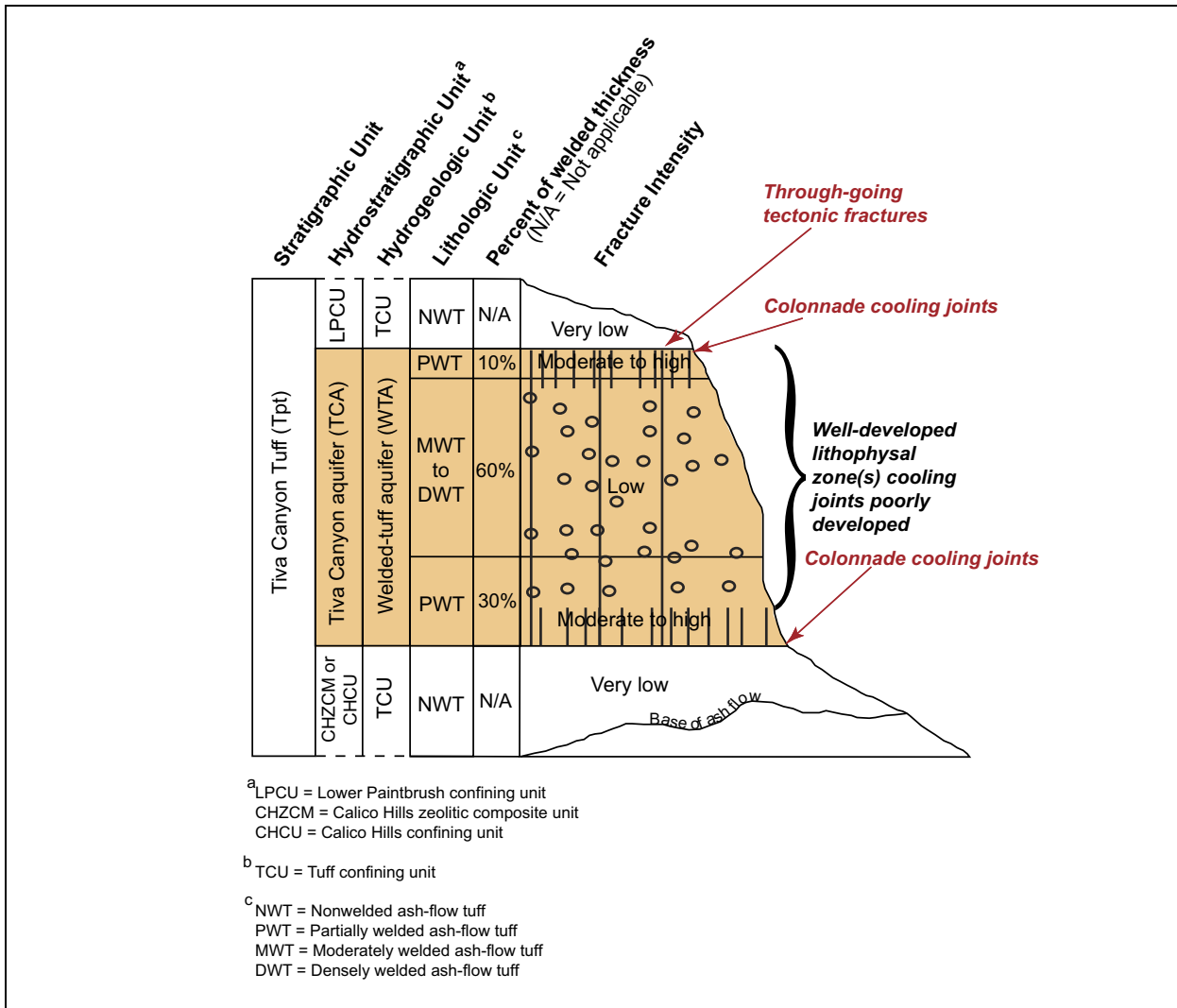
Figure 7-1
Preliminary Conceptual Model of the TCA in Southwestern Pahute Mesa Area
Source: Modified from Drellack, 2010b

4. The presence of only tritium and ^{99}Tc (pending results for ^{14}C and ^{36}Cl) suggests that conclusions drawn from previous calculations about the radionuclides of concern (tritium, ^{14}C, ^{36}Cl, ^{99}Tc, and ^{129}I) are supported by data, but that the mobility or inventory may still be overestimated in some cases.

Uncertainty

The radiological source term, both unclassified and classified, has only general estimates of inventory uncertainty. Additionally, there may be other physical processes that influence the availability of the inventory to groundwater.
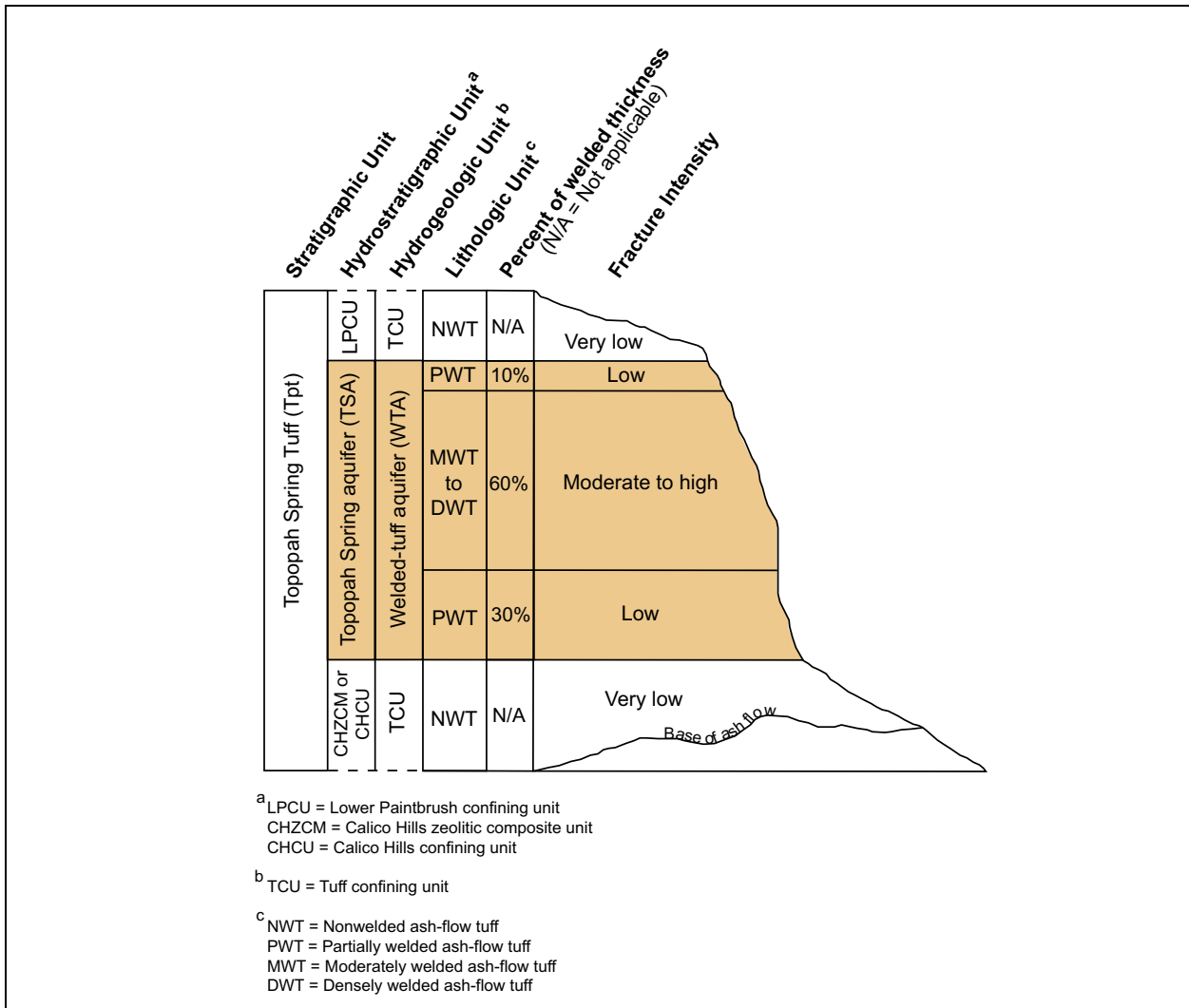
Figure 7-2
Preliminary Conceptual Model of the TSA in Southwestern Pahute Mesa Area
Source: Modified from Drellack, 2010b

8.0   REFERENCES

Anderson, M.P. 2005. "Heat as a Ground Water Tracer." In *Ground Water,* Vol. 43(6): pp. 951–968.

BN, see Bechtel Nevada.

Beauheim, R.L. 2007. "Diffusivity Mapping of Fracture Interconnections." In *Proceedings of the 2007 U.S. EPA/NGWA Fractured Rock Conference*, pp. 235–249. Westerville, OH: U.S. Environmental Protection Agency and National Ground Water Association.

Bechtel Nevada. 2002. *A Hydrostratigraphic Model and Alternatives for the Groundwater Flow and Contaminant Transport Model of Corrective Action Units 101 and 102: Central and Western Pahute Mesa, Nye County, Nevada*, DOE/NV/11718--706. Prepared for the U.S. Department of Energy, National Nuclear Security Administration Nevada Operations Office. Las Vegas, NV.

Blankennagel, R.K., and J.E. Weir, Jr. 1973. *Geohydrology of the Eastern Part of Pahute Mesa, Nevada Test Site, Nye County, Nevada,* Professional Paper 712-B. Denver, CO: U.S. Geological Survey.

Bowen, S.M., D.L. Finnegan, J.L. Thompson, C.M. Miller, P.L. Baca, L.F. Olivas, C.G. Geoffrion, D.K. Smith, W. Goishi, B.K. Esser, J.W. Meadows, N. Namboodiri, and J.F. Wild. 2001. *Nevada Test Site Radionuclide Inventory, 1951-1992,* LA-13859-MS. Los Alamos, NM: Los Alamos National Laboratory.

Byers, F. M., Jr., and D. Cummings. 1967. *Geologic Map of the Scrugham Peak Quadrangle, Nye County, Nevada*. U.S. Geological Survey, Geologic Quadrangle Map GQ-695, scale 1:24,000. Denver, CO: U.S. Geological Survey.

CFR, see *Code of Federal Regulations*.

Caine, J.S., and C.B. Forster. 1999. "Fault Zone Architecture and Fluid Flow: Insights from Field Data and Numerical Modeling." In *Faults and Subsurface Fluid Flow in the Shallow Crust*, Geophysical Monograph 113, pp. 101–127. W.C. Haneberg, P.S. Mozley, J. Casey Moore, and L.B. Goodwin eds. Washington, DC: American Geophysical Union.

Code of Federal Regulations. 2011. Title 40 CFR Part 141, "National Primary Drinking Water Regulations." Washington, DC: U.S. Government Printing Office.

Craig, H. 1961. "Isotopic Variations in Meteoric Waters." In *Science*, Vol. 133(3465): pp. 1702–1703. Washington, DC: American Association for the Advancement of Science.

Criss, R.E. 1999. *Principles of Stable Isotope Distribution*. New York, NY: Oxford University Press.

DOE/NV, see U.S. Department of Energy, Nevada Operations Office.

Drellack, S., National Security Technologies, LLC. 2010a. Personal communication to G. Ruskauff (N-I) and N. DeNovio (Golder Associates, Inc.) regarding the BA Conceptual Model, 15 September. Las Vegas, NV.

Drellack, S., National Security Technologies, LLC. 2010b. Personal communication to N. DeNovio and W. Dershowitz (Golder Associates, Inc.) regarding the TSA Conceptual Model, 26 August Las Vegas, NV.

Drellack, S., National Security Technologies, LLC. 2011a. Personal communication to T. Vogt (N-I) regarding the BA and SPA, 15 July. Las Vegas, NV.

Drellack, S., National Security Technologies, LLC. 2011b. Personal communication to G. Ruskauff (N-I) regarding new buried faults, 12 July. Las Vegas, NV.

Duffield, G.M. 2007. *AQTESOLV for Windows Version 4.5 User's Guide*. Reston, VA: HydroSOLVE, Inc.

EPA, see U.S. Environmental Protection Agency.

Elliott, P.E., and Fenelon, J.M. 2010. *Database of Groundwater Levels and Hydrograph Descriptions for the Nevada Test Site Area, Nye County, Nevada, 1941–2010*, Data Series 533. Reston, VA: U.S. Geological Survey.

FFACO, see *Federal Facility Agreement and Consent Order*.

Faunt, C.C. 1997. *Effect of Faulting on Ground-Water Movement in the Death Valley Region, Nevada and California,* Water-Resources Investigations Report 95-4132. Denver, CO: U.S. Geological Survey.

Federal Facility Agreement and Consent Order. 1996 (as amended March 2010). Agreed to by the State of Nevada; U.S. Department of Energy, Environmental Management; U.S. Department of Defense; and U.S. Department of Energy, Legacy Management. Appendix VI, which contains the Underground Test Area Strategy, was last modified May 2011, Revision No. 4.

Fenelon, J.M., D.S. Sweetkind, and R.J. Laczniak. 2010. *Groundwater Flow Systems at the Nevada Test Site, Nevada: A Synthesis of Potentiometric Contours, Hydrostratigraphy, and Geologic Structures,* Professional Paper 1771. Reston, VA: U.S. Geological Survey.

Fenelon, J., S. Reiner, and K. Halford, U.S. Geological Survey. 2011. Memorandum to B. Thompson (USGS/NNSA) titled "Drawdown Estimation for the ER-20-7 Multi-well Aquifer Test, Pahute Mesa, Nevada National Security Site," 7 March. Henderson, NV.

Geldon, A.L. 2004. *Hydraulic Tests of Miocene Volcanic Rocks at Yucca Mountain and Pahute Mesa and Implications for Groundwater Flow in the Southwest Nevada Volcanic Field, Nevada and California*, GSA Special Papers Vol. 381. 93 p. Boulder, CO: Geological Society of America.

Gillespie, D. 2005. *Temperature Profiles and Hydrologic Implications from the Nevada Test Site Area,* DOE/NV/13609-40; Publication No. 45211. Las Vegas, NV: Desert Research Institute.

HORIBA, see HORIBA, Ltd.

Halford, K., J. Fenelon, and S. Reiner, U.S. Geological Survey. 2010. Memorandum to D. Galloway (RSO–Western Region) titled "AQUIFER-TEST PACKAGE—Analysis of ER-20-8 #2 and ER-EC-11 Multi-well Aquifer Tests, Pahute Mesa, Nevada National Security Site," 27 September. Henderson, NV.

Hickey, J.J. 1989. "An Approach to the Field Study of Hydraulic Gradients in Variable-Salinity Ground Water." In *Ground Water*, Vol. 27(4): pp. 531-539.

HORIBA, Ltd. 2003. *pH Meter F-52/F-53/F-54/F-55 Instruction Manual.* Kyoto, Japan.

Horne, R.N. 1995. *Modern Well Test Analysis: A Computer-Aided Approach*, Second Edition. Palo Alto, CA: Petroway, Inc.

IT, see IT Corporation.

Ingraham, N.L., R.L. Jacobson, J.W. Hess, and B.F. Lyles. 1990. *Stable Isotopic Study of Precipitation and Spring Discharge on the Nevada Test Site*, DOE/NV/10845--03; Publication No. 45078. Las Vegas, NV: Desert Research Institute.

IT Corporation. 1998. *Western Pahute Mesa–Oasis Valley Hydrogeologic Investigation Wells Drilling and Completion Criteria*, Rev. 0, ITLV/13052-049, p. 439. September. Las Vegas, NV.

IT Corporation. 2000a. Written communication. Subject: *Western Pahute Mesa–Oasis Valley Well ER-EC-1 Data Report for Development and Hydraulic Testing*. May. Las Vegas, NV.

IT Corporation. 2000b. Written communication. Subject: *Western Pahute Mesa–Oasis Valley Well ER-EC-6 Data Report for Development and Hydraulic Testing*. May. Las Vegas, NV.

IT Corporation. 2002. Written communication. Subject: *Analysis of Well ER-EC-6 Testing, Western Pahute Mesa–Oasis Valley FY 2000 Testing Program*, Rev. 0. January. Las Vegas, NV.

Knudby, C., and J. Carrera. 2006. "On the Use of Apparent Hydraulic Diffusivity as an Indicator of Connectivity." In *Journal of Hydrology*, Vol. 329(3-4): pp. 377-389.

Kwicklis, E.M., T.P. Rose, and F.C. Benedict, Jr. 2005. *Evaluation of Groundwater Flow in the Pahute Mesa.Oasis Valley Flow System Using Groundwater Chemical and Isotopic Data,* LA-UR-05-4344. Los Alamos, NM: Los Alamos National Laboratory.

Londergan, J. (Navarro-Intera, LLC). 2011. Personal communication to G. Ruskauff (N-I) titled "Comparison of PXD Measurements in the BA/SPA HSU during CRT of the TCA at ER-20-8," 18 August. Las Vegas, NV.

Merlivat, L., and J. Jouzel. 1979. "Global Climatic Interpretation of the Deuterium Oxygen-18 Relationship for Precipitation." In *Journal of Geophysical Research,* Vol. 84(C8): pp. 5029–5033.

N-I, see Navarro-Intera, LLC.

N-I GIS, see Navarro-Intera Geographic Information Systems.

NNES, see Navarro Nevada Environmental Services, LLC.

NNSA/NSO, see U.S. Department of Energy, National Nuclear Security Administration Nevada Site Office.

NNSA/NV, see U.S. Department of Energy, National Nuclear Security Administration Nevada Operations Office.

Navarro-Intera Geographic Information Systems. 2011. ESRI ArcGIS Software.

Navarro-Intera, LLC. 2010a. Written communication. Subject: *Pahute Mesa Phase II ER-20-7 Well Development, Testing, and Sampling Data Report*. June. Las Vegas, NV.

Navarro-Intera, LLC. 2010b. Written communication. Subject: *Pahute Mesa Phase II ER-20-8 #2 Well Development, Testing, and Sampling Data Report*. October. Las Vegas, NV.

Navarro-Intera, LLC. 2010c. Written communication. Subject: *Pahute Mesa Phase II ER-EC-11 Well Development, Testing, and Sampling Data Report*. September. Las Vegas, NV.

Navarro-Intera, LLC. 2011a. Written communication. Subject: "Depth to water level" forms from Field Operations web page. Las Vegas, NV.

Navarro-Intera, LLC. 2011b. Written communication. Subject: *Pahute Mesa Fiscal Year 2010 Long-Term Head Monitoring Data Report*. February. Las Vegas, NV.

Navarro Nevada Environmental Services, LLC. 2010a. *Phase II Transport Model of Corrective Action Unit 98: Frenchman Flat, Nevada Test Site, Nye County, Nevada*, Rev. 1, N-I/28091--004, S-N/99205--122. Las Vegas, NV.

Navarro Nevada Environmental Services, LLC. 2010b. Written communication. Subject: *Pahute Mesa ER-20-7 Well Data Report*. March. Las Vegas, NV.

Navarro Nevada Environmental Services, LLC. 2010c. Written communication. Subject: *Pahute Mesa ER-20-8#2 Well Data Report*. April. Las Vegas, NV.

Navarro Nevada Environmental Services, LLC. 2010d. Written communication. Subject: *Pahute Mesa ER-EC-11 Well Data Report*. April. Las Vegas, NV.

O'Hagan, M.D., and R.J. Laczniak. 1996. *Ground-Water Levels beneath Eastern Pahute Mesa and Vicinity, Nevada Test Site, Nye County, Nevada,* Water-Resources Investigations Report 96-4042. Denver, CO: U.S. Geological Survey.

Pawloski, G.A., T.P. Rose, J.W. Meadows, B.J. Deshler, and J. Watrus. 2002. *Categorization of Underground Nuclear Tests on Pahute Mesa, Nevada Test Site, for Use in Radionuclide Transport Models*, UCRL-TR-208347. Livermore, CA: Lawrence Livermore National Laboratory.

Post, V., H. Kooi, and C. Simmons. 2007. "Using Hydraulic Head Measurements in Variable-Density Ground Water Flow Analyses." In *Ground Water*, Vol. 45(6): pp. 664-671.

Prothro, L.B. 2009. Written communication. Subject: *Analysis and Interpretation of Borehole Image Logs from Well ER-20-7*. October. Las Vegas, NV: National Security Technologies, LLC.

Prothro, L.B. 2010. Written communication. Subject: *Analysis and Interpretation of Borehole Image Logs from Well ER-20-8*. January. Las Vegas, NV: National Security Technologies, LLC.

Prothro, L.B., S.L. Drellack, D.N. Haugstad, H.E. Huckins-Gang, and M.J. Townsend. 2009. *Observations on Faults and Associated Permeability Structures in Hydrogeologic Units at the Nevada Test Site*, DOE/NV/25946--690. Las Vegas, NV: National Security Technologies, LLC.

Rose, T.P., F.C. Benedict, Jr., J.M. Thomas, W.S. Sicke, R.L. Hershey, J.B. Paces, I.M. Farnham, and Z.E. Peterman. 2006. *Geochemical Data Analysis and Interpretation of the Pahute Mesa.Oasis Valley Groundwater Flow System, Nye County, Nevada*, *August 2002,* UCRL-TR-224559. Livermore, CA: Lawrence Livermore National Laboratory; Reno, NV: GeoTrans, Inc., and Desert Research Institute; Denver, CO: U.S. Geological Survey; and Las Vegas, NV: Harry Reid Center for Environmental Studies.

SNJV, see Stoller-Navarro Joint Venture.

Slate, J.L., M.E. Berry, P.D. Rowley, C.J. Fridrich, K.S. Morgan, J.B. Workman, O.D. Young, G.L. Dixon, V.S. Williams, E.H. McKee, D.A. Ponce, T.G. Hildenbrand, W.C. Swadley, S.C. Lundstrom, E.B. Ekren, R.G. Warren, J.C. Cole, R.J. Fleck, M.A. Lanphere, D.A. Sawyer, S.A. Minor, D.J. Grunwald, R.J. Laczniak, C.M. Menges, J.C. Yount, and A.S. Jayko. 1999. *Part A. Digital Geologic Map of the Nevada Test Site and Vicinity, Nye, Lincoln, and Clark Counties, Nevada, and Inyo County, California, Revision 4*, Open-File Report 99-554-A, scale 1:120,000. Denver, CO: U.S. Geological Survey.

Stallman, R.W. 1963. "Computation of Ground-Water Velocity from Temperature Data." In *Methods of Collecting and Interpreting Ground-Water Data*, Vol. 1544-H: pp. H36–H46.

Streltsova, T.D. 1988. *Well Testing in Heterogeneous Formations,* Exxon Monographs Series #5. New York, NY: John Wiley & Sons, Inc.

Stoller-Navarro Joint Venture. 2006. *Groundwater Flow Model of Corrective Action Units 101 and 102: Central and Western Pahute Mesa, Nevada Test Site, Nye County, Nevada*, Rev. 0, S-N/99205--076. Las Vegas, NV.

Stoller-Navarro Joint Venture. 2009. Written communication. Subject: *Preliminary Data Report for Well ER-EC-6 Groundwater Characterization Sampling.* Las Vegas, NV.

Sweetkind, D.S., and S.C. Williams-Stroud. 1996. Written communication. Subject: *Characteristics of Fractures at Yucca Mountain, Nevada: Synthesis Report.* Denver, CO: U.S. Geological Survey.

Sweetkind, D.S., and R.M. Drake, II. 2007. *Characteristics of Fault Zones in Volcanic Rocks near Yucca Flat, Nevada Test Site, Nevada*, Open-File Report 2007-1293. Reston, VA: U.S. Geological Survey.

Thomas, J.M., F.C. Benedict, Jr., T.P. Rose, R.L. Hershey, J.B. Paces, Z.E. Peterman, I.M. Farnham, K.H. Johannesson, A.K. Singh, K.J. Stetzenbach, G.B. Hudson, J.M. Kenneally, G.F. Eaton, and D.K. Smith. 2002. *Geochemical and Isotopic Interpretations of Groundwater Flow in the Oasis Valley Flow System, Southern Nevada,* Water Resources Center, Publication 45190. Las Vegas, NV.

USGS, see U.S. Geological Survey.

U.S. Department of Energy, National Nuclear Security Administration Nevada Operations Office. 2002. *Nevada Test Site Orthophoto Site Atlas,* DOE/NV/11718--604. Aerial photos acquired Summer 1998. Prepared by Bechtel Nevada. Las Vegas, NV.

U.S. Department of Energy, National Nuclear Security Administration Nevada Site Office. 2009. *Phase II Corrective Action Investigation Plan for Corrective Action Units 101 and 102: Central and Western Pahute Mesa, Nevada Test Site, Nye County, Nevada*, DOE/NV--1312-Rev. 2. Las Vegas, NV.

U.S. Department of Energy, National Nuclear Security Administration Nevada Site Office. 2010a. *Completion Report for Well ER-20-7, Corrective Action Units 101 and 102: Central and Western Pahute Mesa*, DOE/NV--1386. Prepared by National Security Technologies, LLC. Las Vegas, NV.

U.S. Department of Energy, National Nuclear Security Administration Nevada Site Office. 2010b. *Completion Report for Well ER-EC-11, Corrective Action Units 101 and 102: Central and Western Pahute Mesa*, DOE/NV--1435. Prepared by National Security Technologies, LLC. Las Vegas, NV.

U.S. Department of Energy, National Nuclear Security Administration Nevada Site Office. 2011a. *Completion Report for Wells ER-20-8 and ER-20-8#2, Corrective Action Units 101 and 102: Central and Western Pahute Mesa*. Prepared by National Security Technologies, LLC. Las Vegas, NV.

U.S. Department of Energy, National Nuclear Security Administration Nevada Site Office. 2011b. *Underground Test Area Quality Assurance Project Plan, Nevada National Security Site, Nevada*, DOE/NV--1450. Las Vegas, NV.

U.S. Department of Energy, Nevada Operations Office. 1997. *Regional Groundwater Flow and Tritium Transport Modeling and Risk Assessment of the Underground Test Area, Nevada Test Site, Nevada*, DOE/NV--477. Las Vegas, NV.

U.S. Department of Energy, Operations Office. 2000. *Completion Report for Well ER-EC-6*, DOE/NV/11718--360. Prepared by Bechtel Nevada. Las Vegas, NV.

U.S. Environmental Protection Agency. 2001. *Monitor Well Development*, Standard Operating Procedure 2044, Rev. 0.1. 23 October. Washington, DC: Environmental Response Team.

U.S. Geological Survey. 2011. *National Field Manual for the Collection of Water-Quality Data: U.S. Geological Survey Techniques of Water-Resources Investigations, Book 9*. As accessed at http://water.usgs.gov/owq/FieldManual on 18 August.

Warren, R.G., G.L. Cole, and D. Walther. 2000. *A Structural Block Model for the Three-Dimensional Geology of the Southwestern Nevada Volcanic Field,* LA-UR-00-5866. Los Alamos, NM: Los Alamos National Laboratory.

Winograd, I.J. 1970. "Noninstrumental Factors Affecting Measurement of Static Water Levels in Deeply Buried Aquifers and Aquitards, Nevada Test Site." In *Ground Water*, Vol. 8(2): pp. 19-28.

Appendix A

Groundwater Chemistry Results

Table A.1-1
Water-Chemistry Data for ER-20-7
(Page 1 of 4)

Analyte	Depth Discrete			Composite Wellhead						
	N-I			N-I		LLNL	USGS			
	2,650 ft	2,535 ft								
	06/30/2009	07/01/2009		09/24/2010						
Miscellaneous and Field Measurements										
Bromide (field) (mg/L)	--	--	--	0.18 [a]			0.21 [a]			
DO (field) (mg/L)	--	---	--	5.99 [a]			3.54 [a]			
pH (field)				7.97 [a]			7.92 [a]			
pH (lab)	8.24 [b]	8.36 [b]	8.49 [b]	8.49 [b]	8.52 [b]	--	--			
SEC (field) (mmhos/cm)	--	---	--	0.522 [a]			0.500 [a]			
SEC (lab) (mmhos/cm)	0.510	0.504	0.515	0.502	0.500	--	--			
Turbidity (NTU)	--	---	--	8.2 [a]			5.0 [a]			
Temperature (°C)	--	--	--	34.1 [a]			34.0 [a]			
Major and Minor Constituents (mg/L)										
Bicarbonate as $CaCO_3$	150	140	150	140	140	--	--	--	--	--
Carbonate as $CaCO_3$	<20	<20	<20	<20	<20	--	--	--	--	--
Bromide	0.29	0.28	0.38	0.15 [b]	0.15 [b]	<0.05	--	--	--	--
Chloride	30	29	29	30	31	29.7	--	--	--	--
Fluoride	5.6	5.5	5.5	6.3	6.3	6.4	--	--	--	--
Sulfate	50	49	49	53	53	49.6	--	--	--	--
Calcium	4.4	4.4	4.1	4.9	4.8	6.6	4.9	5.1	4.3	4.6
Magnesium	0.15 [c]	0.15 [c]	0.13 [c]	<1 [d]	<1 [d]	0.18	<0.4	<0.4	<0.4	<0.4
Potassium	4.3	4.3	4.1	4.9	4.8	3.9	--	--	--	--
Sodium	97	96	98	92	93	118	109	109	102	99
Aluminum	3.9 [b] / 1.9	3.6 [b] / 1.8	3.0 [b] / 1.4	1.7 [b] / 1.5 [b]	1.7 [b] / 1.1 [b]	0.065	1.3	1.1	0.1	0.4
Iron	5.6 [b] / 2.4	6.1 [b] / 2.4	7.4 [b] / 5.8	0.16 [d] / 0.16 [d]	0.17 [d] / <0.10 [d]	0.007	--	--	--	--
Silicon	31 / 26	32 / 26	28 / 24	33 / 33	33 / 32	--	34.6	--	27.3	--
Sulfide	<2 [b]	<2 [b]	<2	<2	<2	--	--	--	--	--
Total Dissolved Solids	430 [b]	430 [b]	410	350 [b]	360 [b]	--	--	--	--	--
Total Inorganic Carbon	--	--	--	--	--	37.9	--	--	--	--
Total Organic Carbon	6.5	7.6	5.7	<0.1	<0.1	0.55	--	--	--	--

Table A.1-1
Water-Chemistry Data for ER-20-7
(Page 2 of 4)

Analyte	Depth Discrete N-I 2,650 ft 06/30/2009	Depth Discrete N-I 2,650 ft 06/30/2009	Depth Discrete N-I 2,535 ft 07/01/2009	Composite Wellhead N-I 09/24/2010	Composite Wellhead N-I 09/24/2010	Composite Wellhead LLNL 09/24/2010	Composite Wellhead USGS 09/24/2010	Composite Wellhead USGS 09/24/2010	Composite Wellhead USGS 09/24/2010	Composite Wellhead USGS 09/24/2010
Trace Constituents (µg/L)										
Antimony	--	--	--	--	--	0.26	<1	<1	<1	<1
Arsenic	5.7 / 3.7	5.0 / 4.0	<3.4 / <3.4	7.2 / 5.0	5.8 / 7.6	5.2	4.2	4.0	4.0	4.5
Barium	<100 [d] / <100 [d]	<100 [d] / <100 [d]	<100 [d] / <100 [d]	1.9 [c] / 1.8 [c]	2.3 [c] / 1.3 [c]	7.1	<15	<15	<15	<15
Beryllium	--	--	--	--	--	<0.15	<1	<2.5	<1	<1
Boron	--	--	--	--	--	<48	209	196	191	192
Cadmium	<5 [d] / <5 [d]	<5 [d] / <5 [d]	<0.4 / <5 [d]	<0.3 / <0.3	<0.3 / <0.3	<0.036	<1	<1	<1	<1
Cesium	--	--	--	--	--	1.12	<1	<1	<1	<1
Chromium	<10 [d] / <10 [d]	<10 [d] / <10 [d]	<10 [d] / <10 [d]	<10 [d] / <0.5	<0.5 / 0.85	0.54	<4.5	<4.5	<4.5	<4.5
Cobalt	--	--	--	--	--	<0.054	<1.3	<1.3	<1.3	<1.3
Copper	--	--	--	--	--	0.78	<2.5	<2.5	<2.5	<2.5
Lead	4.0 [d] / 4.1 [d]	3.9 [d] / 4.7 [d]	3.3 [d] / 3.1 [d]	< 1 / < 1	2.2 [c] / <1	0.51	<0.9	<0.9	<0.9	<0.9
Lithium	-- / 110	-- / 110	-- / 120	-- / 95 [b]	-- / 95 [b]	--	90.4	88.4	84.8	89.5
Manganese	170 / 130	180 / 130	290 / 300	12 / 12	12 / <10 [d]	4.32	11.6	10.2	3.8	4.3
Mercury	<0.2 [d] / <0.2 [d]	<0.2 [d] / <0.2 [d]	<0.2 [d] / <0.2 [d]	0.023 [c] / <0.01	0.017 [c] / <0.01	--	--	--	--	--
Molybdenum	--	--	--	--	--	15.1	15.6	16.0	14.9	15.5
Nickel	--	--	--	--	--	0.36	<15	<15	<15	<15
Rubidium	--	--	--	--	--	12.4	7.6	7.3	4.9	5.6
Selenium	4.7 / 3.5	<2 / <2	2.6 / 2.8	<3 / <3	<3 / <3	2.4	<5	<5	<5	<5
Silver	<0.8 / <0.8	<0.8 / <0.8	<0.8 / <0.8	<1.1 / <1.1	<1.1 / <1.1	<0.06	<3.5	<3.5	<3.5	<3.5
Strontium	-- / 11	-- / 11	-- / <10 [d]	-- / 6.1 [c]	-- / 5.5 [c]	5.9	14.9	15.0	11.2	12.5
Uranium	-- / 6.3	-- / 6.2	-- / 6.3	-- / 8.0	-- / 7.7	7.5	8.2 [e], 7.8 [f]	8.2 [e], 7.6 [f]	8.1 [e], 7.4 [f]	8.1 [e], 7.8 [f]
Vanadium	--	--	--	--	--	1.8	2.2	1.5	1.9	1.9
Zinc	--	--	--	--	--	4.8	<15	<15	<15	<15

Table A.1-1
Water-Chemistry Data for ER-20-7
(Page 3 of 4)

Analyte	Depth Discrete			Composite Wellhead						
	N-I			N-I		LLNL	USGS			
	2,650 ft		2,535 ft							
	06/30/2009		07/01/2009	09/24/2010						
Environmental Isotopes										
δD (‰)	--	--	--	--	--	-113.3	--	--	--	--
$\delta^{18}O$ (%)	--	--	--	--	--	-15.4	--	--	--	--
$\delta^{13}C$ (‰)	--	--	--	--	--	--	--	--	--	--
$^{82}S/^{84}S$ (Ratio)	--	--	--	--	--	--	17.6	--	17.7	--
$^{87}Sr/^{86}Sr$ (Ratio)	--	--	--	--	--	0.71096	0.71103	0.71096	0.71089	0.71091
$^{234}U/^{238}U$ Activity Ratio	--	--	--	--	--	3.020	3.032	3.042	3.049	3.049
Radionuclides (pCi/L)										
Tritium	1.81E+07 ± 0.27E+07	1.82E+07 ± 0.28E+07	1.79E+07± 0.27E+07	1.91E+07 ± 0.29E+07	1.89E+07 ± 0.29E+07	1.77E+07	--	--	--	--
Gross Alpha	7.5 ± 2.2 (2.0) [g]	6.3 ± 1.9 (1.5) [g]	7.6 ± 2.1 (1.7) [g]	8.5 ± 2.5 (1.9) [g]	8.8 ± 2.4 (1.7) [g]	--	--	--	--	--
Gross Beta	13.9 ± 3.2 (3.1) [g]	14.3 ± 3.3 (3.3) [g]	18.0 ± 3.6 (2.8) [g]	16.6 ± 3.4 (2.3) [g]	18.0 ± 3.4 (2.0) [g]	--	--	--	--	--
^{14}C	--	--	--	R	R	--	--	--	--	--
^{90}Sr	--	--	--	1.47 ± 0.43 (0.31) [g]	1.52 ± 0.45 (0.32) [g]	--	--	--	--	--
^{99}Tc	--	--	--	13.4 ± 4.5 (6.1) [g]	16.4 ± 4.7 (6.0) [g]	--	--	--	--	--
^{129}I	--	--	--	<3.0	<2.9	--	--	--	--	--
^{137}Cs	<8.4	<9.2	<8.3	<8.8	<8.9	--	--	--	--	--
^{152}Eu	<40	<61	<47	<52	<58	--	--	--	--	--
^{154}Eu	<47	<55	<57	<51	<59	--	--	--	--	--
^{234}U	--	--	--	--	--	8.16	--	--	--	--
^{235}U	<43	<30	<29	<76	<66	0.124	--	--	--	--
^{236}U	--	--	--	--	--	<7.8E-05	--	--	--	--
^{238}U	--	--	--	--	--	2.66	--	--	--	--

Table A.1-1
Water-Chemistry Data for ER-20-7
(Page 4 of 4)

Analyte	Depth Discrete			Composite Wellhead						
	N-I			N-I		LLNL	USGS			
	2,650 ft		2,535 ft							
	06/30/2009		07/01/2009	09/24/2010						
^{239,240}Pu	0.068 ± 0.031 (0.021) [g]	0.046 ± 0.027 (0.025) [g]	0.030 ± 0.020 (0.020) [g]	0.062 ± 0.032 (0.010) [g]	0.070 ± 0.040 (0.041) [g]	0.10	--	--	--	--
^{241}Am	<7.8	<11	<8.8	<72	<55	--	--	--	--	--
^{243,244}Cm	<19	<21	<22	<50	<46	--	--	--	--	--

[a] Field measurements were made by N-I (formerly NNES) and coincide as closely as possible to the collection time for the associated samples.

[b] Value is an estimate. Hold time was exceeded for pH, sulfide, and total dissolved solids measurements. Measurements of other constituents considered an estimate as a result of failure to meet specific quality control (QC) criteria.

[c] Value is an estimate with a negative bias as a result of failure to meet specific QC criteria.

[d] Contamination was observed in the associated blank. The measured value is reported if greater than the contract required reporting limit; otherwise, the value is reported as less than the contract required reporting limit.

[e] Analyzed using thermal ionization mass spectrometry with isotope dilution.

[f] Analyzed using inductively coupled plasma mass spectrometry.

[g] Detection limit

-- = Not analyzed
R = Data were rejected. High tritium interfered with the ^{14}C analysis.

Note: Values reported with a "/" indicate analysis results from unfiltered/filtered samples.

Table A.1-2
Water-Chemistry Data for ER-20-8 #2
(Page 1 of 4)

Analyte	Depth Discrete — N-I					Composite Wellhead					
	1,710 ft	2,200 ft	2,100 ft			USGS		N-I		LLNL	DRI
	08/31/2009			12/03/2009		12/17/2009		12/18/2009			
Miscellaneous and Field Measurements											
Bromide (field) (mg/L)	--	--	--	--	--	1.33 [a]	1.32 [a]	0.85 [a]	0.99 [a]	0.80 [a]	0.85 [a]
DO (field) (mg/L)	--	--	--	--	--	2.38 [a]	3.09 [a]	2.66 [a]	3.26 [a]	3.15 [a]	2.66 [a]
pH (field)	--	--	--	--	--	8.18 [a]	8.12 [a]	8.18 [a]	8.14 [a]	8.04 [a]	8.18 [a]
pH (lab)	8.45 [b]	8.47 [b]	8.60 [b]	8.43 [b]	8.39 [b]	--	--	8.41 [b]	8.53 [b]	--	--
SEC (field) (mmhos/cm)	--	--	--	--	--	0.383 [a]	0.383 [a]	0.436 [a]	0.437 [a]	0.437 [a]	0.436 [a]
SEC (lab) (mmhos/cm)	0.425	0.428	0.555	0.442	0.441	--	--	0.448	0.449	--	--
Turbidity (NTU)	--	--	--	--	--	2.2 [a]	2.4 [a]	1.6 [a]	2.9 [a]	2.1 [a]	1.6 [a]
Temperature (°C)	--	--	--	--	--	41.8 [a]	41.9 [a]	41.5 [a]	41.5 [a]	41.4 [a]	41.5 [a]
Major and Minor Constituents (mg/L)											
Bicarbonate as $CaCO_3$	110	110	110	120	120	--	--	110	110	--	--
Carbonate as $CaCO_3$	<20	<20	<20	<20	<20	--	--	<10	<10	--	--
Bromide	0.92	0.95	4.0	0.12 [b]	0.12 [b]	--	--	0.12 [b]	0.12 [b]	--	--
Chloride	23	22	24	27	27	--	--	26	26	30.6	--
Fluoride	2.8	2.9	3.3	4.6	4.6	--	--	4.5	4.5	5.7	--
Sulfate	36	37	45	49	49	--	--	49	49	59.6	--
Calcium	-- / 1.9	-- / 1.7	5.3 / 4.9	2.5 / 2.2	2.7 / 2.3	--	--	-- / 1.8	1.8 / 1.9	1.8	--
Magnesium	-- / 0.024 [c]	-- / 0.023 [c]	0.37 / 0.24 [c]	0.12 [c] / <0.007	0.18 [c] / <0.007	--	--	-- / <0.007	<0.007 / 0.011 [c]	0.034	--
Potassium	-- / 3.5	-- / 3.3	6.4 / 5.3	2.8 / 2.9	2.9 / 2.9	--	--	-- / 2.5	2.5 / 2.5	2.2	--
Sodium	-- / 66	-- / 70	100 / 100	82 / 82	82 / 84	--	--	-- / 80	80 / 81	96	--
Aluminum	6.2 / 1.7	6.0 / 1.7	5.8 / 2.4	0.3 / <0.2 [d]	0.43 / <0.2 [d]	0.046	0.046	<0.2 [d] / <0.2 [d]	<0.2 [d] / <0.2 [d]	0.046	R
Iron	38 [c] / 18 [c]	31 [c] / 17 [c]	3.4 [c] / 1.1 [c]	1.0 [b] / <0.001 [b]	1.0 [b] / <0.001 [b]	--	--	<0.1 [d] / <0.1 [d]	<0.1 [d] / <0.1 [d]	<0.03	R
Silicon	30 / 19	29 / 19	29 / 22	24 / 24	25 / 25	25.1	25.9	24 / 24	24 / 24	--	--
Sulfide	<2	<2	<2	<2 [b]	<2 [b]	--	--	<2 [b]	<2 [b]	--	--

Table A.1-2
Water-Chemistry Data for ER-20-8 #2
(Page 2 of 4)

Analyte	Depth Discrete N-I 1,710 ft 08/31/2009	Depth Discrete N-I 2,200 ft 08/31/2009	Depth Discrete N-I 2,100 ft	Depth Discrete N-I 12/03/2009	Depth Discrete N-I 12/03/2009	Composite Wellhead USGS 12/17/2009	Composite Wellhead USGS 12/17/2009	Composite Wellhead N-I 12/18/2009	Composite Wellhead N-I 12/18/2009	Composite Wellhead LLNL 12/18/2009	Composite Wellhead DRI 12/18/2009
Total Dissolved Solids	450	430	750	300	300	--	--	300 [b]	290 [b]	--	--
Total Inorganic Carbon	--	--	--	--	--	--	--	--	--	27.7	--
Total Organic Carbon	35	36	53	<1	<1	--	--	<1	<1	0.7	0.3
Trace Constituents (μg/L)											
Antimony	--	--	--	--	--	0.3	0.3	--	--	0.272	--
Arsenic	4.8 / <3.4	3.5 / <3.4	4.6 / 5.1	7.4 / 9.0	4.4 / 9.2	7.5	7.5	6.9 / 6.8	6.9 / 8.4	--	--
Barium	<100 [d] / <100 [d]	<100 [d] / <100 [d]	<100 [d] / 120	5.5 [c] / 1.2 [c]	5.8 [c] / 1.0 [c]	<3	<3	2.1 [c] / 1.0 [c]	0.91 [c] / 1.3 [c]	1.5	--
Beryllium	--	--	--	--	--	<0.2	<0.2	--	--	<0.048	--
Boron	--	--	--	--	--	118	122	--	--	123	--
Cadmium	0.81 / <0.38	0.43 / 0.66	1.2 / <0.38	<0.52 / <0.52	<0.52 / <0.52	<0.2	<0.2	<0.52 / <0.52	<0.52 / <0.52	<0.06	--
Cesium	--	--	--	--	--	--	--	--	--	1.12	--
Chromium	21 / <10 [d]	14 / <10 [d]	12 / <10 [d]	5.0 [c] / <0.85	4.3 [c] / <0.85	<0.9	<0.9	<10 [d] / <10 [d]	<10 [d] / <10 [d]	0.82	--
Cobalt	--	--	--	--	--	<0.25	<0.25	--	--	<0.033	--
Copper	--	--	--	--	--	3.9	2.3	--	--	1.68	--
Lead	7.7 / 3.8	7.5 / 3.1	5.5 / 4.5	170 / <1.1	170 / 6.5[c]	0.80	0.43	2.3 / 1.2	1.3 / <1.1	0.419	--
Lithium	-- / 150	-- / 150	350 / 360	110 / 110	110 / 110	105	109	-- / 110	110 / 110	--	--
Manganese	470 / 340	410 / 310	94 / 48	16 [b] / <0.2 [b]	17 [b] / <0.2 [b]	11	11	10 / 10	<10[d] / 10	9.2	--
Mercury	<0.20 [d] / <0.20 [d]	0.21 / <0.20 [d]	0.20 / <0.20 [d]	0.071 / 0.040	0.088 / 0.048	--	--	<0.02 [b] / <0.02 [b]	<0.02 [b] / <0.02 [b]	--	--
Molybdenum	--	--	--	--	--	6.3	6.4	--	--	6.2	--
Nickel	--	--	--	--	--	<3	<3	--	--	0.52	--
Rubidium	--	--	--	--	--	8.4	8.4	--	--	8.5	--
Selenium	<3.2 / <3.2	<3.2 / <3.2	5.9 / 6.4	<2.2 / <2.2	<2.2 / <2.2	<1	<1	<5 [d] / <2.2	<2.2 / <2.2	<6.0	--
Silver	<1 / <1	<1 / <1	<1 / <1	<1.2 / <1.2	<1.2 / <1.2	<0.7	<0.7	<1.2 / <1.2	<1.2 / <1.2	<0.018	--
Strontium	-- / 1.9 [c]	-- / 1.0 [c]	5.4 / 6.3 [c]	<0.08 / <0.08	<0.08 / <0.08	2.4	2.4	-- / <0.08	0.08 / <0.08	2.35	--

Table A.1-2
Water-Chemistry Data for ER-20-8 #2
(Page 3 of 4)

Analyte	Depth Discrete					Composite Wellhead					
	N-I					USGS		N-I		LLNL	DRI
	1,710 ft	2,200 ft	2,100 ft								
	08/31/2009			12/03/2009		12/17/2009		12/18/2009			
Uranium	-- / 1.4	-- / 1.4	2.6 / 2.1	2.4 / 2.4	2.4 / 2.4	2.52 [e], 2.43 [f]	2.52 [e], 2.38 [f]	-- / 2.4	2.6 / 2.4	2.335	--
Vanadium	--	--	--	--	--	1.7	1.7	--	--	2.24	--
Zinc	--	--	--	--	--	<3	<3	--	--	2.22	--
Environmental Isotopes											
δD (‰)	--	--	--	--	--	--	--	--	--	-116.7	-115
δ^{18}O (‰)	--	--	--	--	--	--	--	--	--	-15.4	-15.2
δ^{13}C (Inorganic Carbon) (‰)	--	--	--	--	--	--	--	--	--	-2.02	-5.4
δ^{13}C (Organic Carbon) (‰)	--	--	--	--	--	--	--	--	--	--	-26.7
^{14}C (Organic Carbon) (pmc)	--	--	--	--	--	--	--	--	--	--	28.9
^{82}S/^{84}S (‰)	--	--	--	--	--	18.0	18.0	--	--	--	--
^{87}Sr/^{86}Sr	--	--	--	--	--	0.70967	0.70968	--	--	0.70905	--
^{234}U/^{238}U Activity Ratio	--	--	--	--	--	3.87	3.88	--	--	3.895	--
Radionuclides (pCi/L)											
Tritium	680 ± 230 (310) [g]	850 ± 250 (320) [g]	900 ± 250 (320) [g]	730 ± 190 (230) [g]	880 ± 210 (230) [g]	--	--	1,040 ± 270 (320) [g]	880 ± 250 (330) [g]	1,280 ± 70 (97) [f]	--
Gross Alpha	6.1 ± 1.7 (1.3) [g]	5.0 ± 1.5 (1.3) [g]	6.4 ± 1.8 (1.5) [g]	3.0 ± 0.9 (0.9) [g]	3.7 ± 1.5 (1.5) [g]	--	--	2.6 ± 1.8 (2.5) [g]	2.6 ± 1.8 (2.5) [g]	--	--
Gross Beta	8.1 ± 2.0 (2.2) [g]	7.0 ± 1.9 (2.1) [g]	9.8 ± 2.4 (2.5) [g]	4.2 ± 1.3 (1.7) [g]	3.1 ± 1.7 (2.5) [g]	--	--	<2.5	<2.4	--	--
^{14}C	<290 [b]	<290 [b]	<290 [b]	<410 [b]	<410 [b]	--	--	<420	<420	--	--
^{90}Sr	--	--	--	--	--	--	--	<0.49	<0.51	--	--
^{99}Tc	--	--	--	--	--	--	--	<6.9	<6.8	--	--
^{129}I	--	--	--	--	--	--	--	<1.8 [b]	<7.1 [b]	9.27E-05	--

Table A.1-2
Water-Chemistry Data for ER-20-8 #2
(Page 4 of 4)

Analyte	Depth Discrete					Composite Wellhead					
	N-I					USGS		N-I		LLNL	DRI
	1,710 ft		2,200 ft		2,100 ft						
	08/31/2009				12/03/2009		12/17/2009		12/18/2009		
^{137}Cs	<9.2	<9.5	<9.3	<9.5	<9.0	--	--	<9.7	<9.9	--	--
^{152}Eu	<47	<56	<46	<54	<46	--	--	<48	<43	--	--
^{154}Eu	<53	<56	<55	<56	<50	--	--	<59	<61	--	--
^{234}U	--	--	--	--	--	--	--	--	--	3.08	--
^{235}U	<43	<51	<51	<38	<62	--	--	<33	<57	0.0366	--
^{236}U	--	--	--	--	--	--	--	--	--	<2.31E-05	--
^{238}U	--	--	--	--	--	--	--	--	--	0.780	--
^{239,240}Pu	<0.027	0.016 ± 0.015 (0.009) [g, h]	<0.025	<0.040	<0.049	--	--	<0.026	<0.025	--	--
^{241}Am	<83	<8.9	<13	<50	<67	--	--	<48	<86	--	--
^{243,244}Cm	<46	<23	<27	<29	<40	--	--	<30	<49	--	--

[a] Field measurements were made by N-I (formerly NNES) and coincide as closely as possible to the collection time for the associated samples.
[b] Value is an estimate. Hold time was exceeded for pH, sulfide, and total dissolved solids measurements. Measurements of other constituents considered an estimate as a result of failure to meet specific QC criteria.
[c] Value is an estimate with a negative bias as a result of failure to meet specific QC criteria.
[d] Contamination was observed in the associated blank. The measured value is reported if greater than the contract required reporting limit; otherwise, the value is reported as less than the contract required reporting limit.
[e] Analyzed using thermal ionization mass spectrometry with isotope dilution.
[f] Analyzed using inductively coupled plasma mass spectrometry.
[g] Detection limit
[h] Reported value is less than the detection limit plus the error and thus highly uncertain.

-- = Not analyzed
R = Data were rejected. High tritium interfered with the ^{14}C analysis.

Note: Values reported with a "/" indicate analysis results from unfiltered/filtered samples.

Table A.1-3
Water-Chemistry Data for ER-EC-11
(Page 1 of 4)

Analyte	Depth Discrete — N-I									Composite Wellhead					
	2,450 ft	2,750 ft	3,150 ft	3,285 ft	3,285 ft	3,755 ft	3,750 ft (Deep Piezometer)	3,750 ft (Deep Piezometer)	3,300 ft (Intermediate Piezometer)	N-I	LLNL	DRI	DRI	USGS	USGS
	10/09/2009	10/10/2009	10/10/2009	10/17/2009	10/17/2009	10/17/2009	05/02/2010	05/02/2010	05/02/2010	05/18/2010	05/18/2010	05/18/2010	05/18/2010	05/18/2010	05/18/2010
Miscellaneous and Field Measurements															
Bromide (field) (mg/L)	--	--	--	--	--	--	--	--	--	0.46 [a], 0.26 [a], 0.70 [a]					
DO (field) (mg/L)	--	--	--	--	--	--	--	--	--	3.2 [a], 3.4 [a], 3.4 [a]					
pH (field)	--	--	--	--	--	--	--	--	--	7.46 [a], 8.20 [a], 8.24 [a]					
pH (lab)	7.81 [b]	8.05 [b]	8.00 [b]	9.08 [b]	9.04 [b]	8.34 [b]	8.70 [b]	8.65 [b]	8.86 [b]	8.50 [b]	8.58 [b]	--	--	--	--
SEC (field) (mmhos/cm)	--	--	--	--	--	--	--	--	--	0.519 [a], 0.517 [a], 0.512 [a]					
SEC (lab) (mmhos/cm)	0.670	0.663	0.665	0.571	0.564	0.556	0.542	0.541	0.540	0.538	0.545	--	--	--	--
Turbidity (NTU)	--	--	--	--	--	--	--	--	--	3.3 [a], 1.1 [a], 0.7 [a]					
Temperature (°C)	--	--	--	--	--	--	--	--	--	38.7 [a], 43.5 [a], 42.4 [a]					
Major and Minor Constituents (mg/L)															
Bicarbonate as $CaCO_3$	140	140	140	120	120	130	130	130	120	120	110	--	--	--	--
Carbonate as $CaCO_3$	<20	<20	<20	<20	<20	<20	<20	<20	<20	<10	<10	--	--	--	--
Bromide	0.78	0.94	1.1	1.1	1.1	0.61	0.17 [b]	0.17 [b]	0.17 [b]	0.21	<0.023	--	--	--	--
Chloride	56	56	57	38	38	42	49	42	47	43	42	--	--	--	--
Fluoride	3.6	2.9	2.7	2.5	2.5	2.9	2.9	2.9	2.9	3.1	3.0	--	--	--	--
Sulfate	86	86	83	63 [b]	62 [b]	64 [b]	68	66	67	70	70	--	--	--	--
Calcium	2.4 / 2.4	3.8 / 3.8	3.9 / 4.1	4.1 [b] / 4.5 [b]	4.2 [b] / 4.4 [b]	4.3 [b] / 4.5 [b]	-- / 5.8	-- / 7.3	-- / 30	-- / 4.0	-- / 3.9	3.9	--	3.9	3.9
Magnesium	0.039 [c] / 0.020 [c]	0.012 [c] / <0.007	<0.007 / <0.007	0.010 [c] / <0.007	0.014 [c] / <0.007	0.029 [c] / 0.046 [c]	-- / 0.098 [c]	-- / 0.2 [c]	-- / 1.8	-- / <0.013	-- / <0.013	0.009	--	--	--
Potassium	4.0 / 3.9	2.9 / 2.8	2.4 / 2.2	5.4 / 4.7	5.5 / 4.7	1.7 / 1.4	-- / 0.64 [c]	-- / 0.65 [c]	-- / 0.80 [c]	-- / 0.75 [c]	-- / 0.68 [c]	0.7	--	--	--
Sodium	110 / 110	110 / 110	110 / 110	100 / 100 [b]	100 / 100 [b]	97 [b] / 96 [b]	-- / 94	-- / 95	-- / 95	-- / 95	-- / 95	110	--	--	--
Aluminum	1.8 / 0.82	1.2 / 0.47	1.1 / 0.42	1.4 / 0.33	1.5 / 0.32	0.78 / 0.31	0.59 / 0.27 [d]	0.20 [d] / 0.35	3.8 / 2.7	<0.2 [d] / <0.2 [d]	<0.2 [d] / <0.2 [d]	0.031	R	0.030	0.029
Iron	3.5 / 1.4	4.0 / 0.88	1.7 / 0.56	49 [b] / 16 [b]	51 [b] / 16 [b]	20 [b] / 5.1 [b]	15 / 3.7	4.8 / 4.8	19 / 17	0.05 [b] / 0.09 [b]	0.08 [b] / 0.07 [b]	<0.045	R	--	--
Silicon	25 / 24	24 / 23	23 / 23	18 / 15	18 / 15	22 / 20	21 / 20	20 / 20	27 / 23	19 / 19	19 / 19	--	--	19.5	19.4
Sulfide	<2	<2	<2	<2	<2	<2	<2	<2	<2	<2	<2	--	--	--	--

Table A.1-3
Water-Chemistry Data for ER-EC-11
(Page 2 of 4)

Analyte	Depth Discrete								Composite Wellhead					
	N-I								N-I		LLNL	DRI	USGS	
	2,450 ft	2,750 ft	3,150 ft	3,285 ft	3,755 ft	3,750 ft (Deep Piezometer)	3,300 ft (Intermediate Piezometer)							
	10/09/2009	10/10/2009		10/17/2009			05/02/2010		05/18/2010					
Total Dissolved Solids	490	470	470	500	460	430	340	350	350	330	340	--	--	--	--
Total Inorganic Carbon	--	--	--	--	--	--	--	--	--	--	--	28.7	--	--	--
Total Organic Carbon	47	27	26	29	30	19	<0.12	<0.12	<0.12	<0.12	<0.12	0.42	0.02	--	--
Trace Constituents (μg/L)															
Antimony	--	--	--	--	--	--	--	--	--	--	--	0.25	--	<1	<1
Arsenic	<3.4 / 4.6 [c]	<3.4 / <3.4	<3.4 / <3.4	<3.8 / <3.8	<3.8 / <3.8	<3.8 / <3.8	7.5 / 5.0	8.2 / 4.6	12 / 8.2	9.8 / 7.2	9.4 / 11	8.8	--	8.2	8.4
Barium	16 [c] / 100 [b]	19 [c] / 99 [c]	10 [c] / 5.2 [c]	45 [c] / 110 [b]	44 [c] / 140 [b]	35 [c] / 68 [c]	18 [c] / 6.0 [c]	7.3 [c] / 12 [c]	43 [c] / 53 [c]	0.36 [c] / 0.50 [c]	1.2 [c] / 0.41 [c]	1.1	--	<15	<15
Beryllium	--	--	--	--	--	--	--	--	--	--	--	<0.18	--	<1	<1
Boron	--	--	--	--	--	--	--	--	--	--	--		--	161	164
Cadmium	<0.38 / <0.38	<0.38 / <0.38	<0.38 / <0.38	<0.52 / <0.52	<0.52 / <0.52	<0.52 / <0.52	0.87 / <0.33	<0.33 / <0.33	<0.33 / <0.33	<0.33 / <0.33	<0.33 / <0.33	<0.03	--	<1	<1
Cesium	--	--	--	--	--	--	--	--	--	--	--	3.9	--	3.9	3.9
Chromium	240 / 150	40 / 17	24 / 10	51 [b] / 16 [b]	53 [b] / 16 [b]	170 [b] / 36 [b]	120 / 15 [b]	28 / 31	41 / 67	<0.51 / <0.51	<0.51 / <0.51	0.84	--	<4.5	<4.5
Cobalt	--	--	--	--	--	--	--	--	--	--	--	<0.05	--	<1.3	<1.3
Copper	--	--	--	--	--	--	--	--	--	--	--	1.2	--	<2.5	<2.5
Lead	4.9 / 3.4	1.8 / <1.8	<1.8 / <1.8	<1.1 / <1.1	<1.1 / <1.1	<1.1 / <1.1	15 / 2.6 [c]	2.5 [c] / 7.1	5.3 [c] / 6.9	3.2 [c] / 10	8.9 / 8.3	1.0	--	1.3	1.2
Lithium	190 [b] / 190 [b]	180 [b] / 180 [b]	190 [b] / 190 [b]	250 [b] / 240 [b]	250 [b] / 250 [b]	210 [b] / 200 [b]	-- / 170	-- / 170	-- / 170	-- / 170 [b]	-- / 170 [b]	--	--	163	163
Manganese	240 / 210	79 / 56	38 / 29	1,000 [b] / 750 [b]	1,000 [b] / 750 [b]	400 [b] / 280 [b]	270 / 80	76 / 150	250 / 430	2.2 [c] / 3.3 [c]	2.8 [c] / 2.7 [c]	2.0	--	2.1	2.1
Mercury	<0.2 [d] / <0.2 [d]	<0.2 [d] / <0.2 [d]	<0.2 [d] / <0.2 [d]	0.032 / <0.021	<0.021 / <0.021	<0.021 / <0.021	<0.0097 / <0.0097	<0.0097 / <0.0097	<0.0097 / <0.0097	<0.0097 / <0.0097	<0.0097 / 0.016 [c]	--	--	--	--
Molybdenum	--	--	--	--	--	--	--	--	--	--	--	3.9	--	4.3	4.4
Nickel	--	--	--	--	--	--	--	--	--	--	--	0.43	--	<15	<15
Rubidium	--	--	--	--	--	--	--	--	--	--	--	5.5	--	5.4	5.4
Selenium	<3.2 / <3.2	<3.2 / <3.2	<3.2 / <3.2	<2.2 / <2.2	<2.2 / <2.2	<2.2 / <2.2	<2.7 / <2.7	<2.7 / <2.7	<2.7 / <2.7	<2.7 / <2.7	<2.7 / <2.7	<12	--	<5	<5
Silver	<1 / <1	<1 / <1	<1 / <1	<1.2 / <1.2	<1.2 / <1.2	<1.2 / <1.2	<1.1 / <1.1	<1.1 / <1.1	<1.1 / <1.1	<1.1 / <1.1	<1.1 / <1.1	<0.01	--	<3.5	<3.5

Table A.1-3
Water-Chemistry Data for ER-EC-11
(Page 3 of 4)

Analyte	Depth Discrete							Composite Wellhead					
	N-I							N-I		LLNL	DRI	USGS	
	2,450 ft	2,750 ft	3,150 ft	3,285 ft	3,755 ft	3,750 ft (Deep Piezometer)	3,300 ft (Intermediate Piezometer)						
	10/09/2009	10/10/2009		10/17/2009			05/02/2010			05/18/2010			
Strontium	4.1 [c] / 4.9 [c]	2.4 [c] / 2.9 [c]	4.9 [c] / 4.7 [c]	22 [b] / 23 [b]	23 [b] / 25 [b]	21 [b] / 22 [b]	-- / 37	-- / 44	-- / 94	-- / 30 [b]	-- / 30 [b]	34.4	--	35	36
Uranium	6.4 / 5.8	6.9 / 6.6	6.4 / 6.4	0.43 / 0.38	0.44 / 0.38	0.84 / 0.79	-- / 1.7	-- / 1.7	-- / 2.2	-- / 1.6	-- / 1.6	1.64	--	1.754 [e], 1.80 [f]	1.757 [e], 1.84 [f]
Vanadium	--	--	--	--	--	--	--	--	--	--	--	2.6	--	1.5	1.6
Zinc	--	--	--	--	--	--	--	--	--	--	--	0.8	--	<15	<15
Environmental Isotopes															
δD (‰)	--	--	--	--	--	--	--	--	--	--	--	--	-115	--	--
δ^{18}O (‰)	--	--	--	--	--	--	--	--	--	--	--	-15.3	-15.2	--	--
δ^{13}C (DIC) (‰)	--	--	--	--	--	--	--	--	--	--	--	-2.53	-4.7	--	--
δ^{13}C (DOC) (‰)	--	--	--	--	--	--	--	--	--	--	--	--	-23.1	--	--
^{14}C (DOC) (‰)	--	--	--	--	--	--	--	--	--	--	--	--	52.2	--	--
^{82}S/^{84}S (Ratio)	--	--	--	--	--	--	--	--	--	--	--	--	--	18.7	18.7
^{87}Sr/^{86}Sr (Ratio)	--	--	--	--	--	--	--	--	--	--	--	--	--	0.70986	0.70987
^{234}U/^{238}U Activity Ratio	--	--	--	--	--	--	--	--	--	--	--	--	--	4.033	4.045
Radionuclides (pCi/L)															
Tritium	10,000 ± 1,500; 10,589 ± 289	10,100 ± 1,600; 10,393 ± 281	10,331 ± 279; 9,800 ± 1,500	<230	<265; <230	<264;<240	<310	<310	<310	<270	<270	<134	--	--	--
Gross Alpha	7.3 ± 2.0 (1.5) [g]	8.0 ± 2.1 (1.5) [g]	7.0 ± 1.9 (1.6) [g]	<1.8 [b]	2.3 [b] ± 1.3 (1.6) [g]	2.7 [b] ± 1.4 (1.6) [g]	2.9 [b] ± 1.4 (1.7) [g]	2.6 [b] ± 1.3 (1.5) [g]	2.4 [b] ± 1.1 (1.5) [g]	2.4 [b] ± 1.4 (1.8) [g]	3.4 ± 1.5 (1.6) [g]	--	--	--	--
Gross Beta	7.2 ± 2.2 (2.7) [g]	6.8 ± 2.2 (2.8) [g]	4.8 ± 2.0 (2.8) [g]	6.0 ± 2.0 (2.4) [g]	4.7 ± 1.8 (2.4) [g]	<2.5	<2.7	4.0 ± 1.7 (2.5) [g]	<2.5	<2.2	<2.4	--	--	--	--
^{14}C	<420	<420	<420	<420	<420	<420	<390	<390	<390	<390	<390	--	--	--	--
^{90}Sr	--	--	--	--	--	--	--	--	--	<0.59	<0.55	--	--	--	--
^{99}Tc	--	--	--	--	--	--	--	--	--	<7.7	<8.1	--	--	--	--
^{129}I	--	--	--	--	--	--	--	--	--	--	--	--	--	--	--

Table A.1-3
Water-Chemistry Data for ER-EC-11
(Page 4 of 4)

Analyte	Depth Discrete								Composite Wellhead					
	N-I								N-I		LLNL	DRI	USGS	
	2,450 ft	2,750 ft	3,150 ft	3,285 ft		3,755 ft	3,750 ft (Deep Piezometer)	3,300 ft (Intermediate Piezometer)						
	10/09/2009	10/10/2009		10/17/2009			05/02/2010		05/18/2010					
^{137}Cs	<7.8	<8.6	<8.4	<7.3	<9.1	<9.1	<8.9	<8.1	<8.2	<8.6	<4.8	--	--	--	--
^{152}Eu	<38	<54	<41	<46	<43	<42	<47	<53	<41	<53	<30	--	--	--	--
^{154}Eu	<34	<48	<41	<42	<49	<44	<49	<60	<51	<55	<28	--	--	--	--
^{234}U	--	--	--	--	--	--	--	--	--	--	--	2.35	--	--	--
^{235}U	<51	<46	<34	<31	<45	<37	<43	<44	<41	<40	<36	0.0269	--	--	--
^{236}U	--	--	--	--	--	--	--	--	--	--	--	<1.7E-05	--	--	--
^{238}U	--	--	--	--	--	--	--	--	--	--	--	0.577	--	--	--
^{239,240}Pu	<0.026 [b]	<0.016 [b]	<0.023 [b]	<0.027 [b]	<0.008 [b]	<0.007 [b]	<0.016	<0.018	<0.005	<0.027	<0.008	--	--	--	--
^{241}Am	<12	<12	<60	<43	<39	<70	<11	<40	<69	<64	<44	--	--	--	--
^{243,244}Cm	<20	<20	<42	<33	<20	<39	<26	<48	<40	<41	<28	--	--	--	--

[a] Field measurements were made by N-I (formerly NNES) and coincide as closely as possible to the collection time for the associated samples.
[b] Value is an estimate. Hold time was exceeded for pH, sulfide, and total dissolved solids measurements. Measurements of other constituents considered an estimate as a result of failure to meet specific QC criteria.
[c] Value is an estimate with a negative bias as a result of failure to meet specific QC criteria.
[d] Contamination was observed in the associated blank. The measured value is reported if greater than the contract required reporting limit; otherwise, the value is reported as less than the contract required reporting limit.
[e] Analyzed using thermal ionization mass spectrometry with isotope dilution.
[f] Analyzed using inductively coupled plasma mass spectrometry.
[g] Detection limit

-- = Not analyzed
R = Data were rejected. High tritium interfered with the ^{14}C analysis.

Note: Values reported with a "/" indicate analysis results from unfiltered/filtered samples.

Table A.1-4
Major-Ion Data for Wells in the Study Area
(Page 1 of 5)

Site ID	Date	Sample ID [a]	Depth (ft)	HCO$_3$ (mg/L)	CO$_3$ (mg/L)	Br (mg/L)	Cl (mg/L)	SO$_4$ (mg/L)	F (mg/L)	K (mg/L)	Mg (mg/L)	Na (mg/L)	Ca (mg/L)	Charge Balance	Source
ER-20-1	07/02/2001	13365	--	--	--	--	--	--	--	3.7	0.1	155	3.7	--	BN (2005)
	07/26/2005	14109	2,000 [b]	187	1.3		57	83	3.0	3.3	0.1 [c]	128	3.4	-6.2	NSTec (2006)
	07/26/2005	14109	2,000 [b]	--	--	--	--	--	--	3.4	0.1 [c]	125	3.4	--	NSTec (2006)
	10/31/2007	14831.5	2,000 [b]	185	<1.2	--	53	83	3.1	--	--	--	--	--	NSTec (2008)
	10/31/2007	14831	2,000 [b]	185	<1.2	--	57	84	3.2	3.3	0.1	141	3.5	--	NSTec (2008)
ER-20-5 #1	06/03/1996	3921	2,300–2,572	149	8.0	<0.25	27	41	11.5	6.0	0.9	107	11	4.7	IT (1997)
	06/03/1996	12318	2,300–2,572	187 [d]	--	--	26	41	10.3	4.2	0.2	113	6.1	1.4	Rose et al. (1997)
	04/22/1997	3922	2,300–2,572	186	<10	0.10	22	38	8.6	5.7	0.4	105	7.2	2.0	IT (1997)
	04/22/1997	12317	2,300–2,572	186 [d]	--	<0.05	23	39	10.1	4.5	0.3	104	6.6	-0.8	Rose et al. (1997)
	07/09/1998	5164	2,300–2,356	145	10	<0.25	24	41	9.8	--	--	--	--	--	IT (1999)
	07/09/1998	12316	2,300–2,572	182 [d]	--	<0.04	25	40	9.6	5.7	0.4	106	7.2	1.0	LLNL (2003b)
	11/30/2004	13234	--	193 [d]	--	0.07	25	43	10.8	4.6	0.1	118	6.2	1.9	LLNL (2005)
ER-20-5 #3	07/31/1996	3923	3,432–3,881	103	6.4	<0.25	18	35	3.2	6.5	0.6	74	6.1	-6.4	IT (1997)
	07/31/1996	12322	3,432–3,881	109 [d]	--	--	18	35	3.2	3.0	0.1	73	3.1	3.4	Rose et al. (1997)
	04/22/1997	3924	3,432–3,881	115	<10	0.08	15	31	3.0	6.0	0.2	74	3.4	-6.4	IT (1997)
	04/22/1997	12321	3,432–3,881	108 [d]	--	0.98	17	35	3.3	3.1	0.1	70	3.2	2.0	Rose et al. (1997)
	04/30/1998	5166	3,432–3,881	--	--	<0.25	16	33	3.4	7.9	0.4	72	4.1	--	IT (1999)
	04/30/1998	5167	3,432–3,881	--	--	--	--	--	--	4.0	0.2	76	2.7	--	IT (1999)
	04/30/1998	12320	3,432–3,881	107 [d]	--	<0.02	17	33	3.2	2.1	0.1	68	1.8	0.04	LLNL (2003b)
	11/15/2001	12319	3,432–3,881	99 [d]	--	0.76	19	35	3.6	3.3	0.1	87	4.4	14	LLNL (2003b)
	11/29/2004	13235	--	135 [d]	--	0.07	17	35	4.1	3.5	<0.04	80	3.5	1.5	LLNL (2005)
ER-20-7	06/30/2009	14912	2,650	183 [e]	<12	0.29	30	50	5.6	4.3	0.2 [c]	97	4.4	-6.4	SNJV (2009)
	06/30/2009	14913	2,650	171 [e]	<12	0.28	29	49	5.5	4.3	0.2 [c]	96	4.4	-4.3	SNJV (2009)
	07/01/2009	14914	2,535	183 [e]	<12	0.38	29	49	5.5	4.1	0.1 [c]	98	4.1	-5.6	SNJV (2009)
	09/24/2010	15470	--	193 [f]	--	<0.05	30	50	6.4	3.9	0.2	118	6.6	1.8	LLNL (2011b)
	09/24/2010	15383	--	171 [e]	<12	0.15 [c]	30	53	6.3	4.9	--	92	4.9	-7.5	N-I (2011)
	09/24/2010	15384	--	171 [e]	<12	0.15 [c]	31	53	6.3	4.8	--	93	4.8	-7.4	N-I (2011)
	09/24/2010	15457/15488	--	--	--	--	--	--	--	--	<0.4	109	5.0	--	USGS (2011)
	09/24/2010	15459/15460	--	--	--	--	--	--	--	--	<0.4	100	4.4	--	USGS (2011)
ER-EC-1	02/01/2000	8459	2,298–4,750	158 [e]	<6	--	--	--	--	8.2	0.5	120	19	--	IT (2001)
	02/01/2000	8459.4	2,298–4,750	--	--	0.46	95	120	2.6	8.3	0.5	120	20	--	IT (2001)

Table A.1-4
Major-Ion Data for Wells in the Study Area
(Page 2 of 5)

Site ID	Date	Sample ID [a]	Depth (ft)	HCO₃ (mg/L)	CO₃ (mg/L)	Br (mg/L)	Cl (mg/L)	SO₄ (mg/L)	F (mg/L)	K (mg/L)	Mg (mg/L)	Na (mg/L)	Ca (mg/L)	Charge Balance	Source
ER-EC-1 (continued)	02/01/2000	7441/7441.21	2,298–4,750	148 [d]	--	1.1	97	145	2.4	6.0	0.4	154	19	-3.1	DRI (2001)
	06/03/2003	12402	2,298–4,750	102 [e]	--	0.45	88	121	2.7	6.2	0.5	153	20	6.9	DRI (2004)
	06/03/2003	12383	2,298–4,750	149 [d]	--	1.4	97	119	2.3	4.9	0.4	144	19	-3.2	LLNL (2004)
	06/03/2003	12368	2,298–4,750	146 [e]	<6	0.44	95	120	2.6	8.1 [c]	0.4 [c]	150	19	-0.03	SNJV (2004)
	06/03/2003	12368	2,298–4,750	--	--	--	--	--	--	8.0 [c]	0.4 [c]	150	19	--	SNJV (2004)
	06/03/2003	12368.5	2,298–4,750	146 [e]	<6	0.42	92	110	2.6	7.9 [c]	0.4 [c]	150	19	1.9	SNJV (2004)
	06/03/2003	12368.5	2,298–4,750	--	--	--	--	--	--	8.4 [c]	0.4 [c]	150	19	--	SNJV (2004)
	04/02/2009	15200/15202	2,298–4,750	158 [e]	<12	0.53	97	120	2.5	7.3 [c]	0.4 [c]	140	20	-4.3	NNES (2010a)
	04/02/2009	15201/15203	2,298–4,750	158 [e]	<12	0.39	100	120	2.5	7.2 [c]	0.4 [c]	140	20	-4.9	NNES (2010a)
	04/03/2009	15407	2,298–4,750	159 [e]	--	--	94	118	1.7	5.5	0.4	155	18	-0.3	LLNL (2011a)
ER-EC-6 (1,581–5,000 ft)	02/10/2000	8475/8475.4	1,628–4,904	146	<3	0.32	52	77	3.1	3.2	<1.0	130	4.2	3.4	IT (2001)
	02/10/2000	8475.4	1,628–4,904	--	--	--	--	--	--	3.1	<1.0	140	4.1	--	IT (2001)
	02/10/2000	7434.21	1,628–4,904	153 [d]	--	0.84	44	56	3.1	2.0	<0.02	128	4.0	6.7	LLNL (2000b)
ER-EC-6 (1,581–3,820 ft)	06/10/2003	12406	--	134	ND	0.25	50	79	3.0	2.0	0.03	128	4.9	3.8	DRI (2004)
	06/10/2003	12387	--	147 [d]	--	0.90	52	75	2.7	1.8	0.2	120	4.6	-1.2	LLNL (2004)
	06/10/2003	12372	--	146	<6	0.24	53	79	2.8	3.1	1.0 [c]	120	4.2	-0.8	SNJV (2004)
	06/10/2003	12372	--	--	--	--	--	--	--	3.2	1.0 [c]	120	4.1	--	SNJV (2004)
	06/10/2003	12372.5	--	146	<6	0.25	53	79	2.9	2.9	1.0 [c]	120	4.1	-1.0	SNJV (2004)
	06/10/2003	12372.5	--	--	--	--	--	--	--	2.9	1.0 [c]	120	4.2	--	SNJV (2004)
	04/09/2009	15408	--	163 [d]	--	--	47	73	2.0	1.9	0.01	132	4.1	3.0	LLNL (2011a)
	04/09/2009	15209/15210	--	158	<12	0.24	53	78 [c]	2.6	2.8	<1.0	120	4.5	-2.2	NNES (2010a)
	04/09/2009	15208/15211	--	158	<12	0.21	54	79 [c]	2.5	2.6	<1.0	110	4.3	-6.8	NNES (2010a)
ER-EC-11 deep	05/02/2010	15448	3,750	158 [e]	<12	0.17	42	66	2.9	0.7 [c]	0.2 [c]	95	7.3	-7.9	N-I (2011)
	05/02/2010	15446	3,750	158 [e]	<12	0.17	49	68	2.9	0.6 [c]	0.1 [c]	94	5.8	-12	N-I (2011)
ER-EC-11 intermediate	05/02/2010	15450	3,300	158 [e]	<12	0.17	47	67	2.9	0.8 [c]	1.8	95	30	2.9	N-I (2011)
ER-EC-11 main	10/09/2009	15318	2,450	171 [e]	<12	0.78	56	86	3.6	3.9	0.02 [c]	110	2.4	-12	NNES (2010b)
	10/09/2009	15318	2,450	--	--	--	--	--	--	4.0	0.04 [c]	110	2.4		NNES (2010b)
	10/10/2009	15321	2,750	171 [e]	<12	0.94	56	86	2.9	2.8	<0.01	110	3.8	-11	NNES (2010b)
	10/10/2009	15321	2,750	--	--	--	--	--	--	2.9	0.01 [c]	110	3.8		NNES (2010b)
	10/10/2009	15324	3,150	171 [e]	<12	1.1	57	83	2.7	2.2	<0.01	110	3.9	-10	NNES (2010b)
	10/10/2009	15324	3,150	--	--	--	--	--	--	2.4	<0.01	110	4.1	--	NNES (2010b)

Table A.1-4
Major-Ion Data for Wells in the Study Area
(Page 3 of 5)

Site ID	Date	Sample ID [a]	Depth (ft)	HCO₃ (mg/L)	CO₃ (mg/L)	Br (mg/L)	Cl (mg/L)	SO₄ (mg/L)	F (mg/L)	K (mg/L)	Mg (mg/L)	Na (mg/L)	Ca (mg/L)	Charge Balance	Source
ER-EC-11 main (continued)	10/17/2009	15327	3,285	146 [e]	<12	1.1	38	63 [c]	2.5	5.4	0.01	100	4.1 [c]	-6.3	NNES (2010b)
	10/17/2009	15328	3,285	146 [e]	<12	1.1	38	62 [c]	2.5	4.7	<0.01	100	4.4 [c]	-7.1	NNES (2010b)
	10/17/2009	15328	3,285	--	--	--	--	--	--	5.5	0.01	100	4.2	--	NNES (2010b)
	10/17/2009	15327	3,285	--	--	--	--	--	--	4.7	<0.01	100	4.5	--	NNES (2010b)
	10/17/2009	15332	3,755	158 [e]	<12	0.61	42	64 [c]	2.9	1.4	0.05 [c]	96 [c]	4.5 [c]	-8.6	NNES (2010b)
	10/17/2009	15332	3,755	--	--	--	--	--	--	1.7	0.03 [c]	97 [c]	4.3	--	NNES (2010b)
	05/18/2010	15454	--	146 [e]	<6	<0.02	42	70	3.0	0.7	<0.01	95	3.9	-8.1	N-I (2011)
	05/18/2010	15452	--	146 [e]	<6	0.21	43	70	3.1	0.8	<0.01	95	4.0	-8.3	N-I (2011)
	05/18/2010	15405	--	--	--	--	--	--	--	0.7	0.01	110	3.9	--	LLNL (2011b)
	05/18/2010	15455	--	--	--	--	--	--	--	--	--	--	3.9	--	USGS (2010)
PM-3	10/27/1988	3153	1,654	165	--	0.7	95	122	--	12	1.4	141	35	2.2	DOE/NV (1996)
	10/27/1988	3153	1,654	155	--	0.6	97	123	--	11	1.4	138	34	1.7	DOE/NV (1996)
	10/28/1988	3154	--	153	--	0.6	98	124	--	11	1.4	137	34	1.2	DOE/NV (1996)
	10/28/1988	3158	1,455	150	--	0.5	98	130	2.4	10	1.5	130	36	-2.0	DOE/NV (1996)
	05/17/1989	3155	1,490	159	--	0.5	93	125	2.5	11	0.6	137	28	-1.7	DRI (1994b)
	03/17/1992	3157	1,305	158	--	7.4	84	92	2.5	12	4.0	124	19	-1.0	DRI (1994b)
PM-3-1	07/19/2005	14226	1,994 [b]	112	<1.2	--	112	114	2.7	7.4	5.0	114	17		NSTec (2006)
	06/12/2007	14834	1,993 [b]	108	<0.6	--	94	106	2.5	6.9	5.2 [c]	101	15	-8.0	NSTec (2008)
	06/12/2007	14834.5	1,993 [b]	--	--	--	96	114	3.6	--	--	--	--	--	NSTec (2008)
	04/29/2009	15464	1,993 [b]	99	--	--	93	103	2.4	8.8	3.8	130	17	3.9	NSTec (2011)
PM-3-2	10/12/2000	8501	--	142	0.0	--	95	114	--	15	4.4	125	22	1.0	Mizell et al. (2008)
	12/10/2003	13411	1,560 [b]	117	<0.3	--	93	116	3.7 [c]	14	4.9	114	21	-2.6	BN (2005)
	05/25/2004	13270	1,560 [b]	119	<0.7	--	93	114	3.6	16	5.5	119	22	0.1	BN (2005)
	06/12/2007	14835	1,560 [b]	114	<0.6	--	94	109	3.8	12	4.3	88	18	-13	NSTec (2008)
	04/29/2009	15465	1,560 [b]	113	--	--	89	110	3.7	15	5.1	125	21	3.0	NSTec (2011)
	04/29/2009	15466	1,560 [b]	--	--	--	92	112	3.8	15	5.2	126	21	--	NSTec (2011)
U-20 Water Well	05/23/1987	3233	--	111	--	--	12	31	--	1.7	0.3	57	6.4	0.6	Chapman and Lyles (1993)
	04/16/1990	3234	--	113	--	--	12	29	--	1.8	0.2	58	5.7	1.2	Chapman and Lyles (1993)
	08/02/1990	3235	--	111	--	--	11	31	--	1.8	0.7	58	5.4	1.7	Chapman and Lyles (1993)
	09/11/1990	3236	--	107	1.1	--	11	31	--	1.7	0.4	57	6.2	2.1	Chapman and Lyles (1993)
	05/31/1995	5160	--	88	<5	<0.25	11	27	2.4	1.3	0.6	60	7.6	12	IT (1999)

Table A.1-4
Major-Ion Data for Wells in the Study Area
(Page 4 of 5)

Site ID	Date	Sample ID [a]	Depth (ft)	HCO_3 (mg/L)	CO_3 (mg/L)	Br (mg/L)	Cl (mg/L)	SO_4 (mg/L)	F (mg/L)	K (mg/L)	Mg (mg/L)	Na (mg/L)	Ca (mg/L)	Charge Balance	Source
U-20 Water Well (continued)	05/31/1995	3238	--	92 [d]	--	--	12	--	--	2.1	0.3	59	6.2	23	LLNL (1999)
	11/05/1997	4950.22	--	101	6.1	--	12	32	--	1.6	0.3	59	7.8	2.6	DRI (1998c)
	11/05/1997	4950.27	--	93	--	0.1	11	31	2.2	1.4	0.3	61	6.8	7.2	HRC (1998)
	11/05/1997	5130	--	95	--	0.1	11	31	2.4	1.4	0.3	59	6.7	5.4	HRC (1998)
U-20a #2 Water Well	10/14/1964	3162	--	108	ND	--	11	28	2.6	1.9	<0.1	58	5.9	1.0	Blankennagel and Weir (1973)
	10/14/1964	3163	--	108	ND	--	11	28	2.6	1.9	--	58	5.9	0.8	USGS (1994)
	03/10/1966	3164	--	106	ND	--	11	27	2.7	0.2	0.1	55	6.1	-1.2	Blankennagel and Weir (1973)
	03/21/1971	3165	--	113	ND	--	11	29	2.7	2.2	<0.1	57	5.9	-1.4	USGS (1994)
	10/06/1971	3166.21	--	110	ND	--	10	28	2.8	2.2	0.2	55	5.9	-1.2	USGS (1994)
	04/16/1973	3167	--	122 [e]	--	--	12	29	3.1	1.9	0.02	47	1.5	-18	DRI (1994a)
	07/03/1973	3170	--	116 [e]	--	--	11	30	2.7	2.6	0.05	58	0.1	-6.8	DRI (1994a)
	01/16/1975	3173	--	113 [e]	--	--	15	28	2.4	2.2	0.1	70	1.0	2.7	DRI (1994a)
	07/08/1975	3178	--	118 [e]	--	--	10	28	2.7	3.8	0.1	62	1.2	-1.2	DRI (1994a)
	04/01/1988	3184	--	111	--	--	12	33	--	1.7	0.2	59	6.2	1.8	Chapman and Lyles (1993)
	04/10/1988	3185	--	112	--	--	11	38	--	2.3	0.2	63	6.3	2.4	Chapman and Lyles (1993)
U-20ao	12/10/1984	3144	--	114	--	--	3.2	8.1	--	1.9	1.2	38	8.8	2.1	Chapman and Lyles (1993)
U-20c	09/14/1967	3143	--	140	39	--	6.8	10	5.9	0.9	<0.1	95	0.9	-1.1	USGS (1994)
	09/14/1967	3142	--	130	37	--	8.1	18	6.4	1.4	<0.1	95	2.8	0.1	USGS (1994)
U-20n PS#1 DD-H	09/21/1998	12188	4,101–4,111	109 [d]	--	0.40	11	28	4.0	1.7	0.1	61	2.9	-0.9	Smith et al. (1999)
	09/21/1998	5184	--	107	<6	0.40	13	34	4.8	1.3	<0.1	62	3.0	3.4	IT (1998)
	09/21/1998	5184	--	--	--	--	--	--	--	2.0	<0.1	61	3.0	--	IT (1998)
	10/12/1999	12187	--	108 [d]	--	<0.03	11	28	3.6	2.5	0.2	65	4.8	4.1	Davisson et al. (2001)
	07/09/2003	12394	--	90 [d]	--	0.60	11	28	3.6	1.9	0.1	61	3.8	5.4	LLNL (2004)
	11/15/2005	14016	--	94 [d]	--	<0.01	12	33	4.4	1.7	0.1	62	2.0	0.8	LLNL (2006)
UE-20bh #1	12/08/1999	6627.23	2,770	81	--	<0.1	3.5	8.3	--	0.7	<0.1	36	0.5	0.5	DRI (2000)
UE-20d	03/08/1966	3195	2,920	122	ND	--	23	40	3.1	0.2	--	81	1.4	-0.9	Blankennagel and Weir (1973)
	03/08/1966	3196	3,200	120	ND	--	24	42	3.1	0.1	0.1	83	1.4	-0.2	Blankennagel and Weir (1973)
	07/27/1966	3198	2,446–4,500	137	ND	--	23	44	2.8	1.7	0.1	88	4.3	1.7	Blankennagel and Weir (1973)
	07/28/1966	3199	2,446–4,500	143	5.0	--	8.8	53	2.4	0.5	0.1	68	21	3.7	Blankennagel and Weir (1973)
	08/12/1966	3200	2,446–4,500	192	4.0	--	24	40	3.0	2.6	0.1	107	8.5	2.0	Blankennagel and Weir (1973)

Table A.1-4
Major-Ion Data for Wells in the Study Area
(Page 5 of 5)

Site ID	Date	Sample ID [a]	Depth (ft)	HCO₃ (mg/L)	CO₃ (mg/L)	Br (mg/L)	Cl (mg/L)	SO₄ (mg/L)	F (mg/L)	K (mg/L)	Mg (mg/L)	Na (mg/L)	Ca (mg/L)	Charge Balance	Source
	06/23/1987	12263	2,850	97	--	0.6	13	31	4.4	--	0.2	75	7.8	13	Marsh (1991)
	06/30/1987	9007	2,850	93	--	0.55	13	31	4.4	--	0.2	75	7.8	--	DRI (2002)
	06/30/1987	9007.5	2,850	101	--	--	12	31	4.4	--	0.2	75	7.9	--	DRI (2002)
	07/07/1987	12261	2,850	--	--	--	13	34	4.5	3.8	0.3	76	12	--.	Marsh (1991)
	07/07/1987	12255	2,850	--	--	--	13	33	4.5	2.9	0.2	96	11	--.	Marsh (1991)
	07/07/1987	12260	2,850	--	--	--	14	34	4.7	--	--	--	--	--.	Marsh (1991)
	07/07/1987	9008	2,850	--	--	--	13	34	4.5	3.8	0.3	76	12	--	DRI (2002)
	07/07/1987	9010	--	--	--	--	13	33	4.5	2.9	0.2	96	11	--	DRI (2002)
	07/08/1987	9012	2,850	--	--	--	13	35	4.5	2.8	0.2	95	9.6	--.	DRI (2002)
	07/08/1987	12244	2,850	--	--	--	13	35	4.5	2.8	0.2	95	9.9	--.	Marsh (1991)
	07/08/1987	9012.5	--	--	--	--	13	35	4.5	2.8	0.2	95	10	--	DRI (2002)
UE-20n #1 (continued)	07/09/1987	12240	2,850	--	--	0.3	12	36	4.5	3.8	0.2	80	8.8	--.	Marsh (1991)
	07/22/1987	12223	2,750	--	--	0.1	13	36	4.2	3.1	0.2	96	8.8	--.	Marsh (1991)
	07/22/1987	12229	2,750	--	--	--	16	37	4.6	2.8	0.2	94	8.7	--.	Marsh (1991)
	07/22/1987	9020.5	2,850	--	--	0.04	13	35	4.3	3.1	0.2	97	8.9	--	DRI (2002)
	07/22/1987	9019	2,850	--	--	--	16	37	4.6	2.8	0.2	95	8.7	--	DRI (2002)
	07/22/1987	9020	2,850	--	--	0.06	14	37	4.1	3.0	0.2	95	8.7	--	DRI (2002)
	07/23/1987	9022.11	2,600	--	--	--	12	37	3.5	2.4	0.17	88	9.6	--	DRI (2002)
	07/23/1987	12220	2,600	--	--	--	12	37	3.5	2.4	0.2	88	9.6	--.	Marsh (1991)
	08/06/1987	12217	2,750	--	--	0.2	13	34	4.3	2.7	0.2	97	9.7	--.	Marsh (1991)
	08/06/1987	12215	2,750	--	--	0.2	13	34	4.3	3.0	0.2	88	7.8	--.	Marsh (1991)
	10/28/1987	12214	2,750	--	--	0.2	--	76	--	1.8	0.2	65	5.7	--.	Marsh (1992)
	02/09/1988	12213	2,750	--	--	--	--	--	--	1.9	0.2	64	6.3	--.	Marsh (1992)
	05/10/1988	12212	2,750	--	--	--	--	--	--	2.9	0.7	68	6.1	--.	Marsh (1992)

[a] UGTA Geochemistry Database sample identification number.
[b] Depth is from top of the casing.
[c] Value is an estimate.
[d] Data were reported as dissolved inorganic carbon in mg/L HCO₃ units.
[e] Data were converted from mg/L CaCO₃ units to mg/L HCO₃ units by multiplying times 1.219.
[f] Data were converted from dissolved organic carbon in mg/L C units by multiplying times 5.081.

ND = Not detected
-- = Not analyzed

Table A.1-5
Environmental-Isotope Data for Wells in the Study Area
(Page 1 of 2)

Site ID	Date	Sample ID [a]	Depth (ft)	$\delta^{18}O$ (‰)	δD (‰)	$\delta^{13}C$ (‰)	^{14}C (pmc)	$^{36}Cl/Cl$ (ratio)	Source
ER-20-5 #1	06/03/1996	10463	2,300–2,572	-14.8	-116	-3.8	--	--	DRI (1997b)
	06/03/1996	12318	2,300–2,572	-14.9	-114	-2.3	28,169	3.94E-09	LLNL (1996) Rose et al. (1997)
	04/04/1997	3915	2,300–2,572	-14.9	-115	-3.4	--	--	DRI (1997a)
	04/22/1997	12317	2,300–2,572	-15.0	--	-2.8	33,600	3.81E-09	Rose et al. (1997)
	07/09/1998	5164	2,300–2,356	-14.8	-114	-3.9	--	--	DRI (1998a)
	07/09/1998	12316	2,300–2,572	-14.9	--	-2.5	81,657	4.11E-09	LLNL (2003b)
	11/30/2004	13234	--	-14.9	-115	-4.7	96,300	4.39E-09	LLNL (2005)
ER-20-5 #3	07/31/1996	10464	--	-15.2	-115	-6.7	--	--	DRI (1997b)
	07/31/1996	12322	3,432–3,881	-15.1	-114	-5.7	1,450	1.73E-11	LLNL (1996) Rose et al. (1997)
	04/04/1997	3919	3,432–3,881	-15.1	-113	-6.5	--	--	DRI (1997a)
	04/22/1997	12321	3,432–3,881	-15.1	--	-5.8	1,462	1.68E-11	Rose et al. (1997) LLNL (2003a)
	04/30/1998	5166	3,432–3,881	-15.1	-113	-6.8	--	--	DRI (1998b)
	04/30/1998	12320	3,432–3,881	-15.1	-114	-5.6	1,346	1.93E-11	LLNL (1998b) LLNL (2003b)
	11/15/2001	12319	3,432–3,881	-15.0	-114	-4.0	--	--	LLNL (2003b)
	11/29/2004	13235	--	-15.1	-114	-9.3	1,680	2.27E-11	LLNL (2005)
	4/26/2011	15705	--	-15.7	-118	--	--	--	LLNL (2011c)
ER-20-7	09/24/2010	15470	--	-15.4	-113	--	--	--	LLNL (2011b)
ER-20-8-2	12/18/2009	15400	--	-15.2	-115	-5.4	--	--	DRI (2011)
	12/18/2009	15406	--	-15.4	-117	-2.0	--	--	LLNL (2011b)
ER-EC-1	02/01/2000	7441	2,298–4,749	-14.8	-114	-4.3	--	--	DRI (2001)
	02/01/2000	7441.21	2,298–4,749	-14.8	-116	-4.0	5.9	5.46E-13	LLNL (2000a) LLNL (2011c)
	06/03/2003	12402	2,298–4,749	-14.9	-116	-3.8	--	--	DRI (2004)
	06/03/2003	12383	2,298–4,749	-14.9	-116	-3.1	7.2	5.14E-13	LLNL (2004)
	04/02/2009	15380	2,298–4,749	-14.9	-116	-4.6	--	--	DRI (2010)
	04/03/2009	15407	2,298–4,749	-15.0	-116	-2.9	15.2	5.54E-13	LLNL (2011a)
ER-EC-11 main	05/18/2010	15401	--	-15.2	-115	-4.7	--	--	DRI (2011)
	05/18/2010	15405	--	-15.3	--	-2.5	--	--	LLNL (2011b)
ER-EC-6 (1,581–5,000 ft)	02/10/2000	7434	1,628–4,904	-14.9	-114	-4.4	--	--	DRI (2001)
	02/10/2000	7434.21	1,628–4,904	-15.0	-116	-3.4	5.4	5.41E-13	LLNL (2000b) LLNL (2011c)
ER-EC-6 (1,581–3,820 ft)	06/10/2003	12406	--	-15.2	-116	-3.4	--	--	DRI (2004)
	06/10/2003	12387	--	-15.0	-117	-2.7	6.6	5.07E-13	LLNL (2004)
	04/09/2009	15408	--	-15.3	-116	-2.6	16.3	5.62E-13	LLNL (2011a and c)
	04/11/2009	15381	--	-15.1	-116	-4.3	--	--	DRI (2010)

Table A.1-5
Environmental-Isotope Data for Wells in the Study Area
(Page 2 of 2)

Site ID	Date	Sample ID [a]	Depth (ft)	$\delta^{18}O$ (‰)	δD (‰)	$\delta^{13}C$ (‰)	^{14}C (pmc)	$^{36}Cl/Cl$ (ratio)	Source
PM-3 (3,019 ft)	10/27/1988	3153	1,655	-15.1	-116	-6.8	--	--	DRI (1994b)
	10/27/1988	3153	1,655	-15.0	-116	-6.3	--	--	DRI (1994b)
	10/28/1988	3154	1,655	-15.0	-116	-6.7	--	--	DRI (1994b)
	05/17/1989	10453	1,490	-14.8	-116	--	--	--	DRI (1997b)
	05/17/1989	10455	1,780	-14.7	-114	--	--	--	DRI (1997b)
	05/17/1989	10457	1,950	-14.8	-115	--	--	--	DRI (1997b)
PM-3-2	10/12/2000	8501	--	-14.8	-115	-6.8	--	--	Mizell et al. (2008)
U-20 Water Well	05/31/1995	3238	--	--	--	--	9.1	5.67E-13	LLNL (1999)
	11/05/1997	4950.21	--	-14.7	-113	-7.2	--	--	DRI (1998c)
	11/05/1997	4950.23	--	--	--	-6.2	8.6	--	LLNL (1998a)
U-20a #2 Water Well	--	3186	--	-14.8	-114	-13.5	15.3	--	White and Chuma (1987)
U-20n PS#1 DD-H	09/21/1998	12188	--	-14.9	-113	-5.7	160,450	1.09E-09	Smith et al. (1999)
	10/12/1999	12187	--	-15.0	-113	-6.0	153,900	1.60E-09	Davisson et al. (2001)
	07/09/2003	12394	--	-15.0	-114	-4.0	169,000	2.22E-09	LLNL (2004)
	11/15/2005	14016	--	-14.9	-114	-6.4	158,000	1.20E-09	LLNL (2006)
UE-20bh #1	06/20/1993	4423	--	-14.7	-109	-9.2	21.0	6.45E-13	LLNL (1999)
	12/08/1999	6627.23	2,770	-14.7	-110	-10.5	--	--	DRI (2000)
	12/08/1999	6627.21	2,770	--	--	-9.7	22.4	--	LLNL (2000c)
UE-20n #1	05/26/1987	8998	2,407	-14.8	-111	--	--	--	DRI (2002)
	05/26/1987	8998.5	2,407	-14.7	--	--	--	--	DRI (2002)
	05/30/1987	8999	3,003	-14.9	-110	--	--	--	Marsh (1991)
	05/31/1987	9000	3,294	-15.0	-110	--	--	--	Marsh (1991)

[a] UGTA Geochemistry Database sample identification number.

A.1.0 *REFERENCES*

BN, see Bechtel Nevada.

Bechtel Nevada. 2005. Personal communication from D. Hudson to UGTA Geochemistry Database, 1 August. (Ref_ID 481)

Blankennagel, R.K., and J.E. Weir, Jr. 1973. *Geohydrology of the Eastern Part of Pahute Mesa, Nevada Test Site, Nye County, Nevada,* Professional Paper 712-B. Denver, CO: U.S. Geological Survey. (Ref_ID 592)

DRI, see Desert Research Institute.

Chapman, J.B., and B.F. Lyles. 1993. *Groundwater Chemistry at the Nevada Test Site*: *Data and Preliminary Interpretations*, DOE/NV/10845-16; Publication No. 45100. Reno, NV: Desert Research Institute, Water Resources Center. (Ref_ID 441)

DOE/NV, see U.S. Department of Energy, Nevada Operations Office.

Davisson, M.L., G.F. Eaton, N.L. Hakem, G.B. Hudson, I.D. Hutcheon, C.A. Laue, A.B. Kersting, J.M. Kenneally, J.E. Moran, D.L. Phinney, T.P. Rose, D.K. Smith, E.R. Slywester, L. Wang, R. Williams, and M. Zavarin. 2001. *Hydrologic Resources Management Program and Underground Test Area Project FY 2000 Progress Report,* UCRL-ID-145167. Livermore, CA: Lawrence Livermore National Laboratory. (Ref_ID 372)

Desert Research Institute. 1994a. Personal communication from C. Russell to UGTA Geochemistry Database regarding historical results archived by DRI from the Environmental Protection Agency, 1 June. (Ref_ID 64)

Desert Research Institute. 1994b. Personal communication from C. Russell to UGTA Geochemistry Database regarding historical results archived by DRI from the Water Resources Center, 1 June. (Ref_ID 63)

Desert Research Institute. 1997a. Personal communication from C. Russell to UGTA Geochemistry Database, 1 January. (Ref_ID 3)

Desert Research Institute. 1997b. Personal communication from C. Russell to J. Kenneally (LLNL-ANCD) regarding stable isotope data for groundwater from various NTS wells, 1 April. (Ref_ID 327)

Desert Research Institute. 1998a. Personal communication from C. Russell to R. Bangerter (DOE/NV) regarding stable isotopic analysis for ER-20-5 #1, 4 June. (Ref_ID 164)

Desert Research Institute. 1998b. Personal communication from C. Russell to R. Bangerter (DOE/NV) regarding stable isotopic analysis for ER-20-5 #3, 4 June. (Ref_ID 163)

Desert Research Institute. 1998c. Personal communication from R. Hershey to UGTA Geochemistry Database regarding data for 21 sites from the November 1997 Oasis Valley sampling, 1 January. (Ref_IDs 105 and 106)

Desert Research Institute. 2000. Personal communication from R. Hershey to UGTA Geochemistry Database regarding physical, field, major and minor constituents, and environmental tracer data for the 3 Pahute Mesa wells (UE-20bh #1, UE-19h, and UE-18r), 22 August. (Ref_ID 217)

Desert Research Institute. 2001. Personal communication from R. Hershey to UGTA Geochemistry Database regarding water chemistry data for the 6 wells sampled in Frenchman Flat in August 2000 and the 10 Western Pahute Mesa wells (ER-18-2, ER-12-1, and the ER-EC-wells) sampled in FY 2000, 9 July. (Ref_ID 236)

Desert Research Institute. 2002. Personal communication from S. Erikson regarding major ions and isotopes for UE-20n#1 from May to July 1987, 1 March. (Ref_ID 283)

Desert Research Institute. 2004. Personal communication from R. Hershey to UGTA Geochemistry Database, 30 July. (Ref_IDs 398 and 402)

Desert Research Institute. 2010. Personal communication from R. Hershey to UGTA Geochemistry Database regarding DRI sampling results for Wells ER-EC-1 and ER-EC-6, 5 May. (Ref_ID 576)

Desert Research Institute. 2011. Personal communication from R. Hershey to UGTA Geochemistry Database DRI sampling results for Wells ER-EC-11 and ER-20-8-2, 9 June. (Ref_ID 578)

HRC, see Harry Reid Center for Environmental Studies.

Harry Reid Center for Environmental Studies. 1998. Personal communication from I. Farnham to UGTA Geochemistry Database regarding major ion, trace and rare-earth element data for 21 sites from the November 1997 Oasis Valley sampling, 20 November. (Ref_ID 128)

IT, see IT Corporation.

IT Corporation. 1997. Personal communication to UGTA Geochemistry Database, 1 January. (Ref_IDs 14, 15, 26, 27)

IT Corporation. 1998. Personal communication to UGTA Geochemistry Database, 1 January. (Ref_ID 152)

IT Corporation. 1999. Personal communication to UGTA Geochemistry Database, 1 January. (Ref_IDs 133, 137, 139, 140)

IT Corporation. 2001. Personal communication to UGTA Geochemistry Database regarding analysis results from ER-EC wells sampled by IT during FY 2000, 13 August. (Ref_ID 243)

LLNL, see Lawrence Livermore National Laboratory.

Lawrence Livermore National Laboratory. 1996. Personal communication from T. Rose (LLNL-ANCD) to R. Bangerter (DOE/NV) regarding isotopic analyses: Monitoring Well ER-20-5, 13 November. (Ref_ID 382)

Lawrence Livermore National Laboratory. 1998a. Personal communication from T. Rose to UGTA Geochemistry Database regarding dissolved total inorganic carbon, carbon-13, carbon-14, and tritium results for 21 sites from the November 1997 Oasis Valley sampling, 1 January. (Ref_ID 108)

Lawrence Livermore National Laboratory. 1998b. Personal communication from T. Rose (LLNL-ANCD) to R. Bangerter (DOE/NV) regarding isotopic analyses: Monitoring Well ER-20-5, 03 December. (Ref_ID 382)

Lawrence Livermore National Laboratory. 1999. Personal communication from J. Kenneally to UGTA Geochemistry Database regarding updated and QC'd version of the tables published in the LLNL report UCRL-ID-128000, 9 April. (Ref_ID 171)

Lawrence Livermore National Laboratory. 2000a. Personal communication from T. Rose to UGTA Geochemistry Database: Analytical Well Report for Well ER-EC-01, 1 August. (Ref_ID 234)

Lawrence Livermore National Laboratory. 2000b. Personal communication from T. Rose to UGTA Geochemistry Database: Analytical Well Report for Well ER-EC-06, 7 August. (Ref_ID 223)

Lawrence Livermore National Laboratory. 2000c. Personal communication from T. Rose to UGTA Geochemistry Database regarding carbon-14, tritium, and noble gas chemistry for samples collected from Pahute Mesa Wells UE-20bh #1, UE-19h, and UE-18r in December 1999, 1 June. (Ref_ID 202)

Lawrence Livermore National Laboratory. 2003a. Personal communication from T. Rose (LLNL-ANCD) to R. Bangerter (NNSA/NSO ERD): Analytical Well Report for Well ER-20-5, 2 June. (Ref_ID 383)

Lawrence Livermore National Laboratory. 2003b. Personal communication from T. Rose to UGTA Geochemistry Database, 2 June. (Ref_ID 373)

Lawrence Livermore National Laboratory. 2004. Personal communication from T. Rose to UGTA Geochemistry Database, 29 July. (Ref_390)

Lawrence Livermore National Laboratory. 2005. Personal communication from T. Rose to UGTA Geochemistry Database, 2 August. (Ref_ID 480)

Lawrence Livermore National Laboratory. 2006. Personal communication from M. Zavarin to UGTA Geochemistry Database, 29 August. (Ref_ID 518)

Lawrence Livermore National Laboratory. 2011a. Personal communication from M. Zavarin to UGTA Geochemistry Database for Wells ER-12-3, ER-12-4, ER-20-8#2, ER-EC-1, ER-EC-6, ER-EC-11, UE-3e#4-1, UE-3e#4-2, UE-3e#4-3, UE-2ce, and U19v PS1ds, 16 June. (Ref_ID 579)

Lawrence Livermore National Laboratory. 2011b. Personal communication from M. Zavarin to UGTA Geochemistry Database for Wells ER-EC-11, ER-20-8-2, and ER-20-7, 3 August. (Ref_ID 588)

Lawrence Livermore National Laboratory. 2011c. Personal communication from M. Zavarin to UGTA Geochemistry Database for Wells ER-EC-11, ER-20-8-2, and ER-20-7, 4 September. (Ref_ID 591)

Marsh, K.V., comp. 1991. *Hydrology and Radionuclide Migration Program, 1987 Progress Report*, UCRL-53779-87. Livermore, CA: Lawrence Livermore National Laboratory. (Ref_ID 380)

Marsh, K.V., comp. 1992. *Hydrology and Radionuclide Migration Program, 1988 Progress Report*, UCRL-53779-88. Livermore, CA: Lawrence Livermore National Laboratory. (Ref_ID 380)

Mizell, S.A., T.M. Mihevc, and R.L. Hershey. 2008. *Field Reconnaissance and Chemistry Data for Selected Water Sources on the Nevada Test and Training Range*, Publication No. 41247. Prepared for the U.S. Air Force and U.S. Bureau of Land Management. Las Vegas, NV: Desert Research Institute, Division of Hydrologic Sciences. (Ref_ID 594)

N-I, see Navarro-Intera, LLC.

NNES, see Navarro-Nevada Environmental Services, LLC.

NSTec, see National Security Technologies, LLC.

Navarro-Intera, LLC. 2011. Personal communication to UGTA Geochemistry Database for Wells ER-20-4, ER-20-7, ER-20-8, ER-EC-2A, ER-EC-11, ER-EC-12, ER-EC-13, ER-EC-14, and ER-EC-8, 8 July. (Ref_ID 583)

Navarro-Nevada Environmental Services, LLC. 2010a. Personal communication to UGTA Geochemistry Database for Wells ER-8-1, ER-EC-1, ER-EC-6, and ER-20-8-2, 25 February. (Ref_ID 571)

Navarro-Nevada Environmental Services, LLC. 2010b. Personal communication to UGTA Geochemistry Database for drilling sample results for Wells ER-20-7, ER-20-8#2 and ER-EC-11, 5 March. (Ref_ID 573)

National Security Technologies, LLC. 2006. Personal communication from D. Hudson to UGTA Geochemistry Database,11 July. (Ref_ID 519)

National Security Technologies, LLC. 2008. Personal communication from T. Redding to UGTA Geochemistry Database, 29 June. (Ref_ID 550)

National Security Technologies, LLC. 2011. Personal communication from T. Redding to UGTA Geochemistry Database, 25 July. (Ref_ID 587)

Rose, T.P., J.M. Kenneally, D.K. Smith, M.L. Davisson, G.B. Hudson, and J.H. Rego. 1997. *Chemical and Isotopic Data for Groundwater in Southern Nevada*, UCRL-ID-128000. Livermore, CA: Lawrence Livermore National Laboratory. (Ref_ID 377)

SNJV, see Stoller-Navarro Joint Venture.

Smith, D.K., G.F. Eaton, F.C. Benedict, Jr., R.E. Criss, M.L. Davisson, G.B. Hudson, J.M. Kenneally, and T.P. Rose. 1999. *Hydrologic Resources Management Program and Underground Test Area FY 1998 Progress Report*, UCRL-ID-135170. Livermore, CA: Lawrence Livermore National Laboratory. (Ref_ID 369)

Stoller-Navarro Joint Venture. 2004. Personal communication to UGTA Geochemistry Database, 1 July. (Ref_ID 388)

Stoller-Navarro Joint Venture. 2009. Personal communication to UGTA Geochemistry Database for Well ER-20-7, 9 September. (Ref_ID 557)

USGS, see U.S. Geological Survey.

U.S. Department of Energy, Nevada Operations Office. 1996. *Recompletion Report and Summary of Well History for Well PM-3,* DOE/NV-437. Las Vegas, NV. (Ref_ID 593)

U.S. Geological Survey. 1994. Personal communication from D. Wood to UGTA Geochemistry Database regarding water chemistry data,16 June. (Ref_ID 61)

U.S. Geological Survey. 2010. Personal communication from R. Graves to UGTA Geochemistry Database regarding water chemistry data for Well ER-EC-11, 28 September. (Ref_ID 585)

U.S. Geological Survey. 2011. Personal communication from R. Graves to UGTA Geochemistry Database regarding water chemistry data for Well ER-20-7, 22 July. (Ref_ID 586)

White, A.F., and N.J. Chuma. 1987. "Carbon and Isotopic Mass Balance Models of Oasis Valley–Fortymile Canyon Groundwater Basin, Southern Nevada." In *Water Resources Research*, Vol. 23(4): pp. 571–582. Washington, DC: American Geophysical Union. (Ref_ID 99)

Appendix B

LLNL Isotopic Analyses: 2009 ER-20-7 Drilling Fluids

(10 Pages)

Lawrence Livermore National Laboratory

September 15, 2009

To: Bill Wilborn, Federal Sub-Project Director, UGTA Sub-Project

From: Environmental Radiochemistry Group, Lawrence Livermore National Laboratory

RE: Isotopic Analyses: 2009 ER-20-7 drilling fluids

Attached are the analysis results of drilling fluid samples collected from ER-20-7 in 2009. LLNL received 7 drilling fluid samples from SNJV. The first four samples were identified with specific sampling times and collected while drilling through the Tiva Canyon tuff. The following three samples were identified as composite samples from a specific day and collected while drilling through the Topopah Spring tuff and the top of the Calico Hills formation. Thus, the first four samples are associated with the Tiva Canyon tuff aquifer while the latter three are associated with the Topopah Spring tuff aquifer. Figure 1 identifies the approximate drilling depth at the time of sample collection. Approximate drill depths were taken from SNJV daily drilling reports. Figure 1 includes preliminary stratigraphic unit identification, taken from the 07/07/09 daily drilling report.

Samples were analyzed for tritium, plutonium, gamma-emitting radionuclides, and anions. For tritium analyses, samples were run using two different scintillation cocktails and treated or not treated with tritium columns (Eichrom). Use of different scintillation cocktails or sample purification methods produced results that differed by no more than 10%. NSTec/SNJV field measurements taken at approximately the same times are consistent with our values.

Analysis results are reported in Tables 1 to 3. Bromide concentrations are low for all samples except the first. This very high bromide concentration may be the result of incomplete mixing of bromide tracer. Low bromide in all other samples suggests that fluid in these samples is predominantly formation water.

All ER-20-7 drilling fluids had high ^{3}H activities. The ^{3}H activity in the Tiva Canyon tuff samples is somewhat lower than in the Topopah Spring tuff. However, these differences may also be an artifact of drilling fluid mixing with formation waters. The activities measured by LLNL are consistent with field measurements reported in daily drilling reports (Table 1). The activities are also consistent with activities reported by Paragon Labs for fluids sampled on 06/30/09 and 07/01/09 ($\sim 1.8 \times 10^7$ pCi/L).

1
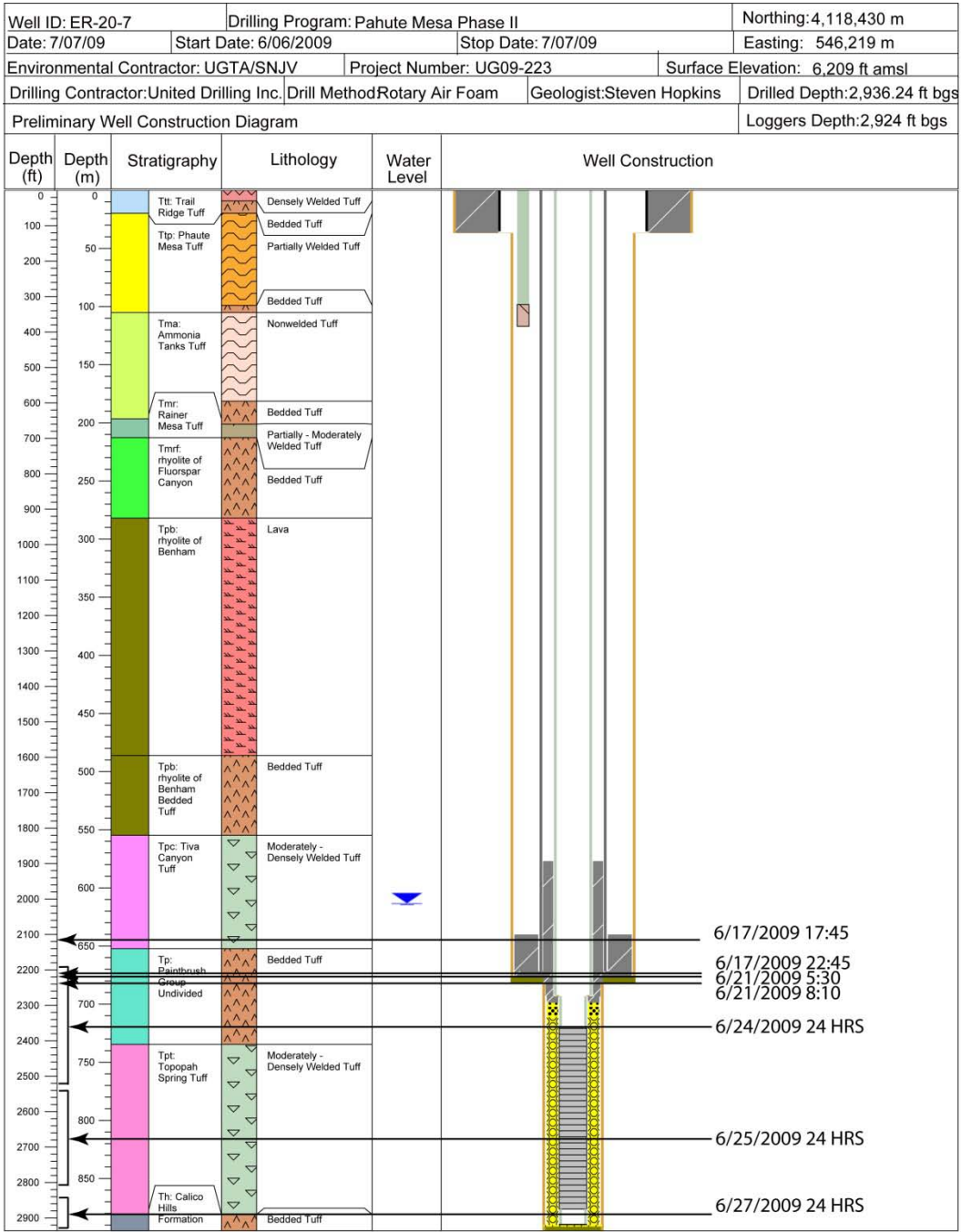
Figure 1. Approximate completion of ER-20-7 and approximate drilling depths during sampling.

SNJV provided LLNL with Paragon Labs analysis of samples collected on 6/30/09 and 07/01/09. As part of their analyses, ^{14}C activities were reported. The reported activities are surprisingly high and inconsistent with LLNL experience measuring ^{14}C activities in NTS hot wells. Figure 2 plots LLNL ^{3}H/^{14}C measurements of Pahute Mesa hot wells and compares these values to those reported by Paragon Labs. The ^{3}H/^{14}C ratio for Paragon Labs ER-20-7 samples are one to two orders of magnitude lower than expected based on past LLNL analyses. We believe that the scintillation counting technique employed by Paragon Labs is not an accurate method in cases where ^{3}H activities are high. We measured ^{3}H and ^{14}C activities in standard solutions that contained only ^{3}H or only ^{14}C. These spectra are plotted in Figure 3. When counting ^{3}H and ^{14}C simultaneously, the energy window used for ^{3}H is 0-12 keV and ^{14}C is 12-156 keV. However, a fraction of the counts in the 12-156 keV window is attributable to ^{3}H and a fraction of the counts in the 0-12 keV window is attributable to ^{14}C. While most liquid scintillation counters correct for this, corrections are imperfect due to the subtle changes in scintillation cocktail behavior under particular solution conditions (e.g. quenching). As a result, our unquenched pure ^{3}H standard resulted in a measured ^{3}H activity of 4.1×10^5 pCi/L and a ^{14}C activity of 3.6×10^4 pCi/L. Importantly, the ^{14}C activity is the result of interference from the large tritium peak and not from ^{14}C. We believe that the ^{14}C measurement reported by Paragon Labs is a result of similar ^{3}H interference (LSC spectra of ER-20-7 samples show no indication of a ^{14}C peak, Figure 4). LLNL will measure ^{14}C activities in ER-20-7 groundwater in FY10 using Accelerator Mass Spectrometry which does not suffer from these types of interferences. We expect ^{14}C activities using this method to provide a more accurate result, and a substantially lower ^{14}C activity in ER-20-7 groundwater.

Plutonium measurements were performed (Table 2). Plutonium was detected in all three samples analyzed. Activities were all below the maximum contaminant level for alpha-emitting radionuclides (15 pCi/L). Isotope ratio measurements for two samples with substantial Pu activity suggest that the source of plutonium is the Benham test. This suggests that the Tiva Canyon and Topopah aquifers are contaminated with Pu from the Benham test. However, the measurements need to be confirmed (re-analysis in underway). Samples will also be shipped to LANL for comparison.

All seven samples were counted for four days each on gamma counters at LLNL. The results are reported in Table 3. All radionuclide activities were below detection in all samples examined except ^{137}Cs in one sample. However, the ^{137}Cs activity in this sample was very close to the limit of detection. Appreciable quantities of gamma-emitting radionuclides are not present in any sample.

While it is important to remember that these samples are drilling fluids and not groundwater samples from a developed well, it does appear that both the Tiva Canyon tuff and Topopah Spring tuff aquifers are contaminated with high activities of ^{3}H. Furthermore, Pu isotope measurements suggest that the Pu contamination is attributable, in both aquifers, to the Benham test. Appreciable quantities of gamma-emitting radionuclides were not detected in any samples and the ^{14}C data reported by Paragon labs

for three ER-20-7 samples appear to be inaccurate and an artifact of interference from ^{3}H. For reference, ^{3}H and ^{239,240}Pu activities at ER-20-5, ER-20-7, and ER-20-8 are plotted in Figure 5. Importantly, we cannot attribute the contamination at ER-20-8 to any particular test due to the lack of test-specific isotopic indicators. Nevertheless, it appears that radiologic contamination may have migrated as much as several kilometers away from underground nuclear test locations.

Questions regarding these analyses should be directed to Mavrik Zavarin.

/s/ Mavrik Zavarin

Mavrik Zavarin
Chemical Sciences Division
Lawrence Livermore National Laboratory
7000 East Ave., L-231
Livermore, CA 94551
(925) 424-6491
Zavarin1@llnl.gov
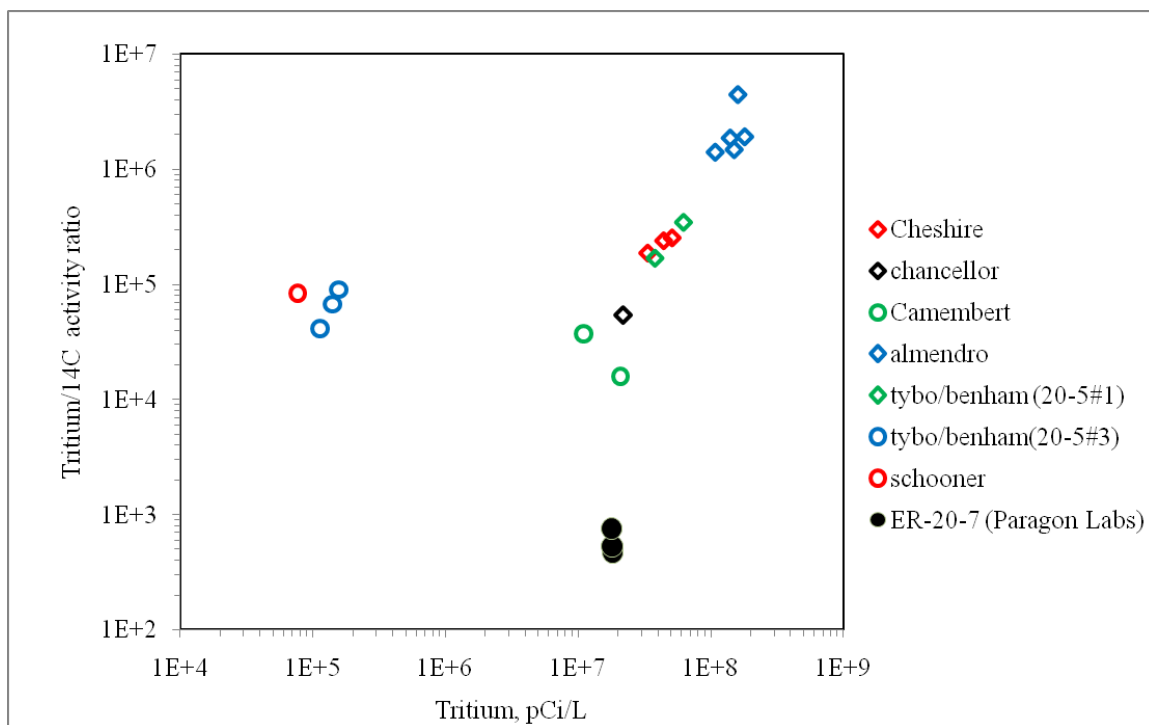
Figure 2. LLNL Pahute Mesa hot well ^{3}H/^{14}C activity ratios compared to values reported by Paragon Labs for ER-20-7.
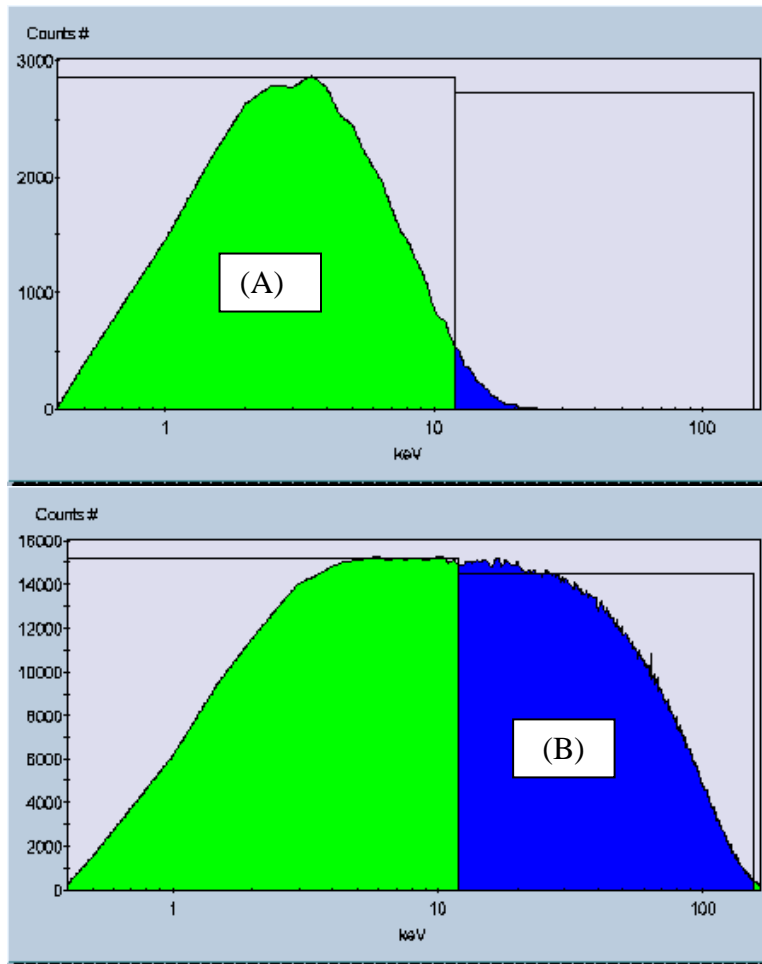
Figure 3. LSC spectra of pure ^{3}H (A) and ^{14}C (B) standards. ^{3}H counting window is 0-12 keV. ^{14}C window is 12-156 keV.
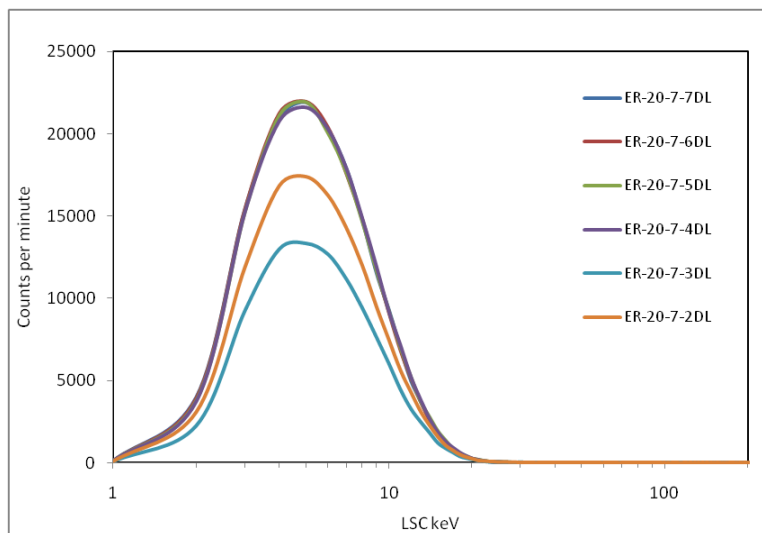
Figure 4. LSC spectra for drilling fluids showing no significant activity indicative of ^{14}C in solution (12-156 keV).
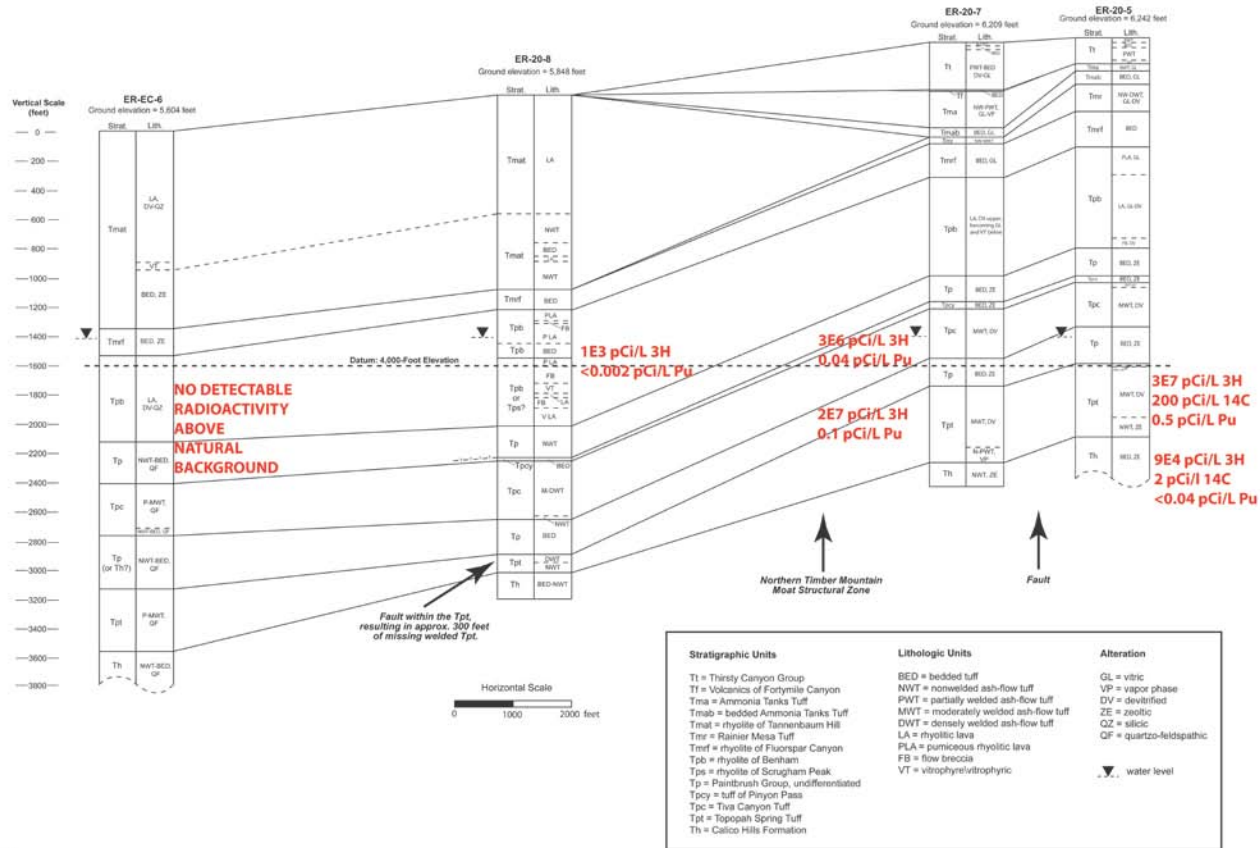
Figure 5. ^{3}H, ^{14}C, and Pu activities in pumped samples and drilling fluids from four locations on Pahute Mesa. Contamination at ER-20-5 and ER-20-7 appears to be, at least in part, from Benham. Source of contamination at ER-20-8 had not been identified. Tritium decay corrected to 6/30/09. ER-20-5 values are an average of recent (1998-2004) LLNL measurements.

Table 1. ER-20-7 LLNL analyses of drilling fluids

Sampling date/time	depth, ft	Unit	Tritium		Tritium, SNJV/NSTec field measurements	Bromide	Fluoride	Chloride	Nitrate	Sulfate
			pCi/L	+/-	pCi/L[a]	------------------- ppm -------------------				
6/17/2009 17:45	2115	Tpc (Tiva Canyon Tuff)	1.98E+6	1E+4	2.48E+6	321	3.0	31.5	<1	63.0
6/17/2009 22:45	2208	Tp (top of Paintbrush)	2.35E+6	1E+4	4.49E+6	3.5	3.0	30.6	<1	62.0
6/21/2009 5:30	2211	Tp (top of Paintbrush)	1.82E+6	9E+3	1.20E+7	7.0	2.3	27.9	<1	61.3
6/21/2009 8:10	2237	Tp (top of Paintbrush)	6.08E+6	3E+4	5.22E+6	4.0	3.9	30.7	<1	61.5
6/24/2009 24 HRS	2193-2526	Tp/Tpt (Painbrush/Topopah)	1.37E+7	7E+4	1.50E+7	2.7	5.6	32.6	<1	65.8
6/25/2009 24 HRS	2540-2809	Tpt (Topopah)	1.83E+7	9E+4	2.16E+7	0.4	6.2	28.6	<1	52.5
6/27/2009 24 HRS	2842-2930	Tpt/Th (Topopah/Calico Hills)	1.80E+7	9E+4	1.74E+7	0.8	6.0	28.5	<1	52.4

[a] Average measurement or measurement made closest in time to sample analyzed at LLNL.

Table 2. ER-20-7 LLNL Pu analyses of drilling fluids

Sampling date/time	depth, ft	Unit	Tritium		^{239,240}Pu	^{239,240}Pu
			pCi/L	+/-	pg/L	pCi/L
6/17/2009 17:45	2115	Tpc (Tiva Canyon Tuff)	1.98E+6	1E+4	~0.03	~0.005
6/21/2009 8:10	2237	Tp (top of Paintbrush)	6.08E+6	3E+4	0.29	0.04
6/27/2009 24 HRS	2842-2930	Tpt/Th (Topopah/Calico Hills)	1.80E+7	9E+4	0.84	0.12

Table 3. ER-20-7 LLNL analyses of drilling fluids, gamma counting

Sampling date/time	depth, ft	Unit	^{60}Co pCi/L	^{125}Sb pCi/L	^{137}Cs pCi/L	^{152}Eu pCi/L	^{154}Eu pCi/L	^{155}Eu pCi/L	^{241}Am pCi/L
Maximum Contaminant Level, MCL			**100**	**300**	**200**	**200**	**60**	**600**	**15**
6/17/2009 17:45	2115	Tpc (Tiva Canyon Tuff)	<6	<18	<6	<19	<12	<22	<43
6/17/2009 22:45	2208	Tp (top of Paintbrush)	<8	<25	<10	<27	<15	<30	<84
6/21/2009 5:30	2211	Tp (top of Paintbrush)	<3	<13	<5	<14	<9	<17	<30
6/21/2009 8:10	2237	Tp (top of Paintbrush)	<4	<16	<6	<18	<11	<23	<82
6/24/2009 24 HRS	2193-2526	Tp/Tpt (Painbrush/Topopah)	<7	<23	<9	<25	<14	<27	<74
6/25/2009 24 HRS	2540-2809	Tpt (Topopah)	<7	<24	<9	<24	<14	<26	<73
6/27/2009 24 HRS	2842-2930	Tpt/Th (Topopah/Calico Hills)	<1	<5	~4	<6	<4	<6	<11

Distribution

Bill Wilborn (paper, electronic)
Environmental Restoration Division
M/S 505
NNSA/NSO
P.O. Box 98518
232 Energy Way
N. Las Vegas, Nevada 89193

George H. Juniel (electronic)
NSTec
P.O. Box 98521, m/s NTS-110
Las Vegas, NV 89193-8521

David L. Finnegan (electronic)
Los Alamos National Laboratory
P.O. Box 1663, MS-J514 CST-7
Los Alamos, New Mexico 87545

Christine Miller (electronic)
Stoller-Navarro Joint Venture
7710 W. Cheyenne Ave.
Las Vegas, Nevada 89129

K.C. Thompson (electronic)
Environmental Restoration Division
NNSA/NSO
P.O. Box 98521 MS 505
232 Energy Way
Las Vegas, Nevada 89193

Appendix C

LLNL Isotopic Analyses: 2009 ER-20-8#2 Drilling Fluids

(6 Pages)

Lawrence Livermore National Laboratory

October 14, 2009

To: Bill Wilborn, Federal Sub-Project Director, UGTA Sub-Project

From: Environmental Radiochemistry Group, Lawrence Livermore National Laboratory

RE: Isotopic Analyses: 2009 ER-20-8#2 drilling fluids

Attached are the results of analyses of drilling fluid samples collected from ER-20-8#2 in 2009. LLNL received 13 drilling fluid samples from ER-20-8#2 (the second hole) with sampling times that indicate drilling was occurring in the Benham aquifer (Tpb) and the top of the Paintbrush group (Tp). We believe that all these fluids are primarily from the Benham aquifer. Figure 1 identifies the approximate drilling depth at the time of sample collection (based on SNJV tritium monitoring data in daily drilling reports). Figure 1 was taken from 9/03/2009 ER-20-8 #2 daily drilling report.

All samples were analyzed for tritium and anions. For tritium analyses, samples were treated with tritium columns (Eichrom) prior to analysis. The samples were also run at a separate LLNL low level tritium analysis laboratory (Environmental Monitoring Radioanalytical Laboratory) to test consistency among laboratories and methods at LLNL. All analyses resulted in equivalent values, within the limits of measurement uncertainty (Figure 2). Bromide concentrations tend to decrease with depth. This suggests that the fraction of formation water in drilling fluid returns increased with depth, as indicated in SNJV drilling logs. The significant increase in tritium activity at 2100 ft correlates with the observed increase in groundwater production rates at that same depth. Results are reported in Table 1.

ER-20-8#2 drilling fluids were below tritium detection limits (~100 pCi/L for low level measurements) in shallow samples but increased with depth starting at 1953 ft. The highest tritium activity was well above background but still low (1395 and 1500 pCi/L from two LLNL labs, respectively). The activities measured at LLNL are consistent with field measurements reported in daily drilling reports. However, activities measured in the field were below their detection limits (estimated to be in the vicinity of 3000 pCi/L). The activities are below any regulatory limits (tritium MCL is 20,000 pCi/L).

While it is important to remember that these samples are drilling fluids and not groundwater samples from a developed well, it does appear that the Benham aquifer at ER-20-8#2 contains tritium above environmental background levels. Furthermore, tritium activities appear to be higher in the deeper section of the aquifer. The data

suggest that contamination from underground nuclear testing has indeed reached ER-20-8#2. These results are in good agreement with tritium measurements from ER-20-8#1 drilling fluids from the same aquifer (maximum activity of 1220 pCi/L measured at LLNL).

Questions regarding these analyses should be directed to Mavrik Zavarin.

/s/ Mavrik Zavarin

Mavrik Zavarin
Chemical Sciences Division
Lawrence Livermore National Laboratory
7000 East Ave., L-231
Livermore, CA 94551
(925) 424-6491
Zavarin1@llnl.gov

Well ID: ER-20-8 #2		Drilling Program: Pahute Mesa Phase II			Northing: 4,119,269.1 m
Date: 9/03/09	Start Date: 8/17/09		Stop Date: 8/30/09		Easting: 546,675.2 m
Environmental Contractor: UGTA/SNJV		Project Number: RU09-601			Surface Elevation: 5,849 ft amsl
Drilling Contractor: United Drilling Inc.	Drill Method: Air Rotary Foam		Geologist: S. Hopkins		Drilled Depth: 2,338.62 ft bgs
Preliminary Well Construction Diagram					Loggers Depth: N/A
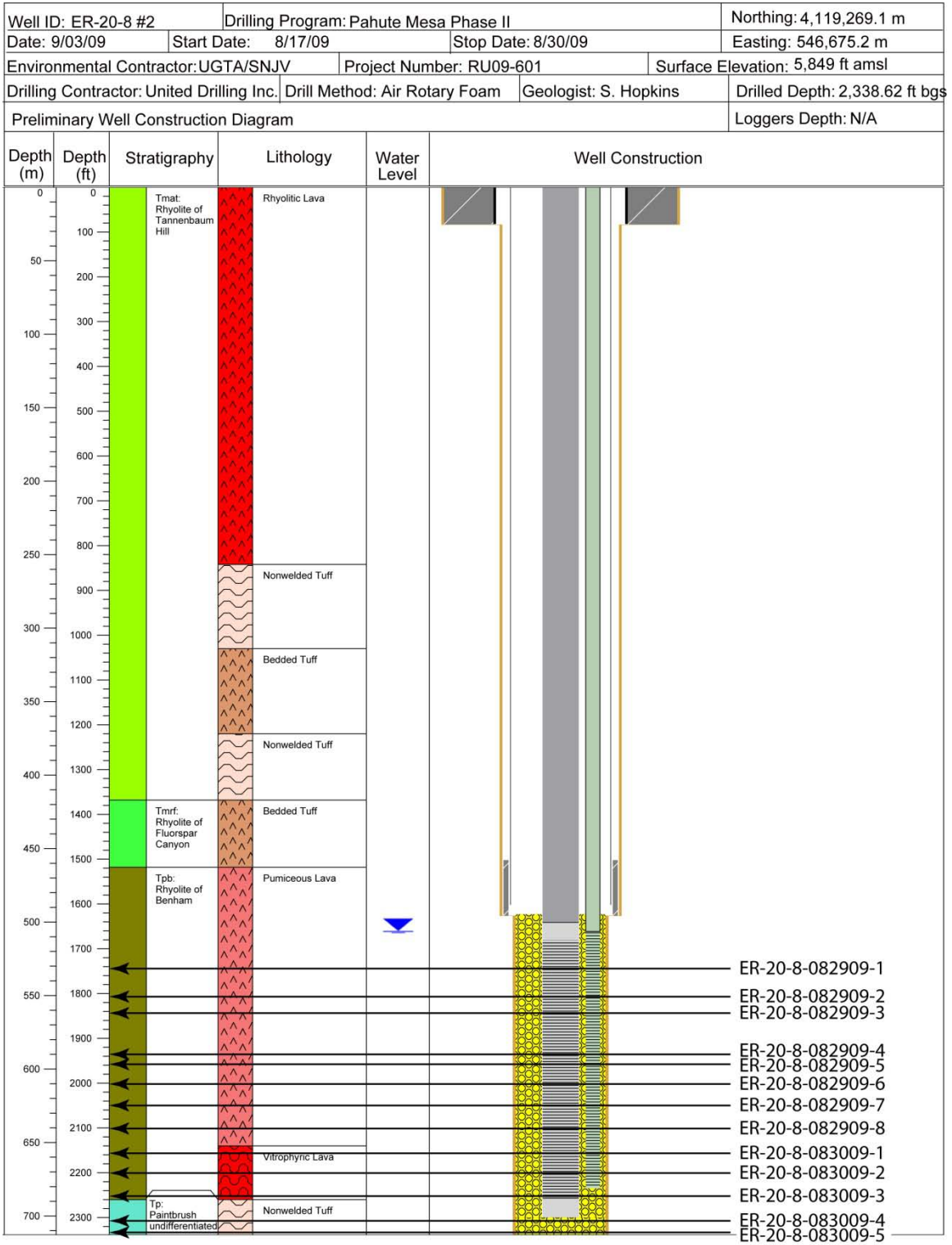
Figure 1. Approximate completion of ER-20-8 #2 and drilling locations during sampling.
Figure from Daily Drilling Reports.

3
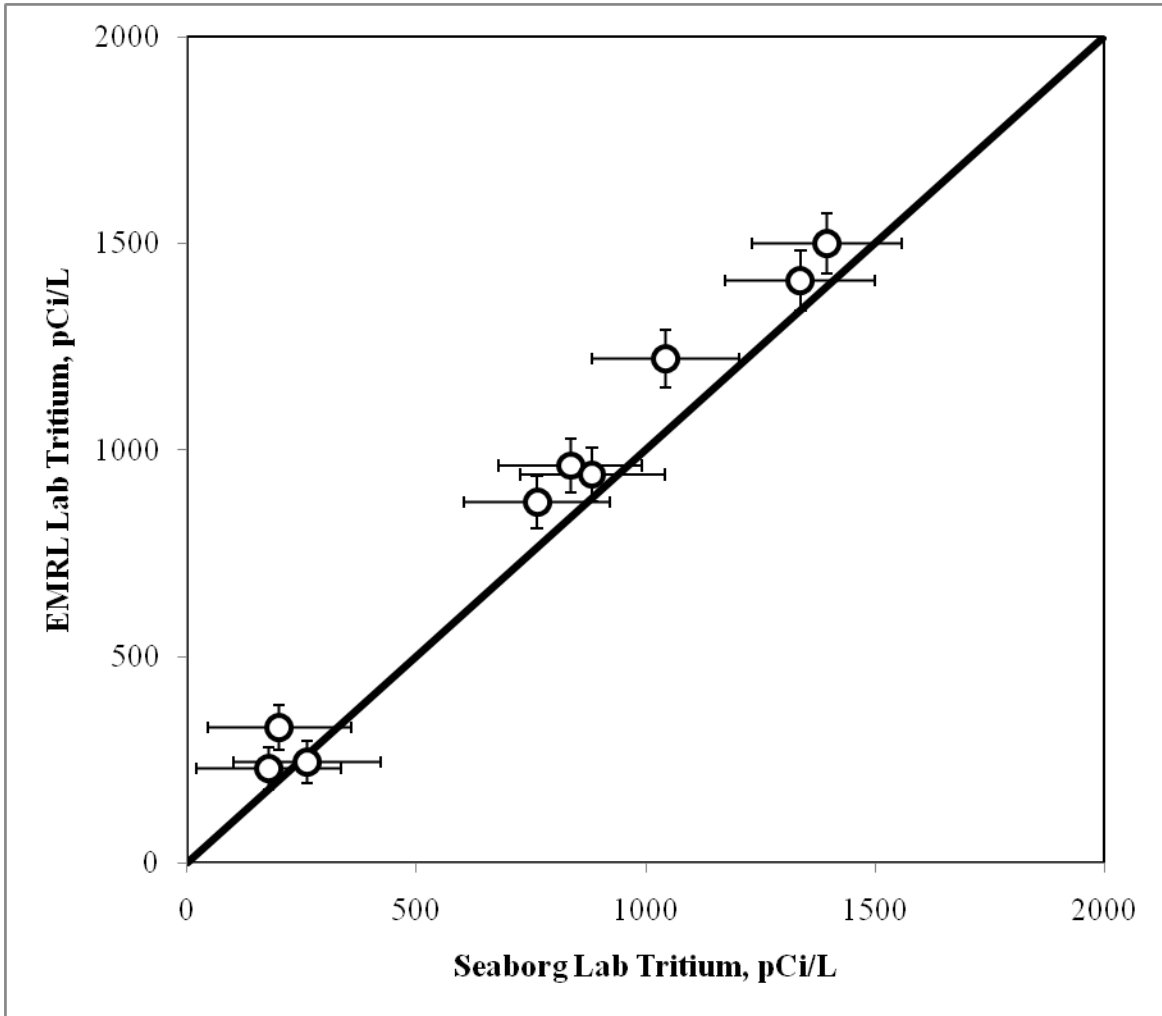
Figure 2. Comparison of measured tritium concentrations in Seaborg Lab (supported by UGTA) and Environmental Monitoring Radioanalytical Laboratory (EMRL) located in the Chemical Sciences Division. Both laboratories located at LLNL.

Table 1. ER-20-8#2 LLNL analyses of drilling fluids.

Sampling date/time	depth, ft	Unit	Tritium		Tritium		Tritium, SNJV/NSTec field measurements	Bromide	Fluoride	Chloride	Nitrate	Sulfate
			pCi/L	+/-	pCi/L[a]	+/-	pCi/L[b]		------------------ ppm -------------------			
8/29/2009 2:05	1744	Tpb (rhyolite of Benham)	ND	-	67	48	9375/4352	8.4	2.5	19.0	<1	42.2
8/29/2009 4:25	1808	Tpb (rhyolite of Benham)	ND	-	39	47	27129/3289	6.2	3.0	19.8	<1	40.6
8/29/2009 5:45	1843	Tpb (rhyolite of Benham)	ND	-	183	50	1407	5.1	3.4	21.1	<1	44.0
8/29/2009 10:30	1936	Tpb (rhyolite of Benham)	ND	-	68	48	1330	3.3	4.1	24.1	<1	44.9
8/29/2009 11:30	1953	Tpb (rhyolite of Benham)	179	158	230	51	0	2.0	4.3	24.7	<1	45.7
8/29/2009 14:30	2001	Tpb (rhyolite of Benham)	262	159	244	52	0	2.6	4.5	25.3	<1	45.4
8/29/2009 18:00	2050	Tpb (rhyolite of Benham)	201	156	329	54	3936	3.1	4.3	24.5	<1	45.4
8/29/2009 23:00	2104	Tpb (rhyolite of Benham)	763	159	873	64	2995	1.9	4.3	24.8	1.1	44.5
8/30/2009 2:00	2157	Tpb (rhyolite of Benham)	836	157	962	65	3700	1.1	4.3	25.4	<1	44.5
8/30/2009 5:30	2203	Tpb (rhyolite of Benham)	883	158	940	65	1883	2.3	4.4	25.5	2.0	46.4
8/30/2009 9:00	2250	Tpb (rhyolite of Benham)	1043	160	1220	70	4161	1.2	4.2	25.7	<1	46.4
8/30/2009 11:40	2310	Tp (top of Paintbrush)	1337	163	1410	72	0	0.7	3.9	25.5	<1	45.4
8/30/2009 13:00	2338	Tp (top of Paintbrush)	1395	163	1500	74	2779	0.8	3.9	26.1	<1	44.8

[a] Samples analyzed at LLNL by independent Environmental Monitoring Radioanalytical Laboratory (EMRL) located in the Chemical Sciences Division.
[b] Average measurement or measurement made closest in time to sample analyzed at LLNL (from SNJV daily drilling reports).

Distribution

Appendix D

LLNL Isotopic Analyses: 2009 ER-EC-11 Drilling Fluids

(5 Pages)

Lawrence Livermore National Laboratory

<div align="right">November 6, 2009</div>

To: Bill Wilborn, Federal Sub-Project Director, UGTA Sub-Project

From: Environmental Radiochemistry Group, Lawrence Livermore National Laboratory

RE: **Isotopic Analyses: 2009 ER-EC-11 drilling fluids**

Attached are the results of analyses of drilling fluid samples collected from ER-EC-11 in 2009. LLNL received 29 ER-EC-11 drilling fluid samples from SNJV with sampling times that indicate drilling was occurring in the bottom of Rainier Mesa tuff (Tmr), the Rhyolite of Fluorspar Canyon (Tmrf), the Rhyolite of Benham (Tpb), the Tiva Canyon Tuff (Tpc), and undifferentiated Paintbrush (Tp). Figure 1 identifies the approximate drilling depth at the time of sample collection (based on SNJV tritium monitoring data in daily drilling reports). Figure 1 was taken from 10/14/2009 ER-EC-11 daily drilling report.

All samples were analyzed for tritium only. Samples 1 to 21 were centrifuged to remove particulate material and, in some cases, subsequently filtered through 0.45um pose size filters, prior tritium column treatment. Cocktail Ecolume was used for LSC. All samples went through 3 counting cycles. The first cycle exhibited chemiluminescence which produced apparent tritium activity that was not observed in subsequent cycles. The counting results of the 2nd and 3rd cycles were equivalent. The last two counting cycles were used to calculate the final results. Duplicate samples of supernatant from sample 4 and 5 were filtered and counted. The results were the same as the column treated fractions. Duplicate samples 17 and 18 were centrifuged for ~1hour and counted. The counting results showed that these two samples had same activities as column treated samples.

Samples 22 to 29 were centrifuged for ~17 hrs and top (presumable organic air foam) layer removed. The aqueous supernatants were filtered using 0.45um pose size filters and 5 mL filtrates were taken for LSC. In this batch, the Ultima Gold cocktail was used. All samples were counted for 5 cycles. The counts stabilized after the 2nd cycle. Counting results of cycles 3, 4 and 5 were used for the final calculations. Sample 22 has above LLD activity, and samples 27 and 28 showed activities slightly above the LLDs.

Groundwater samples collected from the Rhyolite of Benham had consistently high tritium activities (13,180±380 pCi/L) well above our detection limits but below the tritium MCL (20,000 pCi/L). The first sample collected from the Tiva Canyon tuff had

<div align="center">1</div>

measurable tritium activity but subsequent samples did not. This may be an indication that fluids from the Rhyolite of Benham penetrated slightly into the Tiva Canyon tuff. Very low but measurable tritium activities were observed in some Paintbrush tuff samples. However, activities were very near our limit of detection using standard scintillation counting techniques. Samples collected and analyzed during well development and testing will provide more reliable tritium values for the lower aquifers and minimize potential drilling artifacts.

While it is important to remember that these samples are drilling fluids and not groundwater samples from a developed well, it is clear that the Benham aquifer at ER-EC-11 contains tritium above environmental background levels. Tritium contamination of aquifers below the Benham is extremely low or non-existent at this location. Sampling and low level tritium analysis during well development and testing will be necessary to confirm these observations.

Questions regarding these analyses should be directed to Mavrik Zavarin.

/s/ Mavrik Zavarin

Mavrik Zavarin
Chemical Sciences Division
Lawrence Livermore National Laboratory
7000 East Ave., L-231
Livermore, CA 94551
(925) 424-6491
Zavarin1@llnl.gov
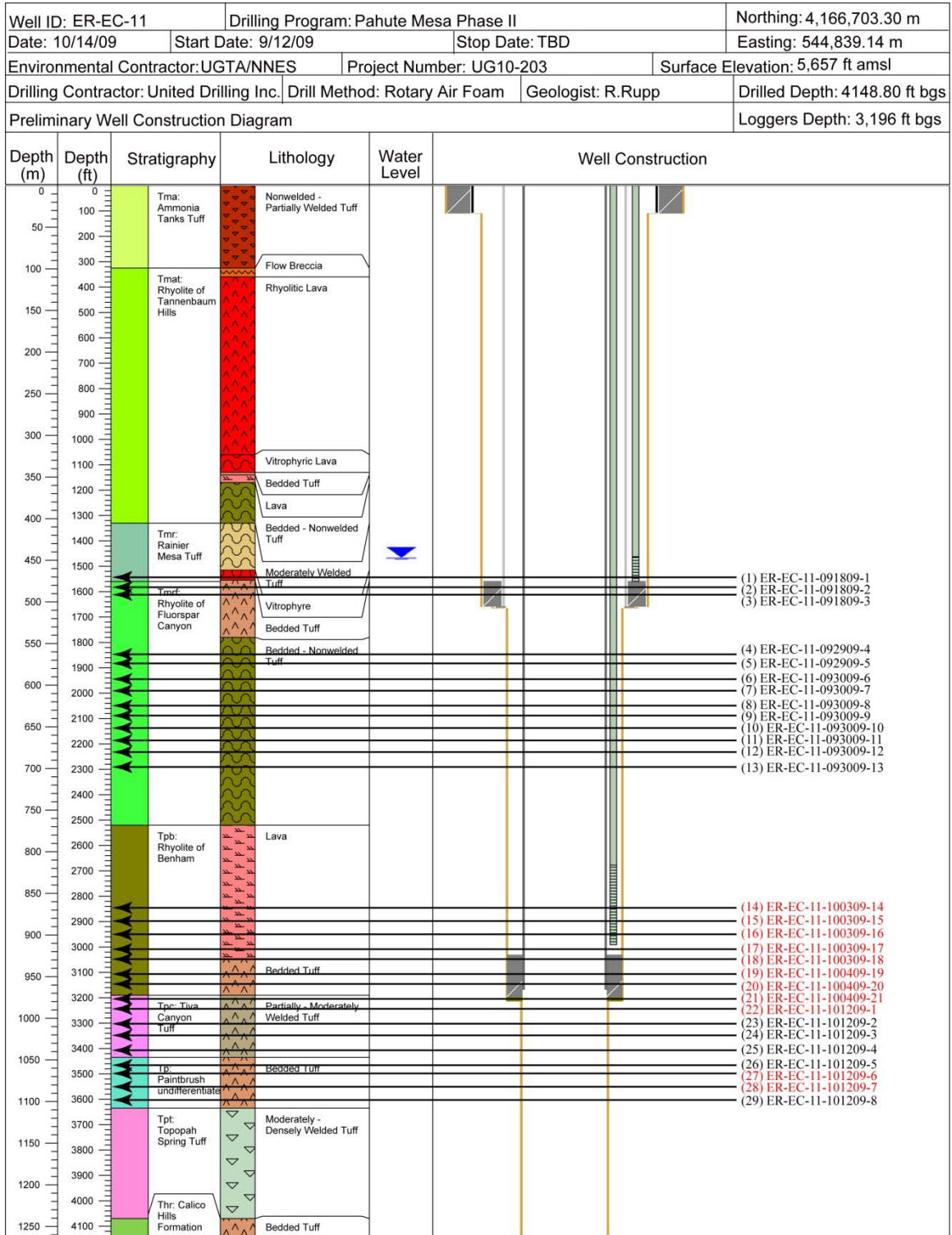
Figure 1. Approximate completion of ER-EC-11 and drilling locations during sampling. Figure from Daily Drilling Reports. Samples in which tritium was detected are highlighted in red.

Table 1. Analysis…

Sample Number	Sampling date/time	depth	Unit	Tritium		LLD[b]	Tritium, SNJV/NSTec field measurements
		ft		pCi/L	+/-	pCi/L	pCi/L[a]
1	9/18/09 12:30	1542	Tmr (bottom of Rainier Mesa tuff)	<229	-	229	2806
2	9/18/09 14:45	1582	Tmrf (top of Rhyolite of Fluorspar Canyon)	<222	-	222	1904
3	9/18/09 16:00	1610	Tmrf (top of Rhyolite of Fluorspar Canyon)	<225	-	225	2876
4	9/29/09 18:15	1843	Tmrf (Rhyolite of Fluorspar Canyon)	<229	-	229	1989
5	9/29/09 21:18	1881	Tmrf (Rhyolite of Fluorspar Canyon)	<225	-	225	1609
6	9/30/09 2:15	1943	Tmrf (Rhyolite of Fluorspar Canyon)	<227	-	227	2281
7	9/30/09 5:15	1988	Tmrf (Rhyolite of Fluorspar Canyon)	<223	-	223	0
8	9/30/09 9:35	2047	Tmrf (Rhyolite of Fluorspar Canyon)	<224	-	224	947
9	9/30/09 11:00	2090	Tmrf (Rhyolite of Fluorspar Canyon)	<226	-	226	1315
10	9/30/09 13:40	2136	Tmrf (Rhyolite of Fluorspar Canyon)	<226	-	226	1483
11	9/30/09 15:35	2185	Tmrf (Rhyolite of Fluorspar Canyon)	<224	-	224	1503
12	9/30/09 17:35	2236	Tmrf (Rhyolite of Fluorspar Canyon)	<226	-	226	1804
13	9/30/09 20:35	2290	Tmrf (Rhyolite of Fluorspar Canyon)	<226	-	226	1116
14	10/3/09 3:25	2847	Tpb (Rhyolite of Benham)	13600	300	305	16101
15	10/3/09 7:20	2900	Tpb (Rhyolite of Benham)	13500	300	303	10113
16	10/3/09 9:30	2949	Tpb (Rhyolite of Benham)	13300	300	302	19627
17	10/3/09 13:40	3004	Tpb (Rhyolite of Benham)	12700	300	294	28191
18	10/3/09 17:35	3043	Tpb (Rhyolite of Benham)	12700	300	296	21087
19	10/4/09 2:00	3103	Tpb (Rhyolite of Benham)	13500	300	305	56640
20	10/4/09 5:30	3148	Tpb (Rhyolite of Benham)	13300	300	305	13230
21	10/4/09 11:45	3206	Tpc (top of Tiva Canyon tuff)	12800	300	298	13941
22	10/12/09 5:45	3244	Tpc (Tiva Canyon tuff)	6480	150	150	94114
23	10/12/09 8:30	3300	Tpc (Tiva Canyon tuff)	<153	-	153	59640
24	10/12/09 10:45	3351	Tpc (Tiva Canyon tuff)	<152	-	152	2834
25	10/12/09 12:30	3403	Tpc (Tiva Canyon tuff)	<151	-	151	3627
26	10/12/09 14:30	3465	Tp (top of paintbrush)	<150	-	150	2486
27	10/12/09 15:35	3498	Tp (Paintbrush)	200	90	150	1748
28	10/12/09 17:30	3555	Tp (Paintbrush)	280	100	151	1381
29	10/12/09 19:20	3601	Tp (bottom of Paintbrush)	<152	-	152	306

[a] Average measurement or measurement made closest in time to sample analyzed at LLNL.
[b] lower limit of detection

Distribution

Bill Wilborn (paper, electronic)
Environmental Restoration Division
M/S 505
NNSA/NSO
P.O. Box 98518
232 Energy Way
N. Las Vegas, Nevada 89193

George H. Juniel (electronic)
NSTec
P.O. Box 98521, m/s NTS-110
Las Vegas, NV 89193-8521

David L. Finnegan (electronic)
Los Alamos National Laboratory
P.O. Box 1663, MS-J514 CST-7
Los Alamos, New Mexico 87545

Christine Miller (electronic)
Stoller-Navarro Joint Venture
7710 W. Cheyenne Ave.
Las Vegas, Nevada 89129

K.C. Thompson (electronic)
Environmental Restoration Division
NNSA/NSO
P.O. Box 98521 MS 505
232 Energy Way
Las Vegas, Nevada 89193

DISTRIBUTION

<u>Copies</u>

W.R. Wilborn   3 hard copies w/electronic media
Environmental Restoration Project
U.S. Department of Energy
National Nuclear Security Administration
Nevada Site Office
P.O. Box 98518, M/S 505
Las Vegas, NV 89193-8518

Bimal Mukhopadhyay   UGTA Website
Environmental Restoration Project
U.S. Department of Energy
National Nuclear Security Administration
Nevada Site Office
P.O. Box 98518, M/S 505
Las Vegas, NV 89193-8518

Bruce Crowe   UGTA Website
Navarro-Intera , LLC
P.O. Box 98952, MS 505
Las Vegas, NV 89193-8518

U.S. Department of Energy   1 electronic media
Office of Scientific and Technical Information
P.O. Box 62
Oak Ridge, TN 37831-0062

U.S. Department of Energy   1 electronic media
National Nuclear Security Administration
Nevada Site Office
Technical Library
P.O. Box 98518, M/S NSF 151
Las Vegas, NV 89193-8518

Naomi Becker   UGTA Website
Los Alamos National Laboratory
Hydrology, Geochemistry, and Geology Group, EES-6
Earth and Environmental Sciences Division
Bikini Atoll Rd., SM30, MS T003
Los Alamos, NM 87545

                            <u>Copies</u>

Sam Marutzky   UGTA Website
Navarro-Intera, LLC
P.O. Box 98952, NSF 167
Las Vegas, NV 89193-8518

Walt McNab   UGTA Website
Lawrence Livermore National Laboratory
7000 East Avenue, L-231
Livermore, CA 94550-9909

Ken Ortego   UGTA Website
National Security Technologies, LLC
P.O. Box 98521, M/S NLV 082
Las Vegas, NV 89193-8521

Chuck E. Russell   UGTA Website
Desert Research Institute
755 E. Flamingo
Las Vegas, NV 89119

Bonnie Thompson   UGTA Website
U.S. Geological Survey
Water Resources Division
160 North Stephanie Street
Henderson, NV 89074

Ed Kwicklis   UGTA Website
Los Alamos National Laboratory
Hydrology, Geochemistry, and Geology Group, EES-6
Earth and Environmental Sciences Division
SM-30 Bikini Atoll Rd., MS T003
Lo Alamos, NM 87545

Gayle Pawloski   UGTA Website
Lawrence Livermore National Laboratory
7000 East Avenue, L-231
Livermore, CA 94550-9900

Greg Ruskauff   UGTA Website
Navarro-Intera , LLC
P.O. Box 98952, NSF 167
Las Vegas, NV 89193-8518

	Copies
Southern Nevada Public Reading Facility c/o Nuclear Testing Archive P.O. Box 98521, M/S NLV 400 Las Vegas, NV 89193-8521	2 electronic media
Northern Nevada Public Reading Facility c/o Nevada State Library & Archives 100 N Stewart Street Carson City, NV 89701-4285	1 electronic media
Environmental Management Records U.S. Department of Energy National Nuclear Security Administration Nevada Site Office P.O. Box 98518, M/S 505 Las Vegas, NV 89193-8518	1 hard copy w/electronic media
Navarro-Intera, LLC Central Files P.O. Box 98952, NSF 156 Las Vegas, NV 89193-8518	1 hard copy w/electronic media